UNIVERSITÀ DI SIENA 1240

Department of Biotechnology, Chemistry and Pharmacy

PhD in Chemical and Pharmaceutical Sciences

Cycle XXXV

Coordinator: Prof. Maurizio Taddei

Catchment based analysis of macronutrients (nitrogen and phosphorus) and organic carbon dynamics: new modelling and participatory tools

Scientific disciplinary sector: CHIM/01

Ph.D. candidate

Francesco Di Grazia

Tutor

Prof. Steven A. Loiselle

Digitally signed by DI GRAZIA FRANCESCO
C=IT

Academic year 2021/2022

Abstract

Ecosystem services (ESs) are increasingly being considered in decision-making with respect to mitigating future climate impacts. To capture complex variation in spatial and temporal dynamics, ecosystem models require spatially explicit data that are often difficult to obtain for model development and validation. Citizen science allows for the participation of trained citizen volunteers in research or regulatory activities, resulting in increased data collection and increased participation of the general public in resource management. Despite the increasing experience in citizen science, these approaches have seldom been used in the modelling of provisioning ecosystem services.

The development of new approaches for the analysis of long-term changes in riverine carbon, hydrological and nutrient cycles is important to identify potential alteration on the biogeochemical cycles and potential impacts on the ecosystem services provided to the local population. The Basin scale approach is useful to evaluate the pressures on river ecosystems that may be distant from the receiving watercourse, including the effects of soil or water management activities that propagate or amplify downstream. However, the lack of process-based and basin-scale models for carbon transport has limited effective basin management of organic carbon fluxes from soils, through river networks and to receiving marine waters.

In the present study, were examined the temporal and spatial drivers in macronutrient (nitrogen and phosphorus) and sediment delivery, carbon storage and sequestration and water yield in a major Italian river catchment and under different NBS scenarios. Information on climate, land use, soil and river conditions, as well as future climate scenarios, were used to explore future (2050) benefits of NBS on local and basin scales, followed the national and European directives related to water quality (Directive 2000/60/EC) and habitat (Directive 92/43/EEC).

It was developed and validate a spatially semi-distributed mass balance modelling approach to estimate organic carbon delivery at a sub-basin scale and which allows exploration of alternative river basin management scenarios and their impact on DOC and POC dynamics. The model is built as an open-source plugin for QGIS and can be easily integrated with other basin scale decision support models on nutrient and sediment export.

Furthermore, was performed an estimation of the benefits of individual and combined NBS approaches related to river restoration and catchment reforestation.

To complete the ESs overall evaluation and prioritization was developed a new method in order to attributing a weight to the best NBS scenarios based on the natural stoichiometric ratio between the elements carbon, silicon, nitrogen, phosphorus (C:Si:N:P).

Acknowledgments

I would like to express my sincere gratitude to those who have contributed to this thesis and supported me on this process.

First and foremost, I want to thank my academic supervisor Prof. Steven Loiselle for believing in me, encouraging me and for helping me grow, both professionally and personally, during this research with his unshakable optimism, patience, inspiration, and friendship.

I would like to present my special thanks to Prof. Bruna Gumiero and Dr. Luisa Galgani for their contributions, precious advice, and direction leading me to the better. They always supported me and shared their time and experiences generously. I would like to thank Elena Troiani for many stimulating discussions and her contribution to this work.

I would like to present my special thanks to my ICRA supervisor Vicenç Acuña and his team, in particular Xavier and Oriana, for hosting me and for many stimulating discussions, contributions, and valuable suggestions. I am grateful to all the wonderful people of ICRA in Girona for their warm reception and hospitality during my stay.

I would like to thank the Eastern Alps District Basin Authority (Autorità di Bacino Distrettuale delle Alpi Orientali) for funding the research and the Veneto Regional Agency for environmental protection (ARPAV) for providing information used in this study.

I would like to thank all the citizen scientists of the lower Piave basin, the municipality of San Donà di Piave and local associations for their participation, effort, enthusiasm, and fundamental data gathering.

I wish to express my deep appreciation to my beloved family. They have always been a strong source of motivation with their support and love. They are great role models and never stopped believing in me.

I wish to extend my gratitude to all my friends for their trust and support.

The last acknowledgement is reserved for the most important person in my life, Simona, who with her love and encouragement, has been my principal support during these years.

Table of Contents

List of figures

List of tables

List of Abbreviations and Symbols

A: absorbance

A^{00}: corrected spectral absorbance

AET: actual evapotranspiration

avg: average

BOD_5: biochemical oxygen demand

ARPAV: Regional agency for environmental protection – Agenzia Regionale per la Prevenzione e Protezione Ambientale - Veneto

C: carbon

C_A: above ground biomass

CAP: common agricultural policy

C_D: dead organic matter

CDOM: Chromophoric fraction of dissolved organic carbon

C factor: crop management factor

CH_4: methane

CO_2: Carbon dioxide

CLC: Corine land cover

d: days

DEM: digital elevation model

DO: dissolved oxygen

DOC: dissolved organic carbon

DOM: dissolved organic matter

IPCC: Intergovernmental panel on climate change

ISPRA: National Institute for Environmental Protection and Research - Istituto Superiore per la Protezione e la Ricerca Ambientale

EEA: European environmental agency

ESDAC: European soil data centre

ESs: ecosystem services

ET0: evapotranspiration

exp: exponent

exp_tot: total export

F_{D1}: DOC reduction factor river

F_{D2}: DOC reduction factor tributary

F_{P1}: POC reduction factor river

F_{P2}: POC reduction factor tributary

FWW: FreshWater Watch

GHG: greenhouse gases

ha: hectare

hr: hour

InVEST: Integrate valuation of ecosystem services and trade-offs

K: soil erodibility

Kc: plant evapotranspiration coefficient

kg: kilograms

km: kilometres

λ: wavelength

L: litre

LS: Basin slope

LU: Land use

LULC: Land Use / Land Cover

m: metre

mm: millimetre

mg: milligram

Mg: megagram

min: minute

MJ: megajoule

μS: micro Siemens

μM: micrometre

MEA: millennium ecosystem assessment

N: nitrogen

NAO: North Atlantic oscillation

NBS: nature-based solutions

NDR: nutrient delivery ratio

NGOs: non-governmental organizations

NH_4^+-N: ammonium

NO_3^--N: nitrate

NNB: national biodiversity network

N_2O: nitrous oxide

NOAA: national oceanic and atmospheric administration

NTU: nephelometric turbidity units

O_2: oxygen

°C: degree Celsius

OC: organic carbon

OM: organic matter

p: p-value or probability value

P: phosphorus

PAWC: plant available water capacity

PET: potential evapotranspiration

P_i: support practice P factor for USLE

PO_4^{3-}-P: phosphate

POC: particulate organic carbon

R_i: rainfall erosivity index

R^2: coefficient of determination

RCP: representative concentration paths

Red: reduction

RMSE: root mean square error

Rv: river

s: second

S: slope

SD: standard deviation

SDR: sediment delivery ratio

Si: silicon

Subb: sub-basin

Sub_load: sub soil load

Surf_load: surface load

T: temperature

T-N: total nitrogen

T-P: total phosphorous

Tons: Tonnes

Trib: tributary

TSS: Total suspended solids

UN: United Nations

USLE: Universal soil loss equation

UV: ultraviolet radiation

W: watt

WFD: Water framework directive 2000/60/EC

Wn (or Wp): water mass

Z: Z parameter

Structure of the thesis

The research described in this thesis was focused on the modelling and analysis of macronutrients (nitrogen and phosphorus) and organic carbon dynamics related to the Piave Basin and the lower basin, in relation to different land use scenarios and considering possible impacts compared to the climate change projected by the IPCC for 2050.

The collection of information and preliminary data was necessary for the identification of information sources and any missing data, in order to proceed with the most suitable models for the evaluation of biogeochemical dynamics and ecosystem services. Data local, regional and national sources was integrated and used in the models developed and analyses performed. Among these, citizen participation in co-design and data collection provided important information for model development and validation. This project on the lower Piave basin is the first in which citizen science activities were integrated with other data sources for this objective, and within the modelling of ecosystem services.

The research described in this thesis can be summarised in 4 main tasks:

1) The development of climate change and variation land use scenarios (chapter 2). These latter included scenarios where Nature-Based Solutions were applied, starting from the 2018 conditions. Each scenario was developed based on consultations with local and regional stakeholders. Temporal trends were explored using photometric and satellite-based images.

2) The development of a macronutrients dynamics analysis approach integrating citizen science monitoring activities (chapter 3).

3) The development of the river basin organic carbon dynamics model. This was divided in 2 sub-chapters, with Chapter 4.1 focused on the analysis of the carbon stock including DOC from CDOM and riparian vegetation monitoring by local population. The second part (Chapter 4.2) on the development of an open-source basin scale model to identify organic carbon (DOC and POC) dynamics across temporal and spatial scales.

4) The Conclusion section, where these models were integrated into the determination of ecosystem services of the river basin, to determine both the best scenario and the best combination of two scenarios. These were prioritised based on the environmental goals of stakeholders in the Piave basin (chapter 6).

Additional ecosystem services models, necessary for the overall determination of best scenarios, including those related to water availability and sediment export and retention, were included in Chapter 5.

The research activities described in the thesis were carried out in collaboration with the Eastern Alps District Basin Authority. Part of the research described here was also performed in Girona, Spain, where I was hosted as a PhD visiting student at ICRA (Catalan Institute for Water Research), a research centre focused on water cycle, hydraulic resources, water quality and treatment, and evaluation technologies for environmental sustainability purposes.

1. GENERAL INTRODUCTION

1.1. Biogeochemical dynamics

Carbon (C), nitrogen (N), phosphorus (P) are essential elements for life and ecosystems processes (Sterner and Elser, 2017). Knowledge of these element cycles is essential for understanding the ecosystem biogeochemistry. Before reaching the ocean, sediment, organic carbon and nutrients from land transit through the continuum formed by soils, groundwater, riparian zones, floodplains, rivers, lakes, estuaries and coastal marine areas. These systems act as successive filters in which the hydrology, ecology and biogeochemical processing are strongly coupled and together act to retain a significant fraction of the nutrients transported (Turner et al., 2003). Retention in the aquatic continuum not only affects the absolute amount of nutrients reaching the ocean, but also modifies the ratio in which C, N and P are transferred, and the chemical form of each of these elements (Bouwman et al., 2013; Ensign and Doyle, 2006).

The quality of surface waters is highly influenced by external perturbations, mostly anthropic, whether they are of a physical nature, such as dams, weirs or sediment or chemical regulation systems, such as agricultural activities or industrial and domestic discharges (X. Li et al., 2017; Liu and Han, 2020). The chemical component of a water course is the result of natural actions such as rock erosion, glacier melting and seasonal meteorological events. Since the last century surface waters have been more significantly affected by human activities, such as soil, agriculture, animal husbandry, industrial waste or the management of the catchment area itself (Ciobotaru, 2015). Anthropic activities can modify the chemical state of the watercourse, bringing an excess of organic matter and/or nutrients or introducing toxic substances or variations in temperature or pH. These changes can exceed the ecosystem resilience and load capacity, compromising its balance and preventing its recovery through self-purification (ISPRA, 2013).

Climate change represents a threat to the balance of the river ecosystem, not only by through extreme events (floods and low flows) but also by increasing its temperature and acidifying its waters (Scanes et al., 2020). The rivers alkalinity, represented by bicarbonate (HCO_3^-) and carbonate (CO_3^{2-}) ions, is in fact compromised by global warming and other anthropic actions, such as intensive agriculture and land use, as higher concentrations of CO_2 and the relative increase in acidity, increase the rate of carbonate dissolution (Drake et al., 2018; Raymond et al., 2018).

Accurate, high spatial and temporal resolution water quality monitoring in inland waters is fundamental for better understanding the biogeochemical dynamics. Recent advances in remote sensing, big data, cloud computing, and machine learning have promoted remote sensing of water environment (Chen et al., 2022). Although some water environment characteristics (optically active parameters) have been widely studied through remote sensing estimation and numerical simulations in the past decades, more features (non-optically active parameters) remain under-explored or even missing (Sagan et al., 2020). Therefore, integrating research considering the key factors of water colour, water quality, and water volume is urgently needed to promote the transformation ability of science research into actionable responses for economic activities and climate change.

1.2. Macronutrients dynamics

Phosphorus and nitrogen are essential elements for life, despite their excess, due to the leaching of fertilizers used in agriculture, zootechnical activities, purification plants and industrial waste. The macronutrients N and P concentration, their molecular form, and stoichiometry at a given location and time are factors that control the productivity of aquatic ecosystems (Stutter et al., 2018). The structure of the riverine ecosystem and the biodiversity present may be strongly influenced by the impact that nutrient loads have on primary production (Balvanera et al., 2006; Bouwman et al., 2013). The dynamic structures of aquatic ecosystems are also influenced by many factors such as temperature, precipitation or geographical location which in turn influence nutrients, physical forces or the organisms themselves (Porter et al., 2012; Straile et al., 2003).

In deep and slow-flowing rivers and floodplain channels, nutrient uptake by macrophytes and emergent plants plays a major role in nutrient cycling.

Nitrogen cycle

The nitrogen (N) cycle is fundamental to the Earth biogeochemistry, with large natural flows of N from the atmosphere into terrestrial and marine ecosystems. N is a very important element for living beings and can be found in the biosphere in various forms, organic and inorganic. All processes involving nitrogen are usually represented through the nitrogen cycle which relates the biosphere to the atmosphere. The largely un-reactive molecular nitrogen (N_2) represents about 78% of the gases present in the atmosphere, through the biological nitrogen fixation is reduced to ammonium compounds (Smith and Smith, 2014). The forms of nitrogen present in the biosphere are obtained through the demolition of some complex organic substances present in the soil by some fungi and bacteria, in this way formed ammonia (NH_3)

and ammonium ion (NH_4^+). This is not the only way in which bioavailable substances containing nitrogen are formed, in fact, through a biological fixation reaction, atmospheric nitrogen is transformed into ammonia thanks to the intervention of some nitrogen-fixing bacteria. At this point other bacteria come into play and transform the newly formed ammonia into nitrite (NO_2^-). After the oxidation of ammonia to nitrite, other bacteria transform the nitrites into nitrates (NO_3^-) which are easier for plants to assimilate. In fact, nitrates are used by plants for the synthesis of complex substances such as proteins and nucleic acids. In addition to this type of fixation (organic) there is another type (inorganic) which occurs due to atmospheric events such as lightning and cosmic radiation which, starting from atmospheric nitrogen and oxygen or hydrogen, give rise to ammonium oxides or hydroxides (Bazilevskaya et al., 2000; Hill et al., 1980).

Based on different reactions, various binary compounds are formed with oxygen, called NO_x (NO and NO_2), which are harmful to humans and the environment as they are the protagonists of the photochemical smog. Having reached the final phase of the cycle, other bacteria, for example the *Pseudomonas*, transform the ammonia back into N_2 through a denitrification reaction (Jin et al., 2015).

Atmospheric nitrogen is also fixed unintentionally through human activities, especially during the combustion of fossil fuels by internal combustion engines, and industrial activity, including electricity production (Houlton et al., 2013). The overall magnitude of anthropogenic relative to natural sources of fixed nitrogen (210 Tg N $year^{-1}$ anthropogenic and 203 Tg N $year^{-1}$ natural) is so large it has doubled the global cycling of nitrogen over the last century (Erisman et al., 2013; Fowler et al., 2013; Smil, 2004).

In freshwater and marine systems, biotic transformations include the autotrophic and heterotrophic uptake of nutrients from the water, their assimilation into biomass, and their release by excretion and microbial decomposition (Bernot and Dodds, 2005; Birgand et al., 2007).

The nitrogen cycle just described represents in a very general way how the various forms of nitrogen are distributed between the biosphere and the atmosphere, but the same processes also occur between the atmosphere and the aquatic environment included in the biosphere. Nitrogen in the form of nitrate or ammonia is fundamental in agriculture for plant grow. This nitrogen can stem from different sources, as mineral fertilizer, manure, organic matter, or bacteria. Animals and humans need proteins, of which nitrogen is a key component. On the other hand, nitrogen emissions can be harmful for humans and for biodiversity and have negative effects on many natural resources.

Nitrogen emissions to the aquatic systems occur from agricultural sources (mainly diffuse sources) and from sewerage systems (mainly point sources). Agriculture is the dominant source of emissions in Europe for each of nitrates to ground and surface waters, as well of emissions of ammonia and nitrous oxide to the air (Sutton et al., 2011). Emission and consequent deposition of ammonia leads to loss of terrestrial biodiversity, while nitrous oxide is a powerful greenhouse gas.

While agriculture is the main source of nitrogen emissions in Europe, it has also been shown that livestock production is the key driver of total nitrogen losses (Sutton et al., 2011). Livestock manure is also a major source of nitrate leaching, for example due to wrong timing of manure application, or due to over-application of manure (Steinfeld and Wassenaar, 2007).

The riparian forest provides protection against erosion, retention of pollutants, excessive nutrients runoff and water temperature (Gumiero and Boz, 2017; Loiselle et al., 2016; Sabater et al., 2003), with benefits for the quality of human life and biodiversity (Ou et al., 2016; Tanaka et al., 2016). In this context, is fundamental the importance of improving our understanding of the benefits of riparian zone restoration (W. Yang et al., 2016; Zhang et al., 2010).

Phosphorus cycle

The global phosphorus cycle is the only major biogeochemical cycle that does not have a significant component in the atmosphere. This is because phosphorus and its derivatives are not gaseous under normal conditions of temperature and pressure. The phosphorus cycle only partially follows the water cycle. During transport from the land to the sea, part of the phosphorus is subtracted from the biogeochemical cycle. For this reason, the global availability of phosphorus is limited. The natural scarcity of phosphorus in aquatic ecosystems is evidenced by the exponential growth of algae in water bodies especially where there are phosphorus discharges.

In terrestrial ecosystems, most phosphorus comes from the leaching of calcium phosphate minerals. Phosphorus enters the biosphere from the soil by uptake by plant roots; weathering of rocks containing phosphorus minerals, primarily apatite $Ca_5(PO_4)_3X$ where X is F, OH or Cl yields relatively little phosphorus. The bioavailability of phosphorus for plants comes from the decomposition of organic molecules, many of which derive from the dissolution of phosphate by microorganisms (fungi and bacteria) (Timofeeva et al., 2022).

In aquatic ecosystems, both marine and terrestrial, phosphorus is present in three different chemical forms: particulate organic phosphorus (POP), dissolved organic phosphates (DOP) and inorganic phosphates. The main form of uptake is orthophosphate (PO_4^{3-}) (Koistinen et al., 2020). In fact, the form of PO_4^{3-} and HPO_4^{2-} an essential nutrient for plants and animals.

Phosphorus is part of DNA and RNA, molecules that provide energy such as ATP, in the form of phospholipids in the cell membrane (Butusov and Jernelöv, 2013).

The main P sources are identified in the civil and industrial sectors. In the agricultural sector, when the phosphorus contained in fertilizers exceeds the amount assimilated by plants, it can leach from agricultural land and reach watercourses (Smith and Smith, 2014).

Knowing the nature and magnitude of P flow in various systems at different geographical scales is crucial for a sustainable management of P for both global food security and conservation of aquatic ecosystems (Biswas Chowdhury and Zhang, 2021; Scholz et al., 2014).

Eutrophication

The excess of nutrients (nitrogen and phosphorus) in surface waters causes eutrophication, which leads to biodiversity loss, algae blooms and fish kills (Fig. 1) (Dodds et al., 2009). The eutrophication process can be determined by natural changes in the environment but, more frequently, it is accelerated by pollutants (detergents, fertilizers, etc.). Phosphorus is a key factor for the development of eutrophic conditions, especially for plant biomass (macro and micro). Furthermore, the main control factors for algal growth are the river flow rate and light limitation (Mainstone and Parr, 2002). At low nutrient concentrations, macrophytes prevail and develop as a function of water flow, the amount of available nutrients, light and other factors. As nutrients and/or available light increase, it is possible for other plants to develop such as *Cladophora*, epiphytes and finally benthic algae, with the latter only developing at very high nutrient concentrations. High concentrations of nitrates accumulate in groundwater causing human health problems and loss of biodiversity (Ahada and Suthar, 2018). In aquatic ecosystems, P is usually less efficiently removed than N (Hejzlar et al., 2009; Passy et al., 2016)

Nutrient eutrophication negatively affects services provided by river ecosystems. In recent decades in Europe, and following improvements in nutrient management and regulation, there has been a significant reduction in total phosphorus and total nitrogen emissions in freshwater ecosystems. Due to policy interventions, economic circumstances, and technological improvements nitrogen emissions from agriculture in Europe have decreased since their peak in around 1985. However, many water bodies still require improvements to bring them in good condition, as required by the Water Framework Directive 2000/60/EC (EU, 2000).

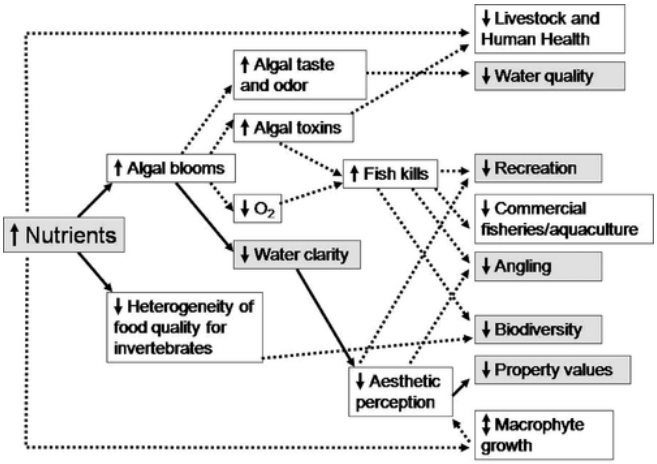

Figure.1 Nutrient dynamics on ecosystem services

1.3. Carbon dynamics

One of the steps towards the mitigation of global climate change, universally accepted by the scientific community, consists in improving the monitoring and management of the biogeochemical cycle of carbon.

There are three main reservoirs of C: atmospheric, terrestrial, and oceanic (M. Li et al., 2017; Prentice et al., 2001). Each of these reservoirs can be described the amount of C contained (stock) and its flow (flux), interpreted as the rate of exchange between environmental compartments. As regards the second parameter, they can be classified as assets or liabilities based on the turnover interval which can be short, with rapid passages of the element from one chemical form to another, or long. The biochemically active compartments for C are the terrestrial and oceanic ones (Cole et al., 2007), where the greatest flux values are recorded in vegetation, soil and seas, in contrast to the slow transformation rate typical of C preserved in fossil form, such as coal or oil, and in carbonate rocks (Brown et al., 2013).

Organic carbon (OC) is commonly divided in two forms: Particulate Organic Carbon (POC) and Dissolved Organic Carbon (DOC) (M. Li et al., 2017; Ouyang, 2003). The inclusion in one category rather than the other takes place by convection depending on the dimension of the subject considered. In the case of DOC, the diameter must be less than or equal to 0.45μm, while if it is exceeded, it falls back to POC (Smith and Smith, 2014).

The relationship between DOC and POC varies in relation to the production processes (allochthonous or autochthonous origin), transformation and degradation (Holland et al., 2020). A study conducted on twelve tributaries of the Arctic Ocean highlighted the ratio of 8:1 between the concentration of DOC and POC (Lobbes et al., 2000), as it finds support in the literature (Tranvik et al., 2009) where inputs into freshwater ecosystems of dissolved matter are reported as significantly exceeding particulate matter.

A wide range of organic compounds of different origins contribute to forming the classes of DOC and POC in rivers (Currie et al., 2002) and their composition is an essential factor in determining the chemical-physical properties of dissolved carbon. In depth knowledge the OC characteristics is fundamental since it influences numerous ecological functions of watercourses. OC is strictly related with the bioavailability of heavy metals, the control of the environmental pH, the absorption of incident light, with effects on the quality and intensity of solar radiation as well as on the thermal regime, and, connected to this phenomenon, the control of ecosystem metabolism (Battin et al., 2008; Stanley et al., 2012).

Prairie (2011) puts particular emphasis on DOC defining it as a "great modulator". In lake environments it constitutes the majority fraction of all available OC and is also the only one

directly assimilable through the cell membrane and usable for respiration by the microbial community (Battin et al., 2008). In this way DOC represents a factor of alteration of the energy balance of freshwater ecosystems.

In the general context of the carbon cycle, inland waters including lake basins, river systems and wetlands play an important role. Many greenhouse gases are produced and consumed by microorganisms that transform organic matter (OM) in aquatic ecosystems and these processes influence its atmospheric concentration with consequences on the climate (Tranvik et al., 2009).

1.3.1. Carbon cycles in natural lotic systems

One of the major difficulties encountered by various authors in dealing with the C cycle in lotic systems consists in analysing separately the processes that act on OC and the drivers that determine them, in fact in real situations they intertwine and condition each other. Three main pathways have been recognized in river systems which can be summarized as follows: production, transport, and sedimentation (Tranvik et al., 2009) (Fig. 2). The first is to be understood as the production of OC from inorganic C (CO_2, CH_4) within the river itself and, as such, autochthonous (arrow 6), or vice versa a process external to the freshwater system and therefore allochthonous (arrow 1). In the twelve Russian rivers sampled by Lobbes et al. (2000), the major contribution to fluvial OM comes from soils and vegetation of the hydrographic basin while only a small part originates in situ from autotrophic organisms.

To the production pathways of OC must be added the release of C by the stocks stored in the soil and in the benthos, arrows 5 and 9 respectively, and the contribution through biomass throughfall and leaching (arrow 2). The origin and size of Particulate OM (POM) modify the DOC formation rate: if initially it is mainly attributable to the leaching of the more soluble component of Coarse POM, subsequently when microbial degradation becomes the dominant process, the contribution of Fine POM grows to have a weight comparable to the fraction with the largest particle size (Yoshimura et al., 2010).

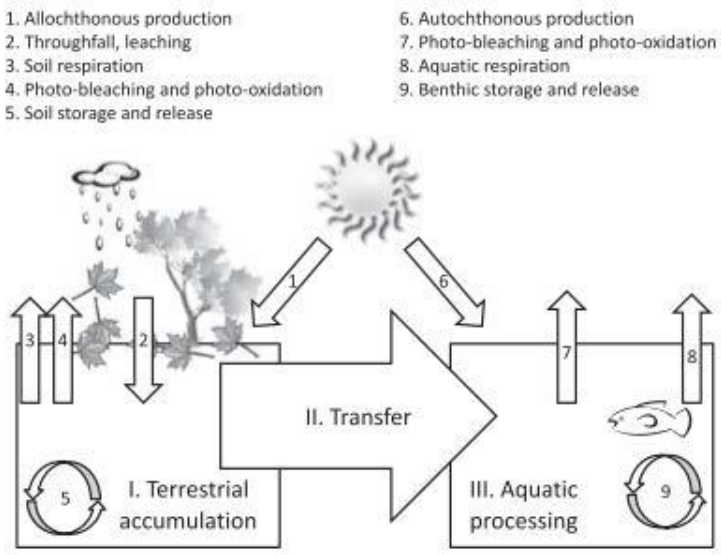

Figure.2 Carbon cycle (Stanley et al., 2012).

The accumulation in the soil and the sedimentation in the riverbeds and in the alluvial plains significantly affect the fluxes and the concentration of OM in aquatic environments. Currie et al. (2002) recognize the highly dynamic nature of the phenomena involving C, observing how, for example, the possibility for DOC to enrich the C reservoir in the soil depends simultaneously on many factors including its production and leaching, the refractoriness to mineralization and the ability of mineral horizons to hold it.

Transport, both within and towards water bodies, is generally mediated by water, however, differences can be noted depending on the diameter of the particles. In fact, dissolved OC, as the name suggests, moves together with the river current towards the mouth. On the contrary, POC undergoes the combined effect of gravitational and hydrodynamic forces, therefore it tends to move with "small discrete movements", it settles more easily and once deposited in the riverbed it can remain there for long periods until a peak in the flow does not puts it back into suspension (Battin et al., 2008).

Upward arrows (3, 4, 7 and 8) indicate respiration and photo-oxidation by which OM is removed from soil and river compartments to be released into the atmosphere in the form of greenhouse gases.

According to Miller and Moran (1997) bacterial metabolism, photodegradation and photosynthesis would control the quantity and speed with which OC is incorporated into the food web and, therefore, would constitute other important factors for the description of the C cycle in lotic systems. How these processes influence each other is still under discussion, whether or not photodegradation has a positive effect on the bioavailability of C for the biological community (Hansen et al., 2016; Stanley et al., 2012).

From several studies has emerged that rivers and streams are highly dynamic systems as

well as active reservoirs that host the processes in which OM is involved during its transport from sources to mouths (Casas-Ruiz et al., 2017; Cole et al., 2007; Soares et al., 2019) rather than passive channels of matter and energy.

The efficiency in retaining and oxidizing OC depends on the development of the microbial physiological activity in relation to the geochemical factors that determine the increase of the water residence time (Battin et al., 2008). This statement emphasizes the drivers controlling the processes that make up the C cycle. The most recurring ones are listed below.

Among the key factors are those that describe the hydrographic basin starting from its geomorphology, hydrology, and geographical position, also considering the possibility of establishing synergistic or, on the contrary, antagonistic effects between one and the other. The extension, the slope, the branching degree of the waterways with the territory (M. Li et al., 2017; Stanley et al., 2012) generally contribute positively to the increase of the OC loads in the riverbed.

The geology of the basin can directly influence the composition of DOM so that, in rivers draining chalky and permeable soils, it contains a lower volume of aromatic C and has a lower molecular weight than that recorded for streams that develop on organic soils such as peat bogs (Yates et al., 2016). The geological characteristics also have indirect consequences on the hydrology of the basin, being able to increase or decrease the connection of the main channel with the aquifer. The lowering of the groundwater level caused, for example, by rising temperatures could induce a greater release of DOC since the soil layer with favourable conditions to its oxidation would extend to greater depths (Worrall et al., 2004). Links between groundwater and drainage networks have proven equally important, as Shang et al. (2018). In fact, the researchers found a positive correlation between the DOC concentration and the proxies used to evaluate soil moisture and the hydrological conditions prior to sampling.

The greater the connectivity at the river-soil interface and the more abundant the precipitation, the greater the flow (M. Li et al., 2017) and therefore the quantity of biodegraded organic compounds in the riverbed. Furthermore, the results demonstrated that these drivers influence DOM even after the passage of the flood peak.

There is a second aspect to which geomorphology and hydrology contribute synergistically. Water Residence Time (WRT) which, by lengthening the retention times of OM, optimizes all the physical and biochemical processes of alteration (Catalán et al., 2016; Maavara et al., 2017). Soares et al. (2019) analysing DOM in the lower reaches of fifteen Swedish rivers concluded that the bioreactivity of dissolved C shows a positive correlation with WRT, in conjunction with other factors including land use. That this increased possibility of participating in chemical

processes then translates into an increase of DOC in solution or, vice versa, into a loss in the atmospheric compartment, according to Casas-Ruiz et al. (2017) depends on the properties of DOM and on the availability of nitrates which, by promoting photosynthesis, promote the autochthonous production of OM.

Land cover affects the quantity and quality of DOC inputs from watercourses and has therefore been frequently researched. A central node is constituted by agriculture since the type of plantations and their extension with respect to the total landscape can modify both the content and the lability of dissolved OC (Stanley et al., 2012).

Equally important is the forest cover that influences the chemical composition of POC and DOC (Lobbes et al., 2000). Furthermore, the crowns of the trees and the root systems, by protecting the soil from erosion, reduce the contribution of C particulate into the riverbed and, consequently, the concentration of DOC which derives from the latter.

In particular, the riparian strips play a key role. The impacts of their alteration could turn out to be disproportionate compared to the amplitude because they are involved in every aspect of the river DOC processes (Stanley et al., 2012). Just think of how photodegradation is encouraged or, conversely, hindered by the absence or presence of dense vegetation.

As can be understood, geographical position is also a fundamental driver on which climate change strongly affects. Taken individually, rainfall affects the hydrology of watercourses by inducing positive daily, monthly, and annual changes in the total OC load in the riverbed (Ouyang, 2003). However, as Ouyang's work highlights, rainfall is not sufficient to account for the OC oscillation which can be better explained by also considering temperature and its effects on biological activity (Shang et al., 2018; Worrall et al., 2004) and C mineralization.

Irradiance, understood as the flow of energy that reaches a unit of surface area in each time interval (W/m^2), affects the aquatic DOC directly and indirectly through numerous mechanisms (Stanley et al., 2012). Various metabolic processes depend on it (Battin et al., 2008), one above all photosynthesis and others including photodegradation, and the thermal regime of the river ecosystem. Some data to support the fact that the geography of a catchment area can affect the dynamics of OC were produced by Li et al. (2017) in a study on the spatial patterns of global river C fluxes. The researchers successfully demonstrated how the individual contribution of each of the three components examined, namely POC, DIC and DOC, varies significantly in relation to the latitude of the river considered, as well as other parameters.

The organic fraction is the majority for watercourses with very high annual flows such as the Amazon River, the Congo or the Yangtze while the inorganic C prevails in rivers that carry a smaller quantity of water. This observation is matched by the DOC flux per continent, which

is minimum in Europe and Oceania, respectively 19.72Tg C/y and 5.67Tg C/y, and maximum in Asia and South America, 87.13Tg C/year and 58.73Tg C/year. Focusing the attention on the latitude at which the mouth of the main rivers is located, it can be noted that between 30°N and 60°N the export of POC and DIC reaches its peak while that of DOC is second only to the range between Equator and 30°S.

For central-southern Europe, the Po Valley region crossed by the river Po is of particular interest since it represents the only one with a DOC yield higher than 3 ton/(km^2*year) and overlooks the Adriatic Sea, a narrow and shallow (Ciglenečki et al., 2020) in which dilution is less effective.

1.3.2. Drivers of carbon cycle alteration

The high complexity of OC dynamics in lotic systems is further increased when considering human impact. In the last period, anthropogenic alterations to global fluvial C fluxes are receiving increasing attention from the international scientific community (M. Li et al., 2017). The TRIPLEX-HYDRA model, simulating the export of fluvial DOC by the major rivers of the planet for the last 50 years, has highlighted a negative trend which is particularly evident in the basins located between 30 and 90°N (Li et al., 2019). While the data collected in almost 200 British sites for a period of time up to 1961 would suggest a positive correlation between the frequency of serious drought events and the concentration of DOC in the riverbed (Worrall et al., 2004), the effects of climate wetting on the arid regions of Scandinavia would indicate that a 10% increase in the average annual rainfall would produce a 30% increase in the mobilization of OC making browning phenomena more frequent in freshwater (De Wit et al., 2016). Catalan et al. (2016) estimated that, in a future scenario where temperatures are 2°C higher than current and where organic matter inputs are constant, changes in surface runoff would induce a 10% acceleration of the decay rate of OC in boreal and tundra biomes. Under the same conditions, however, a slowdown of 13% would be observed in regions with a Mediterranean climate.

Land use change affects natural freshwater ecosystems, nevertheless the extent of the effects on the environment depends on the time scale considered and on the specific characteristics of the basin (Shang et al., 2018). The intensity of anthropic alteration shows a positive correlation with the export of DOC of ancient origin: stored in the organic matter of the soil, in the aquifers or in the form of coal or oil, for a sample of 135 basins obtained from a worldwide database (Butman et al., 2014). The transformation from natural environments to agricultural or urban lands would induce a growth between 3.2-8.9% of the contribution of ancient DOC in the lotic systems of the planet. Outputs higher than expected were recorded in

basins characterized by high population density and highly drained organic soils, vice versa the presence of riparian forests led to lower export values. Restricting the focus to the composition only, in the sites where the human footprint was accentuated, reduction in molecular weight, increase in redox potential and decrease in the degree of aromaticity were observed: in general, an increase in DOC lability (Stanley et al., 2012).

At global scale, dams represent a net removal route for fluvial OC, since for the period 1970-2050 the sedimentation and mineralization of native and non-native organic matter will exceed the internal production of the basin (Maavara et al., 2017).

A further driver to be taken into consideration when analysing the land cover is the riparian vegetation. It is foreseeable that the modification and/or removal of this landscape class will have broad repercussions on the structure of the lotic habitat and, specifically, on the composition, quality, and temporal intervals of the DOC inputs (Stanley et al., 2012). Among the most widespread alterations is the presence on the riparian zones by invasive allochthonous species, such as *Robinia pseudoacacia* L. and *Ailanthus altissima* (Mill.) Swingle, which can induce changes in ecosystem processes and soil properties (Medina-Villar et al., 2015). In the specific case investigated by Medina-Villar et al. (2015), the presence of these two species recorded twice the concentration of nitrogen (N) in the litter compared to natural poplar groves (*Populus alba* L.).

The dissolved fraction of OC plays an important role in the biogeochemical cycle of carbon, and therefore in climate change, but this is not the only reason why it is the subject of an increasing number of studies. Since the early 2000s DOC removal had been identified as one of the major costs in wastewater treatment and as a potential threat to human health if present in drinking water (Worrall et al., 2004). Furthermore, high concentrations of fluvial OC are responsible for the browning that affects various water bodies in Europe (De Wit et al., 2016) and which translates not only into a poor aesthetic value of the basin in question but also into risks for the river ecosystem.

1.4. Water quality legislation

The European Directive on water quality, the Water Framework Directive 2000/60/EC (WFD), has the purpose of preventing further deterioration of aquatic and terrestrial ecosystems and wetlands, protecting, and improving their status. The WFD require the commitment of Member States to facilitate sustainable water use, protecting water resources with a long-term plan aimed at gradually reducing discharges and polluting emissions. Regarding surface waters, monitoring programs are required to obtain a coherent, global, and always updated view. Its implementation has led to rapid and positive results on the decline in fertilizer use in the first 10 years, with a reduction of up to 70% in the European monitored sites (EEA, 2019).

The directive introduces the concept of "surface water status" as the combination of the physicochemical, hydro-morphological, and ecological qualities of a water body. The "ecological status" is defined as a function of the quality and structure of the functioning of aquatic ecosystems. A general definition is first given for all surface waters, indicating 5 ecological states: high, good, moderate, poor, and bad.

The Legislative Decree which is still referred to in Italy is Legislative Decree no. 152 of 3 April 2006 (IR, 2006), and all the updates that followed, also called the "Testo Unico Ambientale", the third part of which concerns the "Rules on soil protection and the fight against desertification, protection of water from pollution and management of water resources". This Legislative Decree transposes the WFD 2000/60/EC and takes up the definition of the ecological status of a water body (with the related 5 classes) and introduces the principle of sustainable development.

Legislative Decree 152/06 has the following purposes:

- Prevent and reduce pollution and remediate polluted water bodies.
- To achieve the improvement of the water status.
- Pursue sustainable and long-lasting uses of water resources.
- Maintain the self-purification capacity of water bodies.
- Mitigate the effects of floods and droughts.
- Maintain the “Good” status of surface water bodies.
- Have all surface water bodies achieve a “Sufficient” rating by 31 December 2008, thus achieving a “Good” status by 22 December 2015.

The water bodies management is provided by the basin authorities that drafting plans and programs, while the Higher Institute for Environmental Protection and Research (ISPRA) merges and processes the data collected by the Regional Agencies for Environmental Protection (ARPA).

In Italy, only 43% of rivers reach the "good" quality objective for their ecological status; on the other hand, 75% of rivers have a good chemical status thanks to the pandemic stop (SNPA data, 2020). It is evident that there is still a lot of work to be done in order to comply with the provisions of the WFD which aimed to achieve good ecological and chemical status of all water bodies in Europe by 2015 now replace to 2030.

The United Nations (UN) Agenda 2030 for Sustainable Development is an action programme to achieve a better and more sustainable future for the environment and humanity. Signed on 25 September 2015 by the governments of the 193 Member Countries of the United Nations, and approved by the UN General Assembly (UN, 2015), the Agenda sets out **17 Sustainable Development Goals (SDGs)**, which are part of a broader programme of action consisting of 169 associated targets to be achieved in the environmental, economic, social and institutional domains by 2030. The UN indicated how the importance of good water quality is reflected in various SDGs, as they involve and concern biodiversity, human health, food availability and energy availability (Fig. 3).

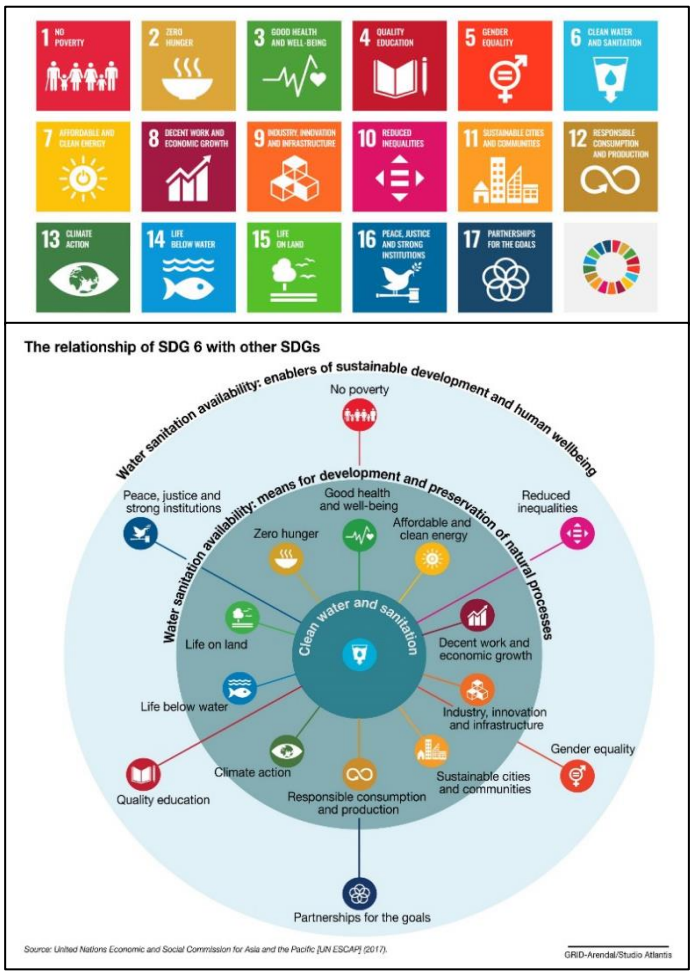

Figure.3 Link between water quality and the SDGs (UN, 2017).

Indicators, LIM and LIMeco

In Italy, firstly the Legislative Decree 152/99 established that a series of chemical-physical parameters should be evaluated to establish the quality of freshwater bodies.

Legislative Decree 152/06 in 2010 continued to make use of the Macro Descriptor Pollution Level index (LIM) that Legislative Decree 152/99 had introduced, classifying the waters based on specific macro-descriptors (Table 1).

Table 1 Macro descriptor parameters and pollution levels.

Parameter	Level 1	Level 2	Level 3	Level 4	Level 5
100-OD (% sat.) (*)	≤ 10 (#)	≤ 20	≤ 30	≤ 50	> 50
BOD_5 (O2 mg/L)	< 2.5	≤ 4	≤ 8	≤ 15	> 15
COD (O2 mg/L)	< 5	≤ 10	≤ 15	≤ 25	> 25
NH_4^+ (N mg/L)	< 0.03	≤ 0.10	≤ 0.50	≤ 1.50	> 1.50
NO_3^- (N mg/L)	< 0.3	≤ 1.5	≤ 5.0	≤ 10.0	> 10.0
T-P (P mg/L)	< 0.07	≤ 0.15	≤ 0.30	≤ 0.60	> 0.60
E. coli (UFC/100 mL)	< 100	≤ 1,000	≤ 5,000	≤ 20,000	> 20,000
Score to attribute on each parameter analysed (75° percentile)	**80**	**40**	**20**	**10**	**5**
Macro-descriptor pollution Level	**480 – 560**	**240 – 475**	**120 – 235**	**60 – 115**	**< 60**

With the Decree n. 260 of 8 November 2010, attachment 1 of Legislative Decree 152/06 is amended: the LIM index of Legislative Decree 152/99 is replaced by the index for the Pollution Level expressed by the Macro-descriptors for the ecological state (LIMeco), which is always a pollution index of the macro-descriptors, which however focuses on dissolved oxygen and nutrients (nitrates and phosphates), i.e. on the trophic state and no longer on microbiological pollution (Table 2).

The LIMeco index of a water body is obtained from the average score of each individual parameter.

Table 2 Pollution levels of river water expressed by Macro-descriptors Pollution Level for the Ecological status (LIMeco).

	LIMeco				
Parameter	Level 1	Level 2	Level 3	Level 4	Level 5
DO%	≤ |10|	≤ |20|	≤ |40|	≤ |80|	> |80|
NH_4^+-N [mg/L]	< 0.03	≤ 0.06	≤ 0.12	≤ 0.24	> 0.24
NO_3^--N [mg/L]	< 0.6	≤ 1.2	≤ 2.4	≤ 4.8	> 4.8
T-P [μg/L]	< 50	≤ 100	≤ 200	≤ 400	> 400
Score for single parameter	**1**	**0.5**	**0.25**	**0.125**	**0**
Total score	**≥ 0.66**	**≥ 0.50**	**≥ 0.33**	**≥ 0.17**	**≤ 0.17**
Score interpretation	**Excellent**	**Good**	**Sufficient**	**Scarce**	**Bad**

In water for drinking use are monitored additional substances and compounds such as antimony and nitrites (Annex 2 of Ministerial Decree 260/10). Other reference standards for the assessment of water resources are Legislative Decree 49/2010, which aims to reduce the destructive effects of floods through the assessment and management of the risks associated with these events, and Directive 91/676/EEC (Nitrates Directive) which aims to protect waters from pollution produced by nitrates of agricultural origin. In 2015, the last inland water monitoring cycle was completed, which follows the six-year timescales of the river basin district management plans, as defined by Legislative Decree 152/06 and related technical standards.

1.5. Ecosystem services

The most accepted definition of ecosystem services (ESs) was first officially proposed in the Millennium Ecosystem Assessment (2005) (MEA) and reads "Ecosystem services are the benefits people obtain from ecosystems. These include *provisioning services* (food, water, timber, and fibre), *regulating services* (climate, floods, disease, wastes, and water quality), *cultural services* (recreational, aesthetic, and spiritual benefits), and *supporting services* (soil formation, photosynthesis, and nutrient cycling)" (Fig. 4). ESs definition comes thanks the publications of Daily (1997) and Costanza et al. (1997), who were able to give voice to an idea that various authors had already tried to expose without however receiving real consensus.

Figure.4 Range of ecosystem services provided by nature to humans. Source: WWF, 2016 (adapted from Millennium Ecosystem Assessment, 2005)

The ecosystem approach aims to provide a holistic and transparent tool with which decision-makers, that is the figures responsible for the management of natural capital whether they are government bodies, NGOs or private individuals, can take the best way to the sustainable development. Interdisciplinarity is therefore an intrinsic feature of this approach which requires overcoming the traditional sectorial nature of science, drawing exponents of each discipline around a single table (Anzaldua et al., 2018). Transparency consists in the need to identify all stakeholders, to give them equal opportunities to express themselves and encourage constructive dialogue based on the scientific knowledge produced by research. To facilitate this process, which is far from simple, some methods of evaluating ecosystem services were developed that summarize their value in comparable units.

There are several reasons that make the ecosystem approach extremely promising, although

with limitations. A non-negligible part of the academic community is skeptical of the idea that ESSs can be the solution to the many environmental and social problems that afflict humanity. One of the most uncomfortable issues concerns the ethics of the concept (Jax et al., 2013; Schröter et al., 2014). In fact, the very definition of ecosystem services implies an anthropocentric vision of nature which becomes a tool through which man can obtain his own well-being. Many authors, including Vira and Adams (2009), say they are concerned that the unreasoned application of a concept of this type in national and international policies could legitimize the commodification of ecosystems or their destruction if their value is considered inferior to more "traditional" development projects. Certainly, the risk exists but, in favor of the ecosystem approach, it should be remembered that the category of cultural services allows the intrinsic value of a species or habitat to be considered. Furthermore, it could be argued that there are currently countless situations in which decisions relating to small and large development plans were taken without considering the possibility of protecting natural ecosystems at all. The introduction of studies on SSE allows to turn the spotlight on the environmental component, favoring the transparency of the objectives of the parties involved (Jax et al., 2013; Vira and Adams, 2009). Other criticisms concern the monetization of ecosystem services. Since this approach is proposed as a pragmatic tool to facilitate the approval of the most sustainable projects, the evaluation phase cannot be avoided. Nevertheless, based on the experience gained in more than twenty initiatives of The Natural Capital Project, Ruckelshaus et al. (2015) state that stakeholders often do not care about the dollar value of services. In some of these works, it was the stakeholders who asked for the ESs to be expressed in biophysical and not market units. It follows that economic evaluation can be used and certainly has some advantages, including the possibility of comparing extremely heterogeneous services with a shared unit of measurement.

Conservation biologists caution against assuming that actions to increase the quality or flux of ESs result in an improvement in the state of biodiversity. In this regard, Cardinale et al. (2012) reviewed the available literature for the last twenty years, taking into consideration about 1700 scientific articles from which it emerged that "there is sufficient evidence that biodiversity influences or is strongly correlated with some regulatory and commodity production services". In summary, therefore, the ecosystem approach has very valid advantages in practice that make it one of the best logical procedures, even if not perfect, available to the scientific community to give prominence to the environment in the decision-making phase. Historically, four main categories have been identified (MEA, 2005) to which seventeen specific services can be attributed (Costanza et al., 1997): supporting, provisioning, regulating and cultural (Fig. 4).

Depending on the authors and as the research progresses, the categories are updated by changing the number and type of services within them, aggregating some or separating others, or simply changing their denomination. In this thesis work I will refer to the classification used by the InVEST (Sharp et al., 2018). **Support services** are the essential prerequisite for all the others to exist nutrient cycling, primary production, and soil formation. The supply of goods instead consists in the production of matter and energy through ecosystems. Sometimes they also include genetic material intended as a resource that can generate biodiversity, while on other occasions it is included in the supporting category. ESs **provisioning** was among the first to be evaluated because, having reference markets, they could be expressed with relative ease in economic terms (Costanza et al., 1997). The group of **cultural** services ranges from recreational to spiritual and religious ones, from education to the sense of belonging of a community or an individual to a particular place.

Nutrients and carbon dynamics are among the **regulatory** services which allow the regulation of climate, water, pollination, extreme events, erosion, etc. One example among others is represented by storage and sequestration, understood as the variation of the C content over time (Sharp et al., 2018), i.e. the process by which ecosystems remove carbon dioxide from the environment by storing it in their own organic tissues. Given the evidence of ongoing climate change, the cause of which is mainly recognized in the excess of greenhouse gases in the atmosphere (Friedlingstein et al., 2020), the mitigation of CO_2 concentration by vegetation plays a decisive role (Gaglio et al., 2019). The availability of water resources is a problem felt in various parts of the world, including the North-East of Italy (Fabbri et al., 2016). One of the critical aspects concerns the quantity of this primary good but another no less important is its quality. In the UK the DOC concentration constitutes a of the largest expenditure items for water purification and its excess can cause damage to human health as well as the well-known browning phenomenon in Scandinavian countries (Škerlep et al., 2020; Worrall et al., 2004). The dark waters of the rivers, too rich in organic matter (OM), pour their content into the coastal strips laying the foundations for eutrophication problems, productivity imbalances (Cozzi et al., 2012) as well as damage to the tourism sector. The riparian strips contribute to limiting this chain of events by retaining part of the OM produced and diluting its release (Deforet et al., 2008), thus suggesting a positive trend both as regards the carbon storage service and water purification. Riverside forests, especially in the alluvial plain, are generally small environments and heavily altered by human action but at the same time they are home to fundamental processes that determine the supply of ESs.

1.6. Citizen science

In the last decade, the number and impact of Citizen Science (CS) projects indicates an increasing role of this approach in scientific research, providing a breeding ground for sharing data at local and global scales, and for policy and management (Geoghegan, H., Dyke, A., Pateman, R., West, S. & Everett, 2016). Citizen science provides an opportunity to gather information in large quantity and over large geographical areas that would be otherwise impossible to collect by professional scientists due to limitations on time and resources (Loiselle et al., 2017).

The term citizen science was coined by social scientist Alan Irwin (1995) to describe 'expertise that exists among those who are traditionally seen as ignorant lay people'. Scientists have since re-defined it as a research technique that enlists the help of members of the public to gather scientific data or simply as the involvement of volunteers in science (Bonney et al., 2009). Dickinson et al. (2012) use the term citizen science to refer to non-professional scientists that engage in research. In addition, there is increasing recognition that citizen science can and should involve the public in the development and design of projects addressing real-world problems (Wiggins and Crowston, 2011).

Citizen science connects people with the natural environment and issues surrounding its management. Involving non-experts in scientific research helps professional scientists in monitoring, collecting data and interpreting natural and human systems (Crain et al., 2014). Buytaert et al. (2014) argue that water science suffers from a lack of spatial and temporal data, despite its critical societal relevance and the complexity of its governance. Buytaert et al. (2014) call for reflection on the role that citizen science can play in generating new knowledge about the water cycle and ecosystem services, particularly in the decision-making process.

Volunteer involvement in scientific research is not new: before careers in scientific fields became widespread, numerous volunteers and amateurs conducted scientific research in across a wide range of disciplines (Haklay, 2013; McKinley et al., 2017), such as astronomy (Raddick et al., 2008), environmental monitoring (Pocock et al., 2017), natural history (Bonney et al., 2009; Miller-Rushing et al., 2012), archaeology (Smith, 2014) and more recently also in life sciences (Den Broeder et al., 2018). The most well-known and one of the first CS projects is the Christmas Bird Count, which started in 1900 as a volunteer-based inventory of winter bird populations (Link et al., 2006). In contrast, the renewed attention for CS in the past 20 years is fuelled by the knowledge-driven society (Lidskog, 2008) and by changing scientific grant regulations (Silvertown, 2009). Most of CS projects were born for local needs and practical issues (Dickinson et al., 2012). Common project topics incorporating CS are climate change,

invasive species, conservation biology, ecological restoration, water quality monitoring, population ecology (Silvertown, 2009).

The significant development of the internet and Geographic Information Systems (GIS) are playing a fundamental part to citizen science diffusion (Haklay, 2013). The existence of easily available low-cost information and communication tools create new possibilities for collecting large volumes of data, exchange, and analysis to other fields of environmental science (Thornhill et al., 2016). In recent years, the ubiquity of smartphones and other devices has resulted in their increasing use to record observations and send them to a central project database. Applications on smartphones that utilises camera and Global Positioning Systems (GPS) allow citizen scientists to send pictures and other data tagged with geospatial information. However, most of these projects use smartphones as record keeping or communication devices while only few CS projects turn smartphones into an actual measurement device (Newman et al., 2012). When such user-generated content has a geographic dimension, it is now commonly referred to as Volunteered Geographic Information (VGI), which has a great potential to engage citizens and to be a significant, timely, and cost-effective source for geographers' understanding of the earth (Goodchild, 2007).

However, CS has limitations. From the data-quality point of view (Cohn, 2008; Kremen et al., 2011), sampling bias and analytical challenges have been noted (Bird et al., 2014; Dickinson et al., 2012). In addition, the use of volunteer labour for the advancement of individual scientific gain has been questioned (Lehr and Fowler, 2006), as has the overreliance on CS observational and monitoring data in ecological settings (Kelling et al., 2009; Shirk et al., 2012). However, the contribution of CS data to scientific articles in peer-reviewed journals has increased substantially, indicating that citizen scientists are being recognised for and contributing to research (Catlin-Groves, 2012; Miller-Rushing et al., 2012).

To address the challenges facing CS and to maximise its potential a global network of coordinating organisations has been founded including: the American Citizen Science Association (CSA), European Citizen Science Association (ECSA) and Australian Citizen Science Association (ACSA), who seek to advance citizen science through the sharing of knowledge, collaboration, capacity building and support. Through a global database (e.g., SciStarter) they help bring together the millions of citizen scientist projects around the world and to sharing the resources, products, and services that enable citizens to pursue and enjoy these activities. The projects are offered by researchers, organizations, and companies (ECSA, 2022).

Citizen science projects may also be considered according to the number of participants

and public learning processes. Roy (2012) described citizen science environmental projects into four categories according to their degree of mass participation (local or mass) and *thoroughness* (a measure of investment of time and resources). Bonney (2009) considered project approach in terms of whether projects were led by experts and participants are only data collector (*contributory*), designed by scientists, but participants are involved in more than one stage of the scientific process (*community-led*), or designed collaboratively, where scientists and participants or communities work together in partnership (*co-created*). FWW has a collaborative approach, they provide platform, but user specifies parameters, protocol, sampling regime.

Wiggins and Crownston (2011) classify projects into five categories. In *action* projects, citizens collaborate with scientists to address local issues and concerns. *Conservation* projects focus on protecting and managing natural resources. *Investigation* projects focus on answering scientific questions. In *virtual* projects, activities are carried out remotely. *Education* projects aim at improving citizens' knowledge.

Haklay's (2013) scheme classifies citizen science projects based on the depth of their engagement with volunteers, within a four-level framework of participation. The least participatory projects are termed *crowdsourcing* and use volunteers simply to collect data from distributed sensors, or to provide computing power. Level 2 *distributed intelligence* are projects which may provide participants with some basic skills before asking them to collect and potentially interpret data. At Level 3 *participatory science*, participants are more involved in steering the direction of the research. The most participatory are referred to as *extreme citizen science*, where citizens are involved at all stages in the development of the project and work to achieve their own goals. This classification scheme is not intended to encourage judgments about how good specific projects are, based on their level of engagement, but Haklay (2013) suggests that participants will benefit most from projects that operate at the highest levels of engagement as appropriate to their aims.

In summary, Citizen Science has the potential to be a valid and robust approach that can improve conservation outcomes by building scientific knowledge informing policy formulation, and inspiring public action (McKinley et al., 2017).

1.6.1. FreshWater Watch

The CS project "FreshWater Watch" (FWW) started in 2012 under the direction of the Earthwatch Europe foundation and currently has more than eighty active groups all over the world, although it is most successful in Europe (Earthwatch Europe, 2021a).

The reasons that led to the birth of FWW revolve around the issues of scarcity and pollution of water resources, problems to which the European continent is no stranger (Anzaldua et al., 2018). Only 40% of European water basins are classified in "good ecological status" despite the importance of fresh water for drinking, domestic, irrigation, industrial use, energy production, etc., as well as representing a fundamental ecosystem for the maintenance of biological diversity (EEA, 2021).

The main objectives of FWW consist in: i) increasing the sense of connection between citizens and the aquatic environment as well as awareness of the critical issues that characterize it; ii) provide volunteers with skills and means to monitor water quality iii) thus develop a prevention tool that can inform the authorities on situations of greatest risk and iv) improve data collection by local communities by facilitating the drafting of reports related to the Sustainable Development Goals (SDGs) (Earthwatch Europe, 2021b). On this front Bishop et al. (2020) have highlighted the potential of CS, specifically the FWW project, which has proved to be a reliable tool for the development of necessary for the description of SDG 6.3.2, "monitors the proportion of bodies of water with good ambient water quality". The advantages have been registered both in countries with not particularly advanced monitoring programs such as Kenya, and where the control bodies have a large and efficient action such as in the United Kingdom.

The possibility of using FWW in such an ambitious way certainly depends on the amount of data collected according to a standardized methodology.

Parameters such as nitrate (NO_3^--N) and phosphate (PO_4^{3-}-P) concentrations, turbidity, and qualitative characteristics such as land use, presence/absence of animal and plant species, etc. were recorded in over 31,000 samplings carried out on more than 2,000 water bodies in about twenty countries (Earthwatch Europe, 2021b). The elaboration made it possible to find 30% of basins with pollution from nitrates and a further 25% from phosphates. In Italy, more than 10% of the monitored environments have high concentrations of NO_3^--N, a percentage which rises to almost 20% if PO_4^{3-}-P are considered (Fig. 5).

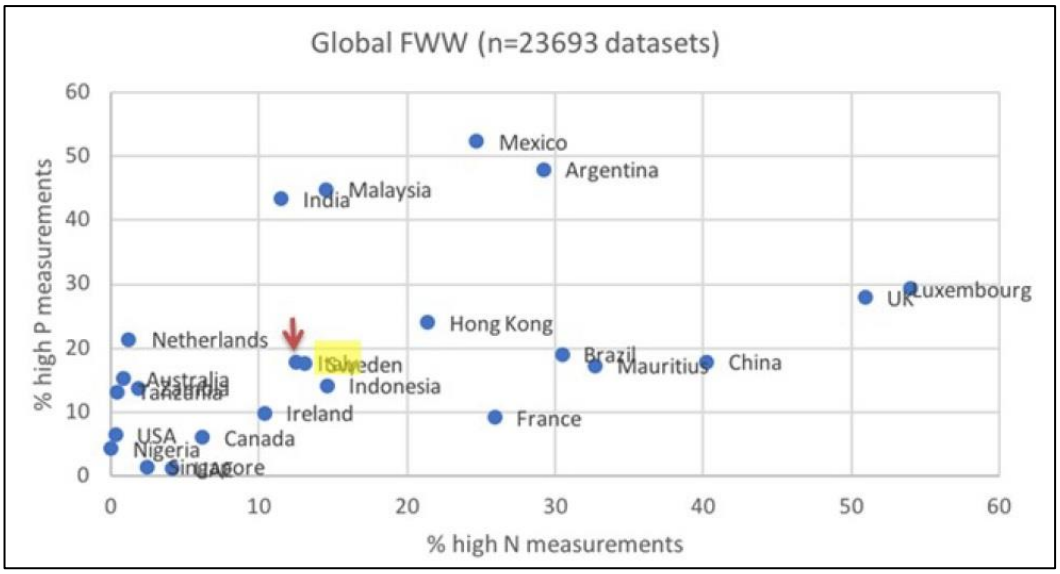

Figure.5 N and P pollution in water bodies monitored by FWW methodology. Red arrow highlight Italy position (Earthwatch Europe, 2021b).

1.6.2. Riparian Vegetation

The riparian buffer strips constitute "the interface between the aquatic and terrestrial environments" (Richardson et al., 2007), the transitional ecotone between the river and the surrounding landscape. This location makes them particularly sensitive to fluvial dynamics, changes in hydrological regimes, altitudinal variations from source to mouth, as well as terrestrial inputs (Naiman and Décamps, 2003). This strip of territory is usually characterized by unique biological communities and specific physicochemical processes and, although capable of producing important ecosystem services, they are strongly threatened by human interventions, especially in the alluvial plains where agriculture and urbanization create the greatest impacts. In these systems, flood events alternating with more or less lasting periods of drought, erosion and sedimentation phenomena, mechanical abrasion, etc. they reappear with generally annual but variable frequency according to the climatic region (Naiman and Décamps, 2003). Therefore, the vegetation that develops in these conditions is mainly composed of specialized taxa, resistant to sudden changes and long periods of soil saturation, also thanks to ad hoc physiological adaptations (Naiman and Décamps, 2003; Richardson et al., 2007).

At temperate latitudes, the most common genera in hygrophilous woods include *Salix, Populus, Alnus* which follow more mesophiles varieties including *Fraxinus, Acer, Ulmus*, *Quercus* and *Carpinus* (NNB, 2021). To these are added other allochthonous and often invasive species whose settlement is facilitated by the high level of disturbance to which the riparian strips are subject. The phenomenon, constantly increasing, is documented all over the planet. Colonization by alien *taxa* is particularly problematic in this type of environment since, based

on the ecological characteristics of the alien species, there can be profound alterations in the functions of the peri-fluvial ecosystem (Medina-Villar et al., 2015; Richardson et al., 2007).

The riparian wood formations represent an important ecological corridor as well as being themselves a peculiar habitat for ecotonal populations; from a physical point of view, their structure retains sediment and woody material reducing the erosion of the channel up to thirty times, at the same time they dissipate the kinetic energy of the current, slowing down its flow and increasing the Water Residence Time (Dosskey et al., 2010; Tabacchi et al., 2000). Therefore, the riparian vegetation contributes to determining the morphology of the river, increasing its heterogeneity, and opening ecological niches necessary for the maintenance of biodiversity. Some relevant biochemical processes also occur in this environment including denitrification, complex phosphorus cycles and DOM production (Naiman and Décamps, 2003). A study conducted by Deforet et al. (2008) demonstrated, for example, the positive correlation between the retention of DOC in the riverbed and the presence of vegetation in the river bars, also underlining the seasonal nature of the phenomenon which is more pronounced in autumn than in summer.

1.7. Research objectives

Sustainable river management should consider potential impacts on ecosystem services in decision-making with respect to mitigating future climate impacts.

The overall objective of the thesis is the development of new approaches for the analysis of long-term changes in riverine carbon, hydrological and nutrient cycles important to identify potential alteration on the biogeochemical cycles and potential impacts on the ecosystem services provided to the local population. To achieve the main objective will be explored a series of scenario of climate and river basin management on the spatial variations of carbon storage and sequestration, macronutrients (N & P) and sediment delivery and water yield combining citizen science and modelling to support decision making for one of Italy's most important rivers. Furthermore, a comparation between different NBS will be performed in relation to their ESs costs and benefits related to nutrient retention under a future climate change scenario (2050). The participation of the local population as citizen scientists, coordinated by experts and using standardised methods will be allowed for both increased engagement with the project as well as a new and fundamental data gathering for the ecosystem service models.

Dissolved organic carbon (DOC) and particulate organic carbon (POC) dynamics play a fundamental role in biogeochemical cycles of freshwater ecosystems. However, the lack of process-based and basin-scale models for carbon transport has limited effective basin management of organic carbon fluxes from soils, through river networks and to receiving marine waters. The development of a new mass balance spatially distributed modelling approach that can estimate organic carbon delivery at basin and sub-basin scales in order to understand and correctly reproduces spatial and temporal changes in DOC and POC fluxes in relation to changes in precipitation, basin morphology and land use, as well as soil carbon content across different sub-basins.

To complete the overall models evaluation and prioritization will be developed a new method to attributing a weight to the best NBS scenarios based on the natural stoichiometric ratio between the elements carbon, silicon, nitrogen, phosphorus (C:Si:N:P).

2. STUDY AREA AND DEVELOPMENT OF SCENARIO ANALYSIS

The development of modelling and analysis tools for the biogeochemical dynamics was focused on the Piave River, and in particular to lower basin, in relation to different land use scenarios and considering possible impacts respect to the climate change predicted by the IPCC for 2050.

The biogeochemical based instruments were developed to allow for a more integrated determination of the river status and its variation over time and space. I explored key catchment biogeochemical dynamics, nutrient loads, and carbon cycles, taking into consideration the related EU directives related to water quality and ecosystem services (WFD 2000/60/EC).

Some of the data was obtained through local, regional, and national sources. Data was obtained through collaborations with ARPAV, UNIPD, Consorzio BIM, Consorzio di Bonifica Veneto Orientale, Autorità di Bacino Distrettuale delle Alpi Orientali and VERITAS spa. Important information has also been obtained from international sources including ESDAC, ESA, NASA, NOAA and the USGS. These data relate to the hydrological variations of the basin and water supply, climatic variations, the ecological and chemical state of the river, the cover and use of the land, riparian vegetation and spatial dynamics of the last 20 years.

My first objective was to determinate the current state of the river, the transformation and storage of nutrients (nitrogen and phosphorus), transformation and storage of carbon, transformation and storage of sediments and annual water availability.

2.1.Study area

The Piave river, located in the north-east of Italy, flows for 220 km into the Adriatic Sea with a drainage basin of 4,500 km^2. Approximately 300,000 people live within the basin boundaries that falls across multiple regions (Veneto, Friuli-Venezia Giulia and Trentino-Alto Adige). The climate is temperate-humid with an average annual precipitation of ~1300 mm but with significant spatial variations from the alpine to valley sub-basins. Land use (Fig. 6) has a clear elevation-based pattern with the upper basin (from 500 to 1800 m a.s.l.) characterised by evergreen and deciduous forests (mainly conifers and broad-leaved trees), with alpine pasture/prairies and rock emergence present at higher elevations (above 1800 m a.s.l.). Agriculture dominates the lower part of the basin (below 500 m a.s.l.), with increased impervious surface cover. Like most alpine rivers in Italy (Surian et al., 2009), the Piave River has been heavy impacted, with modified river channel dynamics and a rapid land use change in the 20^{th} century (Botter et al., 2010). Traditional agricultural activities on mountain slopes are increasingly being abandoned largely because of the development of industry and tourism,

resulting in natural reforestation in the upper parts of the basin (Del Favero and Lasen, 1993), while wine production and agriculture have expanded at lower elevations. Weirs, dams and in-channel gravel mining have contributed to reduced sediment fluxes (Comiti et al., 2011).

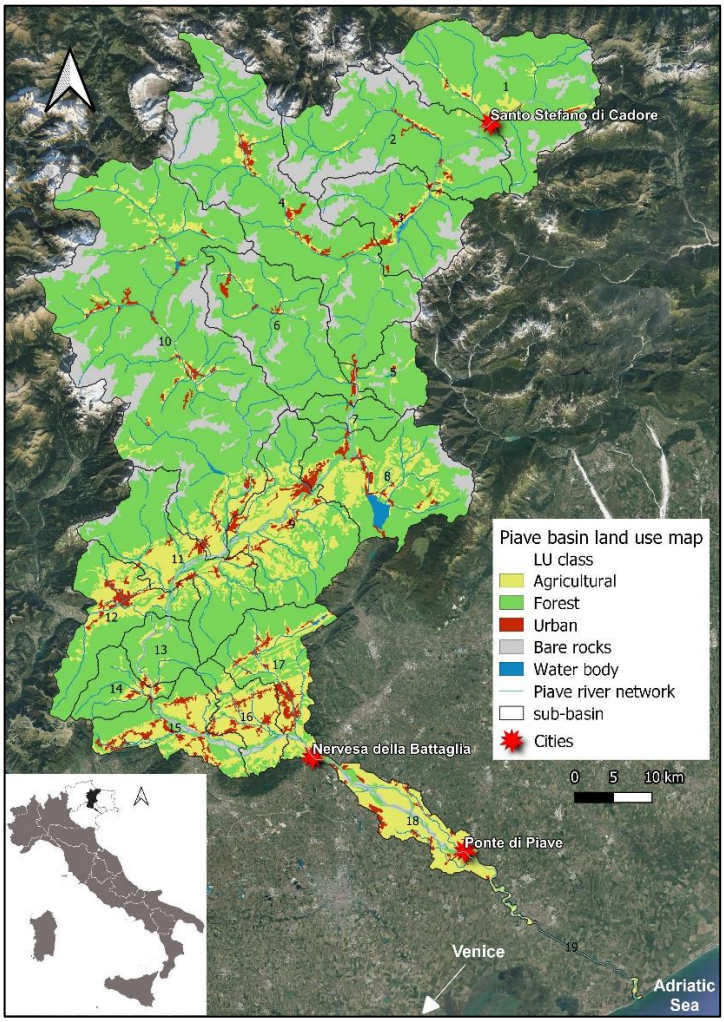

Figure 6 The Piave river basin land use map 2018.

2.2. Development of Nature-Based Solutions scenarios

Different Nature-Based Solutions (NBS) scenarios were tested starting from the 2018 conditions. The baseline scenario (2018) was identified using Corine Land Cover - CLC - (ISPRA, 2018) data and classification, with a spatial resolution of 100 m (Fig. 6). Land use/land cover change (LULC) has a significant impact on the supply and value of multiple ecosystem services, especially climate regulating services, due to the fundamental changes that occur over time in structure and function of forests, agriculture, and other uses (Fu et al., 2017).

The development of future NBS scenarios was based on consultations with local stakeholders. Temporal trends were explored using photometric and satellite-based images. This analysis showed a consistent and continuous increase in riparian vegetation within the Piave river corridor (Picco et al., 2017) over the last five decades and a more recent trend of

agricultural abandonment in the upper basin. This rural exodus, which began after the Second World War, triggered the natural regrowth process of vegetation (Rocchini et al., 2006).

All scenarios were developed as land use modifications following simultaneously the trends of the last decades and the results of recent studies, using QGIS software version 3.18 and update version 3.22 (QGIS Development Team, 2022). The changes are located both in the Basso Piave basin (A1, A2), and in the Upper and Middle Piave basin (B1, C1), and compared with the current conditions (A0, B0, C0). Twenty-four combinations of land use scenarios were explored for each model, 12 scenarios for 2018 and 12 for 2050.

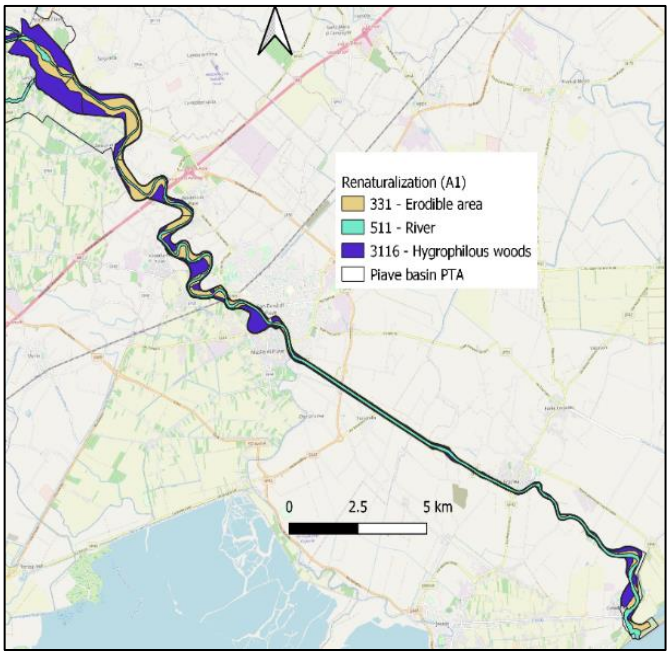

Figure 7 River restoration scenario (A2) in the Lower Piave basin

The **first scenario "A1"** (Fig. 7) was based on two simultaneous changes in the Lower Piave basin between Ponte di Piave and its mouth, the transformation of:

- 645 ha in hygrophilous wood (class 3116) and
- 415 ha in erodible strip (class 331) along the river corridor of the lower basin.

The erodible areas were identified thanks to the study conducted in 2018 by the University of Padua coordinated by Professor Nicola Surian on behalf of ARPAV[1]. Some of these erodible areas close to the riverbanks, for this reason a 20-metre buffer of riparian forest was explored, locates on the edge of the external banks, along the entire length of the lower reaches of the Piave river, to protect the banks themselves.

A1 represents a river restoration scenario to restore the hydro-geomorphological processes which support the entire biological component. This scenario was developed also considering the new Common Agricultural Policy (CAP) 2023-2027 (European Commission, 2022) which provides for funding for the establishment of ecological corridors and the active management of green infrastructures (hedges, buffer strips, groves) whose phytoremediation function of nutrients, pesticides, suspended solids is particularly important. These interventions would

[1]Project: "Application of the MQI (Morphological Quality Index) to selected streams of the Veneto Region, identified as possible highly modified water bodies" – funded by the Regional Environmental Agency (ARPAV), 2017-2018.

improve the chemical and ecological status of water resources as well as an improvement in the quality and ecological connectivity in agriculture and forestry, the protection of biodiversity, the preservation of habitats and landscapes.

The second scenario "A2" (Fig. 8) was focused on a river restoration approach of the river embankment, by replacing the current allochthonous and often invasive corps and forest vegetation with 1,060 ha of hygrophilous forest (class 3116) along the entire river corridor of the lower basin, from Ponte di Piave to the river mouth. The benefits expected from this scenario are linked to the increase in nutrient buffer functions and sediment removal by the riparian vegetation as well an improvement of habitat quality. I also considered the objectives and functions of the new CAP 2023-2027 on the establishment of ecological corridors and green infrastructures and of the sustainable development Agenda 2030. Furthermore, European directives such as the water framework directive (2000/60/EC) and the habitat directive (92/43/EEC), require for Member States to improve the quality of their natural habitats and to build a greater connection between natural areas.

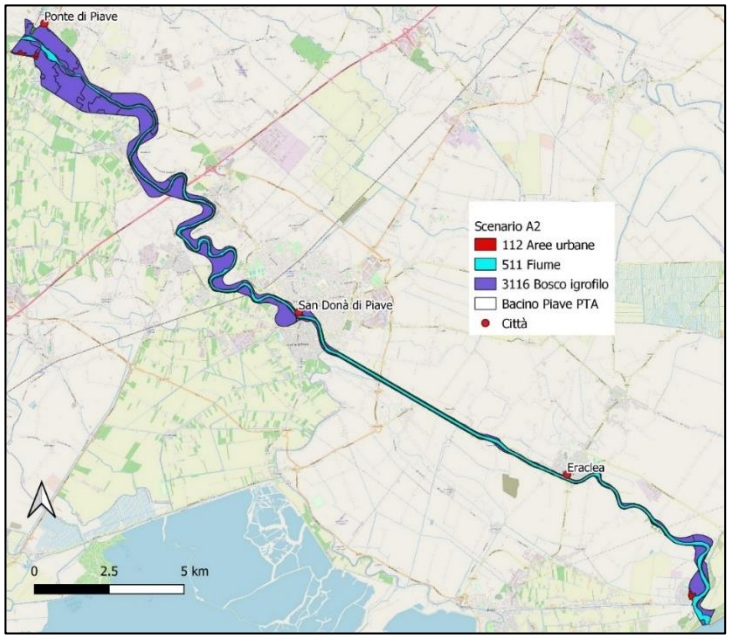

Figure 8 Reforestation scenario (A1) in the Lower Piave basin.

The third scenario "B1" (Fig. 9) was based on the reforestation of agricultural areas with large natural spaces (class 243) of the upper basin in:

- 11,549 ha of mixed woodland (class 313) and
- 3,025 ha of hygrophilous woods (class 3116).

Reforestation has multiple benefits, promoting biodiversity (Wade et al., 2006), reducing surface water runoff and soil erosion (Tasser et al., 2003), controlling sediment loss, and improving soil properties (Seeber and Seeber, 2005). Forests constitute the most important carbon pool within terrestrial ecosystems, playing a substantial role in the process of mitigating climate change. They also must adapt to these changes to be able to provide efficient ecosystem services for human well-being. Afforestation and reforestation are potentially impactful mitigation strategies, as wood production and carbon (C) storage can be combined. Attention

to forests and the biological diversity associated with these ecosystems has risen on the agenda of European policy makers who have adopted the European Green Deal (European Commission, 2020a), the plan on climate targets for 2030, the EU biodiversity strategy for 2030 (European Commission, 2021) and the objectives of carbon neutrality by 2050. The new CAP 2023-2027 provides for the financing of interventions for afforestation of agricultural and non-agricultural land, improving rural landscapes and the forest-wood supply chain, favouring the diversification of farm income. Both permanent and temporary afforestation (short and medium-long cycle) are also favoured with the objectives of improving ecological connectivity in agriculture and forestry and mitigating climate change by subtracting greenhouse gases from the atmosphere, as well as for development of sustainable energy.

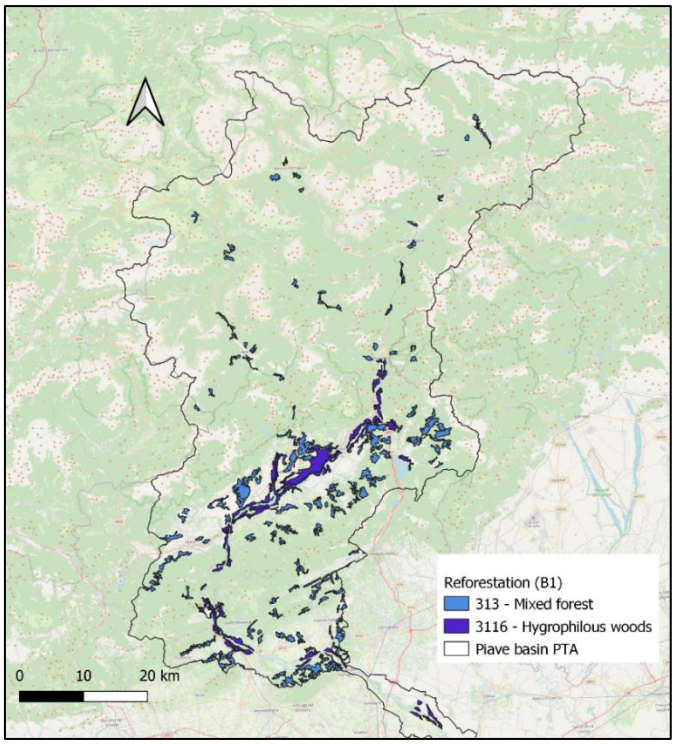

Figure 9 Reforestation scenario (B1) in the upper basin

The fourth scenario "C1" was created to consider the possible impacts of a structure to defend against the flood risk. A flood retention area was selected, based on preliminary information presented in the Environmental Pre-Feasibility Report dated March 2017 by the Veneto Region for the hydraulic safety of the middle and lower basin of the Piave river. The replacement of the land use classes after the acquisition of the flood retention area was envisaged by the project and corresponding at 6 km^2 approximately (Fig. 10). It was possible to convert all the land use contained within the flood retention area into the dominant land use in the baseline scenario (2018), that is meadows and natural pastures (class 321) figure 7a and

7b.

The downscaling of the river was performed to better highlight the areas that most contribute to the export of nitrogen, phosphorus, sediment, and water availability near the river.

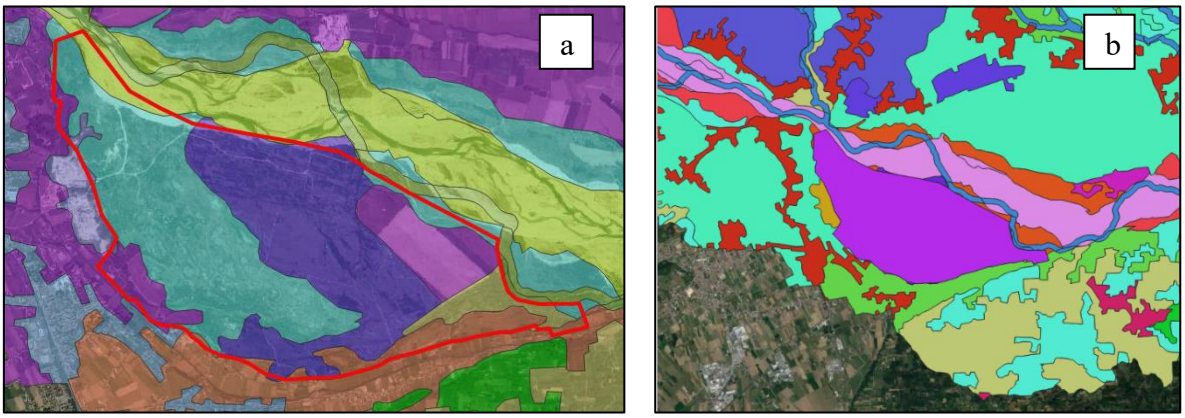

Figure 10 Flood retention basin scenario (C1) map

The biogeochemical models and analysis approaches were used to test the impacts of all twenty-four scenario combinations and compared with the current conditions (A0, B0, C0) determined for the year 2018 (Table 3). The models and the results obtained from the scenarios are discussed individually in the next chapters.

Table 3 Scheme of all scenarios and possible combinations

Year	*Flood Retention Basin*	*Lower Piave section*			*Reforestation*
		A0	*A1*	*A2*	
2018 (CLC & Climatic variation)	*C0 (no)*	C0, A0, B0	C0, A1, B0	C0, A2, B0	*B0 (no)*
	C1 (yes)	C1, A0, B0	C1, A1, B0	C0, A2, B0	
	C0 (no)	C0, A0, B1	C0, A1, B1	C0, A2, B1	*B1 (yes)*
	C1 (yes)	C1, A0, B1	C1, A1, B1	C0, A2, B1	
2050 (CLC & Climatic variation)	*C0 (no)*	C0, A0, B0	C0, A1, B0	C0, A2, B0	*B0 (no)*
	C1 (yes)	C1, A0, B0	C1, A1, B0	C0, A2, B0	
	C0 (no)	C0, A0, B1	C0, A1, B1	C0, A2, B1	*B1 (yes)*
	C1 (yes)	C1, A0, B1	C1, A1, B1	C0, A2, B1	
		COMBINATION = 24			

2.3. Climate change scenario

2.3.1. Introduction

Climate scenarios are representations of future climate that has been constructed for explicit use in investigating the potential impacts of anthropogenic climate change.

The latest special report of the Intergovernmental Panel on Climate Change (IPCC) on climate change and soil underlines that the increase in the global average surface temperature, compared to pre-industrial levels, can substantially influence the processes involved in desertification (water scarcity), land degradation (soil erosion, vegetation loss, forest fires, permafrost thaw) and food security (crop yield and food supply instability) (IPCC, 2019a).

Climate change will have important consequences for ecosystems and humans (Creutzburg et al., 2016; Dai et al., 2016). The Atmosphere-Ocean General Circulation Models (AOGCMs) of the Intergovernmental Panel on Climate Change in the fifth report (IPCC AR5) (Flato et al., 2013) estimate the potential climate changes during the 21st century under different scenarios of greenhouse gas radiative forcing, called representative concentration paths - RCP (Fig. 11) (Moss et al., 2008). Thus, the emission scenarios are plausible representations of the future development of greenhouse gas and aerosol concentrations.

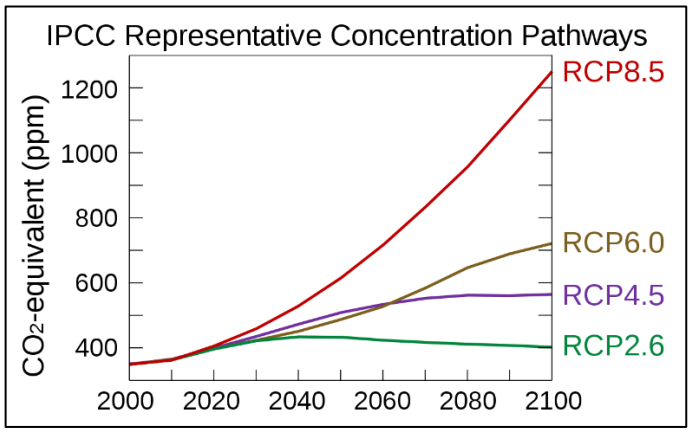

Figure 11 Representative concentration paths (RCPs) and their predictive effects.

The RCP2.6 emission scenario assumes that the international community agrees on the drastic reduction of greenhouse gases. This scenario assumes an additional radiative forcing of 2.6 W/m^2 by the end of the 21st century. The RCP8.5 scenario assumes that humanity continues as before by emitting more and more greenhouse gases. This corresponds to a radiative forcing of 8.5 W/m^2 at the end of the century.

The intermediate scenario RCP4.5 assumes that the emission of greenhouse gases is contained, even if their concentrations in the atmosphere increase further in the next 50 years, the target of +2°C will not be achieved. Compared to 1850, in 2100 the radiative forcing will

amount to 4.5 W/m^2 (about 650 ppm CO_2-equivalent) (Thomson et al., 2011).

Some studies have shown the first adaptations related to increased growth rates of temperate forest in response to climate change to respond to changes in CO_2, temperature and rainfall starting from the mid-20th century (Bascietto et al., 2011; Sass-Klaassen et al., 2016). Conversely, other reports point to varying trends during different periods or overall declines in forest productivity, mainly related to water stress and increases in insects, diseases, and forest fires due to rising temperatures (Creutzburg et al., 2016).

Climate change is predicted to increase rainfall intensity (Kunkel et al., 2013), and result in increased surface water runoff that will cause reduced infiltration into agricultural land (Basche and DeLonge, 2017). with even greater soil losses than in the early 21st century (Borrelli et al., 2017).

In the biogeochemical models, I have used the median climate scenario RCP4.5 which globally predicts +1.4°C (±0.5) by 2050, to assess the impacts of climate change on carbon stocks, nitrogen and phosphorus dynamics, soil loss and future water availability.

The climate scenario is applied to ecosystem services models (Fig. 12) in combination with the different land use scenarios to illustrate the influence of policy decisions on the future of climate and land.

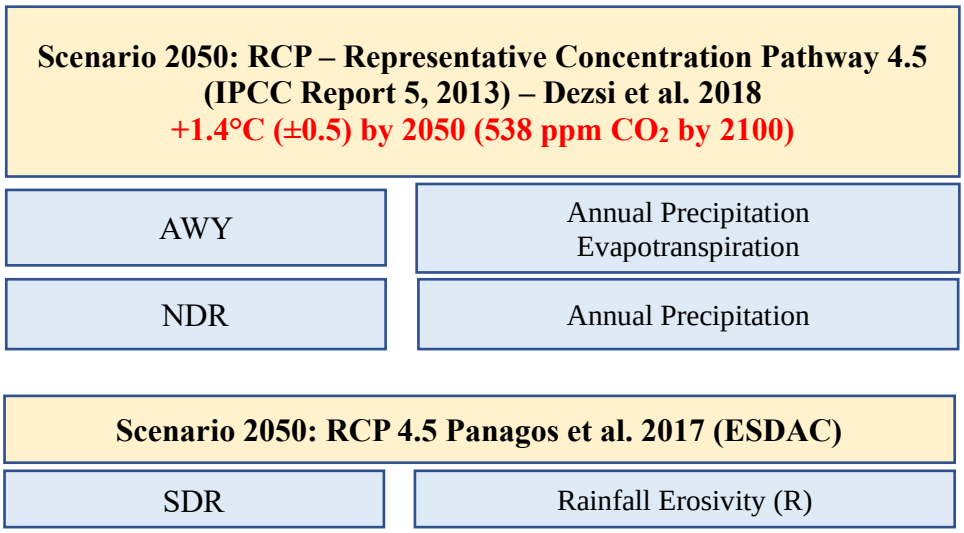

Figure 12 Climate scenario applied to ecosystem services models

2.3.2. Material and methods

The potential influence of climate change on nitrogen, phosphorus and carbon dynamics was explored using data from historical time series and global climate models. The climatic components most directly impacting ecosystem services related to the water, carbon, nitrogen

and phosphorus loads, retention and export are the average monthly precipitation, the number of days with precipitation, average monthly temperature and average monthly maximum temperature.

The climate of the study area has a temperate humid regime with months of maximum precipitation in autumn and late spring (May), with minimum precipitation generally recorded in February and July. The average annual rainfall is highly variable. An analysis of local trends in precipitation and temperature was performed using:

- ARPAV data of Ponte di Piave station (1995–2018) and Valdobbiadene (2010, 2020) stations lower basin; Feltre and Belluno stations (2010, 2020) middle basin; Longarone, Cortina d'Ampezzo (2010, 2020) and Santo Stefano di Cadore stations (1998–2018) upper basin (ARPAV, 2021a);
- NOAA data (National Oceanographic and Atmospheric Centre, Silver Spring, Maryland, USA) from NCEP reanalysis (1948–2018) (NOAA, 2018);
- Global climate projections (2041–2070) (Dezsi et al., 2018).

The climatic components most directly impacting water, carbon and nutrient cycles are the average monthly precipitation, the number of days with precipitation, average monthly temperature, and average monthly maximum temperature. The data were subjected to decomposition methods to explore seasonal, inter-annual trends and teleconnections with global climate indices. The North Atlantic Oscillation (NAO) is an important teleconnection scheme influencing European climates. It is based on a dipolar model of mean sea level pressure over the North Atlantic extending from subtropical to sub-arctic latitudes. It is associated with variations in westerly winds relative to Western Europe, an important factor for winter weather in Europe (Daly et al., 2008; Hurrell et al., 2003).

Further a multiple regression analysis is typically undertaken to identify the independent variables that explain if the chemical parameters (ARPAV, 2021b) are influenced by temperature and precipitation or both.

Future projections were developed with the delta method based on multi-model CMIP5 projections for the 2011–2040 and 2041–2070 periods (referred to as the 2020s and 2050s). The baseline reference data for monthly precipitation were constructed with parameter regression of independent slopes model (PRISM) by Daly et al. (2008). I selected a median emission scenario, represented by (RCP) 4.5 that globally predicts a +1.4°C (±0.5) by 2050.

2.3.3. Results and Discussions

2.3.3.1. Climate change

In 2018, the highest annual precipitation (mm) occurred in the upper catchment with a mean of 1,599 mm/year, while the precipitation mean in the lower catchment was 1,070 mm/year. The wettest month was October (396 mm), the month with the least rain was December (10 mm) (Fig. 13).

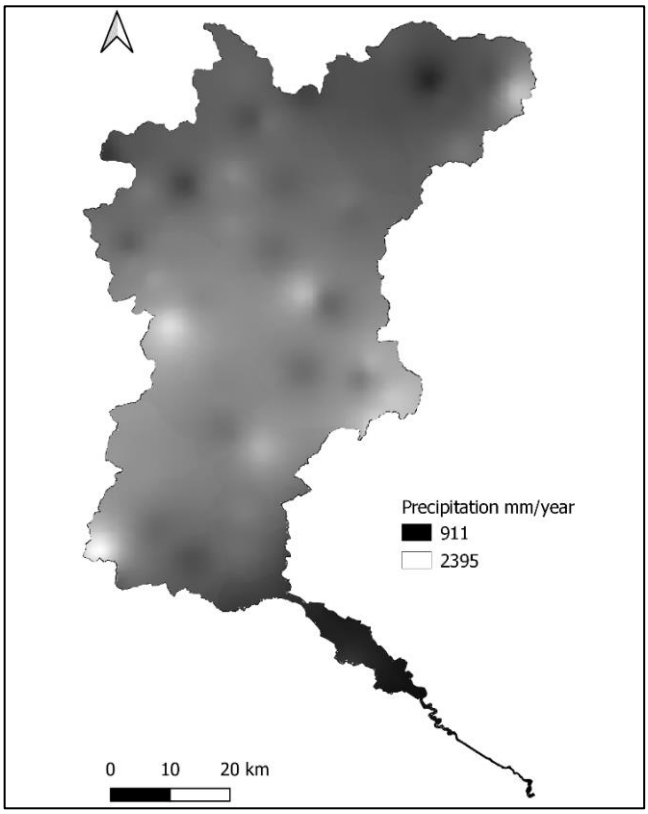

Figure.13 The distribution of precipitation in the Piave River catchment in 2018.

Teleconnections with major climate indices indicated potential links of the catchment climate to conditions in the rest of Europe. The NAO index shows an increased variability since 1950 (Fig. 14), associated with the changes in circulation due to differences in pressure at sea level. There were several long periods in which the anomalous circulation of the NAO persisted, particularly from the 1940s to the 1970s, with a downward trend and lower than normal winter temperatures. After a period of relatively negative NAO values, the last 7 years (2012–2018) have seen a significant increase, associated with warmer-than-usual winter temperatures and changes in the precipitation regimes in much of Europe.

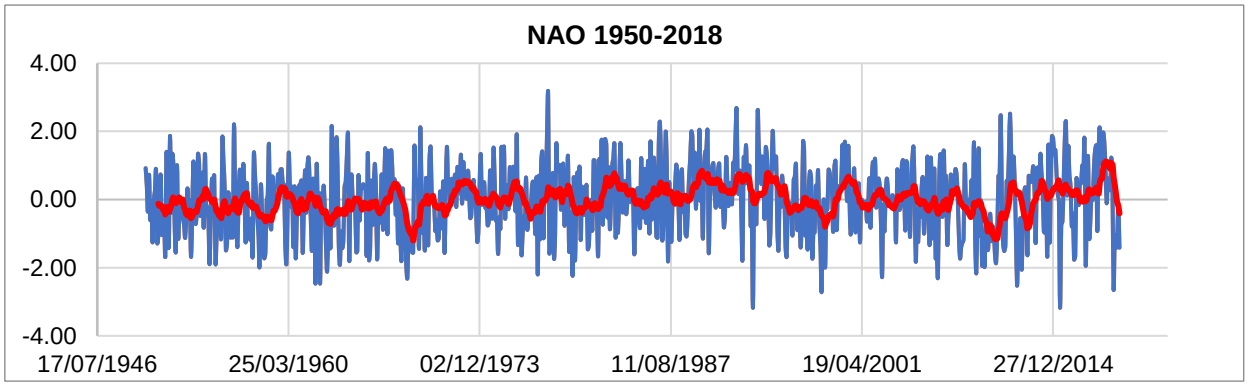

Figure.14 Variability of the NAO indices from 1950 to 2018.

The monthly dynamics of precipitation showed a much lower seasonality with respect to temperature, with the former showing a strong autocorrelation from 1995 to 2018 (Fig. 15 and Fig. 16).

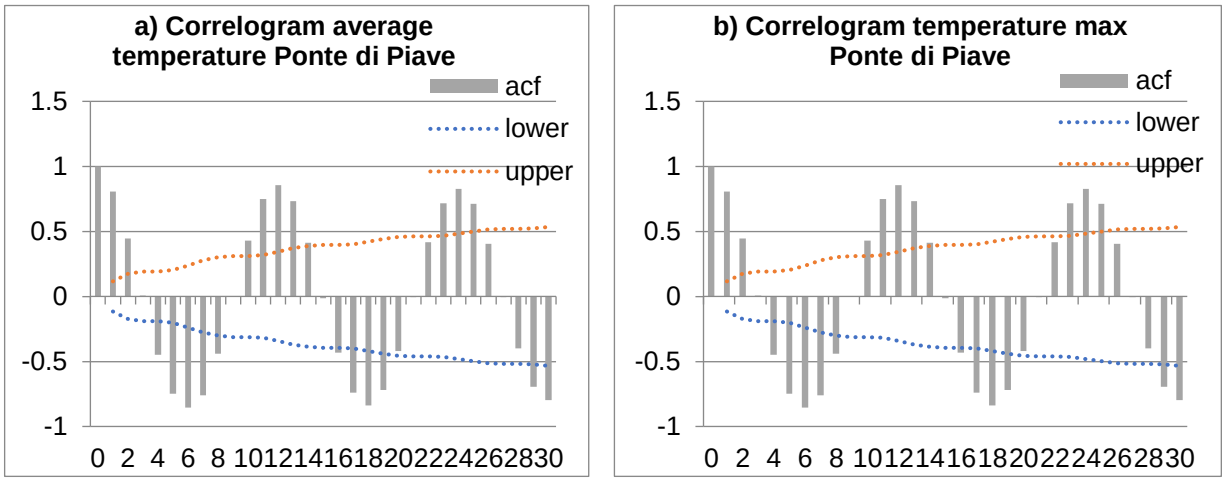

Figure.15 Temperature correlograms (a), (b) showing an elevated seasonal component, indicating the regularity of the monthly average temperature and maximum monthly temperature.

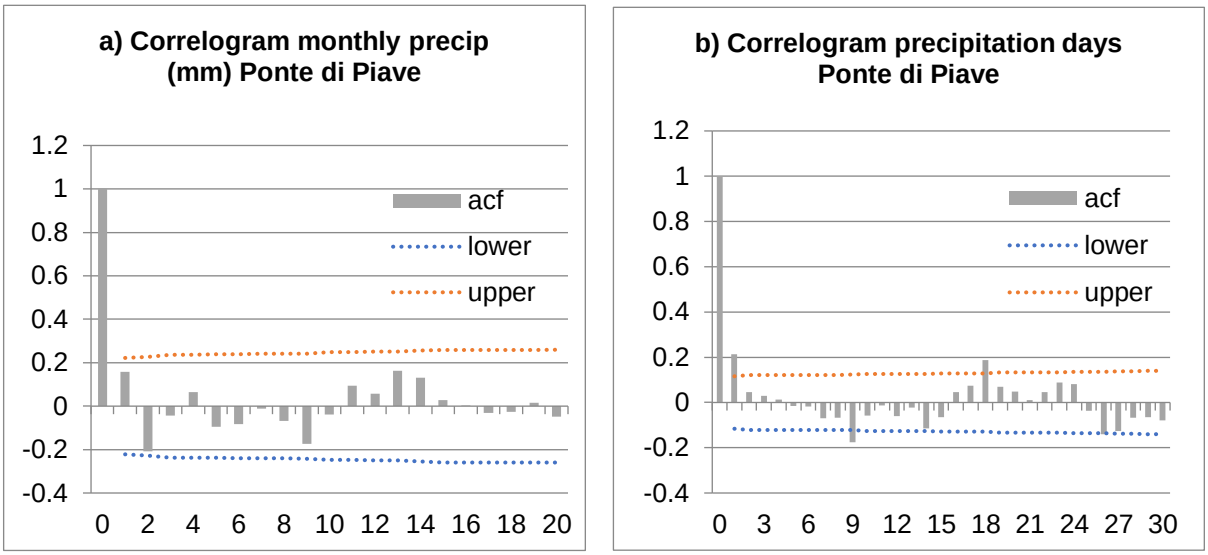

Figure.16 Precipitation correlograms (a), (b) showing a high autocorrelation and more complex dynamics.

There were no significant interannual trends ($\alpha = 0.01$) identified in the seasonal decomposition for temperature and precipitation. However, there was an increase in the irregular component for temperature ($p < 0.001$), indicating a potential increase of more than 1.5°C by 2050. The increase in the monthly maximum is also significant ($p < 0.001$), characterized by an increase (1.2°C by 2050). The irregular component of precipitation (mm and days for months) did not show a clear trend. A clear negative relationship between the monthly NAO indices and precipitation (monthly and precipitation days) was identified. However, the links between the NAO regimes and the hydroclimate are widely regarded as not being constant over time (Bladé et al., 2011). The output of climate models (Baruffi et al., 2012; Meehl et al., 2007) suggests a moderate reduction in expected rainfall in the coming decades. The same models estimate an increase in the temperature of the study area, which implies greater evaporation and a greater hydrological deficit. Current and future trends and variability will have clear impacts on ecosystem services related to nutrient flow within the catchment.

Future projections represent an ensemble average of 15 Atmosphere–Ocean General Circulation Models of the CMIP5 multi-model data set, corresponding to the IPCC Assessment Report 5 (Stocker et al., 2013). I selected the median emission scenario RCP 4.5 that globally predicts a +1.4°C (±0.5) by 2050 (Dezsi et al., 2018). This scenario confirmed a decrease in precipitation in 2050, with an estimated minimum of 758 mm/year and a maximum of 1,968 mm/year (Fig.17).

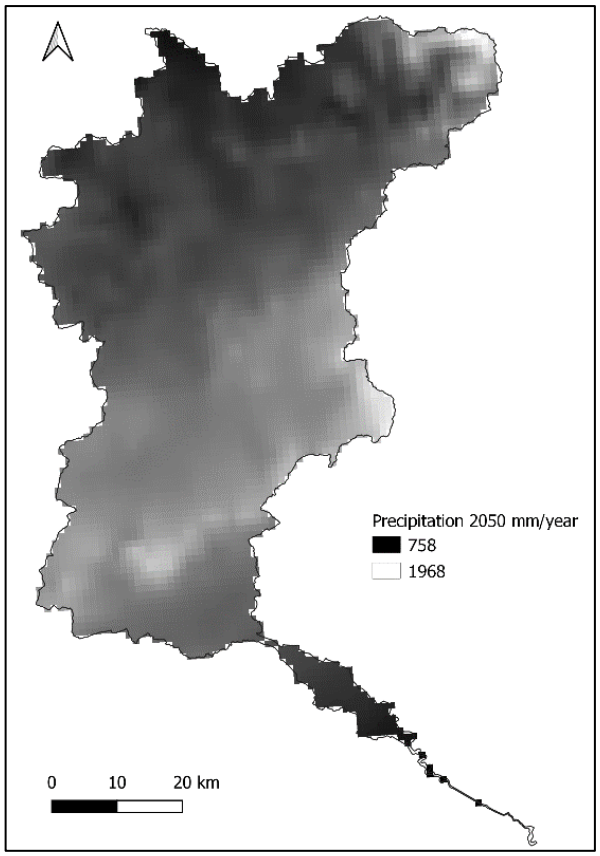

Figure.17 Estimates of yearly annual precipitation in 2050 following IPCC emission scenario RCP 4.5.

The modelled higher temperatures and more intense precipitation cause greater soil washout and increase the transport of sediments with consequences in the organic carbon and phosphate contained in the soil matrix (Orem et al., 2014).

The effect of climate change on the evapotranspiration and water availability of Europe has been carried out for medium-term (2050s) projections. The water availability is dependent on changes in evapotranspiration and in the projected precipitation regime. Water availability is expected to be reduced in the Piave river basin and throughout most of Europe. These values imply important changes that may affect runoff and groundwater recharge. The analysis for the Piave River basin generally conforms to previous European studies (Dezsi et al., 2018).

2.3.3.2. Regression analysis

The multiple regression analysis made it possible to understand which of the parameters considered are influenced by temperature and/or precipitation (1 = significant model, 0 = no significant model in table 4). The analysis was conducted in each of the 7 sampling stations for each single parameter considered. For nitrite (NO_2^--N) the model is significant only in 2 stations, for pH the model is never significant (Table 4). For ammonia (NH_4^+-N), *E. coli* and total phosphorus (T-P) there is a prevalence of stations for which the model is not significant. For suspended solids (TSS), the stations indicating a significant model are slightly higher, but in general this parameter was considered not influenced by temperature and precipitation because the p-values are just < 0.05. Finally, for nitrates (NO_3^--N), phosphates (PO_4^{3-}-P), total nitrogen (T-N), BOD_5 and dissolved oxygen the model is significant in almost all stations.

Table 4 Summary table of the forcing climatic factors models for the water quality of the Piave river (1 = significant model, 0 = no significant model, P = precipitation, T = temperature).

Site	NH_4^+-N (mg L^{-1})	NO_3^--N (mg L^{-1})	NO_2^--N (mg L^{-1})	T-N (mg L^{-1})	BOD_5 (mg O_2 L^{-1})	*E. coli* (MPN/100mL)	PO_4^{3-}-P (mg L^{-1})	T-P (mg L^{-1})	DO_2 (mg L^{-1})	pH	TSS (mg L^{-1})
Cortina d'Am-pezzo	0	1	1	1	0	0	1	1	1	0	1
S. Stefano di Cadore	0	1	0	0	0	0	1	0	1	0	1
Longa-rone	0	1	0	1	1	1	1	1	1	0	1
Belluno	0	1	0	1	1	1	1	0	1	0	1
Feltre	1	1	0	1	1	1	0	0	1	0	1
Valdob-biadene	1	1	0	1	1	0	1	1	1	0	1
Ponte di Piave	1	1	1	1	1	0	1	0	1	0	0
TOT	0	T- P+	0	T- P+	T-	0	1	0	T-	0	P+

The Ponte di Piave station clearly showed a significant model for most of the chemical parameters (Table 5). Understanding the fate and transport of nutrients in watersheds requires knowing the nutrients export and factors that control nutrients mobility through the hydrologic pathway. The regression analysis showed a significant model between NO_3^--N, PO_4^{3-}-P and precipitation. These results indicates that elevated levels of nutrients (nitrate and phosphate) was significantly associated with precipitation events and less with temperature increase.

Table 5 Analysis of forcing climatic factors for water quality at Ponte di Piave.

	NH_4^+-N (mg L^{-1})	NO_3^--N (mg L^{-1})	NO_2^--N (mg L^{-1})	T-N (mg L^{-1})	BOD_5 (mg O_2 L^{-1})	*E. coli* (MPN/100mL)	PO_4^{3-}-P (mg L^{-1})	T-P (mg L^{-1})	DO_2 (mg L^{-1})	pH	TSS (mg L^{-1})
R Square	0.14334	0.1442	0.1696	0.1369	0.1423	0.010997	0.1415	0.012	0.193	0.101	0.003
p-value	0.04194	0.0411	0.02215	0.0489	0.0429	0.797166	0.0438	0.785	0.013	0.112	0.939
Signif.	yes	yes	yes	yes	yes	no	yes	no	yes	no	no
Precip. coeff.	-0.0008	-0.0006	$-2x10^{-06}$	$-5x10^{-04}$	-0.0003	-1.926413	$9x10^{-05}$	$5x10^{-05}$	-0.006	$-4x10^{-4}$	0.002
Temp. coeff.	-0.0034	-0.011	-0.0006	-0.016	-0.0346	-32.63696	0.0006	$-3x10^{-04}$	-0.040	0.006	0.048
p-value Precip.	0.09656	0.0509	0.95644	0.7017	0.9111	0.860313	0.0181	0.558	0.109	0.386	0.949
p-value Temp.	0.21632	0.0384	0.01045	0.0321	0.0212	0.588154	0.1205	0.579	0.064	0.038	0.764

Álvarez-Cabria et al. (2016) determined that the concentration of nitrates in some rivers of northern Spain is directly proportional to precipitation while phosphates are not affected by temperature and precipitation. Zhang et al. (2017) determined that the concentration of suspended solids in rivers is directly proportional to precipitation. Cox and Whitehead (2009) determined that the dissolved oxygen concentration in the Thames River is inversely proportional to temperature. These studies confirm the results obtained from the regression analysis.

2.3.4. Conclusions

The results should have practical relevance for planning of water use for the near- and medium-term future. There is a clear increase in temperature and a reduction in precipitation on the future climate projections to 2050. Uncertainties will remain inherent in predicting future climate change, even though some uncertainties are likely to be narrowed with time.

The regression analysis was fundamental to determine if the climatic conditions (temperature and precipitation) have an influence on the other parameters and what kind of influence is observed.

3. MACRONUTRIENTS POLLUTION DYNAMICS

3.1. Background

The change in land use, and in particular the conversion to agricultural land, strongly impacts the water quality in the river basins (Bu et al., 2014). Fertilizers used in agriculture have far-reaching environmental consequences by changing the natural cycle of nutrients (Xu et al., 2022). Other anthropogenic nutrient sources include point sources, like industrial effluent discharges or water treatment plants. When it rains or snows, water flows over the landscape carrying pollutants from these surfaces to streams, rivers, lakes, and seas. Such processes can affect aquatic ecosystems which have a limited capacity to adapt to these nutrient loads (nitrogen and phosphorus) (Pereda et al., 2021).

CS allows for the participation of trained citizen volunteers in research or regulatory activities, often resulting in an increased data collection on spatial and temporal scales (McKinley et al., 2017). CS also facilitates increased participation of the general public in resource management (Pandeya et al., 2021). Despite the diffuse experience in ecological and environmental projects (Miller-Rushing et al., 2012), CS approaches have seldom been used in ESs studies focused on provisioning services (Schröter et al., 2017), compared to regulating and cultural services (Kabisch et al., 2015; Raudsepp-Hearne et al., 2010). Likewise, data from CS have the potential to support reporting SDGs indicators (Bishop et al., 2020; Fraisl et al., 2020), those related to SDG 6, clean water, and sanitation.

Ecosystem Services delivered by freshwater ecosystems are strongly influenced by the interaction of land management, catchment hydrology and climate conditions. How this interaction plays out over the complex geological, hydrological, and socio-economic conditions of a basin has direct consequences on ESs related to water quantity and quality (Keeler et al., 2012; Pereda et al., 2021). Nutrient retention is a key ES, which was modelled using a range of approaches (Vigerstol and Aukema, 2011) that balance the complexity of model accuracy, feasibility, computational cost and applicability. Models that are based on well-tested, relatively simple algorithms using readily available data are more easily understood and adopted by stakeholders (Sharp et al., 2018) to develop more integrated catchment management, fundamental for both river functioning as well as that of its receiving waters.

Coastal zones receiving river inputs are experiencing major eutrophication with related environmental and economic damage (Josette Garnier et al., 2021). Extreme eutrophication in Europe (Lancelot et al., 2011; McCrackin et al., 2018), North America (Foster et al., 2003; Turner and Rabalais, 1994) and China (Cui et al., 2018; Liu et al., 2018) have had major

consequences on local populations and economies. This is particularly important in Europe, where Member States have invested significantly to achieve good ecological status in water bodies, required by the Water Framework Directive (EU, 2000) and the Common Agricultural Policy (CAP) (European Commission, 2022).

The success of these policies, particularly in Europe (Grizzetti et al., 2012; Romero et al., 2013), the United States (Rabalais et al., 2002; Turner et al., 2007) and China (Ma et al., 2020; Wang et al., 2006), led to a significant reduction in P load in many rivers and marine waters (Minaudo et al., 2015; Torrecilla et al., 2005). Because N loading, largely associated with diffuse agricultural sources, was not simultaneously reduced, a significant excess of N over P in river loading became the rule, and eutrophication problems persisted in coastal zones. Measures taken to reduce N losses from agriculture were less effective than those devoted to urban wastewater treatment, both due to the difficulties in tackling diffuse versus point sources of pollution as well as due to agricultural intensification in some areas (J. Garnier et al., 2021). However, recent studies integrating agricultural activities for the quantification of diffuse nutrient loading (N especially, and P) and nutrient delivery to the marine coastal zone showed success (Garnier et al., 2019; Passy et al., 2016).

This led regional and national decision-makers to explore effective and verifiable measures to reduce nutrient loading through NBS. These efforts are most often focused on improved land use, with particular attention to the riparian interface between terrestrial and aquatic ecosystems, which plays an important role in nutrients and sediments dynamics (Gumiero et al., 2011; Gumiero and Boz, 2017; Mello et al., 2017). The riparian forest provides protection against erosion, retention of pollutants, excessive nutrients runoff and water temperature (Loiselle et al., 2016; Sabater et al., 2003), with benefits for the quality of human life and biodiversity (Saalfeld et al., 2012; Tanaka et al., 2016; H. Yang et al., 2016). In this context, Zhang et al. (2010) and Yang et al. (2016) emphasized the importance of improving our understanding of the benefits of NBS focused on riparian zone restoration.

Besides agricultural intensification, climate change can also enhance eutrophication and its effects on the aquatic environment. Changes in precipitation will modify nutrient delivery through changing surface and river water flows (Glibert et al., 2014a; Wåhlström et al., 2020). These effects are sensitive to precipitation intensity as well as aggregate precipitation as reduced river water flow increases residence time and decreases nutrient dilution (Raimonet et al., 2018; Whitehead et al., 2009). Ecosystems' responses to both climate change and eutrophication may be hard to unravel and thus difficult to predict, but current knowledge suggests that climate change will worsen the present situation (Duan et al., 2014).

The present study utilizes multiple data sources and CS to explore the link between NBS and ESs related to nutrient retention. I compared different riparian zone NBS in relation to their ES costs and benefits related to nutrient retention under a future climate change scenario (2050) in one of Italy's most important rivers.

3.2. Materials and Methods

3.2.1. Nutrient Model

Model development and validation were performed using information from different regional, national, and global datasets and through in situ monitoring, both from the regional environmental agency (ARPAV) and citizen scientists. Geographic and temporal dynamics of the nutrient export and retention in the Piave River catchment were modelled following the mass balance approach of the InVEST nutrient delivery ratio model (version 3.9) (Sharp et al., 2018).

The model is based on mapping nutrient sources and their potential for transport to the river to identify the spatial variation in nutrient retention across the watershed with respect to different land use/land cover conditions (LULC, e.g., vegetative areas) and catchment morphology.

Basin nutrients dynamics were based on nutrient loads across the landscape and the nutrient retention capacity of the landscape. Nutrients loads per LULC were identified from data acquired in collaboration with the regional environmental agency river consortiums and available empirical data. Nutrient flows were divided into sediment-bound (transported via surface flow) or dissolved (and transported via subsurface flow).

The nutrient delivery ratio index (NDR) was simulated for each pixel (20 m resolution) of the catchment, based on the nutrient loads, LULC, and a digital elevation model. At the watershed outlet, the P and N export to the river was calculated based on the weighted aggregation of pixel-level contributions: site-specific information related to the maximum retention efficiency, a runoff proxy (i.e., annual precipitation) representing the spatial variability in runoff potential, and an estimate of the proportion of nutrients delivered via subsurface and surface flows (Fig. 18). The subsurface flow was considered for nitrogen only and was estimated from nitrate concentrations in the ground and surface waters.

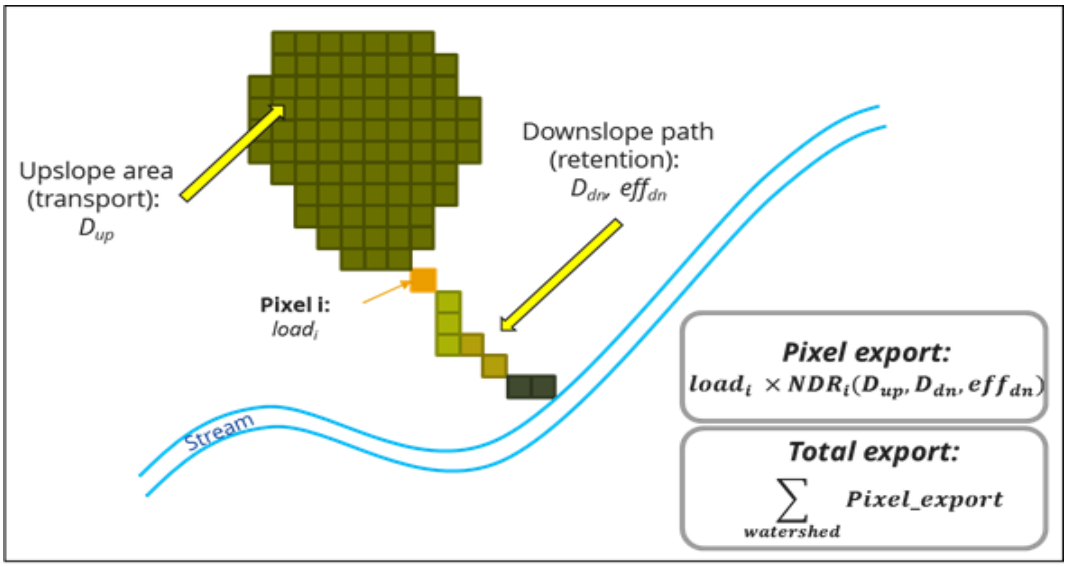

Figure 18 Conceptual representation of nitrogen and phosphorus input models. Each pixel i is characterized by its nutrient load and export (nutrient delivery ratio, NDR), a function of the upslope area and the downslope outflow path (and the retention efficiency of the types of LULC on flow paths). Pixel-level export is calculated on these two factors.

3.2.1.1. Nutrient load

The loadings are the nutrient sources associated with each pixel of the landscape, and the loading of each pixel is modified to account for the local runoff potential. This runoff potential is utilized through a raster of mean annual rainfall, or from the "quickflow" output raster of the Seasonal Water Yield model, i.e., the amount of rain that flows off the earth's surface rapidly (producing a rapid flow) relative to the infiltration into the soil (producing local recharge), determined by the properties of the soil and the type of cover.

For a pixel i:

$$load_{surf,i} = (1 - proportion\_subsurface_i) \cdot modified.load_{n_i} \qquad (1)$$

If no information is available on the proportion of nutrients transported through subsurface flow (proportion_subsurface), the most appropriate value for a conservative and initial estimate of nutrient transport is a proportion_subsurface equal to 0, which means that all nutrients are reaching the flow through the surface flow. In the equation, $modified.load_{n_i}$ denotes the nutrient load adjusted for the potential runoff to the land.

3.2.1.2. Nutrient surface export

The nutrient delivery (NDR) is the product of an export factor, which represents the ability of downstream pixels to transport nutrients without retention, and a topographic index, which represents location on the landscape. For a pixel i:

$$NDR_i = NDR_{0,i}\left(1 + exp\left(\frac{IC_i - IC_0}{k}\right)\right)^{-1} \quad (2)$$

where IC_0 and k are calibration parameters, IC_i is a topographic index and $NDR_{0,i}$ is the proportion of nutrients that are not retained by downstream pixels (regardless of the pixel's position on the landscape). $NDR_{0,i}$ is based on the maximum retention efficiency of the ground between a pixel and the stream:

$$NDR_{0,i} = 1 - eff_i' \quad (3)$$

Moving along a flow path, the additional retention provided by each pixel is calculated, considering the total distance travelled through each type of LULC. Each additional pixel of the same LULC type will contribute less to the total retention, until the maximum retention efficiency for the given LULC is reached. Total retention is limited by the maximum retention value that LULC types along the path can provide, eff_{LULC_i}.

IC, the connectivity index, represents hydrological connectivity, i.e., the probability that the nutrient on a pixel reaches the flow. In this model, the IC is a function of topography only:

$$IC = \left(\frac{D_{up}}{D_{dn}}\right) \quad (4)$$

with

$$D_{up} = \sqrt{A} \quad (5)$$

and

$$D_{dn} = \sum_i \frac{d_i}{S_i} \quad (6)$$

where $D_{up} = \underline{S}$ is the average slope gradient of the upstream contributing area (m/m), A is the upstream contributing area (m^2); d_i is the path length of the flow along the i-th cell in the direction of the steepest slope (m), and S_i is the slope gradient of the i-th cell, respectively.

The export of nutrients from each pixel *i* is calculated as the product of the load and the NDR:

$$x_{exp_i} = load_{surf,i} \cdot NDR_{surf,i} + load_{subs,i} \cdot NDR_{subs,i} \quad (7)$$

The total nutrients at the outlet of each defined watershed are the sum of the contributions of all pixels within that watershed:

$$x_{exp_{tot}} = \sum_i x_{exp_i} \quad (8)$$

3.2.1.3. Nutrient subsoil export

Subsoil nutrient input is limited to nitrogen (nitrate) flux in relation to soil nitrate retention efficiency and distance from the flow. It stabilizes at the value corresponding to the maximum

nutrient retention of the identified subsoil:

$$NDR_{subs,i} = 1 - \text{eff}_{subs}\left(1 - e^{\frac{-5 \cdot \ell}{\ell_{subs}}}\right) \quad (9)$$

Where eff_{subs} is the maximum nutrient retention efficiency that can be achieved through groundwater flow (i.e., retention due to biochemical degradation in soils), ℓ_{subs} is the retention length of the subsurface flow, i.e., the distance after which it can be assumed that the soil retains the nutrient at its maximum capacity, ℓ_i is the distance from the pixel to the stream.

3.2.2. Data Sources for Model Development and Validation

Data required to develop and validate the nutrient N and P models were obtained from multiple sources and include:

A digital elevation model (DEM), of 20 m resolution, obtained from the national research authority - ISPRA (Istituto Superiore per la Protezione e la Ricerca Ambientale) (ISPRA, 2020), was corrected to fill hydrological sinks and checked with the digital watercourse network to ensure routing along the specific watercourse, using QGIS 3.18 (https://www.qgis.org).

LULC raster data (2018) were obtained from Corine Land Use Land Cover IV Level for Italy (ISPRA, 2018), at a 100 m resolution; Current scenario considered CLC 2018 raster modified according to the baseline scenario (A1, A2, B1, C1). Future scenarios (2050) raster were based on the developed land use variation scenarios (A0, A1, A2, B0, B1, C0, C1).

Nutrient runoff proxies were based on raster precipitation data from 2018 (ARPAV, 2021a) at 20 m resolution. These raster data were interpolated using an inverse distance weighting of information from 72 stations. Future Nutrient runoff proxies were based on precipitation estimates for 2050 by Deszi et al. (2018) with high-resolution gridded surfaces at 1 km cell size developed in an Albers Equal Area Conic projection for Europe.

Vector delineation of the watershed and water elements was obtained from the geoportal of ARPAV, relative to the Water Protection Plan 2015 (Piano di Tutela delle Acque) (ARPAV, 2018a, 2018b).

The threshold value for flow accumulation, the number of upriver cells that flow into a cell before it is considered part of a river, was set to 1000, after several tests to compare the river layer output of the model to the measured river network data (ARPAV, 2018a).

Borselli's k for the connection of the surrounding land to the river with respect to the ratio of nutrients reaching the river was set to 2 (Borselli et al., 2008).

The nutrient (N and P) sources associated with each LULC class (kg ha^{-1} $year^{-1}$) were based on 2001 data from ARPAV for Corine LULC classes 111–243 (artificial surfaces and agricultural areas) for each municipality and scaled for relative population changes in 2020. For

Corine LULC classes 3112–523 (forest and semi-natural areas and water bodies), nutrient load data were obtained from the ARPAV relative to 2018 (ARPAV, 2018c). The proportion of subsurface N, a floating-point between 0 and 1, was obtained by intersecting a Corine LULC 2018 vector layer with a groundwater infiltration potential layer (ARPAV, 2018d). In order to obtain the proportion of subsurface N, the groundwater N infiltration risk potential was compared to the protective soil capacity layer (Giandon P., 2016) (Table 6). For each LULC, the final subsurface_N value is weighted for the % of Corine LULC polygons per risk class and calculated as the median of all level 1 Corine LULC classes (i.e., all urban classes, all agricultural classes, all forest classes, etc.) (Table 6).

Table 6 The proportion of subsurface N weighted for the % of Corine LULC per risk class.

Soil Protective Capacity Table			**Assigned Risk Potential**	**Proportion of Subsurface_N to Surface N per Risk Class**
Protection Capacity	**Infiltration Flux**	**Loss of NO_3^-**	**Risk**	**Reference Values (to Be Weighted per % of LULC Polygons)**
High	<12%	<5%	Very low	0.05
Medium high	12–28%	5–10%	Low	0.075
Medium low	29–40%	11–20%	Medium	0.155
Low	>40%	>20%	High	0.2

The proportion of subsurface N value was estimated using groundwater nitrate data from ARPAV for 2018 (ARPAV, 2018e), which has a lower temporal resolution (30%) with respect to surface NO_3^-.

Retention efficiency for N and P, as the maximum nutrient retention expected from each LULC type, were calculated following Pärn et al. (2012), Mayer et al. (2007) and Zhang et al. (2010);

Retention lengths for N and P for each LULC class, as the typical distance necessary to reach the maximum retention efficiency, were based on previous studies of riparian buffers (Mayer et al., 2007; Zhang et al., 2010) and ranged from 10 to 300 m. In the absence of data, the retention length was set to the pixel size.

Subsurface critical length, the distance after which the soil retains N at its maximum capacity, was set to 200 m following Mayer et al. (2007). Maximum retention of N reached through subsurface flow was set to 0.8.

Nitrate and phosphate concentrations were obtained through regulatory (ARPAV) and CS measurements. Quarterly ARPAV monitoring of total nitrogen and total phosphorus in four

stations in the upper catchment and four sites in the lower catchment were used for model development. Data are available online at www.arpa.veneto.it/dati-ambientali/open-data/idrosfera/corsi-dacqua (accessed on 3 August 2021).

Trained citizen scientists used the FreshWater Watch method (https://freshwater-watch.thewaterhub.org/content/freshwater-watch-how-guide, accessed on 3 August 2021) to determine nitrate and phosphate in 12 sites in the lower catchment for model validation. Online and video training followed the standard training program of this global citizen science project [88]. Thirty-five participants in the lower catchment of Piave from Ponte di Piave to the sea collected both observation data (colour, presence of algae, etc.) and semi-quantitative measurements of water quality (nitrate, phosphate, nephelometric turbidity) (Scott and Frost, 2017; Thornhill et al., 2018) from 2019 to 2021. Nitrate (NO_3^--N) and phosphate (PO_4^{3-}-P) were measured in closed plastic tubes, which are designed to mix a fixed volume of water with reagents to produce increasing colour values (peak absorption at 540 nm) with increasing concentration. PO_4^{3-}-P concentrations were estimated colourimetrically using inosine enzymatic reactions in seven specific ranges from 0.02 mg L^{-1} to 1.0 mg L^{-1} PO_4^{3-}-P (<0.02, 0.02–0.05, 0.05–0.1, 0.1–0.2, 0.2–0.5, 0.5–1.0, <1.0 mg L^{-1}) (Strickland and Parsons, 1972). Nitrate–nitrogen concentrations were estimated colourimetrically using N-(1-napthyl)-ethylenediamine (Law Al and Adeloju, 2013), in seven specific ranges from 0.2 mg L^{-1} to 10 mg L^{-1} NO_3^--N (<0.2, 0.2–0.5, 0.5–1.0, 1.0–2.0, 2.0–5.0, 5–10, >10 mg L^{-1}). The median values for each classification were used to allow for quantitative analysis. During the measurements, geo-location and time were recorded automatically using the FreshWater Watch app and transferred to the online database after validation (https://freshwaterwatch.thewaterhub.org/, accessed on 3 august 2021). Once entered, all data underwent quality control by project leaders and citizen scientists.

3.2.3. Cost Analysis of N and P

In order to compare the costs and benefits of different NBS scenarios, an estimate of the economic value associated with phosphorus and nitrogen retention service of the Piave catchment was determined using the reported costs of recent NBS projects focused on nutrient reduction. The projects considered were performed in the same region by the Drainage Authority 'Consorzio di Bonifica Acque Risorgive', from 2003 to 2020 (CBAR, 2021). These projects were financed by the Decree of the Ministries of the Environment and of Labour to reduce the nutrient loads to the Venice Lagoon. I conducted a multiple linear regression after adjusting for inflation to estimate the typical costs of N and P removal. These were compared to recent studies on the costs for nitrate and phosphate removal by improvements to wastewater

treatment (Jiang et al., 2004; Strokal et al., 2016). In general, cost estimation of nutrient reduction is based on the analysis and estimation of different components such as energy consumption, chemicals' consumption, personnel salaries, maintenance expenses, construction materials and their quantities, mechanical equipment and land cost (Bashar et al., 2018; Gratziou et al., 2013). As NBS actions include costs that are not directly related to individual components, using an empirical aggregated approach was deemed more appropriate.

3.3. Results

The changes in nutrient retention-related ESs in the Piave catchment showed the relative impact of different NBS scenarios and the impact of climate change, in particular precipitation and a table for calculating the estimate of:

3.3.1. Results – Nitrogen Model

The results of the model for the nitrogen inputs include a series of output layers – raster – with the same resolution as the digital model of the input terrain, which for the Piave basin is 20 m, and a table of the estimate of:

- Surf_load_: total annual loads in the catchment area of N (kg/year), i.e. the sum of the nutrient contribution from the entire LULC surface without filtering by land cover classes and landscape type.
- Exp_tot_: the total export (kg/year) of N to the river, considering the LULC land cover.
- Sub_load_: Total annual loads in the subsoil of N (kg/year).

3.3.1.1. Comparison of 2018 scenarios

The reforestation scenario C0A0B1 (B1) represented the best scenario for the nitrogen dynamics, with a reduction in both loads (surface and groundwater) and in the nitrogen export. The surface load in scenario B1 decrease by 1.50% (4.45×10^5 kg/year), while the underground load decrease by 0.37% (2.22×10^4 kg/year). In the scenario B1 nitrogen exports decrease by 5.67% (2.46×10^5 kg/year) compared to the values obtained in the current scenario (2018) (Table 7 and Fig. 19). The reduction foreseen in these scenarios is mainly linked to the conversion of agricultural areas into forest cover, this allows a greater absorption of nitrogen by plants.

The increase in surface area in the riparian forest along the river allows it to perform the function of a buffer strip, protecting against widespread contamination, acting as a filter capable of retaining excess nutrients which, in the absence of vegetation, can easily reach the river. In the Lower Piave both the C0A1B0 (A1) and the C0A2B0 (A2) scenarios showed effects on the reduction of nitrogen compared to the current situation.

River restoration scenario A1 (Fig. 20) between the two scenarios envisaged inside the embankments showed overall the best conditions for the reduction of surface (0.06% = 1.92 $x10^4$ kg/year), subsurface (0.09% = $5.22x10^3$ kg/year) and of exports to the river (0.17% = $7.42x10^3$ kg/year) (Table 7).

The flood retention basin scenario (C1) showed a decrease in nitrogen in all its compartments but does not bring a further improvement compared to the base scenarios without intervention for hydraulic safety (Table 7). The combinations of scenario C1 with the other scenarios (A1, A2, B1) showed a reduction in loads and nitrogen retention compared to the base scenarios without a box (Table 7).

Table 7 Variation in nitrogen inputs based on 12 management scenarios of the Piave river basin under current climatic conditions (2018).

2018	NDR Basin			NDR Basin %		
Scenario	surf_load_N (kg/year)	sub_load_N (kg/year)	exp_tot_N (kg/year)	surf_load_N (kg/year) %	sub_load_N (kg/year) %	exp_tot_N (kg/year) %
C0, A0, B0	**2.99 x10^7**	**5.96 x10^6**	**4.47 x10^6**	**2.99 x10^7**	**5.96 x10^6**	**4.47 x10^6**
C0, A1, B0	2.99 x10^7	5.95 x10^6	4.46 x10^6	-0.06	-0.09	-0.17
C0, A2, B0	2.99 x10^7	5.96 x10^6	4.46 x10^6	-0.05	-0.01	-0.13
C0, A0, B1	2.94 x10^7	5.94 x10^6	4.22 x10^6	-1.50	-0.37	-5.67
C0, A1, B1	2.94 x10^7	5.93 x10^6	4.22 x10^6	-1.57	-0.46	-5.84
C0, A2, B1	2.94 x10^7	5.93 x10^6	4.22 x10^6	-1.56	-0.38	-5.80
C1, A0, B0	2.99 x10^7	5.96 x10^6	4.47 x10^6	-0.04	-0.03	-0.08
C1, A1, B0	2.99 x10^7	5.95 x10^6	4.46 x10^6	-0.11	-0.12	-0.25
C1, A2, B0	2.99 x10^7	5.96 x10^6	4.46 x10^6	-0.10	-0.04	-0.21
C1, A0, B1	2.94 x10^7	5.93 x10^6	4.22 x10^6	-1.54	-0.39	-5.72
C1, A1, B1	2.94 x10^7	5.93 x10^6	4.21 x10^6	-1.60	-0.48	-5.89
C1, A2, B1	2.94 x10^7	5.93 x10^6	4.22 x10^6	-1.59	-0.40	-5.85

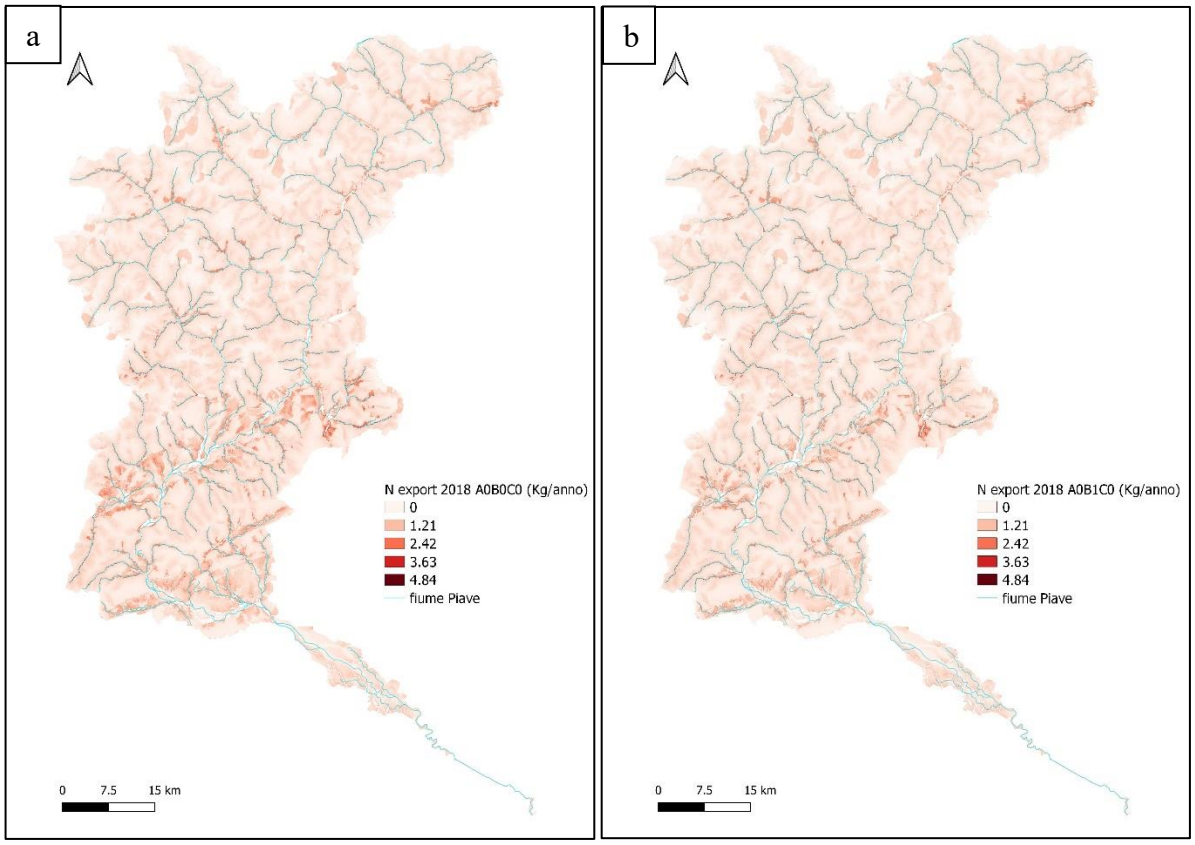

Figure 19 Maps of the spatial distribution of nitrogen exports for 2018. (a) baseline scenario (b) B1 best scenario which envisages reforestation in the upstream basin.

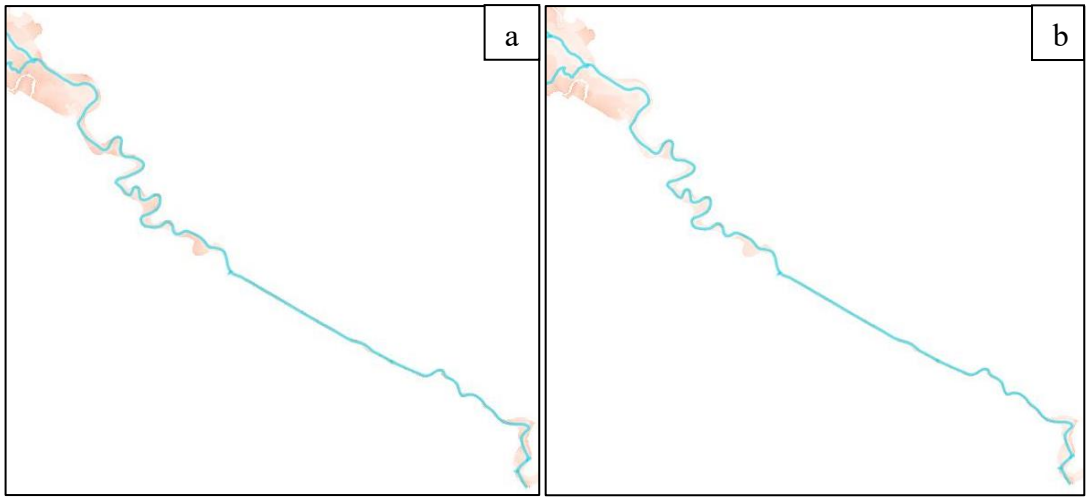

Figure 20 Detail of N exports in the Lower Piave section in 2018. (a) baseline scenario (b) scenario A1.

3.3.1.2. Comparison of 2050 scenarios

The scenarios developed for 2050 showed a significant reduction in the load (surface and underground) and in the export of nitrogen compared to the 2018 scenarios. These results are linked both to the increase in the wooded area and to the variation in the nutrient runoff proxy, i.e. the precipitation according to the selected RCP 4.5 model show a reduction of rainfall and rainy days in the basin area (Dezsi et al., 2018).

The dynamics of nitrogen in the Piave basin forecast for 2050 showed B1 as the best scenario (Table 8 and Fig. 21a) with a reduction of 3.33% (9.80×10^5 kg/year) of surface N loads of 1.68% (9.94×10^4 kg/year) of subsoil loads and of 6.95% (3×10^5 kg/year) of N export compared to current conditions (C0A0B0 2018 in Table 7).

Scenario A1 (Fig. 21b), between the two scenarios envisaged inside the embankments, overall presents the best conditions for the reduction of surface nitrogen loads (1.81%), subsurface nitrogen (1.37%) and export to the river (1.13%). Also in this case, the increase in the riparian vegetation belt in the floodplain of the lower Piave leads to nitrogen reduction effects compared to the baseline situation (2018).

The single scenario that envisages the work for hydraulic safety (C1) showed a less effects in reducing nitrogen compared to B1 and A1 scenarios. While a combination of these scenarios brings a benefit in the reduction of loads and in nitrogen retention (Table 8) compared to the conditions of 2018 (Fig. 22). For example, scenario B1 (6.95%) combined with scenario C1 reduced the N exports of 7.01% (3.03×10^5 kg) less per year, which translates into a reduction difference of 2.31×10^3 kg/year of nitrogen.

Table 8 Variation in nitrogen inputs based on 12 management scenarios of the Piave river basin under future climatic conditions (2050).

2050	NDR Basin			NDR Basin %		
Scenario	surf_load_N (kg/year)	sub_load_N (kg/year)	exp_tot_N (kg/year)	surf_load_N (kg/year) %	sub_load_N (kg/year) %	exp_tot_N (kg/year) %
C0, A0, B0	2.94 x10^7	5.88 x10^6	4.43 x10^6	-1.74	-1.28	-0.96
C0, A1, B0	2.93 x10^7	5.88 x10^6	4.42 x10^6	-1.81	-1.37	-1.13
C0, A2, B0	2.94 x10^7	5.88 x10^6	4.42 x10^6	-1.80	-1.30	-1.09
C0, A0, B1	2.89 x10^7	5.86 x 0^6	4.17 x10^6	-3.33	-1.68	-6.95
C0, A1, B1	2.89 x10^7	5.85 x10^6	4.16 x10^6	-3.40	-1.77	-7.14
C0, A2, B1	2.89 x10^7	5.86 x10^6	4.16 x10^6	-3.39	-1.69	-7.10
C1, A0, B0	2.94 x10^7	5.88 x10^6	4.42 x10^6	-1.79	-1.32	-1.05
C1, A1, B0	2.93 x10^7	5.87 x10^6	4.41 x10^6	-1.86	-1.41	-1.22
C1, A2, B0	2.93 x10^7	5.88 x10^6	4.42 x10^6	-1.85	-1.33	-1.18
C1, A0, B1	2.89 x10^7	5.86 x10^6	4.17 x10^6	-3.37	-1.70	-7.01
C1, A1, B1	2.89 x10^7	5.85 x10^6	4.16 x10^6	-3.44	-1.79	-7.20
C1, A2, B1	2.89 x10^7	5.86 x10^6	4.16 x10^6	-3.43	-1.71	-7.15

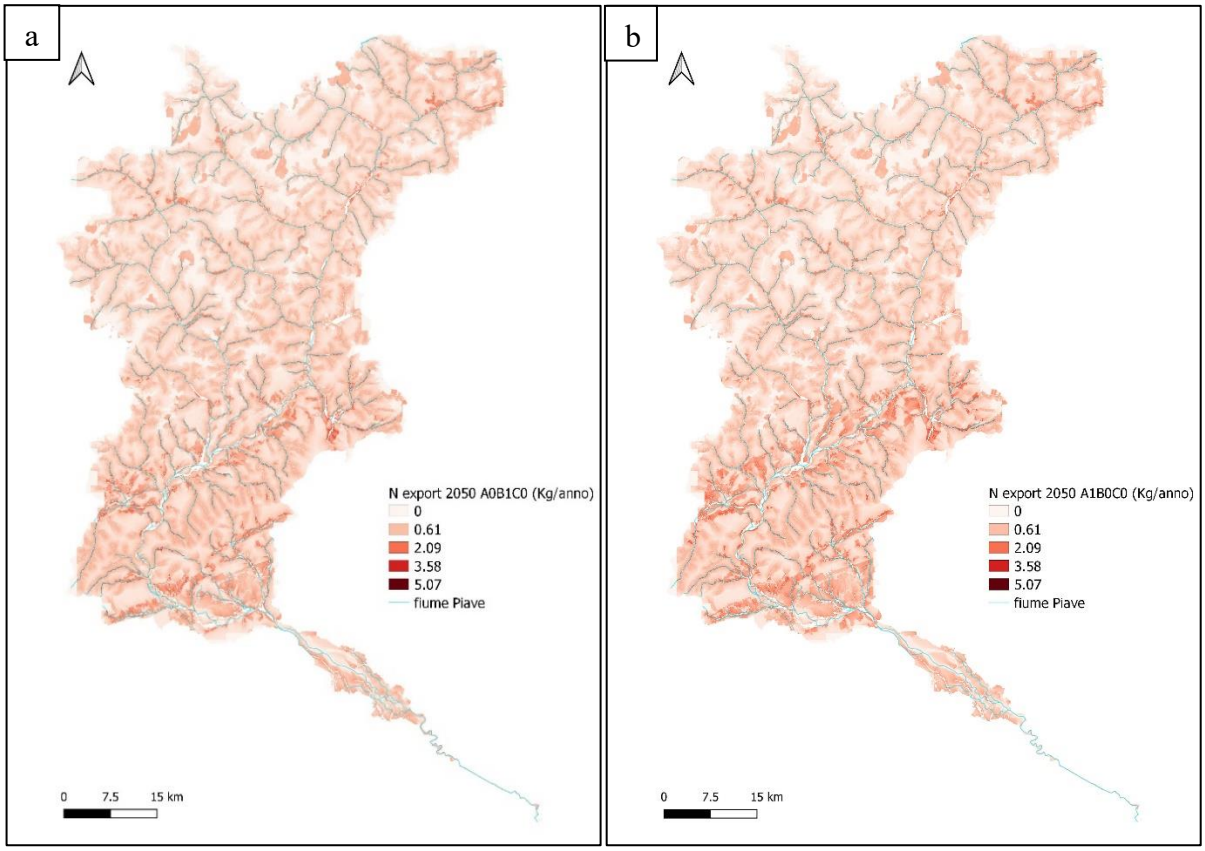

Figure 21 Comparison of maps of spatial distribution of N exports between (a) scenario B1 where the reduction of N exports is more evident compared to scenario A1 (b).

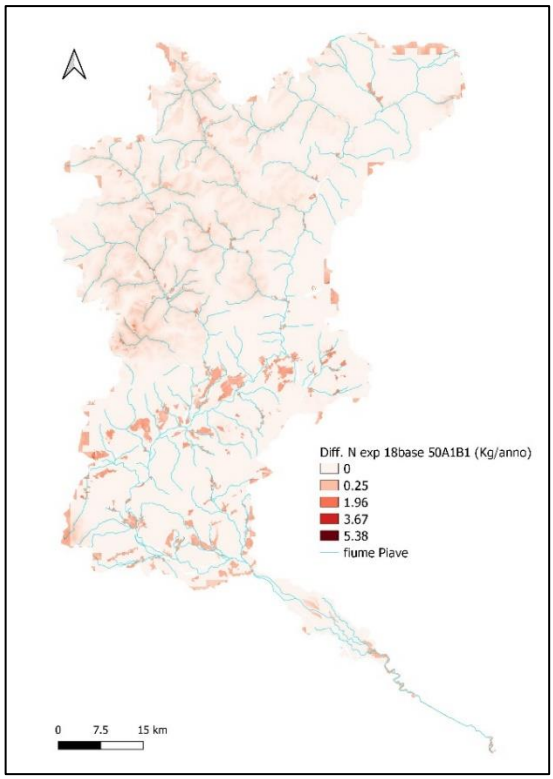

Figure 22 Difference map of N export distributions between the A1B1C0 2050 scenario and the 2018 baseline scenario (A0B0C0).

3.3.1.3. Validation

To validate the model on the N load exported to the river, the ARPAV data of 2018 were used, the data collected by the citizen scientists active in the project in 2020, considering the average monthly concentrations of N and the river flows for 2018. the average monthly flow rate at Ponte di Piave (116 m^3/s) was used, which does not differ significantly from the measurements made at Nervesa della Battaglia (130 m^3/s).

The ARPAV samples for station 65 of Fossalta di Piave (Table 9) show high concentrations of total nitrogen (TN) in winter of 2.17 mg L^{-1} and lower concentrations in summer and autumn of 1.32 mg L^{-1}. Taking these values as a reference, the total load exported to the river was estimated (Table 9).

Table 9 Validation of model data with ARPAV data, estimated loads referring to 2018.

ARPAV 2018	Min	Max	Mean	SD	Export ARPAV (kg/year)
T-N (mg L^{-1})	1.19	2.35	1.62	0.43	5.75 x10^6

For nitrogen, ARPAV (2018) estimated that the total loads (kg/year) in Veneto were around 137,227,512 kg/year, coming from breeding (36.6%) and from fertilizers (63.4%), for a load

unitary average (kg/Ha) of 171.4 kg, and falls under the high load class of fertilizer.

Further validation was done with citizen science (CS) data. Trained citizen scientists collected more than 100 samples along the lower reaches of the Piave River, from Ponte di Piave to its mouth, where the number of environmental agency monitoring stations is limited to one station. Nitrate (NO_3^--N) concentrations are high in autumn (1.63 mg L^{-1}) and low in summer (0.90 mg L^{-1}). Taking these values as a reference, the total load exported to the river was estimated (Table 10).

Table 10 Validation of model data with data from citizen scientists, estimated loads referred to 2020.

CS 2020	Min	Max	Mean	SD	Export CS (kg/year)
NO_3^--N (mg L^{-1})	0.1	7.5	1.37	0.61	4.48 x10^6

From the values obtained with the ARPAV data and from those obtained with citizens' data, it can be deduced that, although the model provides a good approximation of the nitrogen exports of the Piave. It is noted that the model used contains some parameters for which the output values generally show a high sensitivity to the input data. The input data for the N loads on the Piave basin used in the model are given for land use classes a) urban 2) agricultural/zootechnical 3) industrial. For land use classes not included in these categories (wooded areas, pastures and prairies, rocky areas) present in the Piave river basin, the data relating to N were obtained from ARPAV using a layer on the loads of N in Veneto. This indicates that in the absence of specific data relating to the real loads of N on the basin, and relating to a specific year, the results of the model can deviate starting from the concentrations of the ARPAV samplings during 2018. Despite this, the nitrogen model proves valid in estimating the total load of N that can reach the river throughout the catchment area, and it is important to monitor N sources, collect emissions data and monitor any changes that occur in land use, to refine the model to obtain forecasts useful for the management of the river habitat and the services it provides.

3.3.2. Results – Phosphorus Model

The results of the NDR model for the phosphorus inputs include a series of output layers (raster) with the same resolution as the digital model of the input terrain, which for the Piave basin is 20 m, and a calculation table of the estimate of:

- Surf_load_: Total annual loads in the catchment area of P (kg/year), i.e. the sum of the nutrient contribution from all LULC surface area without filtering by land cover classes and landscape type.
- Exp_tot_: the total export (kg/year) of P to the river, considering the LULC land cover.

3.3.2.1. Comparison of 2018 scenarios

The B1 scenario showed the best dynamics in reducing P load and retention compared to the other 2018 scenarios (Figure 23). The annual P load decrease by 5% ($5.55x10^5$ kg/year), while the total P export decrease by 28.71% ($1.50x10^5$ kg/year) (Table 11). The greater presence of forest vegetation brings a benefit for the roots that retain the soil and consequently the phosphorus. Furthermore, phosphorus is one of the essential nutrients for plant growth, as well as being retained by the roots it is also absorbed by them.

The scenario A2 (Fig. 23b), reforestation in the banks of the lower Piave, showed the best effects in reducing the P load (0.18% = $2.06x10^4$ kg/year) and retention (0.56% = $3.33x10^3$ kg/year). This P reduction is linked to the greater presence of riparian vegetation inside the banks foreseen for the scenario.

The scenario that envisages the intervention for hydraulic defence (C1), showed a reduction in P load and export, but not significatively compared to the other base scenarios. Instead, the combination of the hydraulic defence scenario (C1) and the other baseline scenarios showed a better reduction in phosphorus exports (Table 11). For example, the C1 scenario combined with the B1 showed a decrease of 28.91% ($1.51x10^5$ kg/year), with a difference of $1.07x10^3$ kg/year less than the scenario B1 alone.

Table 11 Variation in phosphorus inputs based on 12 management scenarios of the Piave river basin under current climatic conditions (2018).

2018	NDR Basin		NDR Basin %	
Scenario	surf_load_P (kg/year)	exp_tot_P (kg/year)	surf_load_P (kg/year) %	exp_tot_P (kg/year) %
C0, A0, B0	**1.14 x10^7**	**5.97 x10^5**	**1.14 x10^7**	**5.97 x10^5**
C0, A1, B0	1.14 x10^7	5.94 x10^5	-0.20	-0.51
C0, A2, B0	1.14 x10^7	5.94 x10^5	-0.18	-0.56
C0, A0, B1	1.08 x10^7	4.47 x10^5	-5.00	-28.71
C0, A1, B1	1.08 x10^7	4.44 x10^5	-5.21	-29.38
C0, A2, B1	1.08 x10^7	4.44 x10^5	-5.19	-29.44
C1, A0, B0	1.14 x10^7	5.95 x10^5	-0.07	-0.30
C1, A1, B0	1.14 x10^7	5.92 x10^5	-0.27	-0.81
C1, A2, B0	1.14 x10^7	5.92 x10^5	-0.25	-0.86
C1, A0, B1	1.08 x10^7	4.46 x10^5	-5.06	-28.91
C1, A1, B1	1.08 x10^7	4.43 x10^5	-5.27	-29.58
C1, A2, B1	1.08 x10^7	4.43 x10^5	-5.25	-29.64

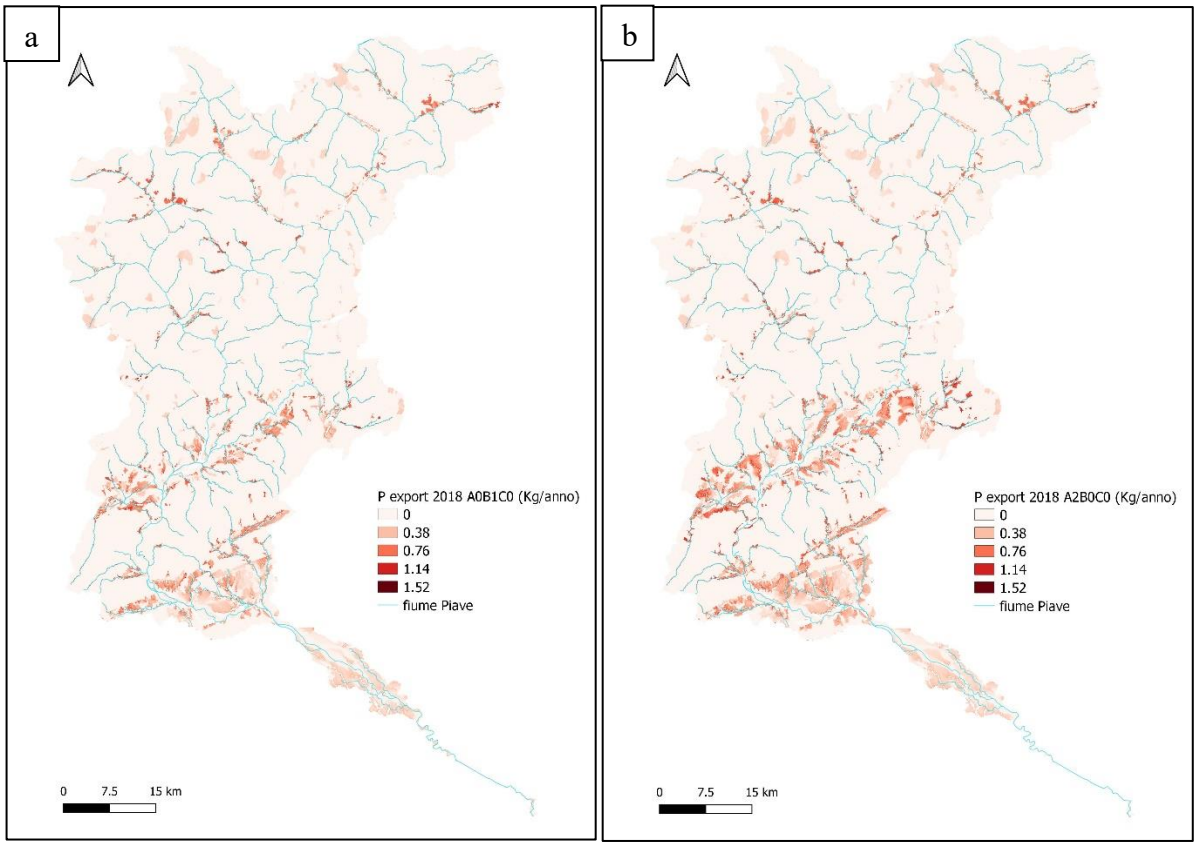

Figure 23 Maps of the spatial distribution of nitrogen exports for 2018. (a) B1 best scenario which envisages reforestation in the upstream basin (b) A2 best scenario inside the banks of the Lower Piave.

3.3.2.2. Comparison of 2050 scenarios

The B1 scenario (Fig. 24a) showed greater reduction of P load (5.67% = $6.26x10^5$ kg/year) and exports (27.58% = $1.45x10^5$ kg/year) compared to the others climate change scenarios to 2050, considering the RCP 4.5 model of rainfall reduction.

Furthermore, the other base scenarios showed an increase in exports of phosphorus: the base scenario (A0) by 2.07% (Fig. 24b), the A1 scenarios by 1.53%, the A2 by 1.49% and C1 by 1.74%, indicating a lower P retention in the middle and lower basins (Table 12). This dynamic, in the long term, leads to an impoverishment of the soils of this nutrient. These factors can be explained by the reduction in rainfall which is witnessed in the climate change scenarios and the reduced size of the area inside the banks of the lower Piave, while the increase in the wooded surface of 14,000 ha upstream allows the reduction of export of P.

The combination of the B1 and A2 scenarios (Fig. 25a, b), both with reforested areas, lead to a reduction in phosphorus exports of 28.34% (Table 12) due to the sum of the positive effects linked to reforestation upstream and within the banks of the lower Piave showed $1.48x10^5$ kg of P less per year.

The scenario C1 which consider the flood retention basin showed an increase in P exports of 1.74% (Table 12). The export of P showed an increase, although to a lesser extent, from the combination of scenario C1 with scenarios A1 and A2. The combination of scenarios C1 and B1 showed a further reduction in both the load (5.74%) and exports (27.81%) of phosphorus (Table 12).

Table 12 Variation in phosphorus inputs based on 12 management scenarios of the Piave river basin in future climatic conditions (2050).

2050	**NDR Basin**		**NDR Basin %**	
Scenario	surf_load_P (kg/year)	exp_tot_P (kg/year)	surf_load_P (kg/year) %	exp_tot_P (kg/year) %
C0, A0, B0	$1.13 x10^7$	$6.09 x10^5$	-0.44	2.07
C0, A1, B0	$1.13 x10^7$	$6.06 x10^5$	-0.65	1.53
C0, A2, B0	$1.13 x10^7$	$6.06 x10^5$	-0.63	1.49
C0, A0, B1	$1.08 x10^7$	$4.52 x10^5$	-5.67	-27.58
C0, A1, B1	$1.07 x10^7$	$4.49 x10^5$	-5.90	-28.29
C0, A2, B1	$1.07 x10^7$	$4.49 x10^5$	-5.87	-28.34
C1, A0, B0	$1.13 x10^7$	$6.07 x10^5$	-0.51	1.74
C1, A1, B0	$1.13 x10^7$	$6.04 x10^5$	-0.72	1.20
C1, A2, B0	$1.13 x10^7$	$6.04 x10^5$	-0.70	1.16
C1, A0, B1	$1.07 x10^7$	$4.51 x10^5$	-5.74	-27.81
C1, A1, B1	$1.07 x10^7$	$4.48 x10^5$	-5.96	-28.52
C1, A2, B1	$1.07 x10^7$	$4.48 x10^5$	-5.94	-28.57

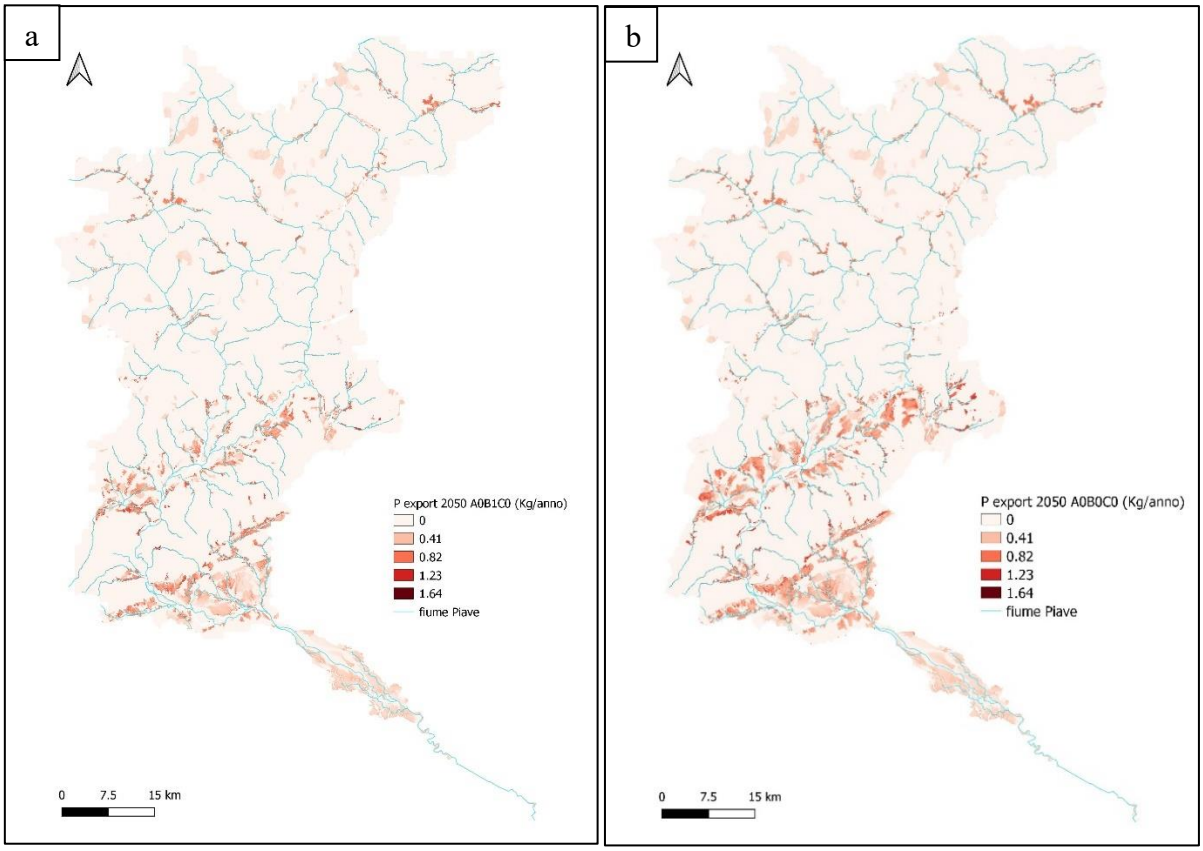

Figure 24 Maps of the spatial distribution of phosphorus exports for 2050. (a) B1 best scenario where the export of P decreases (b) scenario A0B0C0 where the export of P increases.

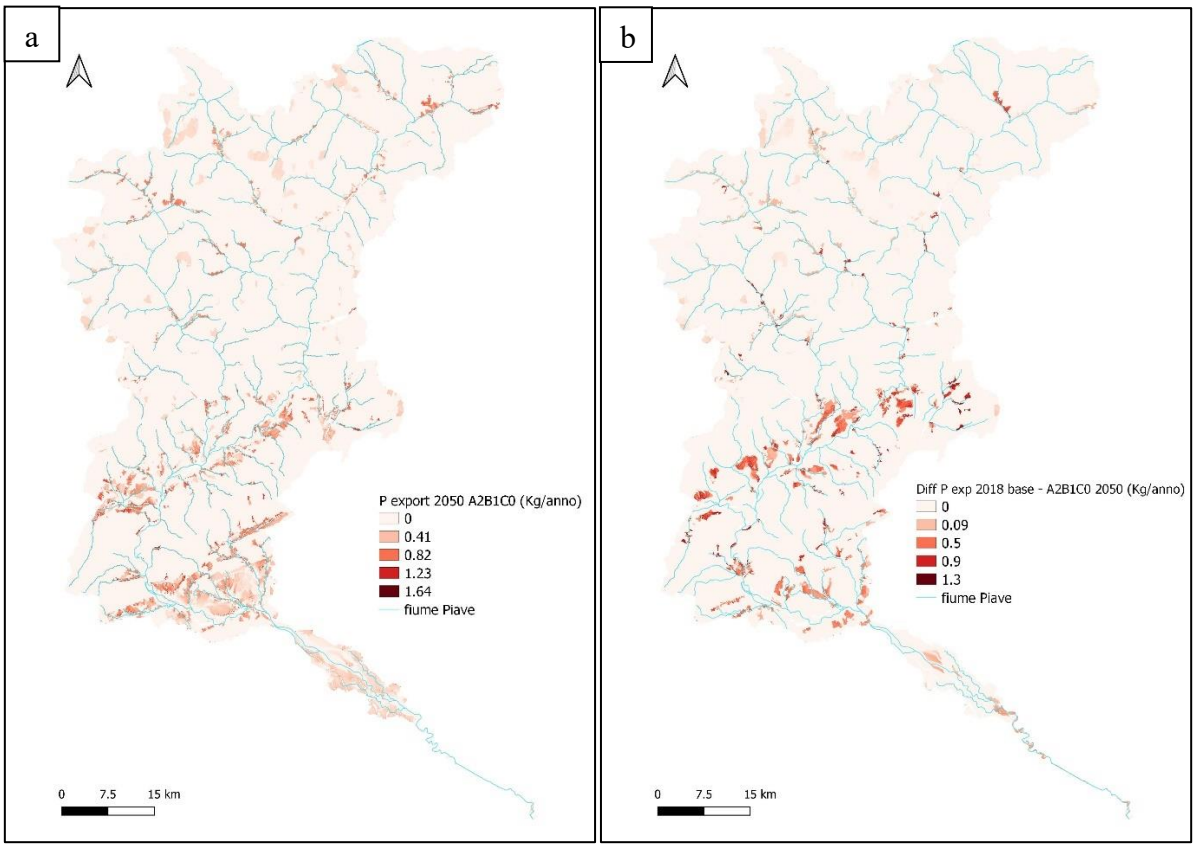

Figure 25(a) Map of the spatial distribution of P exports for the best combination of A2B1 scenarios. (b) Difference map between the 2018 baseline scenario and the 2050 A2B1 scenario.

3.3.2.3. Validation

To validate the model on the P load exported to the river, the ARPAV data of 2018 were used, the 2020 data collected by the citizen scientists active in the project, considering the average monthly concentrations of P and the river flows for 2018. the average monthly flow rate at Ponte di Piave (116 m^3/s) was used, which does not differ significantly from the measurements made at Nervesa della Battaglia (130 m^3/s).

The ARPAV samples for station 65 of Fossalta di Piave show high concentrations of total phosphorus (TP) in autumn (0.037 mg L^{-1}) and low in winter (0.021 mg L^{-1}). Taking these values as a reference, the total load exported to the river was estimated (Table 13).

Table 13 Validation of model data with ARPAV data, estimated loads referring to 2018.

ARPAV 2018	Min	Max	Mean	SD	Export ARPAV (kg/year)
T-P (mg L^{-1})	0.016	0.059	0.029	0.01	1.04 x10^5

Further validation was done with citizen science (CS) data. Trained citizen scientists collected more than 100 samples along the lower reaches of the Piave River, from Ponte di Piave to its mouth, where the number of environmental agency monitoring stations is limited to one station. Phosphate concentrations (PO_4^{3-}-P) are low in winter (0.11 mg L^{-1}) and high in summer (0.52 mg L^{-1}). Taking these values as a reference, the total load exported to the river was estimated (Table 14).

Table 14 Validation of model data with data from citizen scientists, estimated loads referred to 2020.

CS 2020	Min	Max	Mean	SD	Export CS (kg/year)
PO_4^{3-}-P (mg L^{-1})	0.01	1.5	0.032	0.022	8.04 x10^4

The values obtained with ARPAV data and those obtained with citizens' data are very similar and demonstrate that the model provides a good approximation. It should be remembered that the input data for the P loads on the Piave basin used in the model are given for the land use classes a) urban 2) agricultural/zootechnical 3) industrial. For land use classes not included in these categories (wooded areas, pastures and prairies, rocky areas) present in the Piave river basin, the data relating to P were estimated from a layer on N loads in Veneto considering a ratio of N:P equal to 3.67 (derived from the N:P ratio for the municipalities of the Piave basin as the sum of the contributions from urban, agricultural and industrial areas, both for N and for P). In the absence of specific real data on P loads in the basin, the results of the model can deviate from the results obtained from those obtained with ARPAV data. Despite

this, the phosphorus model proves to be valid in estimating the total load of P that can reach the river throughout the basin area.

3.4. Discussions

3.4.1. Nutrient Dynamics and Distribution

There is growing awareness that NBS can help to reduce climate change-related impacts as well as providing ecosystem services (Redhead et al., 2018; Seddon et al., 2020). The results of the simulated nutrient conditions in four different NBS scenarios for 2050 suggest that the nutrient load and export in the Piave river catchment is sensitive to climate change and to an increase in wooded areas, particularly in agricultural areas where there is a trend in agricultural land abandonment (Lasanta et al., 2017; Malavasi et al., 2018). This rural exodus, which began after World War II, triggered the process of natural vegetation regrowth that continues into the present (Rocchini et al., 2006). Reforestation presents multiple benefits, promoting biodiversity (Wade et al., 2006) as well as reducing surface water runoff and soil erosion (Tasser et al., 2003), control sediment loss and improve soil properties (Seeber and Seeber, 2005).

The overall impact of each NBS scenario is clear in the reduced export of both phosphorus and nitrogen, with the largest reduction for a single scenario occurring for B1, the reforested area of the upper catchment (export reduction for N of 328 tonnes/year, export reduction for P of 144 tonnes/year). The values confirm support studies that show increased forest cover and decreased agricultural areas decrease sediment, nitrogen and phosphorus exports (Mello et al., 2017).

The reductions associated with the scenario of A1 in the lower section are less evident but still represent a significant reduction in nutrient export. The lower catchment is heavily impacted by intensive agriculture both inside and outside the riverbanks, leaving very little area for hygrophilous riparian vegetation, with that remaining colonized often by invasive species. NBS actions focused on river renaturalization, and restoration were shown to provide multiple benefits on nutrient mitigation as well as other ESs. The erodible bank expansion in the A1 scenario is also intended to restore river dynamics but, as a consequence, will increase P export (Fox et al., 2016).

While the overall reductions in nutrient export provide a tool for understanding the benefits of NBS related reforestation and restoration activities, key information can be gained from exploring the spatial distribution of ecosystem services based on different scenarios. By using spatially explicit models, it was possible to identify the locations within the catchment with the greatest sensitivity to climate change and NBS actions, in this case with respect to nutrient loads

and nutrient export. As expected, the areas closest to the river network have the highest nutrient export in relation to their retention capacity of the vegetation downslope, substrate, and drainage.

The difference between current and 2050 A1B1 scenarios shows that areas closest to the river have the largest potential for a reduction in P export (Fig. 26). Changes in N export (Fig. 27) were less spatially distinct as nitrate is more mobile (Redhead et al., 2018).

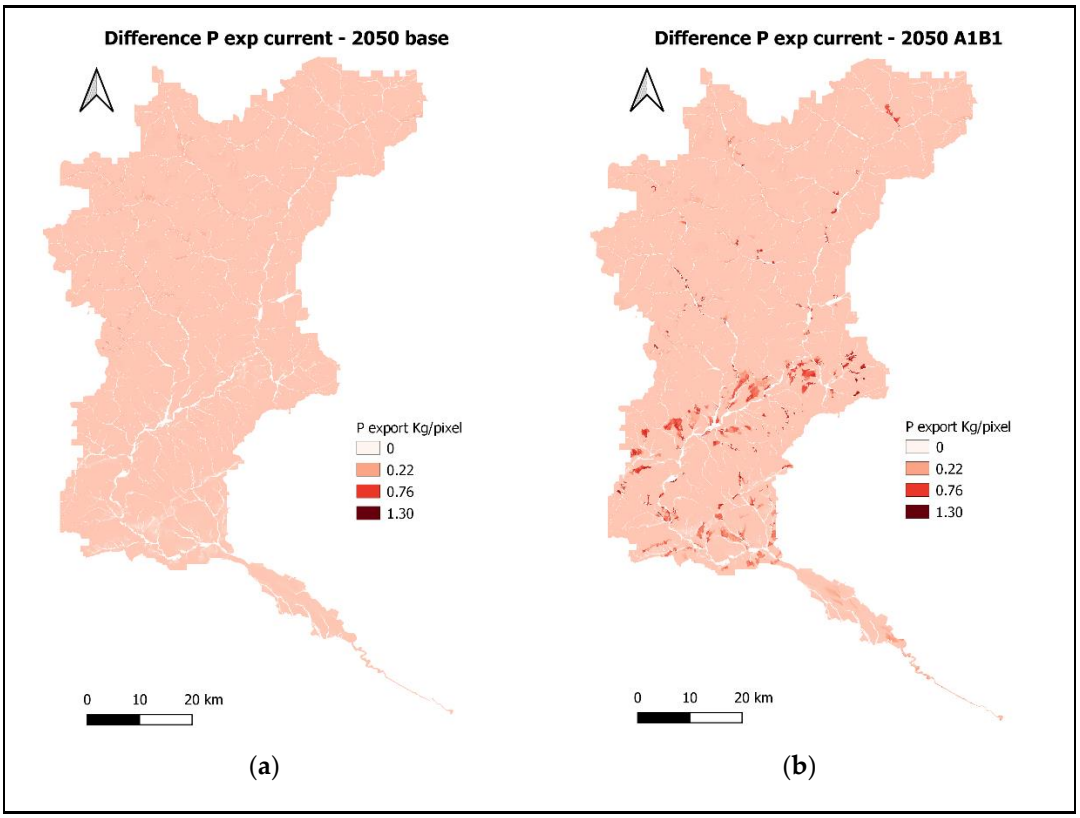

Figure 26 Spatial distribution in the change (reduction) in phosphorus (P) export between 2018 A0B0 and 2050 for scenarios A0B0 (a) and A1B1 (b).

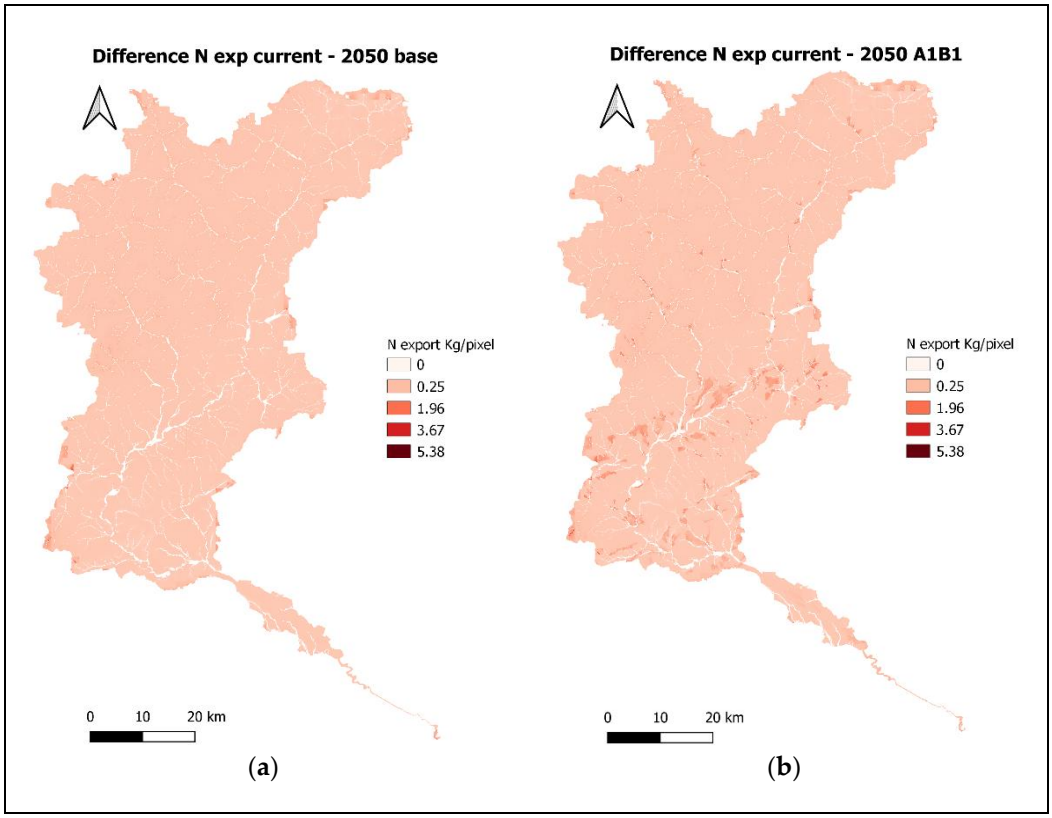

Figure.27 Spatial distribution in the change (reduction) in nitrogen (N) export between 2018 A0B0 and 2050 for scenarios A0B0 (a) and A1B1 (b).

3.4.2. ESs Evaluation of NBS

The selection of the best single or combined NBS depends on the relative value associated with each ecosystem service and the increase or decrease in that service provider. By considering only nutrient reduction, it is possible to compare the impact of each scenario and considering overall changes in main drivers related to climate and land use. The results based on the simulated nutrient load and delivery under four different NBS scenarios, A0B0, A1B0, A0B1 and A1B1, show significant differences. There is a clear potential for a reduction in nitrogen export in 2050 for all scenarios. This was associated with reduced expected precipitation of 1363 mm/year compared to 1653 mm/year in 2018, particularly in the elevated alpine parts of the catchment. In fact, the largest reduction in nitrogen export was achieved by reforestation of the upper catchment (B1). This NBS alone provides a potential reduction of 328 tonnes/year. The costs of natural reforestation are limited, and the benefits to lower catchment and receiving waters (Adriatic Sea) could be translated to support for farmers to manage these lands as productive forests. It is expected that the new European agricultural policy will incentivize this transformation of land use. On the other hand, N and P loads from urban wastewater represent a significant source (Cozzi et al., 2018). Recent studies on lowland rivers that have created riparian buffer strips have shown an elevated efficiency to remove nitrate (Gumiero and Boz, 2017).

The overall best scenario is the combination of NBS approaches in both the lower and upper parts of the river. Under the A1B1 scenario, nitrogen export was reduced by 340 tonnes/year in 2050.

Efforts to reduce phosphorus export are complicated by an expected increase in rainfall intensity in 2050 in relation to the soil characteristics of the Piave river catchment. This increased export is partially mitigated by the A1 and completely reversed in the B1 scenarios. The best scenario is the A1B1 scenario which showed a 148 ton/year reduction in phosphorus export.

To properly estimate the benefits of the proposed NBS, the impacts on other ecosystem services should be considered. Several of these (flood risk reduction, carbon storage and water yield) may be highly significant. However, to explore only those associated with nutrient reduction, I used costs associated with similar NBS projects focused on nutrient reduction to the Venice Lagoon (CBAR, 2021). These projects (Table 15) had a range of secondary benefits that were not evaluated in the present analysis. The estimated costs for the associated reduction for nitrogen and for phosphorus were calculated using a multiple linear regression analysis ($R^2 = 0.79$, $p < 0.001$).

Table 15 The cost of individual NBS projects and the associated annual reduction in N and P in the Veneto region.

Euro	N Tot Ton/Year	P Tot Ton/Year
7,230,000 €	44.9	3.2
4,130,000 €	27.4	1.47
6,600,000 €	43.49	1.4
3,160,000 €	4.9	0.5
825,000 €	1.066	0.45
1,560,000 €	2.14	0.50
2,450,000 €	5.8	0.66
1,650,000 €	4.31	0.66
1,440,000 €	2.56	0.22
1,000,000 €	1.08	0.28
2,066,000 €	18	0.81
1,033,000 €	13.94	1.56
3,430,000 €	5.02	1.08

With an expected intervention cost of EUR 1,128,836 (y-intercept), the cost per ton of N removed by NBS amount was 10.88 EUR/kgN per year. The estimated cost for P was approximately double or 23.83 EUR/kgP per year. These compare well to estimated costs from wastewater treatment upgrades reported by Gratziou and Chrisochoidou (Gratziou et al., 2013), who estimated that for nitrogen removal, the cost of a project varies from 4613 EUR/m3 to 488 EUR/m3, with total annual operation cost ranges from 204 EUR/m3 to 17 EUR/m3. The unit cost for P removal in different treatment alternatives ranges from 80 EUR/kgP to 120 EUR/kgP (Bashar et al., 2018). Jabłonska et al. (2020) estimated the costs of a hypothetical establishment of wetland buffer zones to reduce the non-point source of N and P to be EUR 9 ± 107 M to remove 11%–82% N and 14%–87% P load from the catchment. This translates into a cost that is saved due to the lack of eutrophication and the problems associated with it (Spillman et al., 2007).

Considering the annual reduction in nitrogen and phosphorus exports achieved using NBS (A1 and B1), compared to scenarios with no NBS (A0, B0), the value of these interventions per year is equal to EUR 2,244,677 for A1 and EUR 2,610,888 for B1, using 2018 values. Given the long-term benefits and multiple risks of climate change, as well as the important secondary benefits, the NBS solutions are well justified.

3.5. Conclusions

There is growing awareness that NBS can mitigate climate change impacts while securing ESs. The results from the present study, estimating nutrient load and delivery under four different NBS scenarios, suggest that the nutrient load and delivery in the Piave river catchment would benefit from NBS actions, one of which is already underway through rural abandonment. Upper catchment reforestation has increased wooded areas in agricultural lands that are no longer used by local farmers. Reduced water runoff and sediment loss have had and will continue to have positive impacts on sediment, nitrogen and phosphorus loads to the river.

The proposed NBS for the lower catchment (32 km) riverine corridor, based on increased riparian vegetation and erodible areas (A1), will have a more complex activation due to the intense agricultural and urban use that characterizes this part of the catchment. An increase in vegetated areas in the riparian area will reduce the transport of phosphorus-loaded particulates from agricultural soils as a result of erosion. While A1 has a smaller effect on overall nutrient export with respect to B1, this NBS is likely to have more impacts on other major ecosystem services related to biodiversity and recreational value due to the more elevated population density. Decreasing trends in P export by rivers in Europe have mainly resulted from environmental and agricultural policies leading to reduced nutrient inputs to river catchments. On the other hand, nitrate remains a major challenge in many catchments and already compromised receiving waters, such as the Adriatic Sea. The IPCC Climate Change and Land Report (2019b) emphasizes the need to explore the mitigation potential of restoration actions and the improved management of forests.

It is clear that increased participation in the management and monitoring of our river environments is necessary to improve their status further. Citizen science represented an additional tool to complete the information and for model validation in this study and others. Involving citizen participants directly in monitoring activities can generate a powerful tool to complete the lack of information and improves communities' influence on management policy in their territory. Understanding the direct and indirect influence of human activities is the first step to evaluate the economic value of nutrients removal. Our estimated cost reflects the gains from investing in NBS and shows how the evaluation of ecosystem services can provide a complete evaluation of where and how watersheds can implement these approaches.

This study resulted in the manuscript entitle "Ecosystem Services Evaluation of Nature-Based Solutions with the Help of Citizen Scientists" (Di Grazia et al., 2021) published in September 2021 in the journal Sustainability (IF 2020 of 3.25).

4. CARBON MODELS AND DYNAMICS

4.1. CARBON (STORAGE AND SEQUESTRATION)

4.1.1. Background

Knowing the carbon dynamics is fundamental for developing an accurate model able to predict the possible impacts caused by climate change (Reichstein et al., 2013). C is also crucial in biogeochemical processes and ecosystem for the numerous functions it covers like energy source for trophic chains, regulator of the depth to which solar radiation can penetrate aquatic environments, control factor for the bioavailability of toxic compounds, etc. (Archer, 2010).

Vegetation and forest soils constitute an important terrestrial carbon pool with the potential to absorb and store carbon dioxide (CO_2) from the atmosphere. Since a large fraction of organic carbon (OC) is stored in terrestrial ecosystems, their sustainable management cannot ignore the identification of the areas that contribute most to its storage (Guo et al., 2020).

Evidence of climate change linked to human-induced increases in greenhouse gas (GHG) concentrations is well documented by the IPCC (2019a). The recognized importance of forests in climate change mitigation has led countries to study their forest carbon budgets and to start an assessment to improve and maintain the carbon sequestration of their forest resources (Lal, 2005).

The storage and release capacity of carbon in the Piave basin is an important ecosystem service and, at the same time, sensitive to the land use policies applied in the territory. I developed and validated a model for georeferencing the C stocks currently stored in the territory and the C stocks that will be sequestered over time (Carbon Storage and Sequestration).

4.1.2. Material and Methods

4.1.2.1. Carbon storage and sequestration model

In terrestrial ecosystems C is distributed in four main compartments: aboveground biomass, belowground biomass, soil and dead organic matter. Each may vary with a particular land use or cover and therefore be significantly affected by the effect of land management policies.

Within each land use class, the C density value expressed in Mg/ha of the various compartments was established, based on local data for the Lower Piave basin. The total C density by type of land use is made up of the individual compartment's aggregation, with the georeferencing in raster format of the C density in Mg/pixel currently stored in the study area.

The previous procedure was applied to alternative land use scenarios in which the

geographical distribution or the extension of the land use areas changes. After that the difference between the C stocks of the future and the base scenarios can be determined. Positive values indicate an increase in the C stored in the landscape and therefore its sequestration by the ecosystem, instead negative values show a loss with reduction of the C stock corresponding to a given pixel, therefore a loss towards the atmosphere.

4.1.2.2. Input data for the Piave river basin

To develop the Carbon Storage and Sequestration model, data from numerous sources was collected to produce the necessary spatial information. The land use raster map at 20m resolution) represents the baseline (2018) of the model and can be modified depending on the NBS scenarios (A0, A1, A2, B0, B1, C0, C1). The future land use map represents the combination of the developed land use variation scenarios (A0, A1, A2, B0, B1, C0, C1). The future scenarios (2050), including climate change according to the RCP 4.5 model of the IPCC report AR5 (2014), is located in the study area between the banks of the Lower Piave and in the upper basin (A0, A1, A2, B0, B1, C0, C1).

The biophysical table contains a "lucode" identification number for each land use class which must match in the land use raster and with the respective density value (Mg/ha) for each Carbon pool (aboveground biomass, belowground biomass, soil and dead organic matter).

C_above - The density of C above ground (CA, Mg/ha) for non-forest and cultivated woody biomass land use classes is based on studies and estimated values published in Eggleston et al. (2006), while for types of land use characterized by forest woody biomass the values reported in Nonini and Fiala (2021) were used, except for class 3116 "Hygrophilous woods". For it, in fact, it was possible to make a specific estimate (Eq. 10) thanks to the surveys carried out by the TESAF of the University of Padua (unpublished data):

$$CA = \rho \cdot V \cdot F \quad (10)$$

where ρ (ton/m^3) is the basic density of poplar wood in plantation (Federici et al., 2008); V is the volume of biomass per unit area (m^3/ha) estimated by TESAF and F is the dry biomass to dC conversion factor (IPCC, 2006).

C_below - For land use classes with non-woody biomass the difference between OC Tot and C_above was calculated while for land use with cultivated woody biomass the data are based on studies and values estimated by Eggleston et al. (2006). I assigned the values reported in Nonini and Fiala (2021) to the types of land use with woody biomass.

C_soil - For the lower Piave area: "Soil Organic C layer in the first 30 cm of depth" surveyed between the years 1994 and 2006 on a non-continuous basis by ARPAV (2022a). With the tools available on the QGIS v.3.22 software, the C value of the individual polygons

classified according to land use was extracted. From these, the total area-weighted C-content average of each land use class was calculated. For the remaining part of the basin, as databases of equally high quality are not available, the average density for each class was extrapolated from the OC stocks in the soil made available by the Veneto Region (2007).

C_dead - The density of C in the woody forest land use classes is given by the sum of the dead mass and litter density values (Nonini and Fiala, 2021) (Eq. 11):

$$C_D = \frac{TCS_F \cdot (14.36+7.27)}{100} \quad (11)$$

Calculation of C_D (Mg/ha) in the dead organic matter compartment, where TCSF is the density of total C and 14.36 and 7.27 respectively the percentages of necromass and litter with respect to the total. Following the estimates reported by IPCC (2006) and by Nonini and Fiala (2021), I used 0 Mg/ha for non-forested land use classes, and literature values for land use classes with woody biomass.

4.1.2.3. Characterizations of the chromophoric dissolved organic matter (CDOM)

A field sampling campaign was carried out focused on the carbon element (Fig. 28) present in the river. The study is aimed at identifying possible seasonal variations of CDOM, the chromophoric fraction of DOM (Dissolved Organic Matter) in the aquatic compartment, and therefore represents both a validation of the model and ARPAV data and a further development of ecosystem services models. For each station, measurements were carried out during three campaigns: July, September, and November, useful for describing the temporal variability.

Figure 28 The equipment used during the field sampling.

The objective of the sampling is the description of the CDOM, in the lower course of the Piave river through its absorbance characteristics. In fact, these parameters can be used as indicators of the concentration of organic matter dissolved in the riverbed and of its degree of degradation. Together with the CDOM measurements, a procedure will be set up to estimate the dissolved component of organic carbon (DOC) in the lower course of the Piave river. This will allow comparison with measurements of the same parameter carried out in 2018 by ARPAV, thus providing additional information regarding aquatic C to outline the most precise picture possible.

The sampling sites selection (Fig. 29) considered the sites previously selected in the citizen science activity in order to have accessibility to a larger number of stations and a more comprehensive set of data: CDOM, nitrates, phosphates, specific conductivity, temperature, turbidity. The section of the Piave river considered in this data collection campaign goes from Ponte di Piave to the mouth and includes the Piave Vecchia, the period instead intends to cover at least one phase of low water and one of ordinary flood.

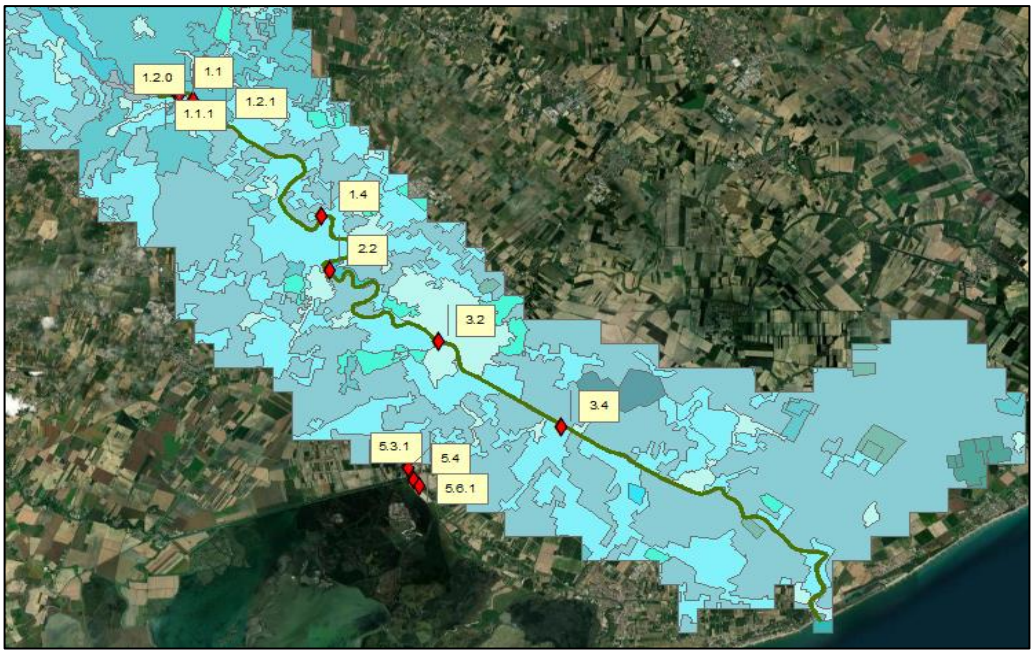

Figure 29 CDOM sampling sites in the lower Piave (green line) indicated with a red diamond. Sites 5.3.1, 5.4, 5.6.1 are located along the Piave Vecchia.

4.1.2.3.1. Field sampling activities

The methodology applied includes:

1. Rinse the sampling device three times with the water from the site sample.
2. When sampling, make sure that the device is fully submerged to collect only surface water without moving the bottom sediment.
3. Carrying out the turbidity test (NTU) using the Secchi tube.
4. Rinse three times the syringe (capacity 24 mL).
5. Taking the sample with the syringe to which a filter is subsequently applied (PES 0.20-0.22µm; brand MilliporeExpress, model Millex-GP).
6. Filling of a numbered test tube (15mL capacity; brand SIGMA-ALDRICH, model SIAL0719) with at least 14mL of filtered sample.
7. Conservation of the sample in a refrigerated environment (in a thermal container with ice cubes or, when possible, in the refrigerator).
8. Steps 3-6 were repeated for a total of three samples at each site.
9. Filling the field form with the information necessary to identify the site, operator, date and time, specific conductance (µs/cm@25°C) and temperature (°C).

4.1.2.3.2. Spectroscopy laboratory activities

The setup of the experimental phases was conducted in the spectrophotometry laboratory on 22 July, 16 September and 11 November 2020 making sure that no more than 48 hours elapsed between taking the samples and observing the DOM.

A preliminary phase consists in setting the spectrophotometer (PerkinElmer Precisely, model Lambda 25 UV/VIS Spectrometer): i) bring to temperature the radiation source lamps, ii) set the number of samples based on the specific collection campaign (UV-WinLab software); iii) make the "baseline" with an empty chamber to eliminate any background noise from the measurements.

At this point, a reference sample containing distilled water ($MilliQ_{t0}$) is analysed, which is then repeated also at the end of the process ($MilliQ_{t25}$) to ensure constant operation of the spectrophotometer, with a carefully cleaned 10mm thick quartz cuvette. The operation is done manually with the use of distilled water and absorbent paper, while the removal of the cellulose fibres from the cuvette is made easy by a flow of gaseous nitrogen. When the result is not satisfactory residues and streaks are eliminated with a 0.2% nitric acid (HNO_3) solution.

Once the instrumentation was ready, the steps listed were followed:

1. Fill the cuvette with a fluid gesture to avoid the formation of gas bubbles.
2. Insert the cuvette into the spectrophotometer taking care to always turn it to the same side.
3. At the end of each measurement check that no condensation has formed on the cuvette, especially if the samples are stored at a temperature lower than room temperature.
4. Between the analysis of a sample and the next, rinse the cuvette with distilled water and clean it thoroughly.
5. Begin and end measurements with analysis of distilled water samples, $MilliQ_{t0}$ and $MilliQ_{t25}$.
6. Store samples in a refrigerated environment.

The spectrophotometer irradiates the filtered samples with radiation, whose wavelength (λ) is located between 200-750 nm and records the absorption by the particles in the aqueous solution.

The data analysis focused on two parameters that describe CDOM, absorbance (*A*) and slope (S), through which it is possible to respectively evaluate the concentration and conditions of degradation of the organic matter (Loiselle et al., 2009b). To determinate S at each wavelength, a nonlinear regression fitting method was used on the open-source software package, Scilab 6.1.0 (ESI Group, 2020). Each run provides estimates of spectral slope and correlation

coefficient (R^2) for all wavelengths between 200 and 700 nm, according to the interval size chosen, with a 1-nm step. The minimization of the least squares between residuals and the experimental data was based on the Levenberg–Marquardt algorithm, which is particularly well suited for nonlinear functions.

The corrected spectral absorbance, $A^{\circ\circ}$ (m^{-1}), was calculated as the mean of the measurements of the samples collected, in triplicate, for each of the eight sites of the study area, corrected by subtracting the baseline and distilled water (Eq. 12).

$$A^{\circ\circ}{}_i = A_i - A_{MQi} - A_{700} \quad (12)$$

Where $A^{\circ\circ}$i is the i-th absorbance corrected for the absorbance of distilled water and g scattering effect (700 nm in the July and September campaigns; 650 nm in the November campaign), Ai is the average absorbance of the samples of a site during a campaign for the i-th wavelength, A_{MQi} is the absorbance of the distilled water for the i-th wavelength. The spectral slope (S, nm^{-1}) describes the rate of decrease in absorbance as wavelength increases, approximating it to an exponential curve (Massicotte et al., 2017). Its value is calculated with Eq. 13 (Loiselle et al., 2009b):

$$a(\lambda) = a^0 \cdot e^{S(\lambda 0 - \lambda)} \quad (13)$$

where a^0 (m^{-1}) is the absorption coefficient at wavelength λ_0 (nm).

4.1.2.3.3. DOC estimation methods from CDOM

In aquatic systems the relationship between the concentration, hereinafter indicated in square brackets [ ], of DOC and the optical absorbance properties of Chromophoric DOM (CDOM) is strong. However, it has been observed on a global scale that its solidity varies according to the ecosystems studied, progressively decreasing from wetlands (R^2 = 0.94) to oceans (R^2 = 0.44) as visible in Figure 30 (Massicotte et al., 2017).

Several researchers in the last decade have dealt with how to estimate [DOC] from CDOM is due to the ease and low cost with which spectroscopic analysis can be performed as an alternative to the traditional procedure for the quantification of DOC (Spencer et al., 2012). The calculation of C flows towards coastal waters could take advantage of a simplified methodology and, with a higher amount of field data, the estimate of the values would be closer to reality, promoting the study of the drivers that condition the spatial and temporal C dynamics.

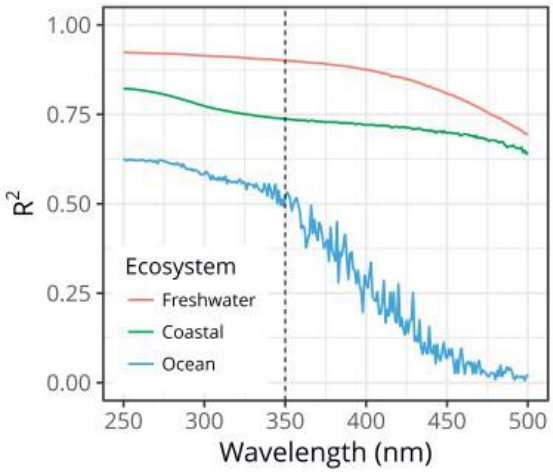

Figure 30 The graph shows the robustness (R^2) of the relationship between the DOC concentration and the absorption coefficient at different wavelengths. The colours highlight three distinct groups of samples belonging to as many ecosystems (Massicotte et al., 2017).

Previous studies interested in ecosystems with characteristics comparable to the Lower Piave are reported in chronological order and briefly described below. For the purposes of this thesis, it is necessary that the estimation method is applied to an environment as similar as possible to that of study, so that the number of potential variables is reduced, and that it is based on a relationship between the absorbance (A, m^{-1}) of CDOM and [DOC].

Fichot and Benner (2011) developed a model for coastal environments in the northern Gulf of Mexico region in which some samples collected in freshwater conditions were also considered, although a correlation analysis between [DOC] and salinity shows an R^2 weak, equal to 0.18, when the latter drops below 20 psu. The relationship is expressed by Eq. 14:

$$ln[DOC] = \alpha + \beta\, ln\left[A_g(275)\right] + \gamma\, ln\left[A_g(295)\right] \qquad (14)$$

where α, β, γ are regression coefficients available in the literature; $A_g(m^{-1})$ the absorption coefficient at the wavelength of 275 and 295 nm respectively and [DOC] the concentration of DOC expressed in µM/L.

Spencer et al. (2012) assembles a dataset comprising 30 US rivers crossing terrains with different lithology and characterized by variable climates and degrees of anthropization.

Analysed optical properties, including A_{254}, A_{350}, A_{440}, were used to describe dissolved OC concluding that absorbance has a strong positive correlation with [DOC] for almost all studied rivers, except for some rivers whose DOM comes from autochthonous, anthropic or allochthonous but clearly photodegraded origin.

At the same time another study was carried out on the Willow Slough River (CA, USA) whose basin is mainly agriculture, with typical Mediterranean climate (Hernes et al., 2013).

The measurements carried out on its waters showed a positive linear correlation ($R^2 = 0.95$; $p<0.0001$) between [DOC] and A_{350} regardless of the current hydrological regime.

The need to synthesize the CDOM and [DOC] data collected up to then in very different ecosystems motivated the work of Massicotte et al. (2017) whose database summarizes another 65 for a total of over 12,800 measurements and elaborate the Eq. 15:

$$log\, A_{CDOM}\,(350) = -15.09 + 9.31 \cdot log[DOC] \quad (15)$$

where A_{CDOM} is the absorption coefficient (m^{-1}) at 350 nm and [DOC] is expressed in μM L^{-1}.

In contrast to the study conducted by Hernes et al. (2013) where the area of interest showed several points in common with the Lower Piave, both in terms of land use and environmental conditions, the one conducted by de Matos Valerio et al. (2018) on the final stretch of the Amazon River showed a lower degree of similarity. However, the researchers divided the analysed samples into two groups based on the different turbidity, distinguishing the main channel with a high load of suspended particles from the tributaries with clearer waters (CW, clearwater). In this publication, the analysis are presented separately before integrating the data into a single model, therefore it is possible to consider only the parameters elaborated for the tributaries closest to the characteristics of the Piave. The correlation between the concentration of dissolved C in low turbidity water bodies and the absorbance at 412 nm ($R^2 = 0.57$; $p<0.05$) is described by the following equation (Eq. 16):

$$[DOC] = a \cdot A_{412} + b \quad (16)$$

where [DOC] is measured in μM/L; *a* and *b* are the coefficients for CW.

Although the results reported by a good number of authors recognizing the absorbance of CDOM as a valid indicator of the fluvial DOC concentration, other scientists suggest caution in using this proxy, especially if the stream is subjected to strong anthropogenic pressures (Yates et al., 2016).

In the Lower Piave scenario it was considered that the most suitable procedure was the one proposed by Hernes et al. (2013).

First, the $A^{\circ\circ}{}_{350}$ (m^{-1}) was converted into an absorption coefficient a_{350} (m^{-1}) with Eq. 17 where L (m) is the length of the cuvette:

$$a_{350} = \frac{A^{\circ\circ}_{350} \cdot 2.303}{L} \quad (17)$$

From the data of Hernes et al. (2013), the linear correlation between [DOC] and a_{350} was calculated obtaining Eq. 18:

$$[DOC] = 0.3527 \cdot a_{350} + 1.0664 \quad (18)$$

The flow calculation (F, Tg year^{-1}), the mass of C exported from the Piave to the Adriatic coast, consists of the product of the flow rate (Q, m^3/s), whose annual value is strongly correlated to F (M. Li et al., 2017), [DOC] and the number of days (*t*) of the period considered (monthly or yearly) (Eq. 19). The flow rate and concentration parameters are assumed to be constant within the time interval *t*.

$$F = Q \cdot [DOC] \cdot t \quad (19)$$

Estimation of the flow rate for the study area was made using the measurements of the complete historical series in the Ponte di Piave station. for the years 2004, 2008, 2012, 2015-2017 (ARPAV, 2018f).

4.1.2.4. Riparian vegetation monitoring

In view of the importance of riparian vegetation on the carbon cycle in river waters, essential information relating to its characteristics were collected from citizens using a specially developed method. The reference procedure of the RiVE methodology is currently being tested and was developed in collaboration with ISPRA (Prof. Gumiero B., personal communication).

Trained citizen scientists collect the observations on the Survey123 for ArcGIS application (ESRI, 2021) or, alternatively, on data sheet paper forms which are subsequently uploaded manually into the ISPRA IT platform (NNB, 2021). The training activities is mandatory and necessary to be able to learn the sampling procedure. The datasheet information consists of:

- Date and sampling location.
- Overall vegetation structure.
- Percentage coverage of the reference botanical species in three different layers (0-1m; 1-3m; >3m).
- Maximum height (m) of the vegetation.
- Size of the transept, homogeneous in structure and composition, perpendicular to the river (length x width, m x m).
- Number of trees fallen or dead.
- Degree of artificiality and banks erosion.
- 2 photographic data: 1 photograph of the entire site, 1 photograph of the site where the river is also visible.

4.1.3. Results

4.1.3.1. Carbon storage model

4.1.3.1.1. Comparison of 2018 scenarios

The comparison between the different base scenarios developed for the 2018 showed the highest C stocks for scenarios that increase the wooded area in the basin (e.g., A2 and B1). The best scenario for carbon sequestration was represented by B1 (reforestation scenario) with an increase of C stored by 1.8% (Table 16). This can be explained based on the definition of the aboveground biomass and dead organic matter compartments: in both it is assumed that the contribution of non-woody biomass is so small that it can be neglected. It follows that the categories of land use characterized by woody biomass record C density values much higher than the others. Since these categories are mainly forest types common to higher altitudes but extremely rare in the agricultural landscape of the hills and plains, the output of the model is justified.

The mountain areas characterized by forest cover are those that most contribute to providing the carbon storage ecosystem service (Fig. 31). The river restoration scenario (A1) inside the Lower Piave banks showed minus impact on the sequestration linked to the small size of the area compared to the basin scale and to the presence of the erodible strip which improves the hydro-geomorphological functions of the river but has no effects on the sequestration of carbon. The conversion of the entire area inside the banks of the lower Piave into riparian forest (A2) showed a greater impact than in scenario A1 in carbon storage. The size of the wooded area inside the banks is small compared to the wooded areas upstream, but the C storage effects produced inside the banks are nonetheless significant for climate change mitigation policies.

The best combination of scenarios, reforestation upstream (B1) and the conversion of hygrophilous forest inside the banks of the lower Piave (A2) (Fig. 32), showed the carbon storage effects of the two scenarios add up, reaching the percentage of 1.90% (Table 16) or 7.78×10^5 tonnes of C stored.

Table 16 Variation in carbon storage based on 8 management scenarios of the Piave river basin under current climatic conditions (2018).

2018	C Basin		C Basin %	C Basin Δ
Scenario	Tot C base (tonnes)	Tot C future (tonnes)	ΔC %	ΔC (tonnes)
C0, A0, B0	**4.10 x10^7**	-	-	-
C0, A1, B0	4.10 x10^7	4.10 x10^7	0.02	9.82 x10^3
C0, A2, B0	4.10 x10^7	4.10 x10^7	0.10	4.11 x10^4
C0, A0, B1	4.10 x10^7	4.17 x10^7	1.80	7.37 x10^5
C0, A1, B1	4.10 x10^7	4.17 x10^7	1.82	7.47 x10^5
C0, A2, B1	4.10 x10^7	4.18 x10^7	1.90	7.78 x10^5

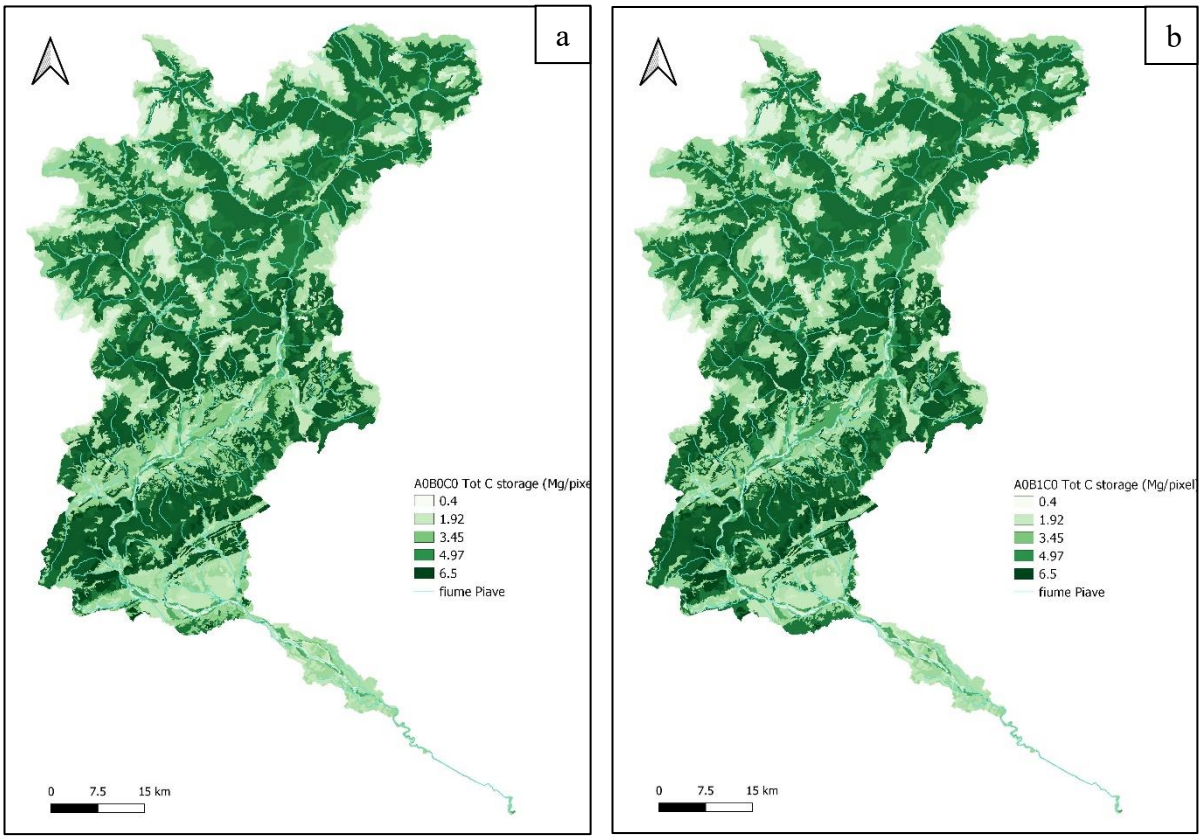

Figure 31 Spatial distribution maps of carbon storage for 2018 referring to the base scenario (a) and scenario B1 of upstream reforestation (b).

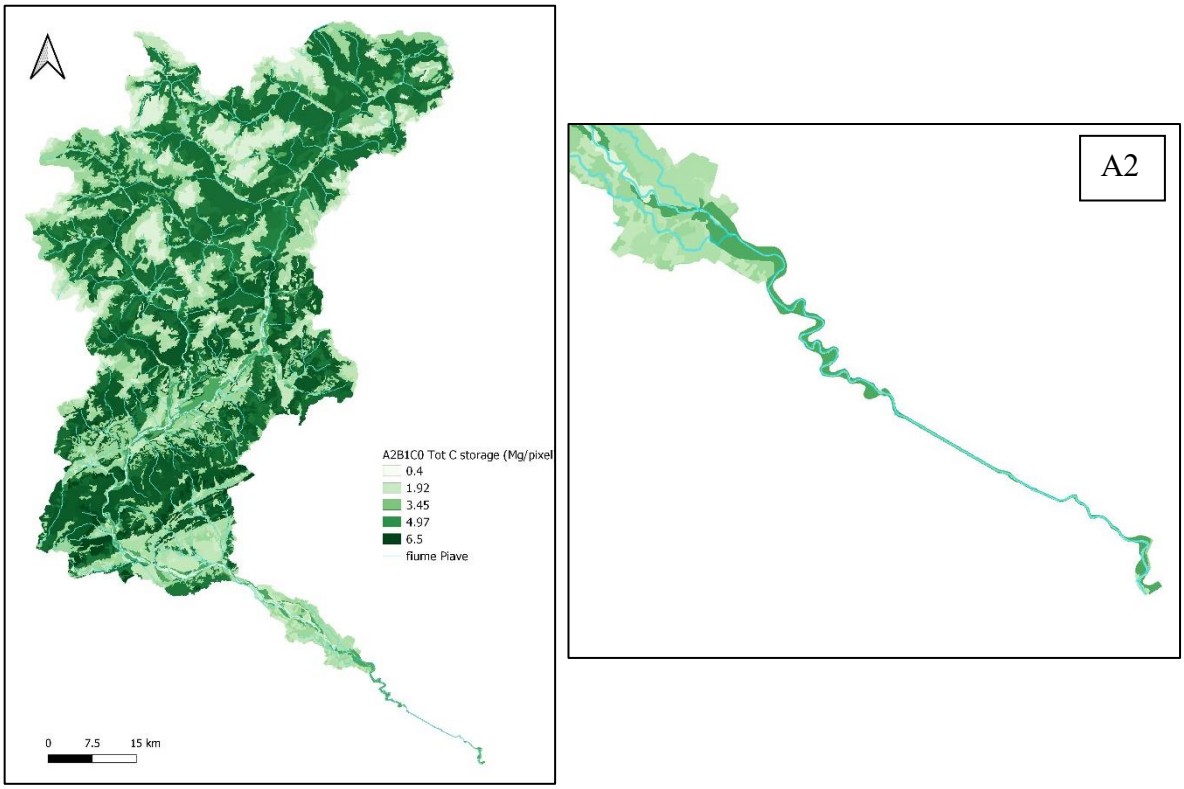

Figure 32 Spatial distribution map of carbon storage for the combination A2B1, reforestation upstream (B1) and inside the banks of the lower Piave (A2) with detail of storage in the lower Piave.

4.1.3.1.2. Comparison of 2050 scenarios

Recent study projections were used to compare 2050 model estimation of SOC, aboveground mass and dead organic matter. The projections of SOC in Italy in the context of climate change (Caddeo et al., 2019) estimated a moderate loss of C. The MIROC5-RCP4.5 model for forest areas showed an increase in aboveground mass and dead organic matter in 2050 (Valipour et al., 2021). The 2050 scenarios showed an increasing trend in carbon storage compared to the 2018 scenarios (Figures 33 and 34). The conversion of agricultural areas into forested areas promote an increase in the stock of C stored and therefore its net sequestration. The sector that undergoes the most significant change is the aboveground biomass which, in the transition from mainly herbaceous to woody vegetation, showed an increase in the density of C per hectare.

Carbon stored by European forests is currently increasing thanks to changes in forest management, as scenario B1 well represented (Table 17). In the lower Piave, scenario A2 showed the best conditions for further storing the 3.45% carbon (Table 17). About half of the carbon is stored in forest soil. However, when forest are damaged or cut, the carbon is released

back into the atmosphere. Furthermore, ploughing agricultural land accelerates the decomposition and mineralization of organic matter. To keep carbon and nutrients in the soil, cultivation should follow the principle of crop rotation using so-called "break crops" and leaving crop residues on the soil surface.

The best combination also in this case is given by the combination of the B1 and A2 scenarios, an increase in wooded area upstream and downstream, that showed a high percentage of carbon stored in the basin equal to 2.28×10^6 tonnes of C.

Table 17 Change in carbon storage based on 12 management scenarios of the Piave river basin under future climate conditions (2050).

2050	C Basin		C Basin %	C Basin **Δ**
Scenario	Tot C base (tonnes)	Tot C future (tonnes)	ΔC %	ΔC (tonnes)
C0, A0, B0	4.10×10^7	4.23×10^7	3.30	1.35×10^6
C0, A1, B0	4.10×10^7	4.23×10^7	3.35	1.37×10^6
C0, A2, B0	4.10×10^7	4.24×10^7	3.45	1.41×10^6
C0, A0, B1	4.10×10^7	4.32×10^7	5.43	2.22×10^6
C0, A1, B1	4.10×10^7	4.32×10^7	5.48	2.24×10^6
C0, A2, B1	4.10×10^7	4.33×10^7	5.57	2.28×10^6
C1, A0, B0	4.10×10^7	4.23×10^7	3.26	1.33×10^6
C1, A1, B0	4.10×10^7	4.23×10^7	3.31	1.36×10^6
C1, A2, B0	4.10×10^7	4.24×10^7	3.40	1.39×10^6
C1, A0, B1	4.10×10^7	4.32×10^7	5.38	2.21×10^6
C1, A1, B1	4.10×10^7	4.32×10^7	5.43	2.23×10^6
C1, A2, B1	4.10×10^7	4.32×10^7	5.53	2.27×10^6

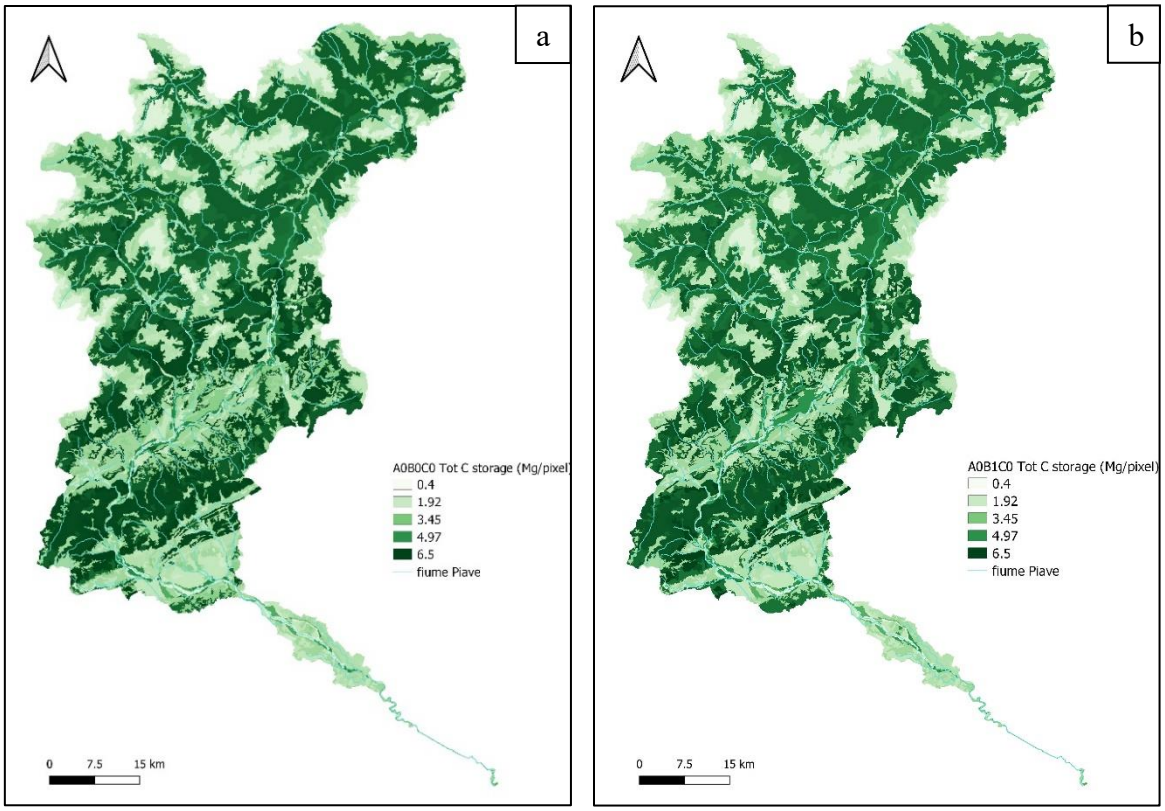

Figure 33 C storage spatial distribution maps base scenario (a) and scenario B1 (b) for 2050.

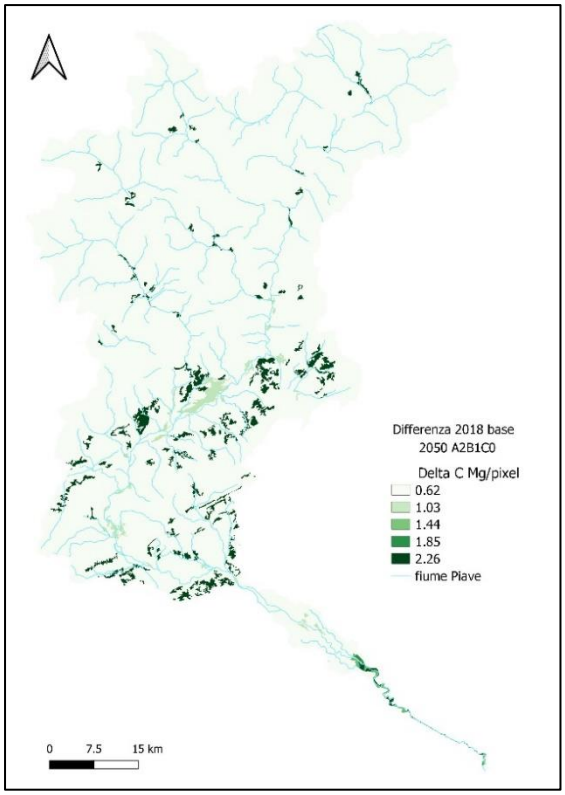

Figure 34 C storage difference map between the 2018 baseline scenario and the best combination of two A2B1 scenarios in 2050.

4.1.3.1.3. Model validation with CDOM

The validation of the C density data for each of the four C pools was performed thanks to the collaboration with TESAF, the citizen scientists monitoring activities and with measurements performed in the field. The collaboration with the Prof. Emanuele Lingua and his research group of the University of Padua has provided information on the riparian vegetation biomass of the lower Piave River.

The wooded biomass and necromass data were used to validate the OC stored in the above ground biomass and dead organic matter. For the root biomass of the riparian forest formations was performed a conservative estimation; in fact, this environment is subject to anthropic and natural coppice, caused by floods, which leads to an alteration of the relationship between the surface mass of the tree and the buried mass (Dr. Niccolò Marchi, TESAF, personal communication).

When the data collection campaign does not cover the area of interest, the validation of the model took place with the comparison of published studies available in the literature e.g., Nonini and Fiala (2021) study area showed geographical and climatic characteristics similar to the lower Piave river.

To validate the carbon storage and sequestration model I also used the spectroscopy analysis result conducted in the Environmental Spectroscopy laboratory at UNISI, on the water samples collected in the July, September and November 2020 campaigns.

The absorbance spectra of CDOM showed a decreasing trend that approximates an exponential curve in the interval between 200 and 250 nm (λ) after which they tend to $0.00 m^{-1}$. Some of the spatial differences' observable within the same collection campaign concern the width of the peak which in the main channel of the Piave reaches a maximum of $2.29\ m^{-1}$, thus always placing itself below the Piave Vecchia except for July (Fig. 35).

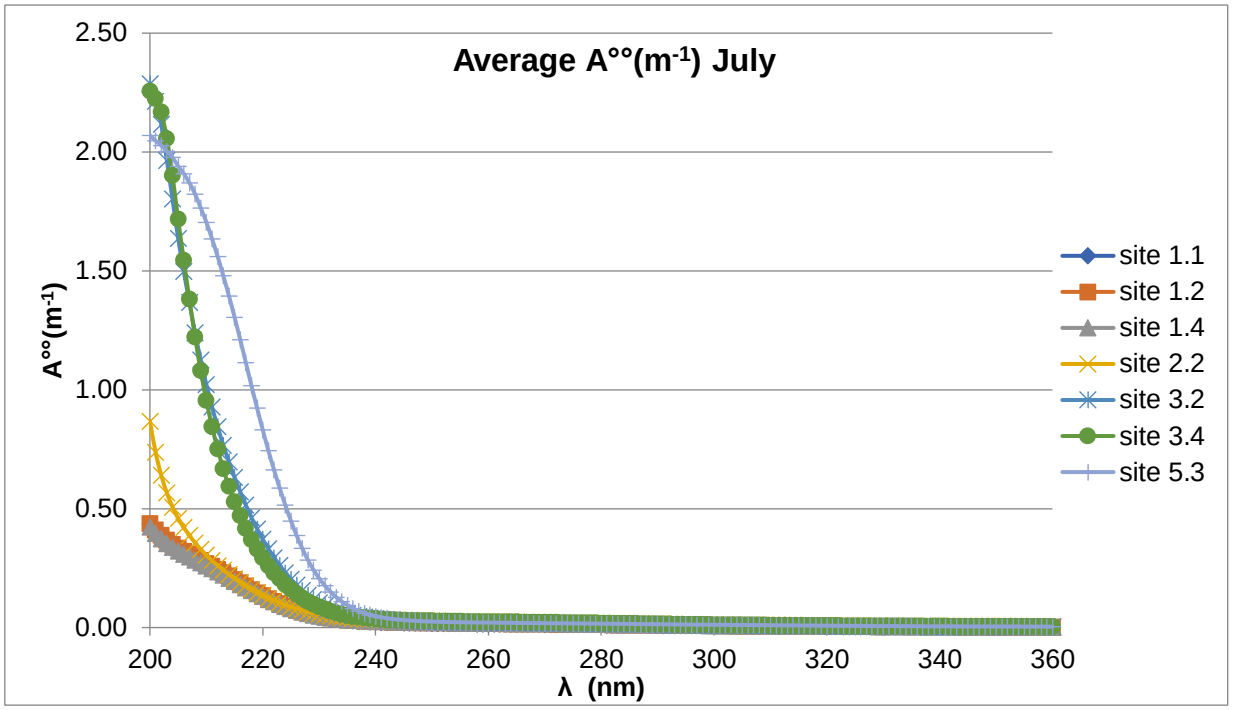

Figure 35 Spectrum of A°° (200-350 nm) average per site observed in the Lower Piave on 20 July 2020.

These anomalous values exactly correspond to the two specific conductance maxima, respectively 30300 µs/cm in section 3.2 and 40300 µs/cm in section 3.4. The sites upstream of Romanziol (site 1.4) were characterized by a strong homogeneity within each data collection period and by lower absorbance measurements than the other samples.

As regards the shape of the spectrum, it is particular the oscillation detected at the lower end of the wavelengths investigated (200-210 nm) at the Piave Vecchia sites in November. On the field, a recent cut of the herbaceous vegetation was observed both on the bank and below the water level. In the literature, a conventional value of λ to refer to has not been established, therefore each researcher uses the most appropriate for his study, some of the most frequently occurring ones are in the range 254-350 nm (Eckard et al., 2020; Spencer et al., 2012). I selected $A^{\circ\circ}_{270}$, $A^{\circ\circ}_{280}$ and $A^{\circ\circ}_{350}$ as benchmarks as they better capture the longitudinal variability of CDOM in the Lower Piave.

Through Pearson's correlation analysis the relationship between $A^{\circ\circ}_{i}$ and specific conductance was investigated, however a positive linear relationship was found only in July at 280 nm ($R^2 = 0.84$; $p<0.05$) (Fig. 36).

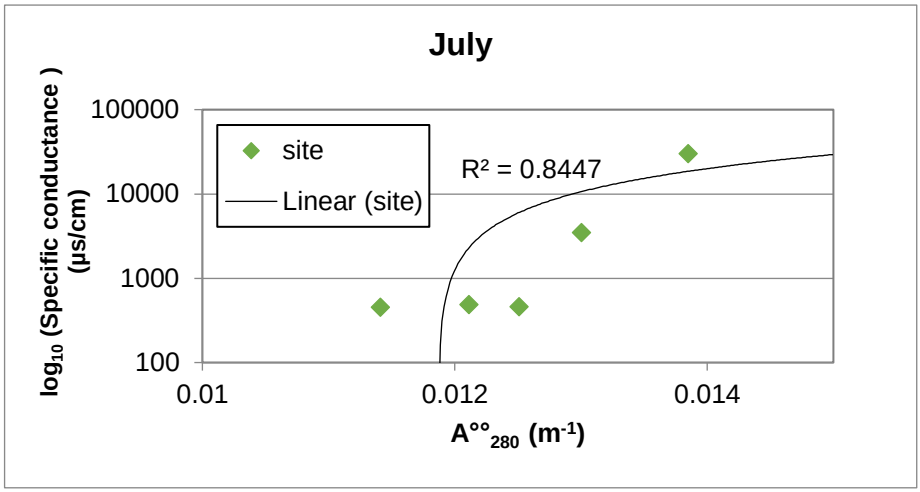

Figure 36 Positive linear correlation between A°°$_{280}$ and specific conductance (on a logarithmic scale) in the sampling of 20 July 2020.

A further interesting results that emerged in the study area was the positive correlation established in July ($R^2 = 0.79$; $p<0.05$) and November ($R^2 = 0.74$; $p<0.05$) between A°°$_{270}$ and the distance (m) of each site from the one most upstream (Fig. 37). This relationship was maintained in the autumn for all wavelengths considered. Furthermore, the seasonal trend was evident, also visible in the absorbance spectra, according to which A°°$_{270}$ in November was higher than in July which in turn exceeds that of September ($p<0.05$).

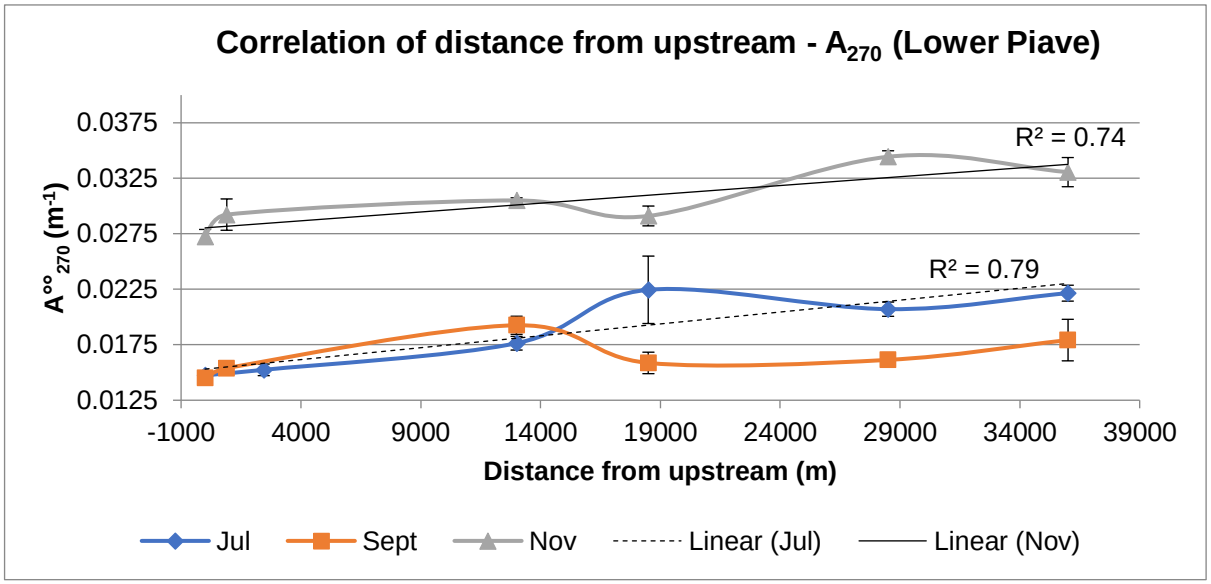

Figure 37 Positive linear correlation between A°°$_{270}$ and distance from upstream (site 1.1) in the three monitoring campaigns.

The slope (S, nm^{-1}) was the second parameter used to describe the CDOM, in particular the state of degradation. The S value in the various stations of the Lower Piave ranges between 0.01 nm^{-1} and 0.021 nm^{-1}, in line with the results of Hernes et al. (2008) and allows to clearly

recognize the main river (PN) from the old riverbed (PV), with a statistically significant difference (t-test, $p<0.05$) between the sites along the PN (Fig. 38) and those on the PV (Fig. 39) respected in almost all cases. While in the Piave Vecchia the seasonal variation was minimal, in the PN it was marked, being characterized by higher values in summer than in autumn. Then, during the first two months observed, there was a similarity of S highlighted by the almost overlapping standard error bars and statistically supported ($p>0.05$).

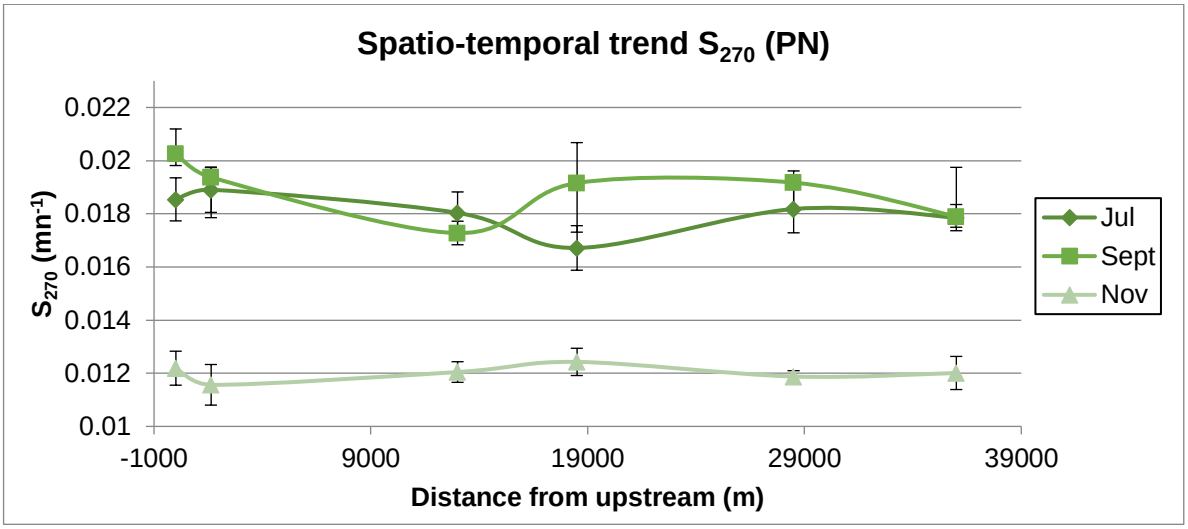

Figure 38 Seasonal and longitudinal trend of S_{270} along the main branch of the Piave.

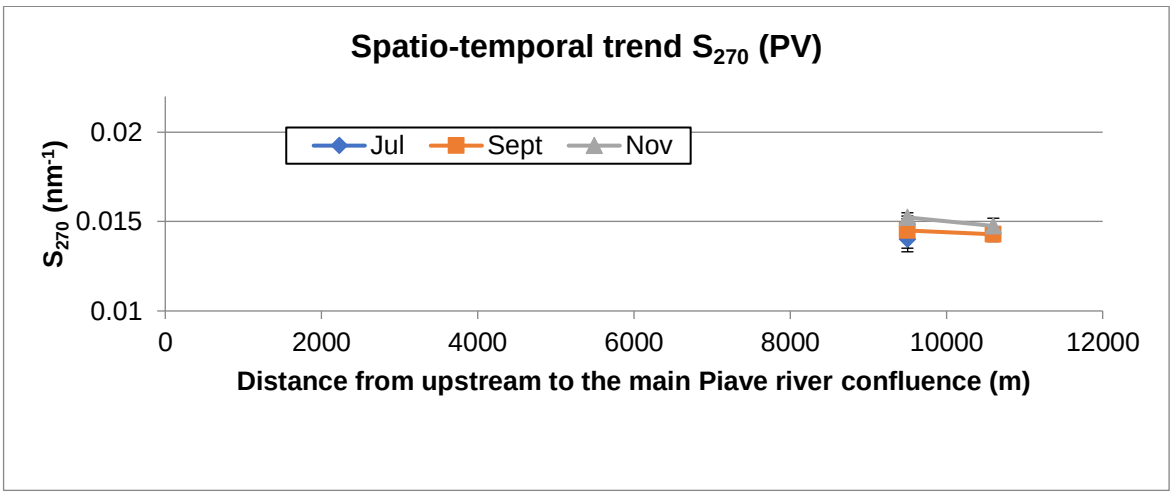

Figure 39 Seasonal and longitudinal trend of S_{270} along the Piave Vecchia.

The DOC estimate showed that the concentrations, whose values were comparable with those measured in the Po delta (Pettine et al., 1998), were higher in autumn (1.66-2.17 mg L^{-1}) and lower during the summer (1.24-1.66 mg L^{-1}) with samples that tend to be more diluted in September than in July (Fig. 40). This seasonal trend differs from that of the largest Italian river where on average DOC does not show significant variations (Pettine et al., 1998).

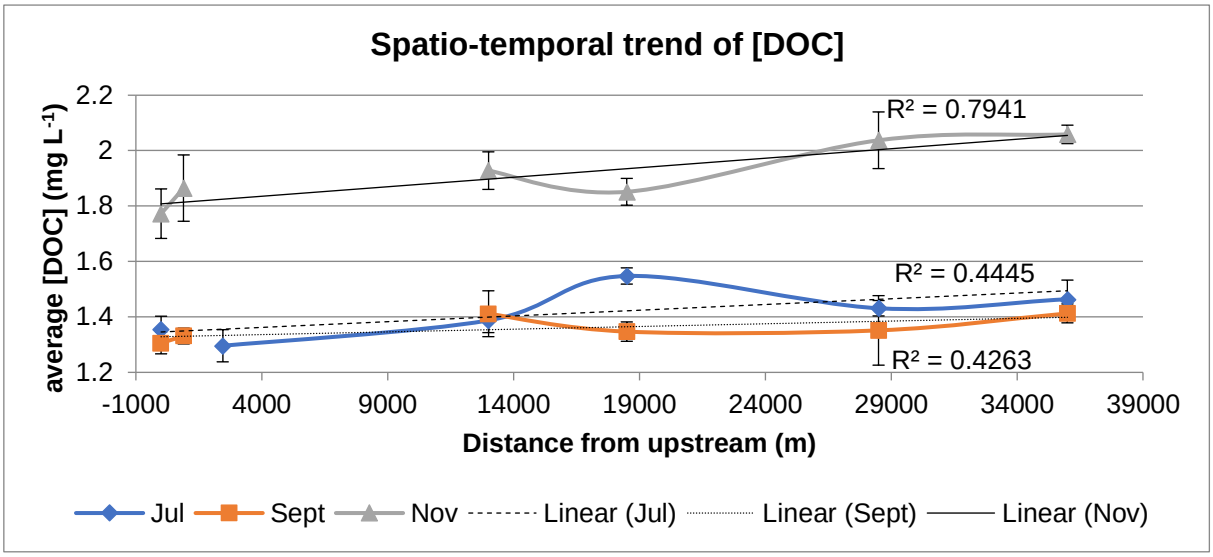

Figure 40 Estimation with the Hernes et al. (2013) method of the DOC average concentration (mg L^{-1}) in the Lower Piave.

The flow in the summer months also appeared similar with values of the same magnitude. Differently in November it was much more consistent reaching the maximum of $4.6x10^3$ Mg of DOC/year. Overall, assuming the DOC average during an entire year as constant, the contribution of dissolved organic C to coastal waters was $1.6x10^3$ Mg/year. This is a conservative value compared to what is reported for the Po Valley in other publications (M. Li et al., 2017; Pettine et al., 1998) (Fig. 41).

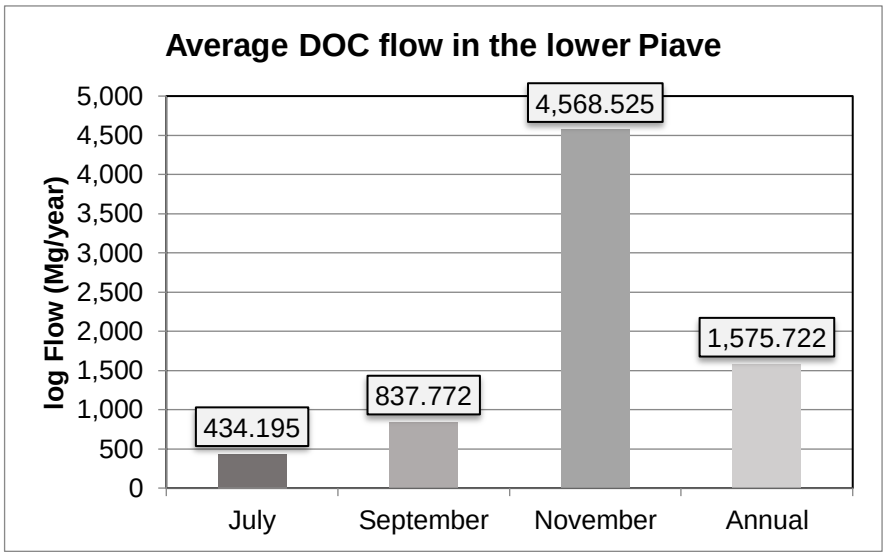

Figure 41 Estimated DOC flow (Mg/year) from the Lower Piave towards the Adriatic Sea in the year 2020.

4.1.3.1.4. Riparian vegetation results

The riparian vegetation sampling activities was carried out by 10 trained citizen scientists in 17 campaigns, from mid-July to early November 2020, along 113 stations located above all upstream of San Donà di Piave and on the Piave Vecchia (Fig. 42).

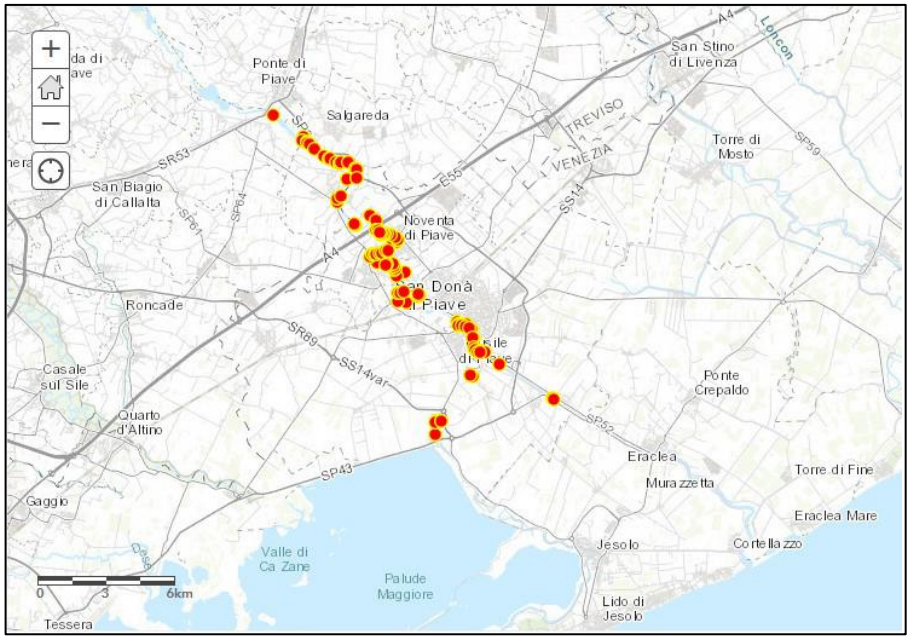

Figure 42 Map of the surveys carried out by citizen scientists during the monitoring of the riparian vegetation in the Lower Piave

The percentage abundance of species in the Lower Piave changed significantly in the cover levels considered. In the tree layer *Populus alba* L., *Populus nigra* L. and *Salix alba* L. contribute in similar proportions to almost 50% of the total cover, nevertheless, in the lower layers their presence decreased to less than 3%. The invasive species *Rubus fruticosus* L. and *Amorpha fruticosa* L. showed an abundance of 22.87% and 19.77%, respectively. The species identified by the CSs in this generic "Other" group, approximately 30% were allochthonous and more than half of them were invasive.

The necromass data was also interesting: in 57% of the transects no dead trees were observed, neither standing nor fallen, in 24% a number between two and five. The reports for which more than five dead plants are reported come from the municipality of Salgareda (TV) south of Ponte di Piave and on the hydrographic left. Regarding bank erosion, the monitoring carried out by the volunteers outlines a substantially homogeneous trend in which 31% of the stations showed strong erosion, slight 30% and none 39%.

4.1.4. Discussions

The ecosystem service evaluation (ES) of C storage in terrestrial ecosystems in the Piave basin, highlighted a very clear difference between the mountain and hill area and that of the plain. The territories bordering the final stretch of the river contribute to a limited extent to the overall C stock, which is promoted above all by the presence of forest formations, substantial on the hills but scarce downstream. The monitoring carried out by citizen scientists (CSs) along the last 40 km of the watercourse, from Ponte di P. to the sea, confirmed the substantial prevalence of agricultural land (57.3%) and the absence of woods.

In the analysis of the ESs it is necessary to make some clarifications on the quality of the input data concerning the densities of C for each environmental compartment and type of land use, since any inaccuracies in subsequent processing could depend on it. For the study region, no local information on C reservoirs is available, except for Soil Organic Carbon (SOC), and this particularly limits the description of belowground and dead C pools. Both reach C densities of less than 17 Mg/ha in all land use classes, vice versa aboveground and SOC pools reach up to 3 and 5 times more respectively in some land uses. As regards the root biomass of the wooded riparian formations, a conservative estimate was made, in fact this environment is subject to anthropic and natural coppice, caused by floods, which involves an alteration of the ratio between the surface mass of the tree and the buried mass (Dr. Niccolò Marchi (TESAF), personal communication). This indicates that apparently young plants may have a much more extensive root system than visible in the field. The necromass data are even less complete for the area of interest, but the low values that were assigned reflect the observations of the CSs on the riparian zone. Considering the number of dead trees or fallen, as a proxy for the intensity of management of the river environment by the local authorities, it can be stated that the watercourse in this stretch of plain is subject to intense maintenance. Large dead vegetation, cut or blown down by floods, is almost completely removed in 72% of the monitored sites and in doing so does not contribute to the dead C pool.

An innovative aspect was the integration of the results of the DOC analyses into the Carbon Storage and Sequestration models. In fact, although river environments are configured as reactors in which organic matter fluxes are higher than terrestrial patches (Cole et al., 2007), carbon storage and sequestration models of river basins do not typically consider carbon sources in water. This is the reason why the Lower Piave section appears as the land use class with the lowest C density in the whole lowland basin.

The first estimates of DOC concentration, carried out through the absorbance characteristics of CDOM, return data with the same order of magnitude as those reported both

in the studies by Spencer et al. (2012) and Hernes et al. (2013) for rivers, as well as those known for surface waters of the northern Adriatic (1.3-1.5 mg L^{-1}) (Ciglenečki et al., 2020). The DOC flux towards the coast was quantified as 1.6 $x10^3$ Mg/year. Considering that the forests of the basin extend overall for 203,641ha and that the Italian forests in the period 1986-2006 stored an average of 7.94 Mg of CO_2 / (ha $year^{-1}$) (Federici et al., 2008), the tons of carbon dioxide sequestered in one year by the forest ecosystems of the basin. The value obtained was converted into tons of elemental 12C, being able to conclude that every year the Piave introduces 0.4% of the C sequestered from the woods of the region in the same period in the form of DOC into the Adriatic Sea. This result describes a conservative estimate that considers only the dissolved component of organic carbon while it has been demonstrated that in other rivers of the Po Valley, such as the Po, and unlike the characteristics of the main temperate rivers, the particulate fraction has higher concentrations than in DOC (Pettine et al., 2001). To this we must add that the stretch of sea into which the Piave discharges is characterized by shallow waters with limited circulation of currents and has been subject in the past to various eutrophic crises (Ciglenečki et al., 2020; Cozzi et al., 2012) therefore the contribution of 1600 tons of DOC per year from the river further promote the microbial activity and the worsening of the conditions of the Adriatic.

Based on the available data, it is not possible to establish whether the flow rate, which has also been identified in the literature as the driver causing the increase in DOC concentrations as one moves away from the mountain (Ejarque et al., 2017), in the Basso Piave can explain the correlation. Q values are available for only one ARPAV station in the study area (Ponte di Piave station) so it is not possible to verify directly whether it is higher or lower downstream.

The results obtained for the study area under different NBS scenarios confirm the greatest benefit in terms of C sequestration in the next 30 years will come from reforestation of approximately 14.500 ha according to the provisions of scenario B1 with an increase of the 5.43% ($2.22x10^6$ tons of C).

4.1.5. Conclusions

The main contribution to climate change mitigation comes from the mountain basin, not only as it constitutes 87% of the entire surface, but also due to the much more widespread presence of forests.

They represent the classes of land use in which the density of C reaches the highest values and the analysis conducted on the Lower Piave highlighted their almost total absence in the study area.

The variation of the floodplain strips to hygrophilous woods, according to the provisions of scenario A, would lead to an improvement in the sequestration ES of approximately 3.40% by 2050, constituting the most advantageous management choice, also compared to scenario C. In the first growth stages of the riparian forests, it is possible that there is an increase of the organic matter exported to the river, a positive trend which will progressively decrease when the forest will become mature. For this reason, the water quality monitoring by citizen scientists will be very important, as they will help to quickly recognize the conditions that can cause the eutrophication of coastal environments.

The DOC dynamics in the lower Piave river are complex and, at least in part, caused by the human impact that has altered its geomorphology, hydrological regime, and land use in the basin. The DOC concentration increases from upstream to downstream in autumn due to the contribution of the fresh allochthonous organic matter coming from the territories drained by the Piave, to which is added the OM transported by the Sile River to the Piave Vecchia (old riverbed). In July the intrusion of sea water rich in very degraded autochthonous DOC which supports the theory of $A^{\circ\circ}_{270}$ with the increasing distance from Ponte di Piave.

The importance of the average DOC flow, estimated through the values of $A^{\circ\circ}_{350}$, has been conservatively quantified as 1600 tons per year. This shows how important it is to deepen the understanding of the drivers that regulate the passage of organic carbon from one stock to another through the river in order to predict the possible impacts of changes in land management on freshwater and coastal ecosystems.

Finally, the Citizen Science initiatives in the Lower Piave basin will be extremely useful, not only for the prevention of eutrophic crises with the water quality monitoring, but also for the collection of environmental parameters, such as temperature and specific conductance, and ecological parameters such as the abundance of species vegetation and height of the tree layer from which it will be possible to make estimates of the above ground C pool.

4.2. MODELLING DISSOLVED AND PARTICULATE ORGANIC CARBON DYNAMICS

4.2.1. Background

Freshwater ecosystems play an important role in regulating climate change, through their capacity to act as carbon sinks, transporter and producers (Ciais et al., 2013). Organic carbon, in both dissolved and particulate form, is a major component of the global carbon cycle and plays a fundamental role in the biogeochemical cycles of all aquatic ecosystems (Gommet et al., 2022). Both particulate (POC) and dissolved (DOC) organic carbon enter freshwater ecosystems from terrestrial ecosystems but are also produced in situ from the fixation of inorganic matter by phytoplankton and aquatic macrophytes. The dominance of either terrestrial or internal organic carbon sources can vary depending on local conditions (Strohmeier et al., 2013). Overall, terrestrial DOC and POC loads to river networks depend both on the availability and mobility of soil organic carbon, as well as the hydrological links between land and river networks (Nakhavali et al., 2021). The concentrations of POC and DOC influence the chemical and biological dynamics of freshwater environments (Perdue et al., 1980; Roulet and Moore, 2006); as an energy source for aquatic organisms (Thurman, 1985), as an attenuator of available solar radiation (visible to UV) (Galgani et al., 2011), as well as a means of transport of macro and micronutrients and pollutants (e.g., toxic heavy metals) (Steinberg, 2003).

Biogeochemical models that consider changing hydrological conditions can provide new insights into the influence of environmental change on aquatic carbon dynamics (Aufdenkampe et al., 2011). However, few studies have used process-based models to examine the influence of land use and climate scenarios on carbon fluxes (Camino-Serrano et al., 2018). Models used to predict DOC export can range from simple regressions to complex process simulations (Futter et al., 2007; Tian et al., 2015; Wu et al., 2014). These models differ in the definitions of the soil carbon pools, the level of detail in the process formulation (e.g., simple first-order kinetics or nonlinear relationships), and the spatial and temporal resolution. The CENTURY modelling framework (Parton et al., 1993) was one of the first models to simulate carbon sequestration services under different land-use change models. Chen et al. (2017) simulated changes in carbon sequestration under land use change using the Dynamics of Land System (DLS) model. However, these studies did not address the links between terrestrial and instream carbon processes (Xu et al., 2019). Neff and Asner (2001) developed a DOC synthesis model, based on CENTURY, which explore DOC flux variations across a wide range of soil conditions. The sensitivity of DOC flux simulations was tested, comparing high versus low rates of DOC bioavailability and extent of DOC absorption. The Terrestrial Ecosystem Model was another

process-based biogeochemical model that couples carbon, nitrogen, water, and heat processes in terrestrial ecosystems to simulate carbon and nitrogen dynamics (Melillo et al., 1993). The DocMod approach (Currie and Aber, 1997) determined DOC production in relation to forest litter decomposition, using inter-connected carbon-litter pools and related carbon transformations, with DOC production in terrestrial environment being an end-point of the overall C turn-over processes along with CO_2. Jutras et al. (2011) developed a 3-parameter DOC-3 model to extend from soil to instream DOC concentrations at a daily basin scale. Michalzik and colleagues' (2003) DyDOC model explored inter-connectedness of C pools and related DOC transformation, with a clear focus on the forest soils. Their model driving factors were precipitation, litter production, and air or soil temperatures at hourly and daily time steps (Fröberg et al., 2007). The Acrotelm and Catotelm DOC production model considers DOC production and storage processes in peatland soil in relation to soil temperature and water-table fluctuations in the context of climate change (Worrall and Burt, 2005). The INCA-C model (Futter et al., 2007; Futter and de Wit, 2008) and the Estimating Carbon in Organic Soils Sequestration and Emissions model (Smith et al., 2010) provided estimates of instream DOC concentrations as well as production, transfer, and mineralization estimates. This model works in forested and mixed land-use basins using daily time series of soil and atmospheric conditions that can be highly variable and difficult to determinate at large basin scales. The ORCHIDEE-SOM model, within the ORCHIDEE land surface model (Krinner et al., 2005), reproduces SOC stock and DOC concentration dynamics by simulating vertical C cycling as well as lateral exports to the river network. It provides a useful tool to explore DOC dynamics, including turnover and decomposition to CO_2, when the required data are available. The Canadian Land Surface Scheme Including Biogeochemical Cycles CLASSIC (Melton et al., 2020). CLASSIC has been used to compare the simulated mean seasonal cycle of gross primary productivity to FLUXNET observations at biome scale (Melton et al., 2020). The SWAT-C model simulates C cycle processes in terrestrial environments (Yang and Zhang, 2016; Zhang et al., 2013), and DOC cycling in river networks (Du et al., 2019), building on the approach developed previously in CENTURY. It has been used across basins of different scales and land uses (Qi et al., 2020) and most recently to model DOC dynamics at high resolution in a large and complex Canadian basin (Du et al., 2023). The SWAT model represents a major breakthrough for riverine DOC modelling, when appropriate information on soil properties (C production and mineralization), channel conditions (e.g., Manning's N) and local meteorology and hydrology are available. Statistical modelling approaches (Ågren et al., 2010; Boyer et al., 1996; Samson et al., 2016) have also shown good results in predicting DOC production with respect to basin conditions.

Lessels et al. (2015) added a DOC model to the Hydrologiska Byråns Vattenbalansavdelning (HBV) hydrological model (Lindström et al., 1997) and a DOC production module based on the static soil organic carbon (SOC) pool. A GIS based modelling framework was developed in the Regional Hydro-Ecological Simulation System (RHESSys) to simulate carbon, water, and nutrient fluxes at the watershed scale (Tague and Band, 2004), while the model by Lessels et al., (2015) also explored DOC dynamics on a basin scale. These models provide important insights to DOC fluxes, but do not address in-stream DOC processes. Moreover, their data requirements often make them less appropriate for large river basins.

In basins where data and regulatory monitoring are limited, or where stakeholders need to explore the impacts of alternative land use scenarios, the Integrated Valuation of Ecosystem Services and Trade-offs (InVEST) modelling suite (Sharp et al., 2018) has been used to estimate of carbon storage and sequestration at basin scale of major C pools (aboveground biomass, belowground biomass, soil, and dead organic matter) in relation to the spatial distribution of land use and catchment conditions. However, these models do not consider links between the terrestrial and aquatic environments and do not address instream dynamics.

There is a clear need for process-based basin-scale models of DOC and POC dynamics that consider the link between terrestrial-aquatic ecosystems as well as the instream transformations. However, for such models to be used for scenario analysis and decision support, or for basin scale analysis in regions which have limited data, a new approach is needed. This approach should be based on data that are both easily available and basin-wide, and should be complementary to other models focused on nutrient and sediment dynamics. Such a model would need to simulate fluxes considering biogeochemical transformation processes and hydrological conditions that can vary at the sub-basin scale and that would also be sensitive to climate change.

In this chapter, I developed and validated an organic carbon flux model to explore the implications of river basin management at sub-basin scale on DOC and POC dynamics, using the Piave River basin (Italy) as a test case. The model was built to be applied as an open-source plugin for QGIS and can be used in basins with limited local data, taking advantage of international datasets and commonly available national data, for example land use and land cover, precipitation, hydrological soil properties, and topography (DEM).

4.2.2. Materials and Methods

4.2.2.1. Carbon flux model

Dissolved and particulate carbon fluxes within a basin depend on the movement and transformation of organic carbon within individual sub-basins and within the main river. We used a mass balance approach within a spatially semi-distributed model to estimate DOC (and POC) fluxes from the terrestrial to river environment, considering hydrological, land-use, and precipitation characteristics of individual sub-basins. More specifically, carbon flow was estimated based on DOC and POC loads of individual land uses, their transport to the river, as well as transformation processes that occur within the tributaries and the main river (per km).

Soil carbon export from each land unit (pixel) to the river were estimated based on its land use / land cover (LULC) and the distance and transport pathways to the river, based on a 20m resolution DEM. The estimates of DOC and POC potential export for each class of LULC were obtained from concentrations reported in available scientific literature (Table 18). Where several values for a single LULC class were found, the mean value was used. Within the distributed model, these values were combined with a monthly water runoff proxy value to estimate the mass of DOC and POC reaching the tributary or river from each land use (Fig. 43).

Table 18. Available studies providing information on DOC and POC concentrations in relation to different land use classes.

LU		DOC (mg L^{-1})		Data source	POC (mg L^{-1})	Data source
Forest	broadleaved forests	17.72	20.5	(Borken et al., 2011); (Camino-Serrano et al., 2016); (Camino-Serrano et al., 2018).	0.58	(Dawson et al., 2004)
	coniferous forests	22.55		(Borken et al., 2011); (Camino-Serrano et al., 2016); (Camino-Serrano et al., 2018).		
Agricultural	grassland	9.17	10.18	(van den Berg et al., 2012); (Camino-Serrano et al., 2018).	1.58	(Kim et al., 2013) (Cai et al., 2015)
	Cropland	4.2		(Camino-Serrano et al., 2018).		
	Vineyard	19.2		(Cattani et al., 2006).		
Urban			24.1	(Maniquiz et al., 2010); (Ortiz-Hernández et al., 2016).	0.56	(Kalev and Toor, 2020)
Bare rocks			0		0	

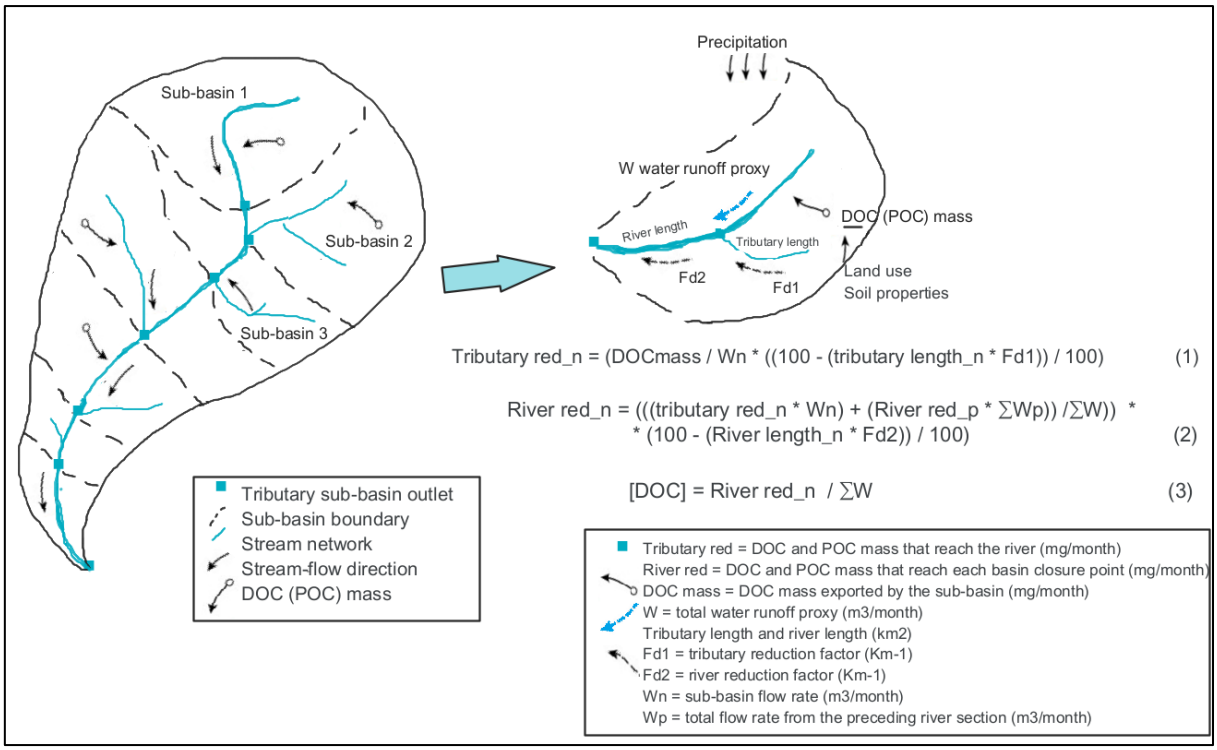

Figure 43. DOC concentrations in the river in each sub-basin were based on the carbon transport to the river and transformation processes within the tributaries of each sub-basin (Trib red$_{n1}$, Trib red$_{n2}$) as well as those transformation processes present within the main river (DOC Rv$_{n1}$, DOC Rv$_{n2}$).

The model simulates the movement of organic carbon (DOC, POC) within each tributary of the sub-basin and into the main river (equation 20). Within each tributary and the main river, DOC and POC loss (retention and transformation) in the sub-basin tributaries and within the main river is calculated (equation 21). The degree of carbon reduction is also a function of the overall length of the tributaries and the main river. The governing equations are:

$$Tributary\ red_n = (DOCmass\ /\ Wn * ((100 - (tributary\ length_n * F_{D1})) / 10 \quad (20)$$

$$River\ red_n = (((tributary\ red_n * W_n) + (River\ red_p * \sum Wp)) / \sum W)) * ((100 - (River\ length_n * F_{D2})) / 100) \quad (21)$$

$$[DOC]or(POC) = River\ red_n / \sum W \quad (22)$$

where the reduction factor (F_{D1} and F_{D2}, Km^{-1}) for DOC, or (F_{P1} and F_{P2}, km^{-1}) for POC, considers the reduction of organic matter in the smaller order streams and main river respectively, based on each kilometer of stream length. Tributary red and River red are the DOC and POC mass flow rates at each tributary and basin closure point (tonnes/month), river length and

tributary length (km) were available from the Basin Authority. DOCmass (or POCmass) is the load (tonnes month^{-1} m^2) from each sub-basin based on land use, monthly precipitation, and soil properties. W is the water runoff proxy (m^3/month). Wp is the total flow rate from the preceding river section (m^3 month^{-1}), Wn is the total flow rate of the sub-basin section (m^3 month^{-1}).

The first sub-basin receives water from its tributaries only, without flow from any preceding river section (Wp = 0). Therefore, river DOC (or POC) is directly determined by the contribution of the tributaries present in the sub-basin and assumes no contribution from emerging groundwater (equation 23).

$$River\ red_n = tributary\ red_n * (100 - (River\ length_n * F_{D2}))/100 \quad (23)$$

The reduction factor for DOC and POC in the tributaries in each sub-basin (F_{D1} or F_{P1}) is assumed to be constant across the sub-basin and approximates the transformation and loss of organic matter for each km of stream length (tributary length$_n$). This reduction is applied to the transportable DOC$_{mass}$ (or POC$_{mass}$) and normalised by a runoff proxy (W) for each pixel. The result is the estimate of DOC or POC load (mg/year) transported within the sub-basin to the main river (Tributary red$_n$), occurring at the point of closure of each sub-basin. The concentration of DOC (River red$_n$) and total flow rate (W_p) from the preceding river section, is summed with the DOC load of the sub-basin (Tributary red$_n$ * W$_n$) to become the influx of DOC into the next sub-basin of the main river. The DOC concentration is then reduced by a riverine reduction coefficient (F_{D2}), considering the river length within this sub-basin, generating a DOC concentration at its closure (River red$_n$). The same approach is used for POC, where the POC river factor (F_{P2}) is more related to a physical retention of the POC along the river.

Longitudinal changes in DOC (or POC) concentration in the river result from LULC related sources (DOC$_{mass}$) of each sub-basin, spatial differences in precipitation, the transport and retention within sub-basin tributaries and the overall reduction within the main river section

4.2.2.2. Organic carbon reduction factors

The composition and concentration of organic matter can be modified by photo-oxidation, microbial respiration, leaching, flocculation, sorption, and settling (Einarsdottir et al., 2017; Galy et al., 2011; Loiselle et al., 2009a; Spencer et al., 2010; Von Wachenfeldt and Tranvik, 2008). Changes in longitudinal DOC and POC concentrations are determined by several factors (e.g., hydrological events, basin slope, soil C), which can have considerable spatial and seasonal variation within a basin (M. Li et al., 2017), with higher values in wetlands and around rainfall events (Harrison et al., 2005; Tian et al., 2015). Different models address these changes through

different approaches. For example, the SWAT-C model simulated DOC and POC movement and transport through: DOC percolation coefficients, the liquid-solid partition coefficient, and POC process coefficients (Du et al., 2019; Qi et al., 2020). Camino-Serrano et al. (2018) considered that free DOC can be adsorbed to soil minerals or remain in solution based on an equilibrium distribution coefficient linked to soil properties(Nodvin et al., 1986). Gommet et al. (2022) consider differences in decomposition rates between labile and refractory DOC pools, which were geographically variable, but within the same order of magnitude. While Berggren and Al-Kharusi (2020) reported a median decomposition half-life of across multiple river sampling locations across Europe.

The initial reduction factors used in the present model were based on these past studies and then tuned by interpolation using DOC and POC measurements made in the Piave river by regional agencies in 2018, 2019 and 2020 (ARPAV, 2021b). It should be noted that there were a limited number of river sections (sub-basins) where DOC was monitored, therefore estimated reduction factors for DOC and POC loss were used to initialise the model, with final values for tributary streams, F_{D1} and F_{P1} (0.45 and 0.07 10^{-2} km^{-1}), and for the main river sections, F_{D2} and F_{P2} (0.9 and 0.01 10^{-2} km^{-1}) following published values. These interpolated values support earlier studies that show that deeper rivers have higher transformation and storage rates of organic matter compared to shallower and faster moving streams (Kalbitz et al., 2003). Similarly, Bouchez et al. (2014) showed that longitudinal reductions in POC due to weathering and oxidation are more limited that those related to DOC.

4.2.2.3. Water runoff proxy

As a detailed hydrological model for the whole basin was not available, a mass balance-based approach was used to estimate the monthly surface runoff: the amount of water running off each pixel towards the river and its tributaries. It is based the Curve Number approach within the seasonal water yield model of the InVEST package (Sharp et al., 2018). The Curve Number method developed by Natural Resources Conservation Service (NRCS) of the United States Department of Agriculture (USDA) (NRCS-USDA, 2007) is widely used for predicting direct surface runoff volume for a given rainfall event and estimating the volumes and peak rates of surface runoff at basin scale (da Silva Cruz et al., 2022). A higher CN value suggests a higher runoff potential, whereas a lower CN value signifies low runoff. This approach was chosen due to its utility to explore future scenarios of land use and climate change (da Silva Cruz et al., 2022).

The model combines a digital elevation model (DEM) and commonly acquired climate and soil information from regional and international sources (Nistor et al., 2018; NRCS-USDA, 2007).

It uses the basic principles of water partitioning (precipitation becoming runoff or evapotranspiration) and routing (upgradient water becoming available to downgradient parcels). These simplified routing processes allow for a large degree of uncertainty and should be interpreted as proxy of runoff rather than predictions of absolute values. The model calculates the monthly water runoff proxy of each pixel based on a modification to the NRCS curve number (NRCS-USDA, 2007), which estimates monthly direct runoff (Guswa et al., 2017; Hamel et al., 2020).

4.2.2.4. Model input data for the Piave river catchment

The Carbon model DOC and POC loads (mg L^{-1}) for each of five LULC classes together with the water runoff proxy (mm) and vectors files containing the tributaries and river networks (km). Five simplified classes (artificial, agricultural, forests, bare rocks, and water bodies) were used. We identified 19 sub-basins using GRASS watershed function on QGIS v.3.22 (2022) while the river networks were obtained from the stream raster generated from the water runoff proxy model.

Monitored DOC concentrations were obtained from the regional environmental agency ARPAV (Agenzia Regionale per la Protezione Ambientale - Veneto) (2021b). These were very limited as DOC monitoring was initiated in 2018 and was not performed in 2021. Seasonal data from 2018 were used for model calibration. Data from 2019, from 5 stations, and from 2020 (two stations) were used for validation.

ARPAV does not monitor POC concentrations, therefore, POC was estimated by using total suspended solids (TSS) concentrations following Nemery et al. (2013), eq. 24. In alpine rivers, both particulate organic carbon (POC) and particulate inorganic carbon (PIC) are closely linked to the TSS transport dynamics (Wheatcroft et al., 2010).

$$POC\% = 28.82 * TSS^{-0.7499} + 0.89 \quad (24)$$

with some adjustment

$$POC = POC\% / 100 * TSSavg \quad (25)$$

The water runoff proxy model used a 20 m DEM available from the national research authority ISPRA (2020), which was corrected to fill hydrological sinks and checked with the digital watercourse network to ensure routing along the specific tributaries using QGIS v.3.22 (2022). Basin area was obtained from the regional geoportal and based on the Water Protection Plan 2015 (ARPAV, 2018b). Monthly average precipitation raster files at 20 m resolution were interpolated using an inverse distance weighting (IDW) of information from 72 stations for 2018, 2019 and 2020 (ARPAV, 2021a). A rain events table containing the number of rain events

for each month was also used. Monthly average evapotranspiration for each pixel was extrapolated from the Reference Evapotranspiration Global Reference Evapotranspiration (Global-ET0) Version 2 dataset (Trabucco and Zomer, 2018). Land Use (LU) raster data, referred to the year 2018, was obtained from Corine Land Use Land Cover Level IV data at a 100 m resolution (ISPRA, 2018). Soil and plant evapotranspiration coefficients (Kc) were estimated for broad land use classes suggested by Allen et al. (1998). Parameters related to flow recharge and accumulation (α, β, γ) used default values (α = 1/12, β = 1, γ = 1) based on similar rivers. The flow accumulation threshold is the number of upstream pixels that flow into a pixel before arriving to the tributary.

4.2.2.5 Root Mean Square Error

The comparison of estimated to measured concentrations of DOC (and POC) used the percentage root mean square error (RMSE):

$$RMSE\% = \sqrt{\frac{\sum_{i=1}^{N}(x_i - \hat{x}_i)^2}{N}} / \overline{x_i}$$

Where x_i is the estimated values, $\hat{x}_i$ is the observations, $\overline{x_i}$ is the average of the observed values and *N* the number of observations.

4.2.3. Results

4.2.3.1. Water runoff proxy

Estimated surface runoff was compared with the available data from four calibrated gauge stations from 2015 to 2020 (ARPAV, 2022b). The average discharge from the lowest sub-basin for the simulated year, 2018, was 125 m^3/s. The four stations were limited to the main Piave river and most did not have a full set of monthly data, especially following the flood event of October 2018 which compromised the measurements from several stations (EFAS, 2018). The surface runoff proxy provided a similar longitudinal trend in flow rate, increasing at lower basins. Considering these five years of data, the overall accuracy was low (RMSE = 81%), underestimating river discharge.

4.2.3.2. DOC flux

The modelled annual average DOC concentrations at 18 sub-basins closure points shows a general increase from the upper to lower basin (Table 19, Fig. 46a). It should be noted that the DOC estimates for the first sub-basin have an intrinsic uncertainty related to the lack of information on source water discharges. As the model is based on precipitation, the first sub-

basin receives low DOC load from source waters, dominated by snow and groundwater.

Table 19. Average annual DOC concentration and mass in each sub-basin calculated by the model following the DOC equations for the year 2018.

Sub-basin	Estimated DOC (mg L^{-1})	DOC mass (tonnes/year)
1	0.67	3.79×10^1
2	0.36	4.08×10^1
3	1.29	1.92×10^2
4	0.69	1.65×10^2
5	1.37	3.48×10^2
6	1.66	5.13×10^2
7	1.87	5.90×10^2
8	1.35	5.29×10^2
9	1.19	5.68×10^2
10	0.81	5.50×10^2
11	0.82	6.10×10^2
12	1.03	8.29×10^2
13	1.15	9.49×10^2
14	1.40	1.19×10^3
15	1.39	1.24×10^3
16	1.49	1.37×10^3
17	1.60	1.55×10^3
18	1.13	1.13×10^3
19	0.86	8.56×10^2

The reduction factors (F_{D1}, F_{D2}) were refined using available DOC data (ARPAV) for 2018 from 5 stations with complete measurements. The resulting DOC estimates captured the over longitudinal trend (RMSE = 83%, Fig. 44a).

The model, using the same reduction factors ($F_{D1} = 0.45$, $F_{D2} = 0.9$) was validated for 2019 and 2020 (RMSE = 59%) and showed a similar trend (Fig. 44b and 44c). It should be noted that the contributions from two sub-basins to the DOC load of the main river were estimated to be negative (sub-basins 4 and 10), and therefore set to zero, indicating that the LULC and hydrology of these basins allowed for a net zero contribution to the DOC in the main river. These sub-basins have hydrological and land use characteristics that create conditions of limited DOC production with respect to the reduction factors for tributaries present, resulting in the equivalent of net zero DOC export.

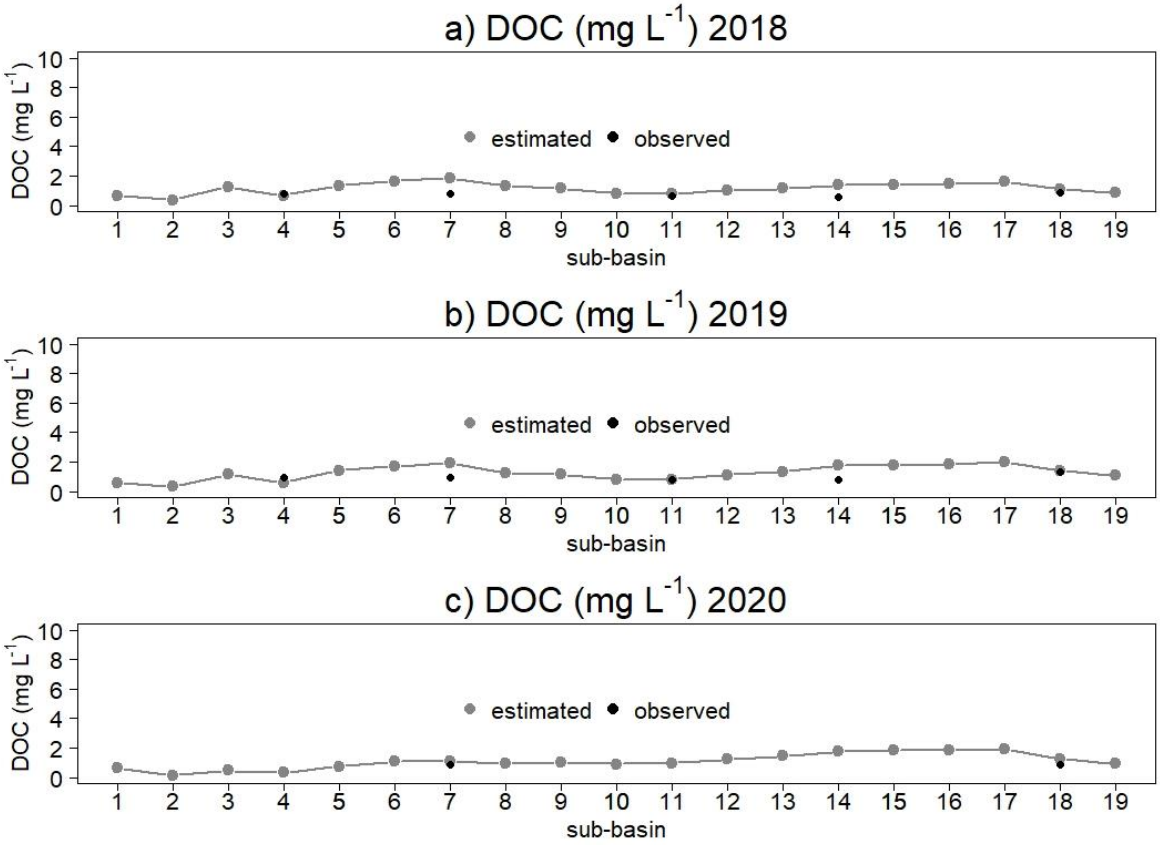

Figure.44. Longitudinal distribution (logarithmic scale) of DOC concentration and comparison with the observed ARPAV values for the years 2018 (a), 2019 (b) and 2020 (c).

The model was run at the monthly frequency to explore seasonal changes in DOC concentrations, along the longitudinal DOC gradient, under present land LULC and meteorological conditions of 2018 (Fig. 45), 2019 and 2020. DOC concentrations were generally higher in June (Fig. 45) with an average value of 1.19 mg L^{-1} (RMSE = 119%), followed by February (1.27 mg L^{-1}, RMSE = 83%) and December (0.86 mg L^{-1}, RMSE = 57%) (Fig. 45). This seasonal change was most evident in the sub-basins in the middle of the basin.

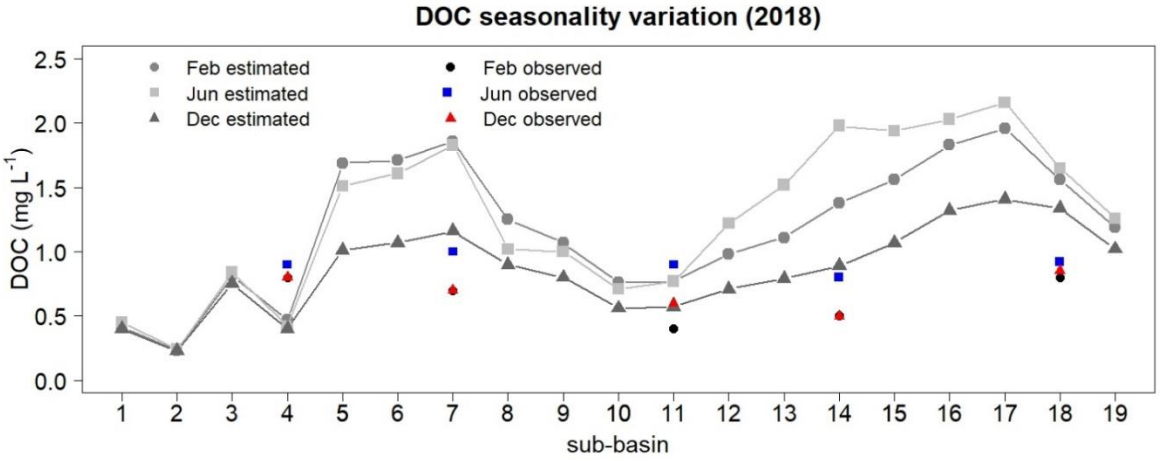

Figure.45. Seasonal variation and distribution across the sub-basin in February, June and December 2018.

4.2.3.3. POC flux

POC flux and POC concentrations showed a general increase along the longitudinal gradient, to the highest concentration at the Piave basin closure point (Table 20).

Table 20. POC concentration and mass in each sub-basin calculated by the model following the POC equations for the year 2018.

Sub-basin	Estimated POC (mg L^{-1})	POC mass (tonnes/year)
1	0.37	2.10 x 10
2	0.33	3.75 x 10
3	0.33	4.96 x 10
4	0.32	7.61 x 10
5	0.33	8.38 x 10
6	0.34	1.04 x 10^2
7	0.34	1.07 x 10^2
8	0.40	1.57 x 10^2
9	0.46	2.21 x 10^2
10	0.40	2.47 x 10^2
11	0.42	3.14 x 10^2
12	0.44	3.58 x 10^2
13	0.45	3.70 x 10^2
14	0.45	3.83 x 10^2
15	0.47	4.15 x 10^2
16	0.48	4.46 x 10^2
17	0.50	4.86 x 10^2
18	0.51	5.07 x 10^2
19	0.51	5.07 x 10^2

To interpolate the reduction factors (F_{P1} = 0.07 and F_{P2} = 0.01) and validate the model, I

used POC estimates (equation 24) from five sites for the years 2018 and 2019, considering the organic fraction to dominate the overall mass of TSS, based on observations for similar rivers in subalpine regions (Némery et al., 2013). The results showed that the simulated POC for the year 2018 (RMSE = 24%) was underestimated in the two sites located in the upper basins and overestimated in the sites 11 and 14 (Fig. 46a). Particulate load in the upper basin is expected to have a higher percentage of inorganic particulates, related to snow and glacier melt and groundwater sources, typical of alpine streams (Chanudet and Filella, 2008). The underestimate in the lower river sub-basin is related to the fact that the model does not determine allochthonous production of organic particulates from primary production. The validation of the model using POC values for 2019 (Fig. 46b) and 2020 (Fig. 46c) showed a reasonable accuracy (RMSE = 41%) with annual POC dynamics similar to 2018 (Fig. 46a). While overall longitudinal and seasonal dynamics follow expected trends, it should be noted that the direct measurement of POC, at regular intervals and for multiple years would improve both the model training as well as validation.

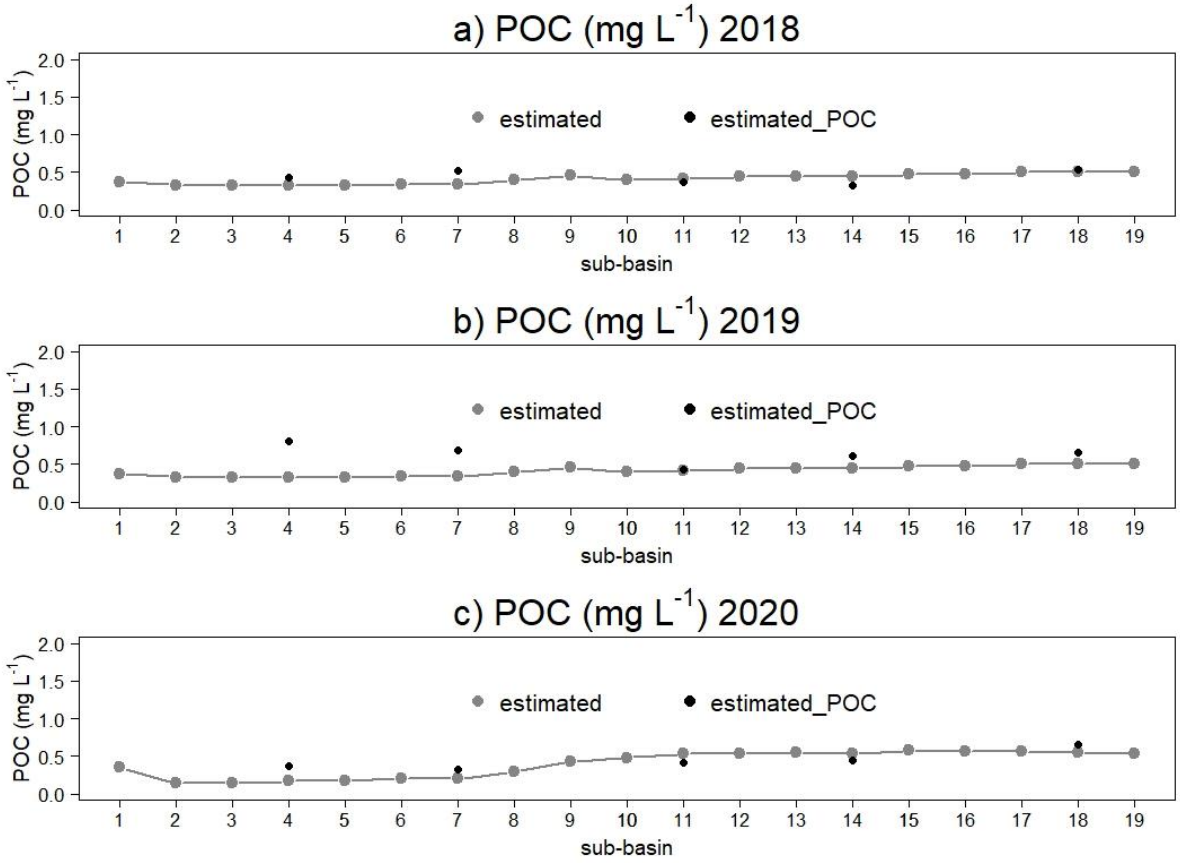

Figure.46. Longitudinal distribution of POC concentration and comparison with the observed ARPAV values for the years 2018 (a), 2019 (b) and 2020 (c).

The model was run at the monthly frequency to compare seasonal changes in POC

concentrations for present day LULC and meteorological conditions. POC concentrations were generally higher in June (Fig. 47) with an average value of 0.43 mg L^{-1} (RMSE= 51%), followed by February (0.33 mg L^{-1}, RMSE= 23%) and December (0.31 mg L^{-1}, RMSE= 35%) (Fig. 47). This was most evident in the sub-basins in the middle of the basin.

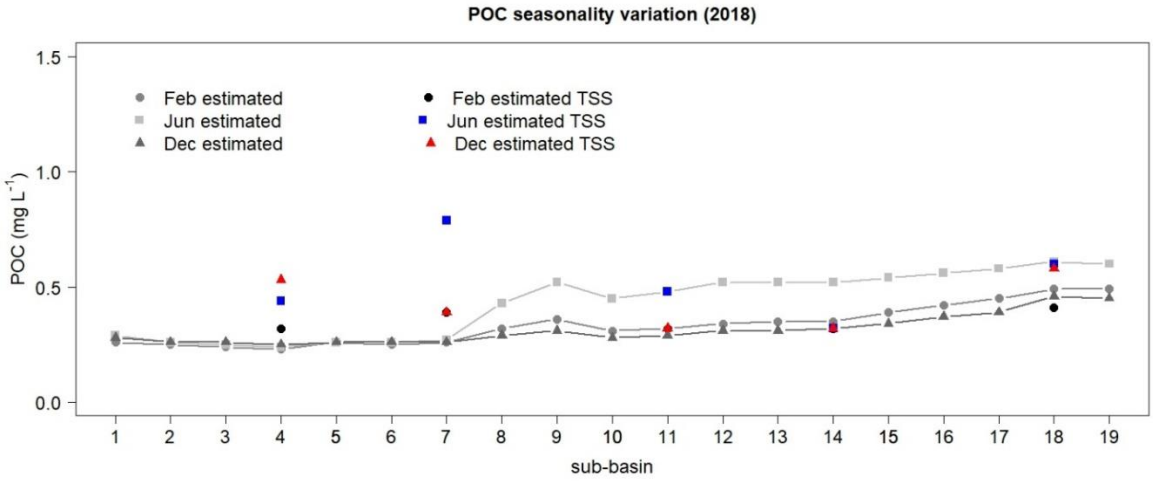

Figure.47 Seasonal variation and distribution of POC across the sub-basin in February, June and December 2018.

4.2.3.4. DOC & POC model Plugin

The DOC & POC model plugin (Fig. 48) was developed for open-source QGIS to allow for the analysis how modifications in land management and climate could be used to explore changes in DOC and POC export at basin and sub-basin scale. The code was written in Python using the associated QGIS Plugin Builder. QGIS is an open-source software for geographic information system (GIS) that is supported by a large community of users and developers. The DOC & POC model plugin code is downloadable from the GitHub repository (https://github.com/dgfrancesco/DOC-POC-model-Di-Grazia-et-al.-). The model plugin can be accessed from the QGIS graphical user interface by opening the Python Console and selecting 'open existing script'. The plugin is intended to be used with other GIS based scenario development tools (e.g., InVEST) that allow stakeholders to explore changes in nutrient and sediment river exports.

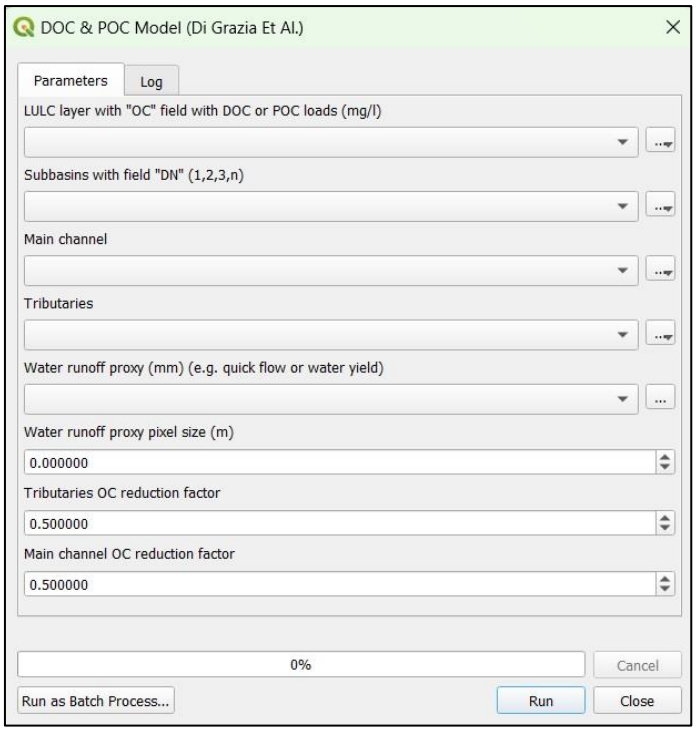

Figure.48 DOC plugin page.

4.2.4. Discussions

4.2.4.1. Estimated dynamics of Organic Carbon export

The organic carbon (DOC and POC) dynamics across the Piave River basin showed longitudinal variations that reflected sub-basin differences in LULC, stream length, instream reduction, and surface runoff hydrology, and seasonal variations in precipitation. Seasonality in DOC and POC fluxes represents one of the major uncertainties in modelling riverine organic matter dynamics (Gommet et al., 2022; Tian et al., 2015). In the coupled hydrology–biogeochemistry DOC model developed by Lessels et al. (2015), in-stream DOC concentrations typically followed streamflow patterns, increasing in the spring from precipitation induced DOC transport from the soil. Our model shows higher DOC concentration in the Piave river in June linked to rainfall events (108 mm) and lower in January and December (77 and 12 mm). It should be noted that flood events are the responsible of for a large part of POC and DOC transport (Bastias et al., 2020; Raymond et al., 2016).

Differences in sub-basin DOC and POC estimated exports show spatial variations in precipitation, basin morphology and land use, as well as soil carbon content across different alpine, subalpine and valley sub-basins. These spatial differences in expected soil erosion and mobilization of dissolved and particulate matter are supported by past studies showing the impact of these factors on river organic matter exports (M. Li et al., 2017; Zhang et al., 2022). The highest DOC mass concentrations were related to sub-basins dominated by urban and forest

land use. The geographical distribution of DOC sources (Fig. 49a) showed the highest density in the upper and middle basin with peaks corresponding to the urban area in the middle sub-basins (sub-basins 5 – 12). Urban DOC export depends on multiple sources; wastewater treatment systems, road runoff, biomass burning aerosols, coal combustion, industrial activities, etc., (Aitkenhead-Peterson et al., 2009; Siudek et al., 2015). The highest POC mass concentrations were related to sub-basins dominated by agricultural land use (sub-basins 8 – 17) (Fig. 49b), similar to past studies showing high POC loads in agricultural areas (Luo et al., 2022).

Final DOC export to the Adriatic Sea (Sub-basin 18) showed values consistent to those measured by the regional agency, with DOC and POC exporting 856 tons/year and 506 tons/year. Changes in OC export have implications on the productivity of the Adriatic Sea, which is a narrow and shallow area of the Mediterranean Sea, where dilution is limited (Ciglenečki et al., 2020). In relation to the Po River, these fluxes are approximately 1% of the total DOC and POC emitted (Pettine et al., 1998).

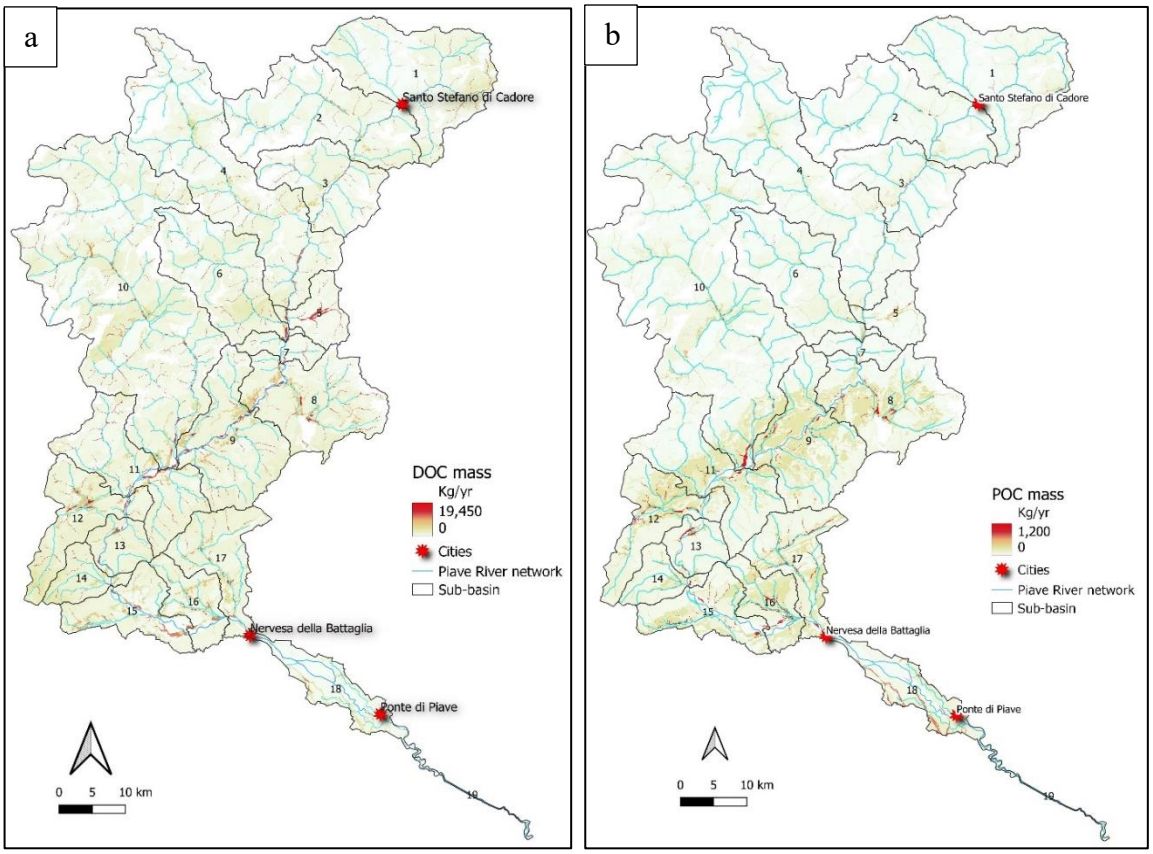

Figure.49 a, b. Spatial distribution of DOC (a) and POC (b) across the 19 sub-basins.

4.2.4.2. Future scenarios

The model was used to explore different scenarios of land use and climate for the Piave river

basin, looking towards 2050. Based on consultations with local stakeholders and a study of 50-year trends, a reforestation scenario was evaluated as the most feasible.

Looking first at projected changes in climate and based on the emission scenario RCP 4.5, a decrease in annual precipitation for the Piave Basin is expected to occur by 2050 (Dezsi et al., 2018). This will lead to a reduction in the water runoff proxy throughout the basin, due to greater evaporation and an increased hydrological deficit. This 2050 climate scenario showed a decrease in DOC export by 25% (214 tons/year) and in POC export by 26% (127 tons/year) with respect to 2018 export. Given an increase in the temperature and reduced runoff, it is likely that soil conditions, as well as river and tributary reduction factors will also change (increased reduction). Qu et al. (2010) using the Global NEWS models estimated that, that in 2050, riverine DOC export will exceed POC in total C export. In particular, POC is expected to decrease by 15-25% as a consequence of human perturbation, land use change and dam construction.

This reduced carbon export, in combination to the expected decrease in both phosphorus and nitrogen exports for the same climate and land use scenario (Di Grazia et al., 2021). suggest a reduced eutrophication threat for the Adriatic Sea in 2050. The area of the Mediterranean Sea has a long history of eutrophication related impacts on biodiversity and ecosystem services. The expected trend in eutrophication is supported by recent studies (Ciglenečki et al., 2020) showing similar reductions in carbon and nutrient concentrations.

4.2.5. Conclusions

The spatially distributed carbon flux model developed in the present study is intended to support decision making by basin scale and sub-basin scale stakeholders, in particular with respect to scenarios of land use and climate. The model can be used, together with other scenario tools to prioritise policy and management options to reduce impacts on receiving waters and improve ecosystem services. The model was applied to a single river basin but is flexible enough basins in different climate and hydrological conditions, given the availability of information on LULC, climate, hydrology, and related indices.

Data requirements for the model are relatively limited. Most of these data can be retrieved from international and national geographic databases, making this approach available for exploring DOC and POC export in data-scarce basins. The model is refined using local data, in particular monthly or seasonal concentrations of DOC and POC at the sub-basin level. The greater number of sub-basins monitored, the more robust will be the reduction factor interpolation.

Further developments of the in-stream OC dynamics should address the different loss dynamics of labile DOC and refractory DOC fractions, as their relative decay rates are significantly different (Du et al., 2020). For example, the turnover time of labile soil OC is typically 1 to 5 years, while the turnover time of refractory fractions could reach 200-1500 years (Iravani et al., 2019). Estimates of relative percentages of labile and refractory OC, related to different LULC classes could be used to improve the model as well as include new information on estimates of CO_2 evasion from the river.

The DOC and POC model was designed as a QGIS plugin for basin scale studies. The model output can be used to evaluate carbon export based on varying land use and climate scenarios, providing an additional tool to support basin management.

This study resulted in the manuscript entitle “Modelling dissolved and particulate organic carbon at basin and sub-basin scales” (Di Grazia et al., 2023) published online in May 2023 in the journal Science of the Total Environment (IF 2022 of 10.75).

5. ADDITIONAL PARAMETER MODELS

5.1. ANNUAL WATER YIELD (WATER AVAILABILITY)

5.1.1. Background

The supply of fresh water is an ecosystem service that contributes to the well-being of society, ensuring the development of agriculture, industry, the improvement of living standards and tourist activities (Cudennec et al., 2009). Land use change is primarily an anthropogenic disturbance of soil that alters surface runoff, affects hydrological processes and water consumption at the catchment level. According to the IPCC Fifth Assessment Report (IPCC, 2014), the climate has warmed over the past half-century in almost all regions of the world (Zhang et al., 2016). Climate change has an impact on rainfall and temperature patterns and consequently affects evapotranspiration and water supply (Wei et al., 2021). The calculation and mapping of the spatio-temporal variations of the water yield are of great importance for the planning and management of water resources. The water yield model is therefore a large-scale spatio-temporal model based on water balance principles.

Compared to other hydrological models, the water yield model has mapping and spatial analysis functions that provide an effective approach for water yield estimation at high spatial resolution and at different scales (Yin et al., 2020). The model considers the annual variability in water volume given likely levels for a given catchment area, but they are vulnerable to variations caused by land use and land cover changes (LULC). LULC changes can alter hydrological cycles, affecting the rate of evapotranspiration, infiltration, and water retention, and modifying the timing and volume of water available in the land (Ennaanay, 2006; WCD, 2000). The maps of the areas where water yields are produced can help avoid unintended impacts on the amount of water entering the river or aid in land use management decisions, balancing uses such as conservation or agriculture.

The analysis focused on estimating the relative contributions of water in different parts of the Piave basin, offering insights into how land use and climate change scenarios influence annual water yield. The components of the water yield model were used to obtain an estimate of the total water availability of the Piave basin and in detail of the lower Piave river.

5.1.2. Materials and Methods

5.1.2.1. Water yield model

The approach is based on determining the amount of water flowing from each pixel as precipitation minus the fraction of water that undergoes evapotranspiration (Fig. 50). The model

does not distinguish between surface, subsurface and base flow, but assumes that all water yield from a pixel reaches the point of interest via one of these paths. Pixel-scale calculations allow us to represent the heterogeneity of key factors in water yield such as soil type, rainfall, vegetation type, etc. Second, in addition to the average annual flow, the model calculates the proportion of available surface water by subtracting the surface water that is consumed for other uses.

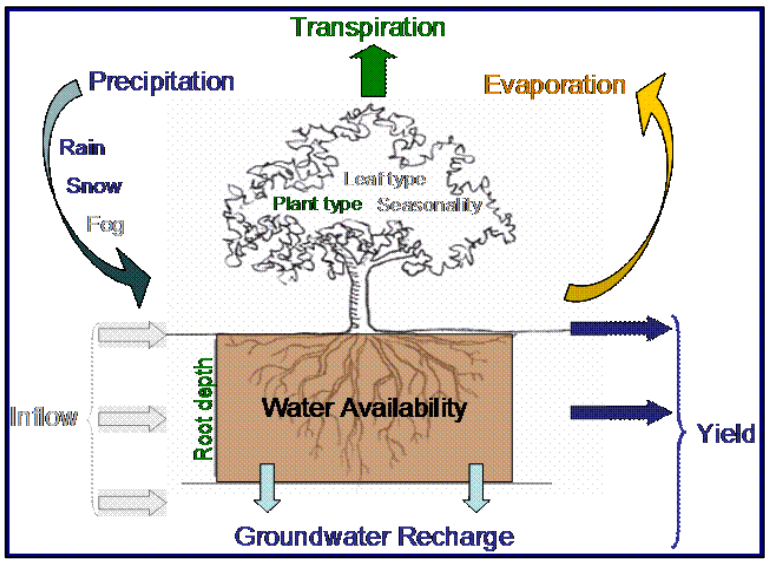

Figure 50 Concept diagram of the simplified water balance method used in the annual water yield model. Aspects of water balance that are in colour are included in the model, those that are in grey are not (InVEST).

The water yield model is based on the Budyko curve and average annual rainfall. The annual water yield Y(x) for each pixel on landscape x is determined:

$$Y(x) = \left(1 - \frac{AET(x)}{P(x)}\right) \cdot P(x) \qquad (26)$$

where *AET(x)* is the effective annual evapotranspiration for pixel x and *P(x)* is the annual precipitation for pixel x.

For vegetated land use/land cover (LULC) types, the evapotranspiration portion of the water balance, *AET(x)/P(x)*, is based on an expression of the Budyko curve proposed by Fu (1981) and Zhang et al. (2004):

$$\frac{AET(x)}{P(x)} = 1 + \frac{PET(x)}{P(x)} - \left[1 + \left(\frac{PET(x)}{P(x)}\right)^{\omega}\right]^{1/\omega} \qquad (27)$$

PET (x) is the potential evapotranspiration and *ω (x)* is a non-physical parameter characterizing the natural climatic properties of the soil, both described below.

Potential evapotranspiration *PET (x)* is defined as:

$$PET(x)=K_c(\ell_x) \cdot ET_0(x) \quad (28)$$

$ET_0(x)$ is the reference evapotranspiration from pixel x and $K_c(\ell_x)$ is the plant (vegetation) evapotranspiration coefficient associated with the LULC ℓ_x on pixel x. $ET_0(x)$ reflects local climatic conditions, based on the evapotranspiration of a reference vegetation such as grass or alfalfa grown at that location. $K_c(\ell_x)$ is largely determined by the vegetative land use/land cover characteristics found on that pixel (Allen et al., 2006). K_c fits the ET_0 values to the type of crop or vegetation in each pixel of the land use / land cover map.

$\omega(x)$ is an empirical parameter that can be expressed as a linear function of $\frac{AWC*N}{P}$, where N is the number of rainfall events per year, and AWC is the volumetric water content of the soil available for the plant. While further research is underway to determine the function that best describes the global data, we use the expression proposed by Donohue et al. (2012) in the InVEST model:

$$\omega(x) = Z\frac{AWC(x)}{P(x)} + 1.25 \quad (29)$$

Where $AWC(x)$ is the volume of water contained in the soil available to the plant (mm). Soil texture and effective rooting depth define the $AWC(x)$, which dictates how much water can be held and released into the soil for a plant to use. It is estimated as the product of the plant's available water capacity (PAWC) and the minimum of the depth of the root-limiting layer and the rooting depth of the vegetation:

$$AWC(x)=Min\ (Rest.layer.depth,\ root.depth) \cdot PAWC \quad (30)$$

The depth of the root-restricting layer is the depth of the soil at which root penetration is inhibited due to physical or chemical characteristics. Vegetation rooting depth is often referred to as the depth at which 95% of the root biomass of a vegetation type is found. PAWC is the plant's available water capacity, i.e., the difference between field capacity and wilting point.

Z is an empirical constant, sometimes referred to as "seasonality factor", that captures the local precipitation pattern and additional hydrogeological characteristics. It is positively correlated with N, the number of rainfall events per year. The value 1.25 is the minimum value of $\omega(x)$, which can be seen as a value for bare soil (when the root depth is 0) (Donohue et al., 2012; Yang et al., 2008), with the values of $\omega(x)$ limited to a value of 5.

For other types of LULC (open water, urban, wetlands), the actual evapotranspiration is directly calculated from the reference evapotranspiration $ET_0(x)$ and has an upper limit defined by precipitation:

$$AET(x)=Min(K_c(\ell_x) \cdot ET_0(x), P(x)) \quad (31)$$

$ET_0(x)$ is the reference evapotranspiration and $K_c(\ell_x)$ is the evaporation factor for each LULC.

The model assumes that all water available for evapotranspiration comes from within the watershed (as rain). This assumption is true in cases where agriculture is rain-fed, or the source of the irrigation water is within the study catchment (not from transfer between catchments or from a deeper aquifer).

5.1.2.2. Input data for the Piave river basin

The water yield model requires some biophysical parameters as basic data, including LULC, reference evapotranspiration, annual precipitation, plant available water content (PAWC), root restricting layer depth, biophysical table, seasonality factor (Zhang parameter), and watersheds. All the data were resampled at a spatial resolution of 20 m.

Current LULC was provided by Corine Land Cover year 2018 (ISPRA, 2018) at a 100 m resolution and modified according to the developed land use change scenario (A0, A1, A2, B0, B1, C0, C1). Future (2050) base and land use change scenarios developed (A0, A1, A2, B0, B1, C0, C1). These LULC codes should match the lucode values in the Biophysics table.

The Precipitation raster was the annual average rainfall 2018 (District Authority of the Eastern Alps, 20 m avg raster from 12 monthly rasters) in the Piave basin (mm). Raster data interpolated using the IDW (Weighted Inverse Distance) interpolation method from information from 72 ARPAV (2021a) monitoring stations in the Piave basin. The future raster of average annual precipitation (2050) was based on the 2050 precipitation estimates by Dezsi et al. (2018) with high resolution gridded surfaces with 1 km cell size developed in an Albers Equal Area Conic projection for Europe. RCP 4.5.

Evapotranspiration raster file with annual average evapotranspiration value for each pixel is the potential soil water loss by both soil evaporation and transpiration by healthy alfalfa (or grass) if sufficient water is available (units: mm). Current Average Annual Reference Evapotranspiration was provided by Global Reference Evapotranspiration (Global-ET_0) Version 2 dataset provides high-resolution (30 arc-seconds) global raster climate data for the 1970-2000 period (Trabucco and Zomer, 2018). Future evapotranspiration raster was based on ET_0 evapotranspiration estimated for 2050 by Dezsi et al. (2018) with high resolution gridded surfaces with 1 km cell size developed in an Albers Equal Area Conic projection for Europe. RCP 4.5.

The Root Restricting Layer Depth was a raster file with average value of the root bounding layer depth for each pixel and was provided by ESDAC at 1Km of resolution (Hiederer, 2013).

The depth of the root-restricting layer is the depth of the soil at which root penetration is strongly inhibited due to physical or chemical characteristics (unit: mm).

The Plant Available Water Content (PAWC) raster file represents the fraction of water that can be stored in the soil profile that is available for plant use (0 to 1 fraction). The data was provided by ESDAC, at initial resolution of 500 m, Available Water Capacity (AWC) for the topsoil fine earth fraction (from LUCAS 2009) (Ballabio et al., 2016).

The vector delimitation of the watershed was obtained from the ARPAV geoportal (ARPAV, 2018b), relating to the 2015 Water Protection Plan (PTA).

The Biophysical Table is a csv file containing the model information corresponding to each of the land use classes in the LULC (2018) raster and variation scenarios. Each row is a land use/land cover class, and the columns should be named and defined as follows:

- *lucode*: unique integer for each LULC class (e.g., 1 urban, 2 agricultural, 3 forest, etc.)
- *LULC_desc*: Descriptive name of the land use / land cover class
- *LULC_veg*: specifies which AET equation to use (Eq. 26 or 30). Values should be 1 for vegetated land use except wetlands and 0 for all other land uses including wetlands, urban, water bodies, etc.
- *root_depth*: the maximum root depth for vegetated land use classes (in mm). This is often given as the depth at which 95% of the root biomass of a vegetation type is found. For land uses where the generic Budyko curve is not used (where evapotranspiration is calculated from Eq. 30), rooting depth is not needed. In these cases, the root depth field is ignored and can be set to a value such as -1 to indicate that the field is not used.
- *Kc*: plant evapotranspiration coefficient for each LULC class (Chapter 6, FAO)(Allen et al., 1998), used to calculate potential evapotranspiration using plant physiological characteristics to modify the reference evapotranspiration, which is based on alfalfa. The evapotranspiration coefficient is to a decimal between 0 and 1.5 (some crops evapotraspirate more than alfalfa in some very humid tropical regions and where water is always available).

The Z parameter is the floating-point value in the order of 1 to 30 corresponding to the seasonal distribution of precipitation (Eq. 28) and calculated based on the Piave-IWMI rain events table, N*0.2, where N=number of rain events per year.

5.1.3. Results and Discussions

The results include a series of output layers – raster – with the same resolution as the input land use, which for the Piave basin is 20 m, and a table for calculating the estimate of:

- precip_mn (mm): average precipitation per pixel in the basin.
- PET_mn (mm): Average potential evapotranspiration per pixel in the basin.
- AET_mn (mm): Average effective evapotranspiration per pixel in the basin.
- wyield_mn (mm): average water yield per pixel in the catchment area.
- wyield_vol (m^3): Volume of water yield in the catchment area.

5.1.3.1. Comparison of 2018 scenarios

The analysis and comparison of the different scenarios showed a general reduction in the available water volumes. The scenario C0A1B0 (A1) (both alone and in combination with C1, Figures 51a and 51b) represented an exception with an increase in water volumes percentage. Other exception was the scenario that envisages the work for the hydraulic safety of the lower course of the river Piave C1A0B0 (C1), where there was no variation in water volumes (Table 21). The evapotranspiration values (PET and AET) increased in the reforestation scenarios (B1, A2) and by the combination of these (A2B1C0/C1), excepted for the current evapotranspiration in scenario A1 which suffered a reduction of the effective evapotranspiration of 0.02% (Table 21). Vegetation promotes evapotranspiration, increasing in intensity in wet soils compared to dry ones and in wooded areas. The highest values of evapotranspiration are represented in mountain forests and along the riparian vegetation strips. The scenarios with the presence of the hydraulic defence work (C1) and the combinations with the other scenarios showed the same dynamics for evapotranspiration and the same volumes of water obtained for the scenarios without intervention for hydraulic defence of the lower course of the Piave (Table 21).

Table 21 Variation in annual water yield based on 12 management scenarios of the Piave river basin under current climatic conditions (2018).

2018	AWY Basin					AWY Basin %				
Scenario	precip mm	PET mm	AET mm	wyield mm	wyield vol_m^3	precip mm %	PET mm %	AET mm %	wyield mm %	wyield vol_m^3 %
C0, A0, B0	**1592.74**	**754.77**	**351.36**	**1237.29**	**4.97 x10^9**	**1592.74**	**754.77**	**351.36**	**1237.29**	**4.97 x10^9**
C0, A1, B0	1592.74	754.76	351.29	1237.36	4.97 x10^9	0.00	0.00	-0.02	0.01	0.01
C0, A2, B0	1592.74	755.64	351.65	1237.00	4.96 x10^9	0.00	0.11	0.08	-0.02	-0.02
C0, A0, B1	1592.74	758.19	352.30	1236.35	4.96 x10^9	0.00	0.45	0.27	-0.08	-0.08
C0, A1, B1	1592.74	758.18	352.23	1236.42	4.96 x10^9	0.00	0.45	0.25	-0.07	-0.07
C0, A2, B1	1592.74	759.05	352.59	1236.06	4.96 x10^9	0.00	0.57	0.35	-0.10	-0.10
C1, A0, B0	1592.74	754.80	351.37	1237.28	4.97 x10^9	0.00	0.00	0.00	0.00	0.00
C1, A1, B0	1592.74	754.79	351.29	1237.36	4.97 x10^9	0.00	0.00	-0.02	0.01	0.01
C1, A2, B0	1592.74	755.66	351.65	1237.00	4.96 x10^9	0.00	0.12	0.08	-0.02	-0.02
C1, A0, B1	1592.74	758.22	352.31	1236.34	4.96 x10^9	0.00	0.46	0.27	-0.08	-0.08
C1, A1, B1	1592.74	758.21	352.23	1236.42	4.96 x10^9	0.00	0.46	0.25	-0.07	-0.07
C1, A2, B1	1592.74	759.08	352.59	1236.06	4.96 x10^9	0.00	0.57	0.35	-0.10	-0.10

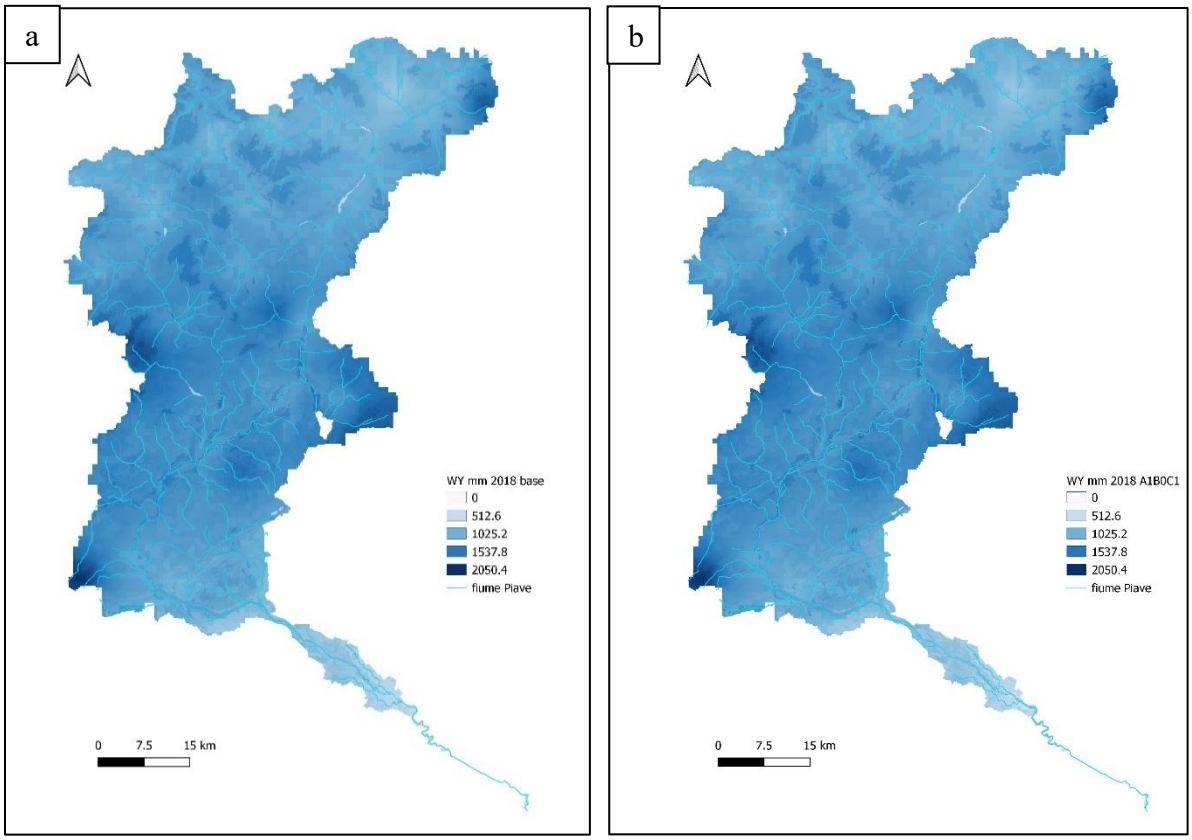

Figure 51 Spatial distribution maps for water yield in the Piave basin. (a) 2018 baseline scenario (b) best combination of A1 and C1 scenarios.

5.1.3.2. Comparison of 2050 scenarios

The available water quantity in the Piave basin will be reduced in the future due to climate change as foreseen in the RCP4.5 climate change scenario (2050). Several studies have assessed the response of water yield to climate change showing a higher sensitivity to precipitation comparing to temperature (Pessacg et al., 2015; Yin et al., 2020).

The model showed reduction in precipitation from 1,592 mm in 2018 to 1,242 mm in 2050 (Table 22), which precipitation will be less frequent but more intense and concentrated in the short term, causing inconvenience linked to the effects of extreme climatic events (Iannuccilli et al., 2021). According to various climatic models, in southern Europe, during the hot season there will be an increase in the summer temperature which will cause a lowering of the relative humidity and an increase in the level of condensation, which will tend to hinder the number of rainy days (Drobinski et al., 2016; Iannuccilli et al., 2021; Panthou et al., 2014).

The analysis and comparison of the different scenarios to 2050 showed an overall loss of water volumes in each scenario (Table 22). Two scenarios estimated a lower leakage by 19.85%, compared to the 2018 conditions (fig. 52a) were the scenario C1A0B0 (C1, fig.52b) and the scenario C0A1B0 (A1) (volume reduction of 9.86 $x10^8$ m^3). The land use changes modelled in these scenarios showed a reduction in forest cover and an increase of pastures and grasslands (C1) and erodible belt (A1) made up of sand and gravel.

Table 22 Variation in annual water yield based on 12 management scenarios of the Piave river basin under future climatic conditions (2050).

2050	AWY Basin					AWY Basin %				
Scenario	precip mm	PET mm	AET mm	wyield mm	wyield vol_m^3	precip mm %	PET mm %	AET mm %	wyield mm %	wyield vol_m^3 %
C0, A0, B0	1,242.77	479.55	247.44	991.64	3.98 $x10^9$	-21.97	-36.46	-29.58	-19.85	-19.85
C0, A1, B0	1,242.77	479.55	247.38	991.71	3.98 $x10^9$	-21.97	-36.46	-29.59	-19.85	-19.85
C0, A2, B0	1,242.77	480.16	247.69	991.40	3.98 $x10^9$	-21.97	-36.38	-29.51	-19.87	-19.87
C0, A0, B1	1,242.77	482.01	248.22	990.87	3.98 $x10^9$	-21.97	-36.14	-29.36	-19.92	-19.92
C0, A1, B1	1,242.77	482.01	248.15	990.93	3.98 $x10^9$	-21.97	-36.14	-29.37	-19.91	-19.91
C0, A2, B1	1,242.77	482.62	248.46	990.62	3.98 $x10^9$	-21.97	-36.06	-29.29	-19.94	-19.94
C1, A0, B0	1,242.77	479.57	247.45	991.64	3.98 $x10^9$	-21.97	-36.46	-29.57	-19.85	-19.85
C1, A1, B0	1,242.77	479.57	247.39	991.70	3.98 $x10^9$	-21.97	-36.46	-29.59	-19.85	-19.85
C1, A2, B0	1,242.77	480.19	247.70	991.39	3.98 $x10^9$	-21.97	-36.38	-29.50	-19.87	-19.87
C1, A0, B1	1,242.77	482.03	248.22	990.86	3.98 $x10^9$	-21.97	-36.14	-29.35	-19.92	-19.92
C1, A1, B1	1,242.77	482.03	248.16	990.93	3.98 $x10^9$	-21.97	-36.14	-29.37	-19.91	-19.91
C1, A2, B1	1,242.77	482.64	248.47	990.62	3.98 $x10^9$	-21.97	-36.05	-29.28	-19.94	-19.94

These LU changes which partly explains the reduction in both potential and current, which however remains more linked to a reduction in rainfall and the consequent water absorption capacity in the soil and by the roots of plants.

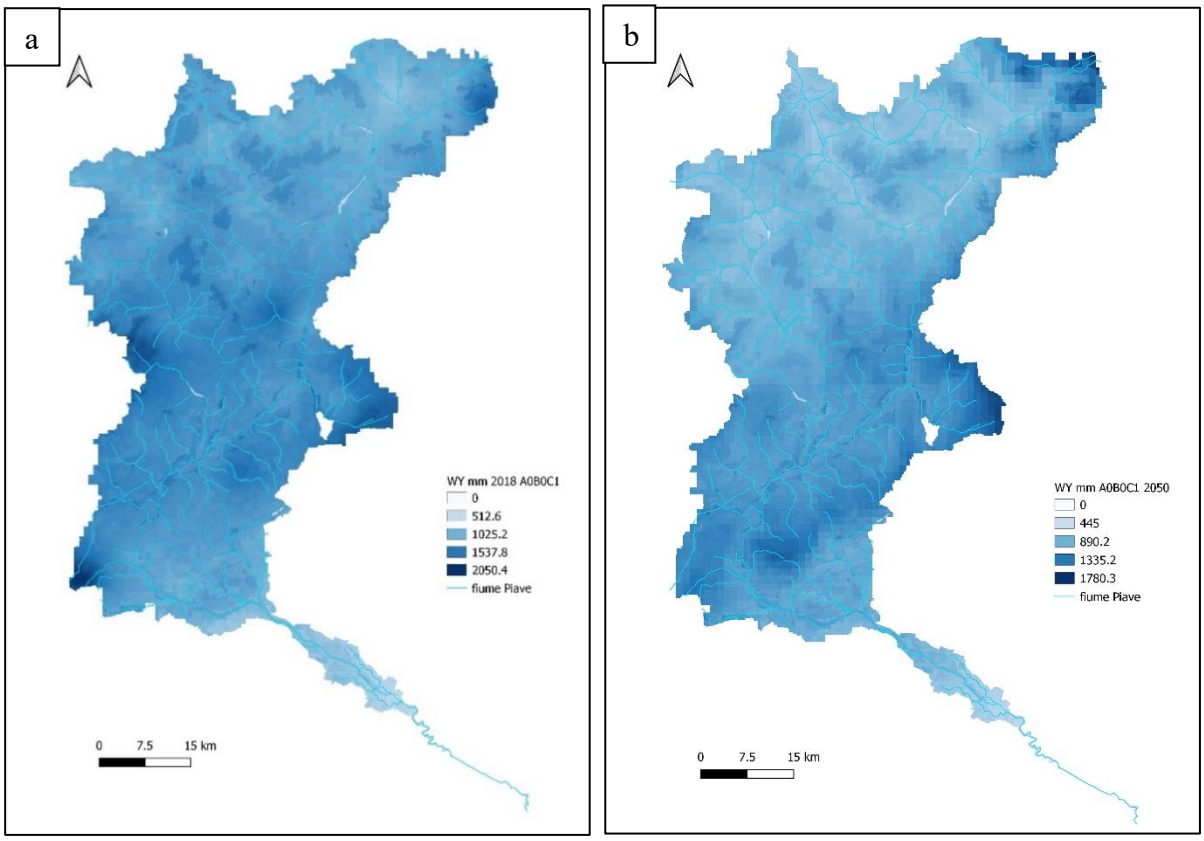

Figure 52 Comparison of water yield C1 scenarios (a) 2018 (b) 2050.

5.1.3.3. Validation

A long-term average flow was used to validate the model. Since the flow data is given in units of flow (m^3/s) and the model calculates the volume of water, the observed flow data is in units of m^3/year. The Piave Basin average flow rate was 195 m^3/s. Considering that the average discharge of the Piave river at Nervesa della Battaglia is 130 m^3/s (ARPAV, 2018g), a value obtained from hydrometric levels and based on years of observations, the model estimation, despite the limitations, was close to the official flow rate of the river.

Climate data (total precipitation and potential evapotranspiration) must match the date of the land use map. Having used the CLC 2018, the precipitation and evapotranspiration values refer to the same year. The other inputs, the depth of the root-limiting layer and the available water content of the plant are less susceptible to temporal variability, so any available data can be used for these parameters.

The ET_0 evapotranspiration data published by ARPAV (2018f) for the year 2018 stand at

values between 600 and 700 mm in the spring/summer 2018 semester. In the mountains and in the foothills, lower values have been estimated between 400 and 600mm. The ET_0 values for the March-August 2018 semester were almost everywhere close to or above the average in almost the entire regional territory and in the eastern part. The values we obtained from the model are in line with the official ARPAV data.

Forecasts of climate change to 2050 (Dezsi et al., 2018) for evapotranspiration, measured as potential (ET_0) and actual (AET_0) evapotranspiration, predict substantial changes for ET_0 and AET_0, with the result that all Europe, except for the northern regions, will experience water deficits, with a pronounced decrease in southern Europe. In particular, the monthly values of ET_0 will decrease in the summer months compared to the winter months in response to climate change. AET_0 projections estimate values above 500 mm of AET_0 mainly in southern Europe, particularly in the Adriatic Sea and in the west of the Italian peninsula, in the north of the Iberian Peninsula and in the south of France. The European regions with low AET_0 are also Sicily, the Alpine chain, and the south of mainland Greece.

Irrigated agriculture constitutes the main sector for water consumption in the Mediterranean countries. Being able to retain as much water as possible in the area so that it can be used in drought periods represents the challenge of the future.

Model results are not intended to elaborate detailed water plans, but rather to evaluate how and where changes in a watershed can affect water yield. It is based on annual averages, which ignore the extremes and do not consider the temporal dimensions of the supply.

I do not consider the spatial distribution of land use / land cover. The empirical model used for water balance (based on Budyko's theory) was tested on scales larger than the pixel dimensions used (Hamel and Guswa, 2015). Complex land use patterns or underlying geology, which can induce complex water balances, may not be well expressed in the model.

I do not consider sub-annual models of water runoff times. Water yield is a supply function. Changes in land use scenarios are likely to affect runoff time as much as annual water yields and are of particular concern when drivers such as climate change are considered. The elaboration of temporal models of outflow requires detailed hydrological data not considered in this approach. However, this model provides a useful initial assessment of how landscape scenarios can affect annual water yields.

The approach used simplifies the demand for water, distributing it over the landscape. For each LULC, a single variable (γd) is used to represent multiple aspects of water resource allocation, which can misrepresent the complex distribution of water across uses and over time. Water demand can differ significantly between plots of the same LULC class. Much of the

water demand can also come from large point source intakes, which are not represented by a LULC class at all.

5.1.4. Conclusions

The water quantity influences biogeochemical cycles and both, its estimation and mapping, are of great importance to water resource planning and management. The availability of water resources is a limiting factor for economic development in many water-stressed countries. The Mediterranean region is one of the most water scarce regions globally, particularly in Southern and Eastern countries (Tarr et al., 2014).

The annual water yield model was used to compare different NBS scenarios at spatial and temporal scales for the Piave river basin. Results for 2018 showed that the river restoration scenario inside the riverbanks (A1) increase the water content compared to the other NBS scenarios in the Piave basin. Future projections (2050) showed a general decrease of the water availability (-19%) related to the reduction in precipitation (-22%) with peaks corresponding to the reforested land use scenarios (A2, B1).

The A1 scenario alone or in combination with C1scenario (flood retention basin) represents the best NBS scenarios for the water availability in the basin both in current and future climatic projections, with an estimated reduction of 9.86 $x10^8$ m^3 from 2018 to 2050.

The water Yield model well captures the Piave basin variability across different NBS and climate scenarios. Despite some limitations the model demonstrates its applicability and efficacy for as sustainable water management.

5.2. SOIL LOSS AND SEDIMENT TRANSPORT

5.2.1. Background

Erosion and retention of terrestrial sediments are natural processes that regulate the concentration of sediments in watercourses (Stallard, 1998). Sediment dynamics in a catchment are mainly determined by climate (particularly precipitation intensity), soil properties, topography and vegetation, and anthropogenic factors such as agricultural activities or the construction and operation of dams (Ferreira and Panagopoulos, 2014; Sánchez-Canales et al., 2015). Major sources of sediments include land erosion (soil particles loosened and carried away by rain and land flow), gullies (channels that concentrate flow), bank erosion, and landslides (Matomela et al., 2022). End receptors include deposits on slopes, floodplains or inundations, and reservoir retention. Land use conversion and changes in land management practices can change the amount of sediment flowing out of a catchment (Zhou et al., 2019).

The extent of this effect is mainly governed by major sources of sediments (land use change will have less effect in basins where sediments do not come primarily from land flow); the spatial distribution of sediment sources and end receptors (e.g., land use change will have less effect if sediment sources are buffered by vegetation).

Soil erosion threatens the sustainability of agricultural productivity and ecosystems. Optimization and management of forest landscape patterns will become increasingly important for soil conservation with the implementation of several afforestation/reforestation projects (Gong et al., 2021).

Changes in sediment load can impact downstream irrigation, water treatment, recreation, and reservoir performance, which can result in reduced soil fertility and reduced water and nutrient holding capacity, with impact on farmers (Dile et al., 2016). It also leads to increased treatment costs for the drinking water supply caused by reduced stream clarity which decreases the value for recreational activities (Butler et al., 2021; Price and Heberling, 2018). Increasing total suspended solids also causes an impact on the health and distribution of aquatic populations, increases tank sedimentation, decreases tank performance, or increases sediment control costs (Lee et al., 2022).

The results of the sediment model include both the sediment load entering the stream on an annual scale, and the amount of sediment eroded into the basin and retained by vegetation and topographic features.

5.2.2. Materials and methods

5.2.2.1. Soil loss and sediment transport model

There are two main aspects to calculating sediment load: 1) quantifying the amount of erosion produced by different points in the landscape and 2) quantifying the amount of that erosion ending up in waterways. The model also estimates the amount of sediment deposited on the landscape along the way. All calculations are performed for each pixel within the catchment area of interest. The amount of erosion produced by each pixel is calculated using the *Universal Soil Loss Equation (usle)* (Borselli et al., 2008), which is the most widely used method for estimating erosion production in a landscape, based on geomorphology, climate and vegetation type. The amount of annual soil loss on pixel *i*, $usle_i$ in tons $ha^{-1}year^{-1}$), is given by:

$$usle_i = R_i \cdot K_i \cdot LS_i \cdot C_i \cdot P_i \quad (32)$$

where

$R_i = rainfall\ erosivity\ (MJ \cdot mm(ha \cdot hr)^{-1})$
$K_i = soil\ erodibility\ (tons\ \cdot ha \cdot hr(MJ \cdot ha \cdot mm)^{-1})$
$LS_i = slope\ length - gradient\ factor$
$C_i = crop\ management\ factor$
$P_i = support\ practice\ factor\ (Renard\ et\ al., 1997).$
$(cf.\ also\ in\ (Bhattarai\ and\ Dutta, 2006)$

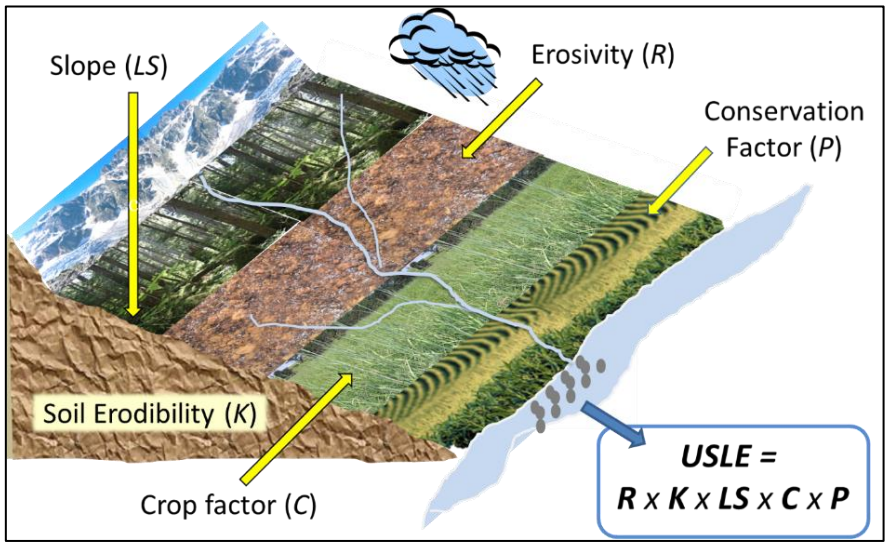

Figure 53 Universal Soil Loss Equation (Borselli et al., 2008).

Rainfall erosivity (R) is a measure of how hard rain falls and hits the ground - heavier rain is more likely to cause erosion than light rain. Soil erodibility (K) is a soil property that indicates the ease with which a particular type of soil detaches and becomes eroded. Slope (LS) is, in general, areas with a steeper slope are more likely to be subject to erosion than flat ones. The Crop Factor (C): A relative measure of how vegetation type affects erosion: Dense vegetation with increased land cover is less likely to produce erosion than sparse vegetation. The conservation practice factor (support practice P): a relative measure of whether

management practices are conducted with the aim of reducing erosion, such as contour farming.

The model (Fig. 53) works on the spatial resolution of the digital elevation model (DEM) input raster. For each pixel, the model first calculates the amount of annual soil loss from that pixel, then calculates the Sediment Export Factor (SDR), i.e. the portion of eroded soil that actually reaches the hydrological flow. Once the sediment reaches the stream, it is assumed that it ends up at the outlet of the catchment area. No in-stream processes are modelled.

5.2.2.2. Sediment export: Sediment Delivery Ratio

The sediment export from a given pixel *i* *Ei* (unit: tons · $ha^{-1}year^{-1}$), is the amount of sediment eroded from that pixel that reaches the flow. Sediment export is given by

$$E_i = usle_i \cdot SDR_i \tag{33}$$

The total export of sediments in basin E (units: tons · $ha^{-1}year^{-1}$) is given by

$$E = \sum_i E_i \tag{34}$$

To determine the total export of sediments, we proceed in two steps:

1) a calculation of the connectivity index (*IC*) for each pixel. The connectivity index describes the hydrological link between sediment sources (from the landscape) and end receptors (such as streams). Higher IC values indicate that sediment erosion from the source is more likely to reach an end receptor, which occurs in the case of sparse vegetation or steeper slopes. Lower *IC* values are associated with more vegetated areas and lower slopes.

IC is a function of both the *upslope* (upstream) area of each pixel (D_{up}) and the flow path between the pixel and the closest flow (Dd_n). If the slope area is large, has a shallow slope and good vegetation cover (hence a low USLE C factor), D_{up} will be low, indicating less potential for sediment to reach the stream. Similarly, if the descent path between the pixel and the stream is long, with a lower slope and good vegetation cover, D_{dn} will be low. *IC* is calculated as follows:

$$IC = \left(\frac{D_{up}}{D_{dn}}\right) \tag{35}$$

$D_{up} = \underline{C}\underline{S}\sqrt{A}$ is the upslope component. Where $\underline{C}$ is the average C factor (*crop management factor*, coverage management factor by type of crop) of the upslope area, $\underline{S}$ is the average slope of the upslope area (m/m) and *A* is the upslope area (m2).

The downslope component D_{dn} is given by

$$D_{dn} = \sum_i \frac{d_i}{C_i S_i} \tag{36}$$

where d_i is the path length of the flow along the i-th cell in the direction of the steepest

slope (m), C_i and S_i are the factor C and the slope gradient of the i-th cell, respectively.

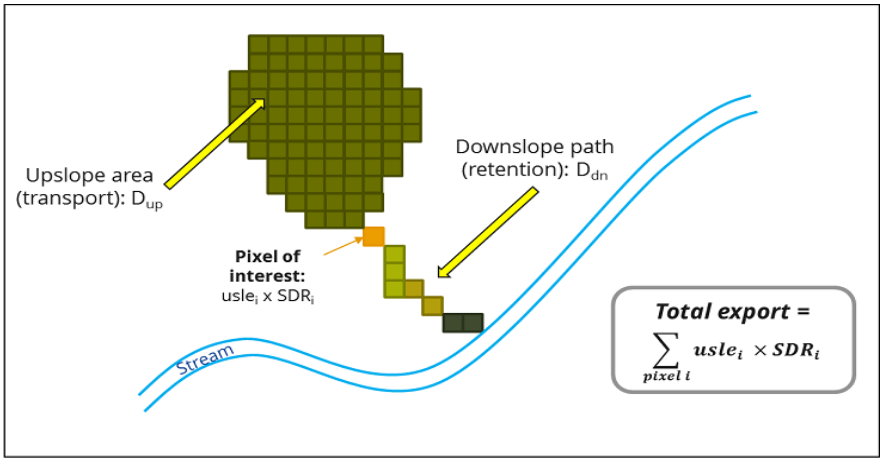

Figure 54 Conceptual approach of the sediment delivery ratio and the connectivity index. The sediment export rate (SDR) for each pixel is a function of the upslope area and the downslope flow path (Natural Capital Project).

2) The SDR factor (Fig. 54) for a pixel *i* is derived from the connectivity index *IC* according to the following relationship (Vigiak et al., 2012)

$$SDR_i = \frac{SDR_{max}}{1+exp\left(\frac{IC_0 - IC_i}{k}\right)} \quad (37)$$

where SDR_{max} is the maximum theoretical SDR, which we set to an average value of 0.8 as a function of soil texture, and IC_0 and k are calibration parameters that determine the shape of the relationship between hydrological connectivity (the degree of connection between plots of land and flow) and the sediment export ratio (percentage of soil loss that reaches the flow). The default values are $k = 2$ and $IC_0 = 0.5$.

5.2.2.3. Input data for the Piave river basin

There are many input data used for sediment load determination. For the Piave river basin, data from numerous sources have been assembled to produce the necessary spatial information and include:

Vector delineation of the watershed and water elements was obtained from the geoportal of ARPAV, relative to the Water Protection Plan 2015 (Piano di Tutela delle Acque) (ARPAV, 2018a, 2018b).

DEM raster at 20m resolution obtained from the from the national research authority - ISPRA (Istituto Superiore per la Protezione e la Ricerca Ambientale) (ISPRA, 2020), was corrected to fill hydrological sinks and checked with the digital watercourse network to ensure routing along the specific watercourse, using QGIS 3.18 (https://www.qgis.org).

LULC raster were obtained from Corine Land Use Land Cover IV Level for Italy (ISPRA,

2018) for current condition (2018) according to the developed land use change scenario (A1, A2, B1, C1). Future LUCL maps (2050) considering the combination of all the land use scenarios developed (A0, A1, A2, B0, B1, C0, C1), as descript in the sub-chapter 2.2.

Soil erodibility, K_i, is a measure of the potential for soil particles to detach and be transported by rainfall and surface runoff (units: tons·ha·h· (ha·MJ·mm)$^{-1}$). Soil Erodibility was extrapolated from Soil Erodibility in Europe High Resolution dataset provided by ESDAC (500m) (Panagos et al., 2014, 2012).

Rainfall erosivity index (R_i) raster dataset, with an erosivity index value for each cell. This variable depends on the intensity and duration of the rains in the basin area. For calculation, R equals the annual average of EI values, where E is the kinetic energy of rainfall (in MJ ha^{-1}) and I_{30} is the maximum intensity of rain in 30 minutes (in mm.hr^{-1}) (InVEST 2018). The greater intensity and duration of the rainfall events generally increase the erosion potential (units: MJ·mm· (ha·hr·year)$^{-1}$). Current: 500m res. Rainfall erosivity in Europe ESDAC (Bezak et al., 2022; Panagos et al., 2022, 2017). Future: 500m res. (MJ mm ha^{-1} hr^{-1} year^{-1}) Future rainfall erosivity ESDAC (projections 2050 based on climate change).

C_i Factor is the crop management factor or land cover management factor C and accounts the crop type for the *USLE* soil loss equation with a range value between 0 and 1. The C values for the Piave river basin were obtained based on the study by Panagos et al. (2015a), European Soil data Centre (Table 23).

P_i factor for USLE is a value between 0 and 1 that considers the effects of ploughing, cutting, or terracing compared to straight row farming up and down the slope. P values for the Piave river basin were obtained based on the study by Panagos et al. (2015b), European Soil data Centre. For the area of interest, P = 0.97513.

Drainage lines layer is a raster with values equal to 0 and 1, where 1 correspond to pixels artificially connected to the flow (from roads, rain pipes, etc.) and 0 is assigned to all other pixels. The flow path will stop at these "artificially connected" pixels, before reaching the flow network, and the corresponding exported sediment is assumed to reach the outlet of the basin. In some situations, the connectivity index defined by the topography does not represent the actual flow paths, which may instead be affected by artificial connectivity. For example, sediment in urban areas or near roadways is likely to be carried away to the stream with little retention. The drainage lines raster identifies pixels that are artificially connected to the flow, regardless of their geographic location (for example, their distance from the flow network). From the DEM model corrected with the routedem model (InVEST), the “flow_direction_Piave” raster.

Table 23 Crop Management Factors – Land cover management factors C_i by crop type used in the model for the Piave Basin, by Panagos et al. (2015a).

Land use type	CLC18 class	C Factor
Urban, industrial, mining, roads, railways	111, 112, 121, 122, 131, 132, 142	0.078
Arable land and predominantly agricultural areas	211, 212, 243	124.65
Rice fields	213	0.15
Vineyards	221	0.3454
Orchards	222	0.2188
Surfaces with herbaceous cover not under rotation system	231	0.0988
Complex cultivation patterns	242	0.1478
Natural and forest areas	3112, 3113, 3114, 3115, 3116, 3117, 3122, 3123, 3124, 3131, 3132	0.0013
Pastures, grasslands, mixed vegetation	321, 3211, 3212	62.4548
Heaths and bushes	322	0.042
Transitional woodland-shrub	324	0.0242
Beaches, dunes, sands	331	0.078
Sparsely vegetated areas	333	0.2509
Bare rocks, streams and other water bodies	332, 335, 511, 512, 523	0

5.2.3. Results and Discussions

The model results include the following parameters:

- Sediment export (unit: tons/catchment per year): total amount of sediment exported in the stream by catchment area.
- Total USLE (unit: tons/watershed per year): Total amount of potential soil loss in each watershed calculated from the Universal Soil Loss Equation (USLE).
- Sediment retention (unit: tons/catchment per year): Difference in the amount of sediment exported to the river in the catchment in question and a hypothetical catchment where all land use types have been converted to bare land.
- Sediment deposition (unit: tons/catchment per year): total amount of sediment deposited on the landscape in the reference catchment area, which does not reach the watercourse.

5.2.3.1. Comparison of 2018 scenarios

The scenario B1 (C0A0B1, Figure 55) showed the best effect in reducing soil loss compared to the 2018 base scenarios with a percentage of 7.20% ($1.67x10^6$ tons) of soil preserved in the basin (Table 24). The combination of the scenario B1 and scenario A2 increased the soil retention in the basin to $1.68x10^6$ tonnes (Figure 56a). The scenario with the hydraulic safety work (C1A0B0) showed an increase in the soil loss in the basin of $4.60x10^3$ tons, it is probably linked to the land use change in pastures and prairies by removing the actual vegetation. Even if the combination of scenario C1, with scenario B1, showed an increase in the reduction of soil loss, this remained below the reduction effect obtained from scenario B1 alone.

The B1 scenario was also the best for the sediment export (5.95%) with a reduction of 1.89 $x10^5$ tons of sediment exported in the basin. This reflects the retention of nutrients which increased in scenario B1 by 0.07% and decreased the sediment deposition by 7.40% (Table 24). In this case the combination of scenario B1 and A2 further reduced the export of sediments (Figure 56b).

Table 24 Variation in soil loss and sediment transport based on 12 management scenarios of the Piave river basin under current climatic conditions (2018).

2018	**SDR Piave Basin**				**SDR Piave Basin %**			
Scenario	usle_tot (ton/basin)	sed_exp (ton/basin)	sed_ret (ton/basin)	sed_dep (ton/basin)	usle_tot %	sed_exp %	sed_ret %	sed_dep %
C0, A0, B0	**$2.41 x10^7$**	**$3.27 x10^6$**	**$2.54 x10^8$**	**$2.08 x10^7$**	**$2.41 x10^7$**	**$3.27 x10^6$**	**$2.54 x10^8$**	**$2.08 x10^7$**
C0, A1, B0	$2.41 x10^7$	$3.27 x10^6$	$2.54 x10^8$	$2.08 x10^7$	-0.01	0.00	0	-0.01
C0, A2, B0	$2.41 x10^7$	$3.27 x10^6$	$2.54 x10^8$	$2.08 x10^7$	-0.01	0.00	0	-0.01
C0, A0, B1	$2.24 x10^7$	$3.08 x10^6$	$2.54 x10^8$	$1.93 x10^7$	-7.20	-5.95	0.07	-7.40
C0, A1, B1	$2.24 x10^7$	$3.08 x10^6$	$2.54 x10^8$	$1.93 x10^7$	-7.21	-5.95	0.07	-7.41
C0, A2, B1	$2.24 x10^7$	$3.08 x10^6$	$2.54 x10^8$	$1.93 x10^7$	-7.22	-5.95	0.07	-7.41
C1, A0, B0	$2.41 x10^7$	$3.27 x10^6$	$2.54 x10^8$	$2.08 x10^7$	0.02	0.01	0.00	0.02
C1, A1, B0	$2.41 x10^7$	$3.27 x10^6$	$2.54 x10^8$	$2.08 x10^7$	0.01	0.00	0.00	0.01
C1, A2, B0	$2.41 x10^7$	$3.27 x10^6$	$2.54 x10^8$	$2.08 x10^7$	0.01	0.00	0.00	0.01
C1, A0, B1	$2.24 x10^7$	$3.08 x10^6$	$2.54 x10^8$	$1.93 x10^7$	-7.19	-5.94	0.07	-7.39
C1, A1, B1	$2.24 x10^7$	$3.08 x10^6$	$2.54 x10^8$	$1.93 x10^7$	-7.21	-5.95	0.07	-7.40
C1, A2, B1	$2.24 x10^7$	$3.08 x10^6$	$2.54 x10^8$	$1.93 x10^7$	-7.21	-5.95	0.07	-7.41

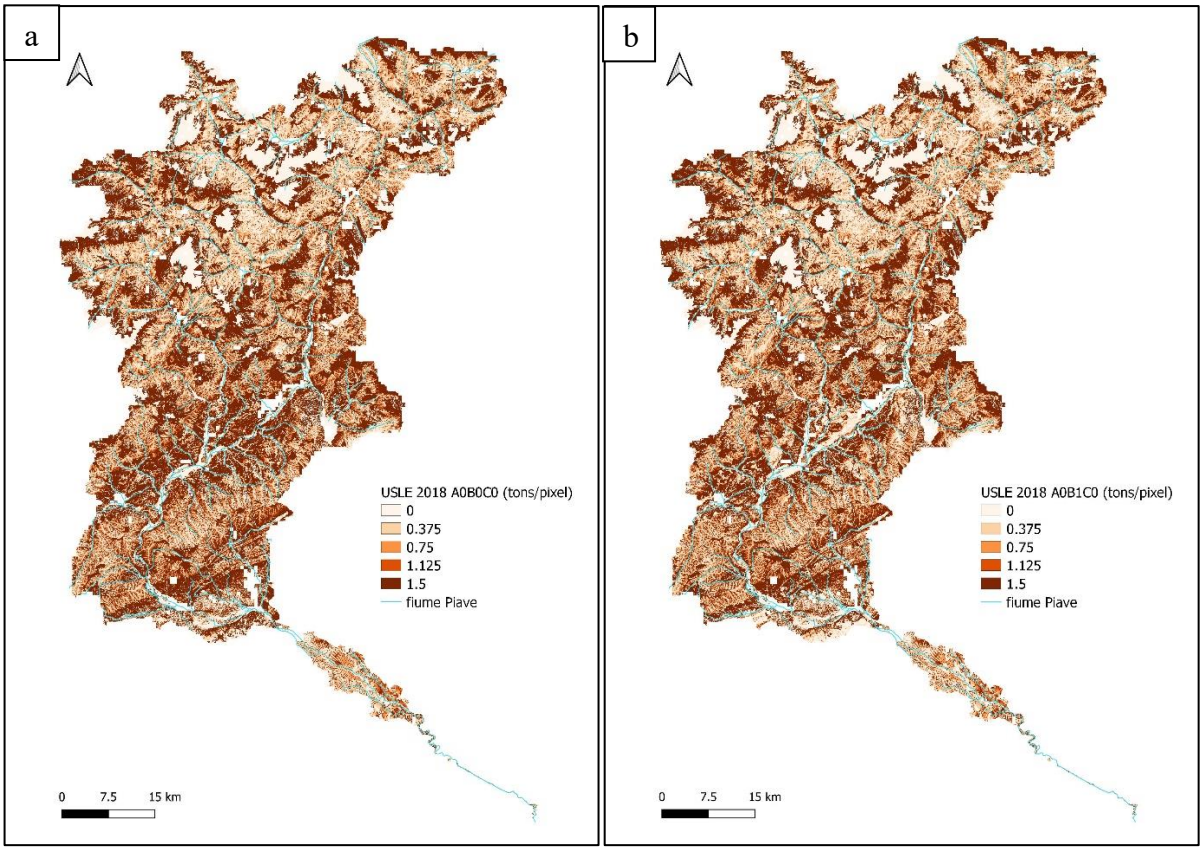

Figure 55 Comparison between USLE land loss maps 2018 (a) baseline scenario (b) scenario B1.

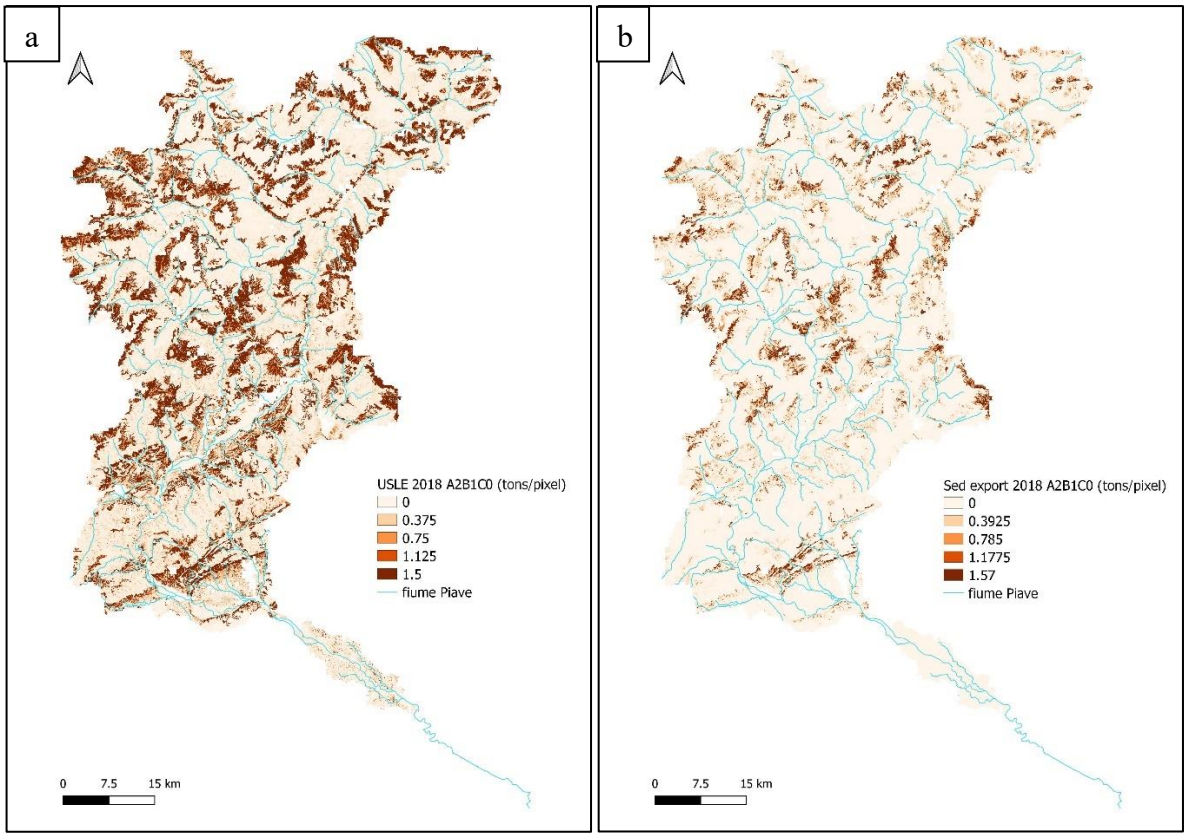

Figure 56 Maps (a) USLE soil loss and (b) sediment export for the best combination of A2B1 scenarios.

5.2.3.2. Comparison of 2050 scenarios

The scenario B1 showed the best effects in reduction of soil loss (USLE) compared to the others 2050 climate change scenarios (RCP 4.5) (Fig. 57a, b). The soil loss amounted to 0.29% ($6.99x10^4$ tons) unlike the base scenario (A0) which showed an increase of 5.39% ($1.33x10^6$ tons) of soil lost in the basin area (Table 25). The greater presence of forest vegetation that replaced agricultural areas with large natural spaces in the upper basin translates into a greater presence of roots that better hold the soil and counteract possible increases in erosion due primarily to the erosion of rain (R factor).

Sediment dynamics showed an increase in export and retention in all scenarios and combinations of scenarios developed for 2050 (Table 25). Instead, the sediments' deposition showed an increase in the base scenario A0 and in the scenarios A1 and A2 of 4.99% and a reduction of 0.86% in B1 scenario (Table 25), also linked in this case to the greater coverage in wooded areas in the Piave mountain basin.

The loss of soil showed in the combination of scenario B1 with both scenario A1 and scenario A2 a further percentage improvement in the reduction of soil loss of 0.30% corresponding to $7.16x10^4$ tons/basin for scenario A1 and $7.21x10^4$ tons/basin for scenario A2 (Table 25).

With regards to the deposition of sediments, a reduction is evident in scenario B1 and in its combinations with A1 and A2, with and without work for hydraulic safety, the reduction percentage remained almost unchanged (Table 25).

Table 25 Variation in soil loss and sediment transport based on 12 management scenarios of the Piave river basin under future climatic conditions (2050).

2050	**SDR Piave Basin**				**SDR Piave Basin %**			
Scenario	usle_tot (ton/basin)	sed_exp (ton/basin)	sed_ret (ton/basin)	sed_dep (ton/basin)	usle_tot %	sed_exp %	sed_ret %	sed_dep %
C0, A0, B0	$2.54 x10^7$	$3.53 x10^6$	$2.69 x10^8$	$2.19 x10^7$	5.39	7.83	5.85	4.99
C0, A1, B0	$2.54 x10^7$	$3.53 x10^6$	$2.69 x10^8$	$2.19 x10^7$	5.39	7.83	5.85	4.99
C0, A2, B0	$2.54 x10^7$	$3.53 x10^6$	$2.69 x10^8$	$2.19 x10^7$	5.38	7.83	5.85	4.99
C0, A0, B1	$2.40 x10^7$	$3.37 x10^6$	$2.70 x10^8$	$2.06 x10^7$	-0.29	3.18	5.91	-0.86
C0, A1, B1	$2.40 x10^7$	$3.37 x10^6$	$2.70 x10^8$	$2.06 x10^7$	-0.30	3.18	5.91	-0.87
C0, A2, B1	$2.40 x10^7$	$3.37 x10^6$	$2.70 x10^8$	$2.06 x10^7$	-0.30	3.18	5.91	-0.87
C1, A0, B0	$2.54 x10^7$	$3.53 x10^6$	$2.69 x10^8$	$2.19 x10^7$	5.41	7.84	5.85	5.01
C1, A1, B0	$2.54 x10^7$	$3.53 x10^6$	$2.69 x10^8$	$2.19 x10^7$	5.40	7.84	5.85	5.00
C1, A2, B0	$2.54 x10^7$	$3.53 x10^6$	$2.69 x10^8$	$2.19 x10^7$	5.40	7.84	5.85	5.00
C1, A0, B1	$2.40 x10^7$	$3.37 x10^6$	$2.70 x10^8$	$2.06 x10^7$	-0.28	3.19	5.91	-0.85
C1, A1, B1	$2.40 x10^7$	$3.37 x10^6$	$2.70 x10^8$	$2.06 x10^7$	-0.29	3.19	5.91	-0.86
C1, A2, B1	$2.40 x10^7$	$3.37 x10^6$	$2.70 x10^8$	$2.06 x10^7$	-0.29	3.19	5.91	-0.86

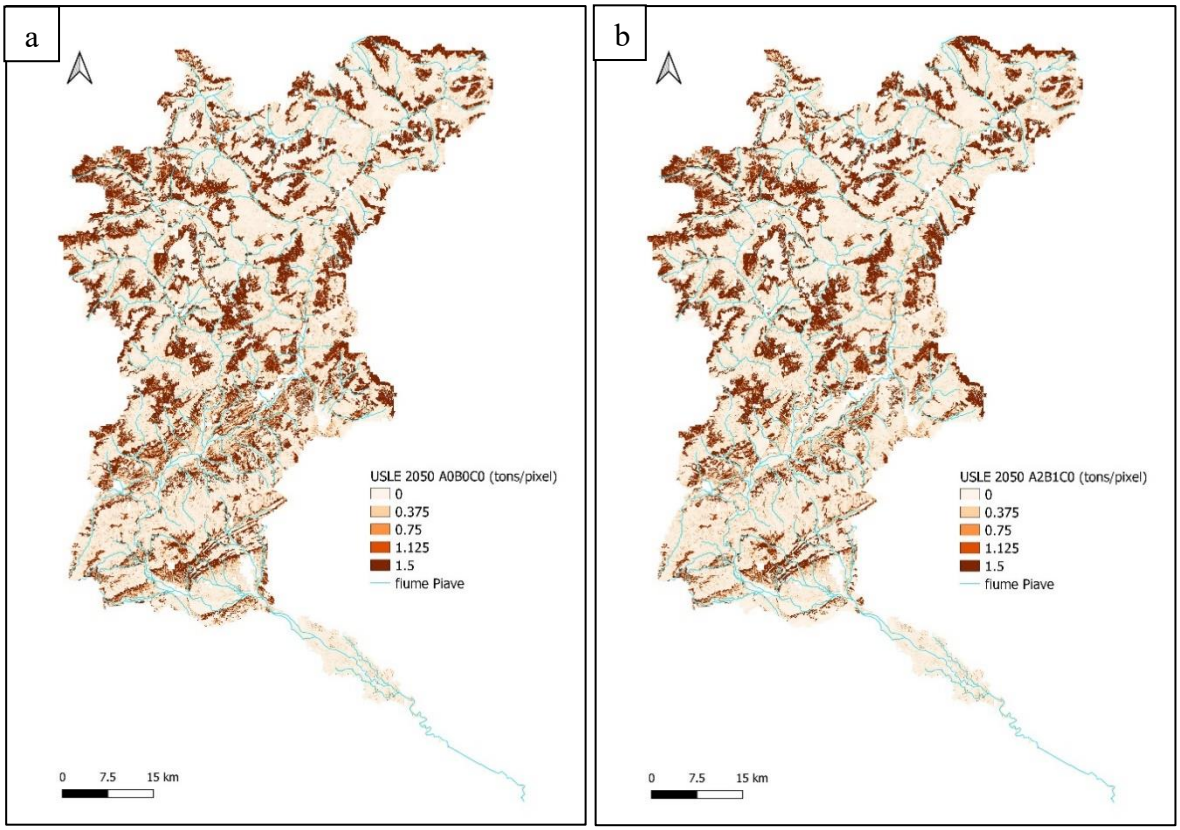

Figure 57 Comparison of land loss USLE maps for 2050 scenarios (a) base (A0B0C0) and (b) best scenario B1.

5.2.3.3. Validation

To validate the model on the total sediment load exported to the river, the total suspended solids (TSS, mg L^{-1}) ARPAV sampling data relating to the year 2018 were considered.

Table 26 Validation of model data with ARPAV data, TSS estimate referring to 2018.

ARPAV 2018	Min	Max	Mean	SD	Export ARPAV (tons/year)
TSS mg L^{-1}	3	136	27.3	38	7.17 x10^6

The average value of total suspended solids in the Piave for the year 2018 was 27.3 mg L^{-1} (Table 26), with rather high values (> 100 mg/L TSS) in the late autumn and winter months. This data was reported on an annual basis using the average flow rate of 116 m^3/s of the Fossalta di Piave station. The value obtained with by ARPAV data (Table 26) and compared with the total sediment export data (3.27x10^6 tons) of the model (Table 24) it can be seen that, although the model provides a good approximation, it nevertheless has a limited number of parameters for which the output values generally show a high sensitivity to the input data.

The USLE model have limitations related to the low number of parameters. As in all geo-spatial models, the outputs are very sensitive to input parameters and errors in the empirical

parameters of the USLE equations. Among the main limitations of the model is its dependence on the USLE. This equation is widely used but only represents overland (rill/inter-rill) erosion processes. Other sources of sediment include gully erosion, streambank erosion, and mass erosion. Mass erosion (landslide) can be a significant source in some areas or certain land use changes, such as road construction.

Erosion is a major cause of soil degradation with consequences for land and aquatic resources. Recent studies using models based on a high spatial resolution universal soil loss equation (RUSLE) revisited semi-empirical modelling approach (GloSEM) can predict the future rate of erosion by modelling the change in the erosion potential of precipitation (factor R) using alternative scenarios of the Shared Socioeconomic Pathway and Representative Concentration Pathway (SSP-RCP) (Borrelli et al., 2020). Climate projections for all global dynamic's scenarios indicate a trend towards a more vigorous hydrological cycle that could increase global water erosion (+30 to +66%). In EU agricultural land, the mean change in rainfall erosivity 2010-2050 varies by +23.9% in RCP4.5.

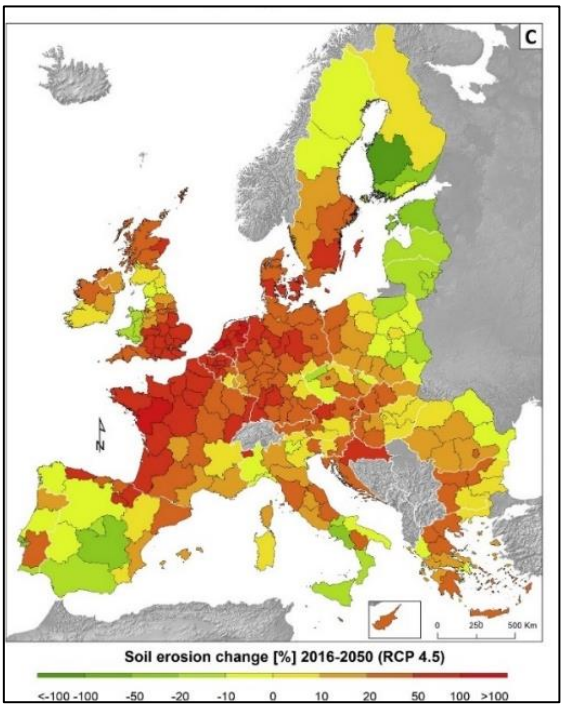

Figure 58 Map of soil erosion estimate in Europe for climate scenario RCP4.5 (from Panagos et al., 2021).

In the Mediterranean basin (Italy, Spain, Portugal, and southern France) where erosional events in late spring and early autumn are the dominant ones, there is a relatively modest increase in erosivity (7% – 12%). In 2050, the average soil losses in Europe under the RCP2.6 and RCP4.5 scenarios are projected to be 3.47 and 3.46 t ha^{-1} $year^{-1}$, respectively. In the RCP4.5 scenario, soil loss by water erosion is estimated to increase by 76% in agricultural land and decrease for the remainder (Fig. 58) (Panagos et al., 2021).

Improving knowledge of future rates of soil erosion, accelerated by human activity, is important for making decisions for local, regional and national strategies for soil conservation. Predicting future rates of erosion provide a useful knowledge base to support decision-makers in considering the development of more resilient agricultural systems, such as forestry agriculture, regenerative agriculture or other emerging techniques that can go beyond current conservation agriculture strategies. These must consider that we may face major climate change now and in the coming decades.

5.2.4. Conclusions

Sediment export and retention are important ecosystem processes causing soil erosion and sediment loading in waterways consequently affecting the health of aquatic habitats downstream. The Comparison between the 2018 NBS scenarios showed a -7% of soil losses in the Piave basin. Most sediment export and retention occurred from forest or vegetated land use land cover types. The model validation confirms that the outputs obtained are consistent with the ARPAV official data, demonstrating that the SDR model is an appropriate tool for estimating soil-loss potential by water at regional/national levels.

In addition, both sediment concentration and export, can influence the water turbidity which represents an important determinant of water quality with consequent effects to the aquatic lives. Therefore, the temporal distribution of rainfall and corresponding sediment export becomes important, since these two factors determine the sediment concentration as well as turbidity in the waterbody. Future projections of 2050 clearly showed that reforestation can reduce soil loss and preserve soil functions (e.g., carbon sink).

The study revealed the potential of SDR model to quantify the sediment export and retention in the Piave River basin and it would help the policy makers in making informed decisions for planning sustainable conservation and strategies for soil and water.

6. ECOSYSTEM SERVICES EVALUATION AND PRIORITIZATION

6.1. Background

In this last phase of the research was reached the ESs quantification and their relationship with the environmental management priorities of the Piave basin, with particular focus at the lower Piave basin. The integration of the concept of ecosystem functions and services in territorial management and planning is essential for the local decision making. The local authorities can control the pressures that threaten the ecosystem and their functionality, "building" a governance model based on tools such as payments for ecosystem services.

After a careful analysis of all the single NBS scenarios produced by the development of the ecosystem services models, the attention was focused on the scenarios for the year 2050. The 2050 scenarios include climate change according to the RCP 4.5 model of the IPCC report AR5 (2014), an intermediate scenario which assumes a radiative forcing at 2100 of 4.5 W/m^2.

Twelve future scenarios were developed for each model. Starting from these scenarios, it was possible to compare each NBS scenario and each combination of scenarios to evaluate which showed the best positive effect for ecosystem services, so that for each scenario it was possible to evaluate which ones would bring the optimal results for the Piave. The best individual baseline scenarios and the best combination of two scenarios (e.g., A1B1) were identified for each ecosystem service (Figure 59-63).

6.2. Ecosystem services assessment – Selection of the best scenarios

The B1 scenario was the best scenario for the service related to the **soil loss reduction** in the Piave basin projected for 2050, with a reduction of the soil loss of 0.29% compared to current conditions (Fig. 59). The greater presence of forest vegetation in the agricultural areas with large natural spaces in the upper basin translates into a greater presence of roots systems which means that they hold the soil better, reducing the hydrogeological risk. In the Lower Piave, scenario A2 presents the best conditions for reducing soil loss, since the belt of hygrophilous forest along the rivers reduces bank erosion. The combination of the scenarios B1 and A2 increased another percentage point in the reduction of soil loss which results in a total of 7.21×10^4 tonnes of soil not lost in the basin.

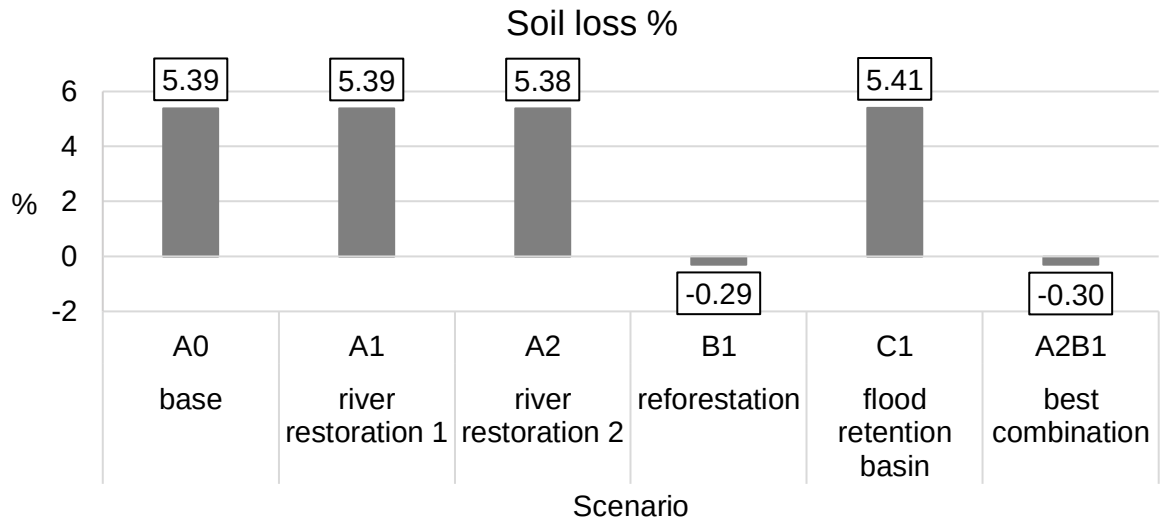

Figure 59 Percentage loss of soil for the baseline scenarios and the best combination of scenarios.

For the service relating to **phosphorus exports** in the basin for 2050, the best scenario is represented by B1 with a reduction of phosphorus load of 27.58% compared to current conditions (Fig. 60). Phosphorus is closely linked to the sediment and in some of its forms it is adsorbed by soil particles (Regelink et al., 2015). In this case the greater presence of forest vegetation brings a benefit because it allows the roots to retain the soil and consequently the phosphorus. Furthermore, phosphorus is one of the essential nutrients for plant growth, as well as being retained by the roots it is also absorbed by them. In the Lower Piave, scenario A2 presents the best conditions for reducing the phosphorus load, again linked to the greater presence of riparian vegetation inside the banks. The combination of the two scenarios B1 and A2 leads to a reduction in phosphorus exports of 28.34% for the sum of the positive effects linked to reforestation upstream and in the floodplain of the lower course of the Piave.

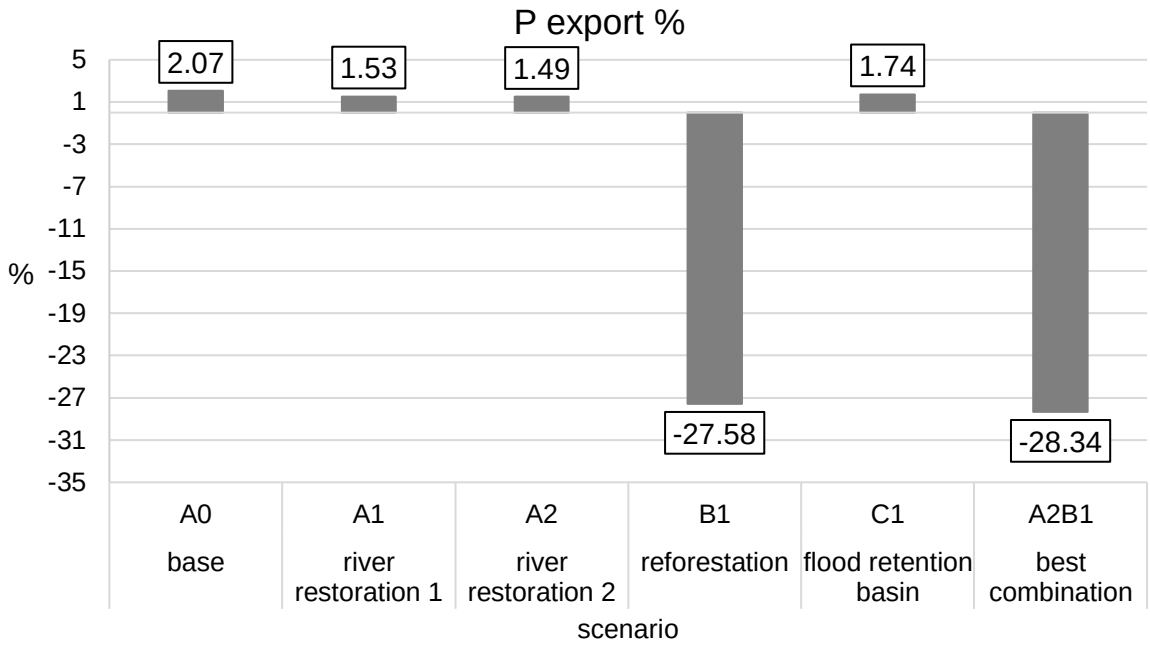

Figure 60 Percentage export of phosphorus for the baseline scenarios and the best combination of scenarios.

The service linked to the **nitrogen export** in the Piave basin for the 2050 showed B1 as the best scenario with a reduction of the nitrogen load of 6.95% compared to current conditions (Fig. 61). By increasing the forest cover, nitrogen, which is also an essential nutrient for plants, is absorbed by plants. Furthermore, the increase in riparian vegetation increases its buffer function against diffuse pollution, retaining the excess of nutrients which, in the absence of vegetation, can easily reach the river. In the Lower Piave, scenario A1 presents the best conditions for reducing the nitrogen load that reaches the river.

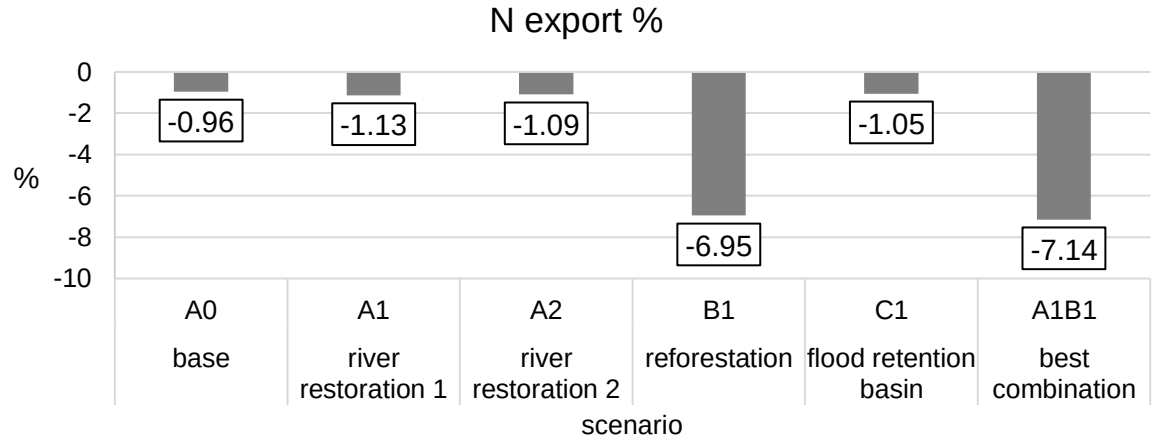

Figure 61 Export percentage of nitrogen for the basic scenarios and the best combination of scenarios.

Scenario B1 represents the best scenario for the **carbon storage and sequestration** ecosystem service contributing 5.43% (Fig. 62) more than the other baseline scenarios. Carbon

stored by European forests is currently increasing due to changes in forest management (CORDIS, 2016), as scenario B1 well represents. In the lower Piave, scenario A2 presents the best conditions for further carbon storage. About half of the carbon is stored in the soil of forests, so when forests are damaged or cut, the carbon is released back into the atmosphere.

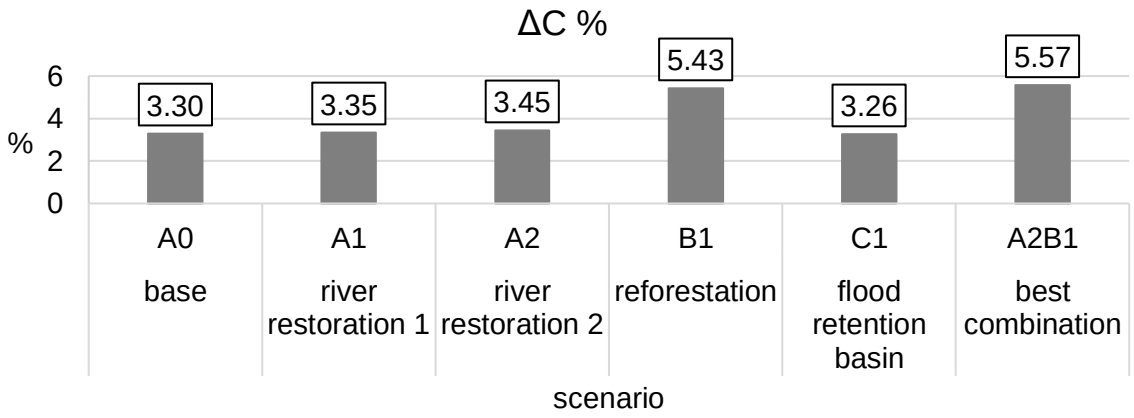

Figure 62 Percentage carbon storage for baseline scenarios and best combination of scenarios.

The **water availability** model predicts a loss of water volumes in all scenarios (Fig. 63). Scenario C1 represents the scenario with the least loss of water volumes (19.85%) with a reduction of 9.86×10^8 m^3. The second-best scenario is represented by A1, followed by the combination of the two scenarios (C1A1). According to IPCC models, the amount of water available in the Piave basin will decrease in the future due to climate change. Precipitation will be less frequent but more intense and concentrated in the short term, causing inconvenience related to the effects of extreme climatic events (Iannuccilli et al., 2021). Being able to retain as much water as possible in the area so that it can be used in periods of drought represents the challenge of the future.

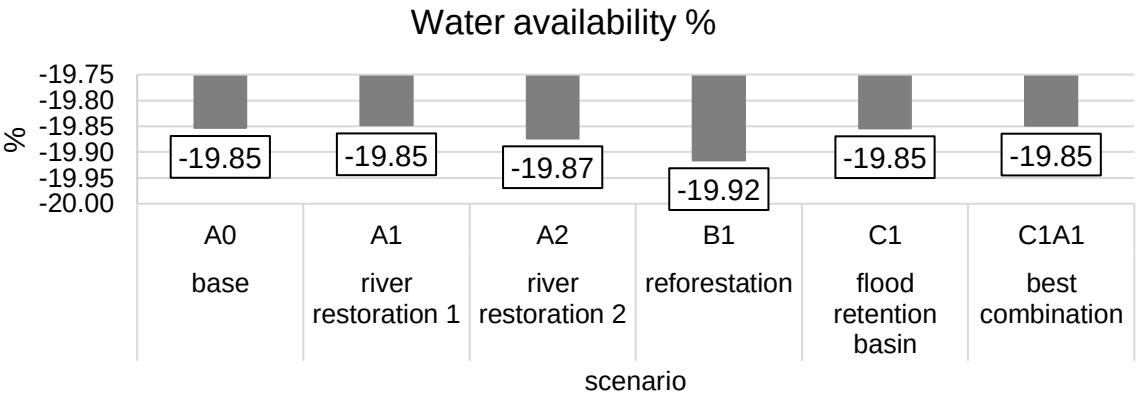

Figure 63 Percentage water availability for the baseline scenarios and the best combination of scenarios.

6.3.Method of prioritization

Several environmental objectives were identified related to the management of the river and the ecosystem services provided. Ecosystem services were associated with each environmental objective based on the relationship between the service provided and the objective itself, to identify the best scenarios with respect to each objective. The individual objectives have been determined based on the most recent legislation and the priorities of the Veneto Region (PAC), of the Eastern Alps Basin District Authority (Water Protection Plan), of the European directives (Water Framework Directive 2000/60/EC, Habitats Directive 92/43/EEC) and IPCC reports. The environmental goals considered in the analysis are:

- Control and reduction of the Piave River eutrophication
- Control and reduction of the Adriatic Sea eutrophication
- Protection and conservation of the soil
- Improving responses to climate change (COP27)

For each goal, the Drivers, Pressures, and Impacts (DPSIR model) were identified in relation to the Piave river as envisaged in the Water Management Plan produced by the Eastern Alps Basin District Authority in compliance with the Water Framework Directive (WFD 2000/60/CE).

For each goal, ecosystem services were selected that have both a direct and indirect impact. The relative weight assigned to each ecosystem service linked to the specific objective was evaluated considering the relationship between the current state, the determined impacts, and the variations on the relative pressures of each service at present (base scenario year 2018, as per the previous reports of the project) and future (year 2050).

For each goal and its ecosystem services were evaluated all single and combined scenarios. For each ecosystem services were identified the single scenario that produced the best positive effects to meet this objective. Furthermore, all possible combinations of scenarios were also evaluated with the same method.

The weight attributed to the best scenario were based on the natural stoichiometric ratio between the elements carbon, silicon, nitrogen, phosphorus (C:Si:N:P). These weights were related according with the control and reduction of the eutrophication of the Piave river, the Adriatic Sea and for the protection and management of agricultural resources. The ideal soil water content was also used for agriculture. For the goal of improving the basin's responses to climate change was considered the relationship between carbon dioxide (CO_2) and nitrogen oxide (N_2O) and their global warming potential.

6.3.1. Control and reduction of the Piave River eutrophication

The eutrophication of the river is linked to an excess of nutrients, substances essential for plant growth, among which a decisive role is played by the bioavailable forms of nitrogen and phosphorus. Studying the distribution of nutrients is very important for assessing the risk of eutrophication in water bodies. The supply of nutrients is a natural process that allows aquatic plants to carry out their biological cycle; however, when the nutrients intake exceed, there is an exponential growth of phytoplankton, in particular of the more opportunistic species, also causing a strong change in the composition of the phytoplankton community. The consequences are linked: the excessive development prevents sunlight from penetrating into the water, inhibiting the photosynthesis of the vegetation located deeper; the increase in organic mass promotes the process of bacterial decomposition, an aerobic process which leads to a reduction of the oxygen available for other microorganisms (phytoplankton) and for the fish causing their death.

To give weight to the models I chose to follow the Redfield–Brzezinski ratio where the Si:N:P ratio is 15:16:1 (Brzezinski, 1985). The N:P ratio (Redfield-Brzezinski ratio) is an important indicator that serves to specify which nutrient limits eutrophication. If the N:P ratio > 16, phosphorus (P) is the limiting factor for algae growth. If N:P is between 14 and 16, both N and P are limiting factors (Mills et al., 2008) and if the ratio is N:P < 14, it indicates that nitrogen (N) is the limiting factor for the growth of algae (Hodgkiss and Lu, 2004; Redfield et al., 1963). Turner et al. (2003) estimated the ratio 16:1 DIN:DIP for phytoplankton and 1:1 DSi:DIN for diatoms (DIN = dissolved inorganic nitrogen; DIP = dissolved inorganic phosphorus or orthophosphate).

Applying this Si:N:P ratio 15:16:1 and considering the ratio of nitrogen to phosphorus of the river during the study period, together with the contribution of silicon, nitrogen and phosphorus from sediment loss to the river, it was identified a ratio between phosphorus, nitrogen and sediment exports of 1.6:1:0.5 (Fig. 64, “Relative weight” column), where an increase in P export will be more impactful than an increase in N or Si. proportion reducing P brings greater benefits than reducing N.

In addition, as a support to the priority analysis, the scenario A1 was identified as the best to the habitat quality, and from some relevant information of the citizen scientists where the participants were underlined the aesthetic, historical and recreational values of the Piave river (cultural ecosystem service).

➢ Control and reduction of the Piave River eutrophication

Drivers	Land use change	Increase of Urban areas	Agriculture			**Indicators**	**Ecosystem services models**	**Relative weight**	**Scenarios**	**Ecosystem service**
Pressures	Agriculture	Withdrawals	Wastewater Treatment plants	Urban runoff	Traffic	P concentration	P export	5.2	B1, A2	Nutrient retention (Self-purification)
						N concentration	N export	3.1	B1, A1	
Impacts	Water quality	Diffuse pollution	Point sources pollution	Soil erosion	Habitat	Land use	Soil loss	1.6	B1, A2	Soil (carbon sink)
						Precipitation				Surface water for non-potable use

Additional ESs	Habitat	+	A1	Habitat
	Cultural (CtN)	+	A1	Aesthetic, landscape
				Recreation and education

Scenarios
B1 – Reforestation upper basin (14,574ha)
A2 – Reforestation inside the lower basin riverbanks (1,070ha)

Figure 64 Summary scheme of the components (DPSIR), weights and scenarios considered for control and reduction of eutrophication in the Piave river.

6.3.2. Control and reduction of the Adriatic Sea eutrophication

The amount of nutrients (N, P, Si) transported to the coastal zone by large river systems, as well as the balance between these elements, are the main factors determining the problems of coastal marine eutrophication (Josette Garnier et al., 2021). Many of these problems are the consequence of the new production of non-siliceous algae, supported by nitrogen and phosphorus supplied by rivers in excess of the dissolved silica component (Royer, 2020).

The European Environment Agency (EEA) published the Report "Nutrient enrichment and eutrophication in Europe's seas" which analyzes whether and how Europe has been able to reverse the eutrophication trends in its regional seas (EEA, 2019). The assessment is based on available monitoring data, mainly collected in the context of the Water Framework Directive, the Marine Strategy Framework Directive and the Regional Maritime Conventions. According to the EEA assessment, following the mapping for eutrophication assessment of 2,400,000 km^2 of European seas, approximately 563,000 km^2 (23%) of these areas are eutrophically challenged.

In the case of the Adriatic Sea, the anthropogenic contribution of nutrients from rivers such as the Po and the Piave, associated with agriculture and the urban contribution of large coastal cities, has determined a strong impact on the quality of sea water, determining conditions of eutrophication (Giani et al., 2012). The waters of the Adriatic in summer are stratified, and this limits the mixing of the water column, leading to a high eutrophication and frequency of hypoxic events (lack of oxygen dissolved in the water). Historical data from 1972 to 2010

indicate a trend of reversal of the phenomenon starting from the 2000s, thanks to lower concentrations of chlorophyll, decrease in river nitrogen loads (except for the Po river from which the load has increased), phosphorus and silica, with a related decrease in hypoxic events since the late 1980s and 1990s. The change in the ratio of dissolved mineral components is due to the reduction of phosphate concentrations thanks to the new regulations on polyphosphates in detergents and the lower nutrient influx from the Po River between 2000 and 2008, following a dry climatic period with reduced precipitation. The 2003-2007 drought resulted in a marked decrease in the net primary production of phytoplankton and chlorophyll. Nutrient and chlorophyll concentrations remained low after the return of higher river flows in 2008-2016, possibly due to better control of nutrient loads by watersheds (Totti et al., 2019).

The main limiting factors for phytoplankton growth are light, temperature and nutrients. Nutrients, mainly PO_4^{3-}, are limiting only in case of prolonged dry periods. Nitrogen concentrations have a strong influence on the marine ecosystem, altering the phytoplankton community and controlling the total biomass, also affecting the biomass of commercial fish stocks. The relationship between nitrogen loading and fish stocks is complex and also depends on local hydrographic conditions (the presence of deep hypoxic zones) and pressure from fishing activities (de Mutsert et al., 2016). A comparison of 30 coastal ecosystems shows that when the spatial extent of bottom hypoxia is < 20% of the ecosystem surface, the fish stock per unit load N (kg wet weight per kg N) varies between 0.1 and 2.1, but when the spatial extent was > 20%, the stocks per load N are consistently < 0.5.

Comparison of N:P ratios from 2011 to 2012 in the Bay of Durres (South Adriatic) (Gjyli et al., 2016), indicated an alternation of limitation for N and co-limitation of N and P. Comparing the ratio N: P in the Bay of Durres with the southern Adriatic Sea for both 2011 and 2012, N was found to be limiting for the bay while in open waters N and P are co-limiting of primary production. This study showed that there is a strong positive relationship between primary production (total chlorophyll a, Chl a) and nitrogen in coastal waters and a moderate positive relationship between primary production and N:P ratio in coastal waters.

In the Northern Adriatic, the formation and deposition of macroaggregates (mucilage) of bacterial-rich organic matter also fuels a high biological demand for oxygen, anoxia, and mass mortality in the May-September period (Ciglenečki et al., 2020; Degobbis, 1989). Mucilage episodes are unique for the North Adriatic both in terms of size, reaching up to 3 m in diameter, and in their abundance and spatial coverage, occupying hundreds of km^2 both in coastal waters and in the open sea. Sporadic occurrence of mucilage episodes increased in frequency from 1980 to 2004 (Danovaro et al., 2009). Major episodes (2-6 weeks in duration) occurred every

year during 1988-1991, 1996-1998 and 2000-2004. After a sustained episode from December 2006 to April 2007, relatively short-lived episodes were recorded in 2014 (August) and 2018 (July-August) (Malone and Newton, 2020).

The relative inputs of N and P can influence potentially toxic phytoplankton abundance and mycotoxins production (Glibert et al., 2014b; Glibert and Burford, 2017). Many toxic marine dinoflagellate species are more abundant when N is in a stoichiometric excess over P (N:P > 16), as is the case in the Upper Adriatic where N:P ratios increased from an average of 64 during the 1960s to >100 in the most recent years (Malone and Newton, 2020).

In addition to eutrophication, the ecosystem of the Adriatic Sea is subject to further pressures due to climate change: sea level rise, salinity increase, precipitation decrease, water temperature increase, with consequent water acidification and increase the number of thermophilic non-native species.

The most recent data on the ratio between N:P in the Adriatic Sea are 22:1 (DIN:TP 11:0.5), as reported in the environmental data report by ISPRA (2019). Applying this ratio and considering the nitrogen to phosphorus ratio of the river during the study period, a nitrogen to phosphorus export ratio of 1.4:1 was identified (Fig. 65). Also in this case, proportionally, there is a greater benefit by reducing P with respect to N, but N must in any case be monitored for the effects it produces in promoting the flowering of toxic algal species.

In addition, to support the priority analysis, the scenario A1 was identified as the best to the habitat quality, as a support ecosystem service, must be taken into consideration in the indications on the management choices of the lower Piave area.

➢ Control and reduction of the Adriatic Sea eutrophication

Drivers	Land use change	Increase of Urban areas	Agriculture			**Indicators**	**Ecosystem services models**	**Relative weight**	**Scenarios**	**Ecosystem service**
Pressures	Agriculture	Withdrawals	Wastewater Treatment plants	Urban runoff	Traffic	P concentration	P export	5.8	B1, A1	Nutrient retention (Self-purification)
Impacts	Water quality	Diffuse pollution	Point sources pollution			N concentration	N export	4.2	B1, A2	
						Land use				
						Precipitation				

Additional ESs	Habitat	+	A1	

Scenarios
B1 – Reforestation upper basin (14,574ha)
A1 – River restoration inside the lower basin riverbanks
(riparian forest 645ha + erodible belt 415ha)

Figure 65 Summary scheme of the components (DPSIR), weights and scenarios considered for control and reduction eutrophication in the Adriatic Sea.

6.3.3. Protection and conservation of the soil

Soil is a limited and non-renewable resource of fundamental environmental and socio-economic importance. Each soil has its own chemical-physical characteristics and a specific endowment of mineral elements and organic matter which determine the granulometric composition and structure, like the partition between soil, air, and water (Costantini and Dazzi, 2013). The optimal water content of a well-structured soil depends on the rainfall regime and for the purposes of agricultural production it has optimal values when it has values equal to 25% (Gardner et al., 2000). Macroporosity is normally occupied by air while micropores are occupied by water. The soil is the site of biogeochemical processes mediated by microorganisms which determine the degradation of fresh organic matter, rich in carbon, and its transformation into mature organic matter characterized by a lower C/N ratio (Huang et al., 2005; Madsen, 2011).

The Community Agricultural Policy and in particular the "farm to fork" strategy (European Commission, 2020b), promotes forms of agricultural production with lower inputs and greater environmental sustainability also with the aim of reducing climate-altering emissions which are 30% of agro-zootechnical origin. Although there is not yet a directive on soil conservation, the importance of this resource and the role it could play in terms of carbon stocks are being warned by many.

Agriculture is therefore one of the productive activities most exposed to the effects of climate change, it can be counted among the causes of climate change and at the same time it can play a very important role in the decarbonization process.

Water is the most important resource involved in the photosynthetic process, an essential resource to express the yield potential of the soil and to allow varieties of plants and animals to benefit from other factors that increase their agricultural production yield (Waraich et al., 2011).

In the Italian agricultural context, climate change deriving from the increase in temperature and therefore of evapotranspiration, from the increase in the frequency of extreme phenomena and from a different precipitation distribution, more abundant in the autumn-winter period and less in the spring-summer period , according to the most accredited forecasting models, could negatively influence the productivity of crops and in particular the spring-summer crops which will have to make greater use of irrigation (Bozzola et al., 2018).

Among the measures to mitigate the effects of climate change are early sowing to prevent critical phases of crops, such as flowering, from taking place in conditions of particular thermal and water stress. In addition, the cultivation of early varieties with shorter cycles and the selection of genetic material more tolerant to water stress or more capable of extracting water

from the soil. In all cases, in the absence of natural rainfall, the use of irrigation is a necessity to ensure the production of fruit and vegetables and summer cereals.

The correct regulation of excess water to recharge the aquifers and an optimal management of the water resource, as well as the protection of the quality of surface and groundwater freshwater represents a strategic priority in the context of a climate change process such as the one described by the reports of the IPCC (2019a).

The causes of the contraction of the water resource, in which agriculture plays a key role as a large user, are attributable to losses in the irrigation water distribution network, growing pollution of water bodies (sediments, dissolved salts, heavy metals, agro-pharmaceuticals and pathogens) (Ceccon et al., 2017).

The Water Framework Directive (2000/60/EC) requires Member States to facilitate sustainable water use based on the long-term protection of available water resources, ensuring that all needs are met to an acceptable level, including that of maintaining flow rates and water levels compatible with the health of ecosystems and with the quality of natural environments. Following the reduction in precipitation and the consequent decrease in water availability, critical situations have arisen for the water supply in numerous territorial contexts.

A healthy soil, in addition to the availability of water, is largely composed of the mineral component, consisting of the presence of fundamental chemical elements necessary for the development of vegetable biomass and for the functionality of ecosystems.

The already known C:N:P ratios for planktonic biomass and their importance in understanding biological processes and nutrient cycling in aquatic ecosystems have prompted ecologists to look for similar patterns in terrestrial ecosystems. Several studies indicate the existence of ratios similar to the Redfield ratio in plants, and such data can provide insight into the nature of nutrient limitation in terrestrial ecosystems (Bai et al., 2020; Fazhu et al., 2015; Li et al., 2012). Although the soil is characterized by high biological diversity, structural complexity and spatial heterogeneity, the concentrations of the elements of the individual phylogenetic groups within the soil microbial community can vary, but on average the atomic ratios C:N:P both in soil (186:13:1) and soil microbial biomass (60:7:1) are well constrained on a global scale (Cleveland and Liptzin, 2007). Elemental stoichiometry with direct evidence of microbial nutrient limitation suggests that measuring the proportions of C, N, and P in microbial biomass may represent another useful tool for assessing nutrient limitation of ecosystem processes in terrestrial ecosystems.

Considering the C:N:P ratio of the soil and that 25% water (W) is contained in the soil, we weighed the elements in order to obtain the optimal ratio of W:C:P:N at 4:1:1: 0.5 (Fig. 66).

The loss of arable soil is the most influential factor for agriculture, followed by the availability of water and the availability of nutrients which increases its productivity as a result of soil fertilization.

In addition, to support the priority analysis, the scenario A1 was identified as the best to the habitat quality, as a support ecosystem service, must be taken into consideration in the indications on the management choices of the lower Piave area.

➢ Protection and conservation of soil

Drivers	Land use change	Increase of Urban areas	Agriculture				**Indicators**	**Ecosystem services models**	**Relative weight**	**Scenarios**	**Ecosystem service**
Pressures	Agriculture	Withdrawals	Exploitation/ removal of animals/ plants	Atmospheric depositions	Physical alteration of canals/ riverbed/ riparian vegetation/ riverbank		Land use	Soil loss	6.2	B1, A2	Soil (carbon sink)
							Precipitation	Water availability	1.5	C1, A1	Surface water for non-potable use
Impacts	Water quality and quantity	Diffuse pollution	Point sources pollution	Soil erosion	Sea water and salt intrusion	Habitat loss	P concentration	P export	1.5	B1, A1	Nutrient retention (Self-purification)
							N concentration	N export	0.8	B1, A1	
Additional ESs	Habitat	+	A1								

Scenarios
B1 – Reforestation upper basin (14,574ha)
A2 – Reforestation inside the lower basin riverbanks (1,070ha)

Figure 66 Summary scheme of the components (DPSIR), weights and scenarios considered for the protection and conservation of agricultural resources.

6.3.4. Improving responses to climate change (COP27)

Climate change and environmental degradation are a significant threat to Europe and the world. The Intergovernmental Panel on Climate Change (IPCC, 2021) has described the profound, irreversible and devastating effects associated with the climate crisis, emphasizing that only further drastic reductions in greenhouse gas emissions can limit global warming to 1.5°C and avoid the most serious consequences of anthropogenic climate change. Although the EU (2020a) and many other parties of the Paris Agreement have set more ambitious goals for COP27, according to the latest UNFCCC (2022) synthesis report, the world community is still far from being on track to contain global warming within 2°C and remain within the limit of 1.5°C. Despite this, the EU is leading the green transition and showing the way for the implementation of the Paris Agreement by having an ambitious and binding legislative framework that regulates all sectors of the economy to comply with the agreements. Between 1990 and 2020, total EU greenhouse gas emissions decreased by 31%, while the economy grew

by more than 60%. Climate action is the EU's top priority, and the European Green Deal (2020a) aims to make Europe the first climate-neutral continent by 2050.

Currently, the World Meteorological Organization (WMO, 2022) has calculated that the concentration of carbon dioxide (CO_2) in the atmosphere is 40% higher than the level recorded at the beginning of the industrial era (400 ppm) and that CO_2 is responsible for 63% of global warming global warming caused by man while methane (CH_4) is responsible for 19% of global warming of anthropic origin (concentration of 1870 ppb), nitrous oxide (N_2O) of 6% (concentration of 330 ppb). The Global Warming Potential (GWP or Global Warming Potential) (IPCC, 2006) expresses the contribution to the greenhouse effect of each climate-changing gas in relation to the effect of CO_2, whose reference potential is equal to 1. The GWP is therefore the measure of how much a molecule of a certain greenhouse gas (CO_2, CH_4, N_2O, HFC, etc.) contributes to the greenhouse effect. Each GWP value is calculated for a specific time interval (typically 20, 100 or 500 years).

The increasing use of nitrogenous fertilizers for agricultural food crops is increasing atmospheric concentrations of N_2O. Three quarters of N_2O emissions are due to agricultural activities. Nitrous oxide remains in the atmosphere for an average of 114 years: it is estimated that for the same mass its contribution to the greenhouse effect is 300 times greater than that of carbon dioxide. According to an estimate published in 2020 in the journal Nature (Tian et al., 2020), nitrous oxide emissions have increased by 30% over the past forty years compared to pre-industrial levels.

Considering both the concentration of CO_2 and N_2O (400 ppm and 330 ppb) and their relative GWP (1:300), we applied a ratio between the two greenhouse gases of 4.2:1 (Fig. 67).

Programs to reduce the impact of agricultural N_2O emissions are focused on better management of the use of nitrogenous fertilizers (sustainable agriculture) and a reforestation policy. A greater forest cover allows a greater sequestration of CO_2 and a better control of the flows of nitrate and other sub-compounds of fertilizers. Even if some of the effects of climate change are already irreversible, the agreements reached at COP27 should aim at mitigating these impacts through more incisive global and local policies.

In addition, to support the priority analysis, the scenario A1 was identified as the best to the habitat quality, as a support ecosystem service, must be taken into consideration in the indications on the management choices of the lower Piave area.

➢ Improving response to climate change (COP27)

Drivers	Climate change	Land use change	Increase of Urban areas	Agriculture		**Indicators**	**Ecosystem services models**	**Relative weight**	**Scenarios**	**Ecosystem service**
Pressures	Atmospheric depositions	Withdrawals	Exploitation/ removal of animals/ plants	Physical alteration of canals/riverbed/ riparian vegetation/ riverbank	Traffic	Carbon Stock	C storage	8.1	B1, A2	Reduction of greenhouse gas emissions
						N concentration	N export	1.9	B1, A1	Plant-based resources
Impacts	Temperature increase	Habitat loss				Land use				Temperature regulation
										Soil (carbon sink)

Additional ESs	Habitat	+	A1	

Scenarios
B1 – Reforestation upper basin (14,574ha)
A2 – Reforestation inside the lower basin riverbanks (1,070ha)

Figure 67 Summary scheme of the components (DPSIR), weights and scenarios considered to improve responses to climate change.

7. CONCLUSIONS

Traditional approaches to water resource management are aimed to optimize the provision of reliable water supplies, energy, and flood protection, while seeking to maintain a static condition. However, this limited focus on direct provisional services has significantly altered the functioning of freshwater ecosystems, resulting in the decline of biodiversity on a global scale and the loss of ecosystem services for local and regional populations. At the same time, climate change has direct and indirect impacts on basic hydrological and chemical functions of terrestrial and freshwater environments, further exacerbating the stress on river ecosystems.

Climate change presents new challenges to maintaining freshwater environments by presenting new and uncertain hydro-climatic conditions, increasing the probability of climate-infrastructure misalignments with respect to historical climate variations. For this reason, global policies are aimed at encouraging new approaches in climate change mitigation and adaptation, increasing the ecological resilience in the design and management of freshwater environments. Improving the resilience of freshwater systems management requires a better consideration of ecosystem functions, services and needs. Integrating an improved understanding of nutrient and carbon dynamics into catchment management and policy making can deliver broad benefits to both people and the environment. It is therefore necessary to combine novel modelling approaches and the development of alternative scenarios that potentially more compatible with the needs of river ecosystems and its basin. Approaches that aim at greater adaptability of ecosystems and include the precautionary principle by avoiding negative side effects on ecosystem services are a fundamental requirement for sustainable development (Hallegatte, 2009). This new approach foresees an emerging water management paradigm that integrates the functioning of natural ecosystems and aims to simultaneously enhance the ecological and engineering resilience of water management systems.

For the Piave basin, a general objective should be to promote the integration of ecological resilience principles into basin planning and design, not only to enhance natural capital, but also to help sustain critical services for populations. and improve the overall resilience of the river basin for the future.

The results of the present study indicate that the most suitable and effective land use change scenario for the purpose of conserving and increasing the ecosystem services would be to favour reforestation of predominantly low production agricultural areas located in the upper basin (scenario B1). This scenario presents numerous benefits, compared to the status quo, and compared to the other scenarios considered, in particular: i) the reduction of the macro-nutrient flows to the Piave river, ii) the reduction of the eutrophication of the Adriatic Sea, iii) the

improvement of the responses to the change climate change (COP27), and iv) the conservation of the soil and biodiversity. Increasing natural areas and reforestation meets the objectives of the European Green Deal and coincides with the interventions envisaged in the new CAP 2023-2027.

The scenarios proposed in the Lower Piave (A1, A2) present numerous benefits for an improvement in river environment and services provided. By transforming the use of the land, inside the banks, from agricultural to natural, there would follow the partial redevelopment of the dynamics of the river by restoring erodible areas and in the remaining areas the evolution of the hygrophilous forest. While scenario A2 only foresees the hygrophilous forest without additional changes except for a control of the expansion of invasive species. Both actions would have positive impacts on nutrient flows to and within the river, as well as indirect impacts on carbon flow.

Scenario C1, based on a possible flood retention basin against the hydraulic risk, also presents benefits, especially on the availability of water and a reduction in phosphorus exports.

The present project also demonstrated that it is possible to increase participation in the management and monitoring of our river environment. Citizen science was found to be a useful approach to fill information gaps for model validation. Involving citizen participants directly in monitoring activities also improves communities' influence on management policy in their territory.

Organic carbon dynamics in the lower Piave river are complex and, at least in part, caused by the human impact that has altered its geomorphology, hydrological regime and land use in the basin. The modelled DOC concentrations increase from upstream to downstream in autumn due to the contribution of the fresh allochthonous organic substance coming from the territories drained by the Piave, to which is added that transported by the Sile River and introduced from the Piave Vecchia. In July the intrusion of sea water rich in degraded autochthonous DOC also influenced overall carbon concentrations and export.

The carbon delivery model, developed for the Piave River, was designed to be used in future river studies. It has been integrated with basin scale tools utilising the QGIS platform. It allows the development of and comparison of alterative scenarios to optimise ecosystem services. Data requirements for the model were easily retrievable from international and national databases, making it appropriate for modelling DOC and POC in data-scarce basins. The model is refined using local data, in particular monthly or seasonal concentrations of DOC and POC at the sub-basin level. The great number of sub-basins monitored, the more robust the reduction factor interpolation will be and therefore, more accurate the model outputs. The

model output can be used to evaluate carbon export based on varying land use and climate scenarios, providing an additional tool to support land use options that reduce carbon loss to receiving waterbodies, either marine or lake.

The suite of models developed was aimed to support the development of policies and tools that integrate social, economic, and ecological perspectives in the management of the Piave basin. The study benefited from the great availability of local and regional authorities and the citizens of the Lower Piave, to develop integrated models and analyses that made it possible to explore in detail the biochemical conditions of the territory, in particular the activities of Citizen Science. The study introduced several innovative aspects, from the methodological point of view of ecosystem services assessments. These innovations have been published in international scientific journals.

8. REFERENCES

Ågren, A., Buffam, I., Bishop, K., Laudon, H., 2010. Modeling stream dissolved organic carbon concentrations during spring flood in the boreal forest: A simple empirical approach for regional predictions. J. Geophys. Res. Biogeosciences 115, 1012. https://doi.org/10.1029/2009JG001013

Ahada, C.P.S., Suthar, S., 2018. Groundwater nitrate contamination and associated human health risk assessment in southern districts of Punjab, India. Environ. Sci. Pollut. Res. 25, 25336–25347. https://doi.org/10.1007/S11356-018-2581-2/FIGURES/6

Aitkenhead-Peterson, J.A., Steele, M.K., Nahar, N., Santhy, K., 2009. Dissolved organic carbon and nitrogen in urban and rural watersheds of south-central Texas: Land use and land management influences. Biogeochemistry 96, 119–129. https://doi.org/10.1007/S10533-009-9348-2/FIGURES/4

Allen, R., Pereira, L., Raes, D., Smith, M., 2006. Crop evapotranspiration —guidelines for computing crop water requirements. FAO Irrigation and drainage paper 56. , Evapotranspiración del cultivo Guías para la determinación de los requerimientos de agua de los cultivos. ESTUDIO FAO RIEGO Y DRENAJE 56. Rome.

Allen, R.G., Pereira, L.S., Raes, D., Smith, M., 1998. Crop evapotranspiration - Guidelines for computing crop water requirements, FAO Irrigation and drainage paper 56. Rome.

Álvarez-Cabria, M., Barquín, J., Peñas, F.J., 2016. Modelling the spatial and seasonal variability of water quality for entire river networks: Relationships with natural and anthropogenic factors. Sci. Total Environ. 545–546, 152–162. https://doi.org/10.1016/J.SCITOTENV.2015.12.109

Anzaldua, G., Gerner, N. V., Lago, M., Abhold, K., Hinzmann, M., Beyer, S., Winking, C., Riegels, N., Krogsgaard Jensen, J., Termes, M., Amorós, J., Wencki, K., Strehl, C., Ugarelli, R., Hasenheit, M., Nafo, I., Hernandez, M., Vilanova, E., Damman, S., Brouwer, S., Rouillard, J., Schwesig, D., Birk, S., 2018. Getting into the water with the Ecosystem Services Approach: The DESSIN ESS evaluation framework. Ecosyst. Serv. 30, 318–326. https://doi.org/10.1016/J.ECOSER.2017.12.004

Archer, D., 2010. The global carbon cycle. Princeton University Press.

ARPAV, 2022a. Carta del contenuto di carbonio organico nei suoli (%) — GeoPortale ARPAV [WWW Document]. URL https://gaia.arpa.veneto.it/layers/geonode_data:geonode:SOCperc_50k250k (accessed 1.31.23).

ARPAV, 2022b. La rete idrometrica e le portate - Agenzia Regionale per la Prevenzione e Protezione Ambientale del Veneto [WWW Document]. URL https://www.arpa.veneto.it/temi-ambientali/idrologia/file-e-allegati/rapporti-e-documenti/idrologia-regionale/idrologia-regionale-la-rete-idrometrica (accessed 1.8.23).

ARPAV, 2021a. Meteo e Clima, from 1994 to 2021 [WWW Document]. URL https://www.arpa.veneto.it/dati-ambientali/open-data/clima (accessed 1.8.23).

ARPAV, 2021b. Fiumi - concentrazione dei parametri di base - Agenzia Regionale per la Prevenzione e Protezione Ambientale del Veneto [WWW Document]. URL https://www.arpa.veneto.it/dati-ambientali/open-data/idrosfera/corsi-dacqua/fiumi-concentrazione-dei-parametri-di-base (accessed 1.8.23).

ARPAV, 2018a. Corpi idrici fluviali (Progetti di Piano, 2020) — Geomap ARPAV [WWW Document]. URL http://geomap.arpa.veneto.it/layers/geonode%3Acorpi_idrici_fluviali (accessed 8.10.21).

ARPAV, 2018b. Bacini Idrografici del Piano di Tutela delle Acque — Geomap ARPAV [WWW Document]. URL http://geomap.arpa.veneto.it/layers/geonode%3Abacinipta (accessed 8.10.21).

ARPAV, 2018c. Carichi di azoto agricolo, da allevamento e da fertilizzanti — Geomap ARPAV [WWW Document]. URL http://geomap.arpa.veneto.it/layers/geonode%3Acarichi_azotoagricolo (accessed 8.10.21).

ARPAV, 2018d. Carta del rischio di percolazione dell'azoto — Esplora mappe - Geomap ARPAV [WWW Document]. URL http://geomap.arpa.veneto.it/maps/270 (accessed 8.10.21).

ARPAV, 2018e. Acque sotterranee - Concentrazione di nitrati — [WWW Document]. URL https://www.arpa.veneto.it/dati-ambientali/open-data/idrosfera/acque-sotterranee/acque-sotterranee-concentrazione-di-nitrati (accessed 8.10.21).

ARPAV, 2018f. Bilancio Idroclimatico - agg. 2018 - Agenzia Regionale per la Prevenzione e Protezione Ambientale del Veneto [WWW Document]. URL https://www.arpa.veneto.it/arpavinforma/indicatori-ambientali/indicatori-ambientali-del-veneto/clima-e-rischi-naturali/clima/bilancio-idroclimatico-agg.-2018/2018 (accessed 1.30.23).

ARPAV, 2018g. La rete idrometrica e le portate — [WWW Document]. URL https://www.arpa.veneto.it/temi-ambientali/idrologia/file-e-allegati/rapporti-e-documenti/idrologia-regionale/idrologia-regionale-la-rete-idrometrica (accessed 8.10.21).

Aufdenkampe, A.K., Mayorga, E., Raymond, P.A., Melack, J.M., Doney, S.C., Alin, S.R., Aalto, R.E., Yoo, K., 2011. Riverine coupling of biogeochemical cycles between land, oceans, and atmosphere. Front. Ecol. Environ. 9, 53–60. https://doi.org/10.1890/100014

Bai, Y., Chen, S., Shi, S., Qi, M., Liu, X., Wang, H., Wang, Y., Jiang, C., 2020. Effects of different management approaches on the stoichiometric characteristics of soil C, N, and P in a mature Chinese fir plantation. Sci. Total Environ. 723, 137868. https://doi.org/10.1016/J.SCITOTENV.2020.137868

Ballabio, C., Panagos, P., Monatanarella, L., 2016. Mapping topsoil physical properties at European scale using the LUCAS database. Geoderma 261, 110–123. https://doi.org/10.1016/J.GEODERMA.2015.07.006

Balvanera, P., Pfisterer, A.B., Buchmann, N., He, J.S., Nakashizuka, T., Raffaelli, D., Schmid, B., 2006. Quantifying the evidence for biodiversity effects on ecosystem functioning and services. Ecol. Lett. 9, 1146–1156. https://doi.org/10.1111/J.1461-0248.2006.00963.X

Baruffi, F., Cisotto, A., Cimolino, A., Ferri, M., Monego, M., Norbiato, D., Cappelletto, M., Bisaglia, M., Pretner, A., Galli, A., Scarinci, A., Marsala, V., Panelli, C., Gualdi, S., Bucchignani, E., Torresan, S., Pasini, S., Critto, A., Marcomini, A., 2012. Climate change impact assessment on Veneto and Friuli plain groundwater. Part I: An integrated modeling approach for hazard scenario construction. Sci. Total Environ. 440, 154–166. https://doi.org/10.1016/J.SCITOTENV.2012.07.070

Basche, A., DeLonge, M., 2017. The Impact of Continuous Living Cover on Soil Hydrologic Properties: A Meta-Analysis. Soil Sci. Soc. Am. J. 81, 1179–1190.

https://doi.org/10.2136/SSSAJ2017.03.0077

Bascietto, M., Cherubini, P., Scarascia-Mugnozza, G., 2011. Tree rings from a European beech forest chronosequence are useful for detecting growth trends and carbon sequestration. https://doi.org/10.1139/x03-214 34, 481–492. https://doi.org/10.1139/X03-214

Bashar, R., Gungor, K., Karthikeyan, K.G., Barak, P., 2018. Cost effectiveness of phosphorus removal processes in municipal wastewater treatment. Chemosphere 197, 280–290. https://doi.org/10.1016/J.CHEMOSPHERE.2017.12.169

Bastias, E., Bolivar, M., Ribot, M., Peipoch, M., Thomas, S.A., Sabater, F., Martí, E., 2020. Spatial heterogeneity in water velocity drives leaf litter dynamics in streams. Freshw. Biol. 65, 435–445. https://doi.org/10.1111/FWB.13436

Battin, T.J., Kaplan, L.A., Findlay, S., Hopkinson, C.S., Marti, E., Packman, A.I., Newbold, J.D., Sabater, F., 2008. Biophysical controls on organic carbon fluxes in fluvial networks. Nat. Geosci. 2008 12 1, 95–100. https://doi.org/10.1038/ngeo101

Bazilevskaya, G.A., Krainev, M.B., Makhmutov, V.S., 2000. Effects of cosmic rays on the Earth's environment. J. Atmos. Solar-Terrestrial Phys. 62, 1577–1586. https://doi.org/10.1016/S1364-6826(00)00113-9

Berggren, M., Al-Kharusi, E.S., 2020. Decreasing organic carbon bioreactivity in European rivers. Freshw. Biol. 65, 1128–1138. https://doi.org/10.1111/FWB.13498

Bernot, M.J., Dodds, W.K., 2005. Nitrogen retention, removal, and saturation in lotic ecosystems. Ecosystems 8, 442–453. https://doi.org/10.1007/S10021-003-0143-Y/FIGURES/6

Bezak, N., Borrelli, P., Panagos, P., 2022. Exploring the possible role of satellite-based rainfall data in estimating inter- and intra-annual global rainfall erosivity. Hydrol. Earth Syst. Sci. 26, 1907–1924. https://doi.org/10.5194/HESS-26-1907-2022

Bird, T.J., Bates, A.E., Lefcheck, J.S., Hill, N.A., Thomson, R.J., Edgar, G.J., Stuart-Smith, R.D., Wotherspoon, S., Krkosek, M., Stuart-Smith, J.F., Pecl, G.T., Barrett, N., Frusher, S., 2014. Statistical solutions for error and bias in global citizen science datasets. Biol. Conserv. 173, 144–154. https://doi.org/10.1016/j.biocon.2013.07.037

Birgand, F., Skaggs, R.W., Chescheir, G.M., Gilliam, J.W., 2007. Nitrogen Removal in Streams of Agricultural Catchments—A Literature Review. http://dx.doi.org/10.1080/10643380600966426 37, 381–487. https://doi.org/10.1080/10643380600966426

Bishop, I.J., Warner, S., Noordwijk, T.C.G.E. van, Nyoni, F.C., Loiselle, S., 2020. Citizen

Science Monitoring for Sustainable Development Goal Indicator 6.3.2 in England and Zambia. Sustain. 2020, Vol. 12, Page 10271 12, 10271. https://doi.org/10.3390/SU122410271

Biswas Chowdhury, R., Zhang, X., 2021. Phosphorus use efficiency in agricultural systems: A comprehensive assessment through the review of national scale substance flow analyses. Ecol. Indic. 121, 107172. https://doi.org/10.1016/J.ECOLIND.2020.107172

Bladé, I., Liebmann, B., Fortuny, D., van Oldenborgh, G.J., 2011. Observed and simulated impacts of the summer NAO in Europe: implications for projected drying in the Mediterranean region. Clim. Dyn. 2011 393 39, 709–727. https://doi.org/10.1007/S00382-011-1195-X

Bonney, R., Cooper, C.B., Dickinson, J., Kelling, S., Phillips, T., Rosenberg, K. V., Shirk, J., 2009. Citizen science: A developing tool for expanding science knowledge and scientific literacy. Bioscience. https://doi.org/10.1525/bio.2009.59.11.9

Borken, W., Ahrens, B., Schulz, C., Zimmermann, L., 2011. Site-to-site variability and temporal trends of DOC concentrations and fluxes in temperate forest soils. Glob. Chang. Biol. 17, 2428–2443. https://doi.org/10.1111/J.1365-2486.2011.02390.X

Borrelli, P., Robinson, D.A., Fleischer, L.R., Lugato, E., Ballabio, C., Alewell, C., Meusburger, K., Modugno, S., Schütt, B., Ferro, V., Bagarello, V., Oost, K. Van, Montanarella, L., Panagos, P., 2017. An assessment of the global impact of 21st century land use change on soil erosion. Nat. Commun. 2017 81 8, 1–13. https://doi.org/10.1038/s41467-017-02142-7

Borrelli, P., Robinson, D.A., Panagos, P., Lugato, E., Yang, J.E., Alewell, C., Wuepper, D., Montanarella, L., Ballabio, C., 2020. Land use and climate change impacts on global soil erosion by water (2015-2070). Proc. Natl. Acad. Sci. U. S. A. 117, 21994–22001. https://doi.org/10.1073/PNAS.2001403117/SUPPL_FILE/PNAS.2001403117.SAPP.PDF

Borselli, L., Cassi, P., Torri, D., 2008. Prolegomena to sediment and flow connectivity in the landscape: A GIS and field numerical assessment. CATENA 75, 268–277. https://doi.org/10.1016/J.CATENA.2008.07.006

Botter, G., Basso, S., Porporato, A., Rodriguez-Iturbe, I., Rinaldo, A., 2010. Natural streamflow regime alterations: Damming of the Piave river basin (Italy). Water Resour. Res. 46, 6522. https://doi.org/10.1029/2009WR008523

Bouchez, J., Galy, V., Hilton, R.G., Gaillardet, J.Ô., Moreira-Turcq, P., Pérez, M.A., France-Lanord, C., Maurice, L., 2014. Source, transport and fluxes of Amazon River particulate

organic carbon: Insights from river sediment depth-profiles. Geochim. Cosmochim. Acta 133, 280–298. https://doi.org/10.1016/J.GCA.2014.02.032

Bouwman, A.F., Bierkens, M.F.P., Griffioen, J., Hefting, M.M., Middelburg, J.J., Middelkoop, H., Slomp, C.P., 2013. Nutrient dynamics, transfer and retention along the aquatic continuum from land to ocean: Towards integration of ecological and biogeochemical models. Biogeosciences 10, 1–23. https://doi.org/10.5194/BG-10-1-2013

Boyer, E.W., Hornberger, G.M., Bencala, K.E., McKnight, D., 1996. Overview of a simple model describing variation of dissolved organic carbon in an upland catchment. Ecol. Modell. 86, 183–188. https://doi.org/10.1016/0304-3800(95)00049-6

Bozzola, M., Massetti, E., Mendelsohn, R., Capitanio, F., 2018. A Ricardian analysis of the impact of climate change on Italian agriculture. Eur. Rev. Agric. Econ. 45, 57–79. https://doi.org/10.1093/ERAE/JBX023

Brown, D.G., Robinson, D.T., French, N.H.F., Reed, B.C., 2013. Land Use and the Carbon Cycle: Advances in Integrated Science, Management, and Policy. Cambridge University Press, Cambridge.

Brzezinski, M.A., 1985. THE Si:C:N RATIO OF MARINE DIATOMS: INTERSPECIFIC VARIABILITY AND THE EFFECT OF SOME ENVIRONMENTAL VARIABLES1. J. Phycol. 21, 347–357. https://doi.org/10.1111/J.0022-3646.1985.00347.X

Bu, H., Meng, W., Zhang, Y., Wan, J., 2014. Relationships between land use patterns and water quality in the Taizi River basin, China. Ecol. Indic. 41, 187–197. https://doi.org/10.1016/J.ECOLIND.2014.02.003

Butler, B., Pearson, R.G., Birtles, R.A., 2021. Water-quality and ecosystem impacts of recreation in streams: Monitoring and management. Environ. Challenges 5, 100328. https://doi.org/10.1016/J.ENVC.2021.100328

Butman, D.E., Wilson, H.F., Barnes, R.T., Xenopoulos, M.A., Raymond, P.A., 2014. Increased mobilization of aged carbon to rivers by human disturbance. Nat. Geosci. 2014 82 8, 112–116. https://doi.org/10.1038/ngeo2322

Butusov, M., Jernelöv, A., 2013. Phosphorus in the Organic Life: Cells, Tissues, Organisms 13–17. https://doi.org/10.1007/978-1-4614-6803-5_2

Buytaert, W., Zulkafli, Z., Grainger, S., Acosta, L., Alemie, T.C., Bastiaensen, J., De Bièvre, B., Bhusal, J., Clark, J., Dewulf, A., Foggin, M., Hannah, D.M., Hergarten, C., Isaeva, A., Karpouzoglou, T., Pandeya, B., Paudel, D., Sharma, K., Steenhuis, T., Tilahun, S., Van Hecken, G., Zhumanova, M., 2014. Citizen science in hydrology and water resources: Opportunities for knowledge generation, ecosystem service management, and

sustainable development. Front. Earth Sci. 2, 26. https://doi.org/10.3389/FEART.2014.00026/BIBTEX

Caddeo, A., Marras, S., Sallustio, L., Spano, D., Sirca, C., 2019. Soil organic carbon in Italian forests and agroecosystems: Estimating current stock and future changes with a spatial modelling approach. Agric. For. Meteorol. 278, 107654. https://doi.org/10.1016/J.AGRFORMET.2019.107654

Cai, Y., Guo, L., Wang, X., Aiken, G., 2015. Abundance, stable isotopic composition, and export fluxes of DOC, POC, and DIC from the Lower Mississippi River during 2006–2008. J. Geophys. Res. Biogeosciences 120, 2273–2288. https://doi.org/10.1002/2015JG003139

Camino-Serrano, M., Graf Pannatier, E., Vicca, S., Luyssaert, S., Jonard, M., Ciais, P., Guenet, B., Gielen, B., Peñuelas, J., Sardans, J., Waldner, P., Etzold, S., Cecchini, G., Clarke, N., GaliÄ, Z., Gandois, L., Hansen, K., Johnson, J., Klinck, U., Lachmanová, Z., Lindroos, A.J., Meesenburg, H., Nieminen, T.M., Sanders, T.G.M., Sawicka, K., Seidling, W., Thimonier, A., Vanguelova, E., Verstraeten, A., Vesterdal, L., Janssens, I.A., 2016. Trends in soil solution dissolved organic carbon (DOC) concentrations across European forests. Biogeosciences 13, 5567–5585. https://doi.org/10.5194/BG-13-5567-2016

Camino-Serrano, M., Guenet, B., Luyssaert, S., Ciais, P., Bastrikov, V., De Vos, B., Gielen, B., Gleixner, G., Jornet-Puig, A., Kaiser, K., Kothawala, D., Lauerwald, R., Peñuelas, J., Schrumpf, M., Vicca, S., Vuichard, N., Walmsley, D., Janssens, I.A., 2018. ORCHIDEE-SOM: Modeling soil organic carbon (SOC) and dissolved organic carbon (DOC) dynamics along vertical soil profiles in Europe. Geosci. Model Dev. 11, 937–957. https://doi.org/10.5194/GMD-11-937-2018

Cardinale, B.J., Duffy, J.E., Gonzalez, A., Hooper, D.U., Perrings, C., Venail, P., Narwani, A., MacE, G.M., Tilman, D., Wardle, D.A., Kinzig, A.P., Daily, G.C., Loreau, M., Grace, J.B., Larigauderie, A., Srivastava, D.S., Naeem, S., 2012. Biodiversity loss and its impact on humanity. Nat. 2012 4867401 486, 59–67. https://doi.org/10.1038/nature11148

Casas-Ruiz, J.P., Catalán, N., Gómez-Gener, L., von Schiller, D., Obrador, B., Kothawala, D.N., López, P., Sabater, S., Marcé, R., 2017. A tale of pipes and reactors: Controls on the in-stream dynamics of dissolved organic matter in rivers. Limnol. Oceanogr. 62, S85–S94. https://doi.org/10.1002/LNO.10471

Catalán, N., Marcé, R., Kothawala, D.N., Tranvik, L.J., 2016. Organic carbon decomposition

rates controlled by water retention time across inland waters. Nat. Geosci. 2016 97 9, 501–504. https://doi.org/10.1038/ngeo2720

Catlin-Groves, C.L., 2012. The citizen science landscape: From volunteers to citizen sensors and beyond. Int. J. Zool. 2012, 1–14. https://doi.org/10.1155/2012/349630

Cattani, I., Fragoulis, G., Boccelli, R., Capri, E., 2006. Copper bioavailability in the rhizosphere of maize (Zea mays L.) grown in two Italian soils. Chemosphere 64, 1972–1979. https://doi.org/10.1016/J.CHEMOSPHERE.2006.01.007

CBAR, 2021. Consorzio di Bonifica Acque Risorgive. Interventi Riqualificazione [WWW Document]. URL https://www.acquerisorgive.it/ambiente/documentazione/interventi-riqualificazione/ (accessed 9.14.21).

Ceccon, P., Fagnano, M., Grignani, C., Monti, M., Orlandisi, S., 2017. Agronomia, Edises. Edises.

Chanudet, V., Filella, M., 2008. Size and composition of inorganic colloids in a peri-alpine, glacial flour-rich lake. Geochim. Cosmochim. Acta 72, 1466–1479. https://doi.org/10.1016/J.GCA.2008.01.002

Chen, D., Deng, X., Jin, G., Samie, A., Li, Z., 2017. Land-use-change induced dynamics of carbon stocks of the terrestrial ecosystem in Pakistan. Phys. Chem. Earth, Parts A/B/C 101, 13–20. https://doi.org/10.1016/J.PCE.2017.01.018

Chen, J., Chen, S., Fu, R., Li, D., Jiang, H., Wang, C., Peng, Y., Jia, K., Hicks, B.J., 2022. Remote Sensing Big Data for Water Environment Monitoring: Current Status, Challenges, and Future Prospects. Earth's Futur. 10, e2021EF002289. https://doi.org/10.1029/2021EF002289

Ciais, P., Sabine, C., Bala, G., Bopp, L., Brovkin, V., Canadell, J., Chhabra, A., DeFries, R., Galloway, J., Heimann, M., Jones, C., Le Quéré, C., Myneni, R.B., Piao, S., Thornto, P., 2013. Carbon and Other Biogeochemical Cycles, in: Heinze, C., Tans, P., Vesala, T. (Eds.), Climate Change 2013: The Physical Science Basis. Contribution of Working Group I to the Fifth Assessment Report of the Intergovernmental Panel on Climate Change. Cambridge University Press, Cambridge, United Kingdom and New York, NY, USA, pp. 465–570.

Ciglenečki, I., Vilibić, I., Dautović, J., Vojvodić, V., Ćosović, B., Zemunik, P., Dunić, N., Mihanović, H., 2020. Dissolved organic carbon and surface active substances in the northern Adriatic Sea: Long-term trends, variability and drivers. Sci. Total Environ. 730, 139104. https://doi.org/10.1016/J.SCITOTENV.2020.139104

Ciobotaru, A.-M., 2015. Influence of human activities on water quality of rivers and

groundwaters from Braila county. Analele Univ. din Oradea– Ser. Geogr. 1, 05–13.

Cleveland, C.C., Liptzin, D., 2007. C:N:P stoichiometry in soil: Is there a “Redfield ratio” for the microbial biomass? Biogeochemistry 85, 235–252. https://doi.org/10.1007/S10533-007-9132-0/TABLES/4

Cohn, J.P., 2008. Citizen Science: Can Volunteers Do Real Research? Source Biosci. 58, 192–197. https://doi.org/10.1641/B580303

Cole, J.J., Prairie, Y.T., Caraco, N.F., McDowell, W.H., Tranvik, L.J., Striegl, R.G., Duarte, C.M., Kortelainen, P., Downing, J.A., Middelburg, J.J., Melack, J., 2007. Plumbing the global carbon cycle: Integrating inland waters into the terrestrial carbon budget. Ecosystems 10, 171–184. https://doi.org/10.1007/S10021-006-9013-8/TABLES/1

Comiti, F., Da Canal, M., Surian, N., Mao, L., Picco, L., Lenzi, M.A., 2011. Channel adjustments and vegetation cover dynamics in a large gravel bed river over the last 200 years. Geomorphology 125, 147–159. https://doi.org/10.1016/J.GEOMORPH.2010.09.011

CORDIS, 2016. Final Report Summary - FORMIT (FORest management strategies to enhance the MITigation potential of European forests) | FP7 | CORDIS | European Commission [WWW Document]. URL https://cordis.europa.eu/project/id/311970/reporting/it (accessed 1.29.23).

Costantini, E.A.C., Dazzi, C., 2013. The Soils of Italy 295–302. https://doi.org/10.1007/978-94-007-5642-7

Costanza, R., D’Arge, R., De Groot, R., Farber, S., Grasso, M., Hannon, B., Limburg, K., Naeem, S., O’Neill, R. V., Paruelo, J., Raskin, R.G., Sutton, P., Van Den Belt, M., 1997. The value of the world’s ecosystem services and natural capital. Nat. 1997 3876630 387, 253–260. https://doi.org/10.1038/387253a0

Cox, B.A., Whitehead, P.G., 2009. Impacts of climate change scenarios on dissolved oxygen in the River Thames, UK. Hydrol. Res. 40, 138–152. https://doi.org/10.2166/NH.2009.096

Cozzi, S., Falconi, C., Comici, C., Čermelj, B., Kovac, N., Turk, V., Giani, M., 2012. Recent evolution of river discharges in the Gulf of Trieste and their potential response to climate changes and anthropogenic pressure. Estuar. Coast. Shelf Sci. 115, 14–24. https://doi.org/10.1016/J.ECSS.2012.03.005

Cozzi, S., Ibáñez, C., Lazar, L., Raimbault, P., Giani, M., 2018. Flow Regime and Nutrient-Loading Trends from the Largest South European Watersheds: Implications for the Productivity of Mediterranean and Black Sea’s Coastal Areas. Water 2019, Vol. 11, Page

1 11, 1. https://doi.org/10.3390/W11010001

Crain, R., Cooper, C., Dickinson, J.L., 2014. Citizen science: A tool for integrating studies of human and natural systems. Annu. Rev. Environ. Resour. https://doi.org/10.1146/annurev-environ-030713-154609

Creutzburg, M.K., Scheller, R.M., Lucash, M.S., Evers, L.B., Leduc, S.D., Johnson, M.G., 2016. Bioenergy harvest, climate change, and forest carbon in the Oregon Coast Range. GCB Bioenergy 8, 357–370. https://doi.org/10.1111/GCBB.12255

Cudennec, C., Leduc, C., Koutsoyiannis, D., 2009. Dryland hydrology in Mediterranean regions—a review. https://doi.org/10.1623/hysj.52.6.1077 52, 1077–1087. https://doi.org/10.1623/HYSJ.52.6.1077

Cui, L., Lu, X., Dong, Y., Cen, J., Cao, R., Pan, L., Lu, S., Ou, L., 2018. Relationship between phytoplankton community succession and environmental parameters in Qinhuangdao coastal areas, China: A region with recurrent brown tide outbreaks. Ecotoxicol. Environ. Saf. 159, 85–93. https://doi.org/10.1016/j.ecoenv.2018.04.043

Currie, W., Aber, J., 1997. Modeling leaching as a decomposition process in humid montane forests. Ecology 78, 1844–1860.

Currie, W.S., Yanai, R.D., Piatek, K.B., Prescott, C.E., Goodale, C.L., 2002. Processes affecting carbon storage in the forest floor and in downed woody debris, in: kimble, J.M., Lal, R., Birdsey, R., Heath, L.S. (Eds.), The Potential of U.S. Forest Soils to Sequester Carbon and Mitigate the Greenhouse Effect. CRC Press, Boca Raton, pp. 135–157. https://doi.org/10.1201/9781420032277-9/PROCESSES-AFFECTING-CARBON-STORAGE-FOREST-FLOOR-DOWNED-WOODY-DEBRIS-WILLIAM-CURRIE-RUTH-YANAI-KATHRYN-PIATEK-CINDY-PRESCOTT-CHRISTINE-GOODALE

da Silva Cruz, J., Blanco, C.J.C., de Oliveira Júnior, J.F., 2022. Modeling of land use and land cover change dynamics for future projection of the Amazon number curve. Sci. Total Environ. 811, 152348. https://doi.org/10.1016/J.SCITOTENV.2021.152348

Dai, E., Wu, Z., Ge, Q., Xi, W., Wang, X., 2016. Predicting the responses of forest distribution and aboveground biomass to climate change under RCP scenarios in southern China. Glob. Chang. Biol. 22, 3642–3661. https://doi.org/10.1111/GCB.13307

Daily, G.C., 1997. Introduction: What are Ecosystem Services?, in: Nature's Services: Societal Dependence on Natual Ecosystems. Island Press, Washington, DC.

Daly, C., Halbleib, M., Smith, J.I., Gibson, W.P., Doggett, M.K., Taylor, G.H., Curtis, J., Pasteris, P.P., 2008. Physiographically sensitive mapping of climatological temperature and precipitation across the conterminous United States. Int. J. Climatol. 28, 2031–2064.

https://doi.org/10.1002/JOC.1688

Danovaro, R., Umani, S.F., Pusceddu, A., 2009. Climate Change and the Potential Spreading of Marine Mucilage and Microbial Pathogens in the Mediterranean Sea. PLoS One 4, e7006. https://doi.org/10.1371/JOURNAL.PONE.0007006

Dawson, J.J.C., Billett, M.F., Hope, D., Palmer, S.M., Deacon, C.M., 2004. Sources and sinks of aquatic carbon in a peatland stream continuum. Biogeochem. 2004 701 70, 71–92. https://doi.org/10.1023/B:BIOG.0000049337.66150.F1

de Mutsert, K., Steenbeek, J., Lewis, K., Buszowski, J., Cowan, J.H., Christensen, V., 2016. Exploring effects of hypoxia on fish and fisheries in the northern Gulf of Mexico using a dynamic spatially explicit ecosystem model. Ecol. Modell. 331, 142–150. https://doi.org/10.1016/J.ECOLMODEL.2015.10.013

De Wit, H.A., Valinia, S., Weyhenmeyer, G.A., Futter, M.N., Kortelainen, P., Austnes, K., Hessen, D.O., Räike, A., Laudon, H., Vuorenmaa, J., 2016. Current Browning of Surface Waters Will Be Further Promoted by Wetter Climate. Environ. Sci. Technol. Lett. 3, 430–435. https://doi.org/10.1021/ACS.ESTLETT.6B00396/ASSET/IMAGES/LARGE/EZ-2016-00396D_0004.JPEG

Deforet, T., Marmonier, P., Rieffel, D., Crini, N., Fritsch, C., Giraudoux, P., Gilbert, D., 2008. The influence of size, hydrological characteristics and vegetation cover on nitrogen, phosphorus and organic carbon cycling in lowland river gravel bars (Doubs River, France). Fundam. Appl. Limnol. 171, 161–173. https://doi.org/10.1127/1863-9135/2008/0171-0161

Degobbis, D., 1989. Increased eutrophication of the northern Adriatic sea: Second act. Mar. Pollut. Bull. 20, 452–457. https://doi.org/10.1016/0025-326X(89)90066-0

Del Favero, R., Lasen, C., 1993. La vegetazione forestale del Veneto, 2nd ed, Padova : Libreria progetto,. Libreria Progetto Editore, Padova.

Den Broeder, L., Devilee, J., Van Oers, H., Schuit, A.J., Wagemakers, A., 2018. Citizen Science for public health. Health Promot. Int. 33, 505–514. https://doi.org/10.1093/HEAPRO/DAW086

Dezsi, Ş., Mîndrescu, M., Petrea, D., Rai, P.K., Hamann, A., Nistor, M.-M., 2018. High-resolution projections of evapotranspiration and water availability for Europe under climate change. Int. J. Climatol. 38, 3832–3841. https://doi.org/10.1002/joc.5537

Di Grazia, F., Gumiero, B., Galgani, L., Troiani, E., Ferri, M., Loiselle, S.A., 2021. Ecosystem services evaluation of nature-based solutions with the help of citizen

scientists. Sustain. 13, 10629. https://doi.org/10.3390/SU131910629/S1

Dickinson, J.L., Shirk, J., Bonter, D., Bonney, R., Crain, R.L., Martin, J., Phillips, T., Purcell, K., 2012. The current state of citizen science as a tool for ecological research and public engagement. Front. Ecol. Environ. https://doi.org/10.1890/110236

Dile, Y.T., Karlberg, L., Daggupati, P., Srinivasan, R., Wiberg, D., Rockström, J., 2016. Assessing the implications of water harvesting intensification on upstream–downstream ecosystem services: A case study in the Lake Tana basin. Sci. Total Environ. 542, 22–35. https://doi.org/10.1016/J.SCITOTENV.2015.10.065

Dodds, W.K., Bouska, W.W., Eitzmann, J.L., Pilger, T.J., Pitts, K.L., Riley, A.J., Schloesser, J.T., Thornbrugh, D.J., 2009. Eutrophication of U. S. freshwaters: Analysis of potential economic damages. Environ. Sci. Technol. 43, 12–19. https://doi.org/10.1021/ES801217Q/SUPPL_FILE/ES801217Q_SI_001.PDF

Donohue, R.J., Roderick, M.L., McVicar, T.R., 2012. Roots, storms and soil pores: Incorporating key ecohydrological processes into Budyko's hydrological model. J. Hydrol. 436–437, 35–50. https://doi.org/10.1016/J.JHYDROL.2012.02.033

Dosskey, M.G., Vidon, P., Gurwick, N.P., Allan, C.J., Duval, T.P., Lowrance, R., 2010. The role of riparian vegetation in protecting and improving chemical water quality in streams. J. Am. Water Resour. Assoc. 46, 261–277. https://doi.org/10.1111/J.1752-1688.2010.00419.X

Drake, T.W., Tank, S.E., Zhulidov, A. V., Holmes, R.M., Gurtovaya, T., Spencer, R.G.M., 2018. Increasing Alkalinity Export from Large Russian Arctic Rivers. Environ. Sci. Technol. 52, 8302–8308. https://doi.org/10.1021/ACS.EST.8B01051/SUPPL_FILE/ES8B01051_SI_002.XLS

Drobinski, P., Alonzo, B., Bastin, S., Da Silva, N., Muller, C., 2016. Scaling of precipitation extremes with temperature in the French Mediterranean region: What explains the hook shape? J. Geophys. Res. Atmos. 121, 3100–3119. https://doi.org/10.1002/2015JD023497

Du, X., Faramarzi, M., Qi, J., Lei, Q., Liu, H., 2023. Investigating hydrological transport pathways of dissolved organic carbon in cold region watershed based on a watershed biogeochemical model. Environ. Pollut. 324, 121390. https://doi.org/10.1016/J.ENVPOL.2023.121390

Du, X., Loiselle, D., Alessi, D.S., Faramarzi, M., 2020. Hydro-climate and biogeochemical processes control watershed organic carbon inflows: Development of an in-stream organic carbon module coupled with a process-based hydrologic model. Sci. Total Environ. 718, 137281. https://doi.org/10.1016/J.SCITOTENV.2020.137281

Du, X., Zhang, X., Mukundan, R., Hoang, L., Owens, E.M., 2019. Integrating terrestrial and aquatic processes toward watershed scale modeling of dissolved organic carbon fluxes. Environ. Pollut. 249, 125–135. https://doi.org/10.1016/J.ENVPOL.2019.03.014

Duan, H., Ma, R., Zhang, Y., Loiselle, S.A., 2014. Are algal blooms occurring later in Lake Taihu? Climate local effects outcompete mitigation prevention. J. Plankton Res. 36, 866–871. https://doi.org/10.1093/PLANKT/FBT132

Earthwatch Europe, 2021a. Earthwatch Europe [WWW Document]. URL https://earthwatch.org.uk/ (accessed 1.29.23).

Earthwatch Europe, 2021b. FreshWater Watch [WWW Document]. URL https://www.freshwaterwatch.org/ (accessed 1.29.23).

Eckard, R.S., Bergamaschi, B.A., Pellerin, B., Spencer, R.G., Dyda, R., Hernes, P.J., 2020. Organic Matter Integration, Overprinting, and the Relative Fraction of Optically Active Organic Carbon in a Human-Impacted Watershed. Front. Earth Sci. 8, 67. https://doi.org/10.3389/FEART.2020.00067/BIBTEX

ECSA, 2022. European Citizen Science Association (ECSA) – Engage with us [WWW Document]. URL https://www.ecsa.ngo/ (accessed 1.30.23).

EEA, 2021. Ecological status of surface waters in Europe. European Environment Agency (EEA) [WWW Document]. URL https://www.eea.europa.eu/ims/ecological-status-of-surface-waters (accessed 1.30.23).

EEA, 2019. Nutrient enrichment and eutrophication in Europe's seas: Moving towards a healthy marine environment. European Environmental Agency (EEA), Biological Reviews. Blackwell Publishing Ltd, Luxemboroug.

EFAS, 2018. Assessment report on the flood events in Spain and Italy during autumn 2018 | Copernicus EMS - European Flood Awareness System [WWW Document]. URL https://www.efas.eu/en/report/assessment-report-flood-events-spain-and-italy-during-autumn-2018 (accessed 10.25.22).

Einarsdottir, K., Wallin, M.B., Sobek, S., 2017. High terrestrial carbon load via groundwater to a boreal lake dominated by surface water inflow. J. Geophys. Res. Biogeosciences 122, 15–29. https://doi.org/10.1002/2016JG003495

Ejarque, E., Freixa, A., Vazquez, E., Guarch, A., Amalfitano, S., Fazi, S., Romaní, A.M., Butturini, A., 2017. Quality and reactivity of dissolved organic matter in a Mediterranean river across hydrological and spatial gradients. Sci. Total Environ. 599–600, 1802–1812. https://doi.org/10.1016/j.scitotenv.2017.05.113

Ennaanay, D., 2006. Impacts of land use changes on the hydrologic regime in the Minnesota

River basin. University of Minnesota.

Ensign, S.H., Doyle, M.W., 2006. Nutrient spiraling in streams and river networks. J. Geophys. Res. Biogeosciences 111, 4009. https://doi.org/10.1029/2005JG000114

Erisman, J.W., Galloway, J.N., Seitzinger, S., Bleeker, A., Dise, N.B., Roxana Petrescu, A.M., Leach, A.M., de Vries, W., 2013. Consequences of human modification of the global nitrogen cycle. Philos. Trans. R. Soc. B Biol. Sci. 368. https://doi.org/10.1098/RSTB.2013.0116

EU, 2000. Directive 2000/60/EC of the European Parliament and of the Council of 23 October 2000 establishing a framework for Community action in the field of water policy. Off. J. Eur. Parliam., EU.

European Commission, 2022. Common Agricultural Policy (CAP) Strategic Plans 2023-2027 [WWW Document]. URL https://agriculture.ec.europa.eu/cap-my-country/cap-strategic-plans_en (accessed 1.30.23).

European Commission, 2021. Biodiversity strategy for 2030 [WWW Document]. URL https://environment.ec.europa.eu/strategy/biodiversity-strategy-2030_en (accessed 1.30.23).

European Commission, 2020a. A European Green Deal [WWW Document]. URL https://commission.europa.eu/strategy-and-policy/priorities-2019-2024/european-green-deal_en (accessed 1.30.23).

European Commission, 2020b. Farm to Fork Strategy [WWW Document]. URL https://food.ec.europa.eu/horizontal-topics/farm-fork-strategy_it (accessed 1.30.23).

Fabbri, P., Piccinini, L., Marcolongo, E., Pola, M., Conchetto, E., Zangheri, P., 2016. Does a change of irrigation technique impact on groundwater resources? A case study in Northeastern Italy. Environ. Sci. Policy 63, 63–75. https://doi.org/10.1016/J.ENVSCI.2016.05.009

Fazhu, Z., Jiao, S., Chengjie, R., Di, K., Jian, D., Xinhui, H., Gaihe, Y., Yongzhong, F., Guangxin, R., 2015. Land use change influences soil C, N and P stoichiometry under 'Grain-to-Green Program' in China. Sci. Reports 2015 51 5, 1–10. https://doi.org/10.1038/srep10195

Federici, S., Vitullo, M., Tulipano, S., De Lauretis, R., Seufert, G., 2008. An approach to estimate carbon stocks change in forest carbon pools under the UNFCCC: the Italian case. iForest - Biogeosciences For. 1, 86. https://doi.org/10.3832/IFOR0457-0010086

Ferreira, V., Panagopoulos, T., 2014. Seasonality of soil erosion under Mediterranean conditions at the Alqueva dam watershed. Environ. Manage. 54, 67–83.

https://doi.org/10.1007/S00267-014-0281-3/FIGURES/7

Fichot, C.G., Benner, R., 2011. A novel method to estimate DOC concentrations from CDOM absorption coefficients in coastal waters. Geophys. Res. Lett. 38. https://doi.org/10.1029/2010GL046152

Flato, G., Marotzke, J., Abiodun, B., Braconnot, P., Chou, S.C., Collins, W., Cox, P., Driouech, F., Emori, S., Eyring, V., Forest, C., Gleckler, P., Guilyardi, E., Jakob, C., Kattsov, V., Reason, C., Rummukainen, M., 2013. Evaluation of Climate Models, in: Stocker, T.F., Qin, D., Plattner, G.-K., Tignor, M., Allen, S.K., Boschung, J., Nauels, A., Xia, Y., Bex, V., Midg, P.M. (Eds.), Climate Change 2013: The Physical Science Basis. Contribution of Working Group I to the Fifth Assessment Report of the Intergovernmental Panel on Climate Change. Cambridge University Press, Cambridge, United Kingdom and New York, NY, USA.

Foster, I.D.L., Chapman, A.S., Hodgkinson, R.M., Jones, A.R., Lees, J.A., Turner, S.E., Scott, M., 2003. Changing suspended sediment and particulate phosphorus loads and pathways in underdrained lowland agricultural catchments; Herefordshire and Worcestershire, U.K., in: The Interactions between Sediments and Water. Springer Netherlands, pp. 119–126. https://doi.org/10.1007/978-94-017-3366-3_17

Fowler, D., Coyle, M., Skiba, U., Sutton, M.A., Cape, J.N., Reis, S., Sheppard, L.J., Jenkins, A., Grizzetti, B., Galloway, J.N., Vitousek, P., Leach, A., Bouwman, A.F., Butterbach-Bahl, K., Dentener, F., Stevenson, D., Amann, M., Voss, M., 2013. The global nitrogen cycle in the twenty-first century. Philos. Trans. R. Soc. B Biol. Sci. 368. https://doi.org/10.1098/RSTB.2013.0164

Fox, G.A., Purvis, R.A., Penn, C.J., 2016. Streambanks: A net source of sediment and phosphorus to streams and rivers. J. Environ. Manage. 181, 602–614. https://doi.org/10.1016/J.JENVMAN.2016.06.071

Fraisl, D., Campbell, J., See, L., Wehn, U., Wardlaw, J., Gold, M., Moorthy, I., Arias, R., Piera, J., Oliver, J.L., Masó, J., Penker, M., Fritz, S., 2020. Mapping citizen science contributions to the UN sustainable development goals. Sustain. Sci. 2020 156 15, 1735–1751. https://doi.org/10.1007/S11625-020-00833-7

Friedlingstein, P., O'Sullivan, M., Jones, M.W., Andrew, R.M., Hauck, J., Olsen, A., Peters, G.P., Peters, W., Pongratz, J., Sitch, S., Le Quéré, C., Canadell, J.G., Ciais, P., Jackson, R.B., Alin, S., Aragão, L.E.O.C., Arneth, A., Arora, V., Bates, N.R., Becker, M., Benoit-Cattin, A., Bittig, H.C., Bopp, L., Bultan, S., Chandra, N., Chevallier, F., Chini, L.P., Evans, W., Florentie, L., Forster, P.M., Gasser, T., Gehlen, M., Gilfillan, D., Gkritzalis,

T., Gregor, L., Gruber, N., Harris, I., Hartung, K., Haverd, V., Houghton, R.A., Ilyina, T., Jain, A.K., Joetzjer, E., Kadono, K., Kato, E., Kitidis, V., Korsbakken, J.I., Landschützer, P., Lefèvre, N., Lenton, A., Lienert, S., Liu, Z., Lombardozzi, D., Marland, G., Metzl, N., Munro, D.R., Nabel, J.E.M.S., Nakaoka, S.I., Niwa, Y., O'Brien, K., Ono, T., Palmer, P.I., Pierrot, D., Poulter, B., Resplandy, L., Robertson, E., Rödenbeck, C., Schwinger, J., Séférian, R., Skjelvan, I., Smith, A.J.P., Sutton, A.J., Tanhua, T., Tans, P.P., Tian, H., Tilbrook, B., Van Der Werf, G., Vuichard, N., Walker, A.P., Wanninkhof, R., Watson, A.J., Willis, D., Wiltshire, A.J., Yuan, W., Yue, X., Zaehle, S., 2020. Global Carbon Budget 2020. Earth Syst. Sci. Data 12, 3269–3340. https://doi.org/10.5194/ESSD-12-3269-2020

Fröberg, M., Berggren Kleja, D., Hagedorn, F., 2007. The contribution of fresh litter to dissolved organic carbon leached from a coniferous forest floor. Eur. J. Soil Sci. 58, 108–114. https://doi.org/10.1111/J.1365-2389.2006.00812.X

Fu, B.P., 1981. On the calculation of the evaporation from land surface (in Chinese). Chinese J. Atmos. Sci. 5, 23–31. https://doi.org/10.3878/J.ISSN.1006-9895.1981.01.03

Fu, Q., Li, B., Hou, Y., Bi, X., Zhang, X., 2017. Effects of land use and climate change on ecosystem services in Central Asia's arid regions: A case study in Altay Prefecture, China. Sci. Total Environ. 607–608, 633–646. https://doi.org/10.1016/J.SCITOTENV.2017.06.241

Futter, M.N., Butterfield, D., Cosby, B.J., Dillon, P.J., Wade, A.J., Whitehead, P.G., 2007. Modeling the mechanisms that control in-stream dissolved organic carbon dynamics in upland and forested catchments. Water Resour. Res. 43, 2424. https://doi.org/10.1029/2006WR004960

Futter, M.N., de Wit, H.A., 2008. Testing seasonal and long-term controls of streamwater DOC using empirical and process-based models. Sci. Total Environ. 407, 698–707. https://doi.org/10.1016/J.SCITOTENV.2008.10.002

Gaglio, M., Aschonitis, V., Pieretti, L., Santos, L., Gissi, E., Castaldelli, G., Fano, E.A., 2019. Modelling past, present and future Ecosystem Services supply in a protected floodplain under land use and climate changes. Ecol. Modell. 403, 23–34. https://doi.org/10.1016/J.ECOLMODEL.2019.04.019

Galgani, L., Tognazzi, A., Rossi, C., Ricci, M., Angel Galvez, J., Dattilo, A.M., Cozar, A., Bracchini, L., Loiselle, S.A., 2011. Assessing the optical changes in dissolved organic matter in humic lakes by spectral slope distributions. J. Photochem. Photobiol. B Biol. 102, 132–139. https://doi.org/10.1016/J.JPHOTOBIOL.2010.10.001

Galy, V., Eglinton, T., France-Lanord, C., Sylva, S., 2011. The provenance of vegetation and environmental signatures encoded in vascular plant biomarkers carried by the Ganges–Brahmaputra rivers. Earth Planet. Sci. Lett. 304, 1–12. https://doi.org/10.1016/J.EPSL.2011.02.003

Gardner, C.M.K., Robinson, D., Blyth, K., Cooper, J.D., 2000. Soil Water Content, in: Smith, K.A. (Ed.), Soil and Environmental Analysis. CRC Press, Boca Raton, pp. 13–76. https://doi.org/10.1201/9780203908600-6

Garnier, Josette, Billen, G., Lassaletta, L., Vigiak, O., Nikolaidis, N.P., Grizzetti, B., 2021. Hydromorphology of coastal zone and structure of watershed agro-food system are main determinants of coastal eutrophication. Environ. Res. Lett. 16, 023005. https://doi.org/10.1088/1748-9326/abc777

Garnier, J., Marescaux, A., Guillon, S., Vilmin, L., Rocher, V., Billen, G., Thieu, V., Silvestre, M., Passy, P., Raimonet, M., Groleau, A., Théry, S., Tallec, G., Flipo, N., 2021. Ecological Functioning of the Seine River: From Long-Term Modelling Approaches to High-Frequency Data Analysis, in: Handbook of Environmental Chemistry. Springer Science and Business Media Deutschland GmbH, pp. 189–216. https://doi.org/10.1007/698_2019_379

Garnier, J., Riou, P., Le Gendre, R., Ramarson, A., Billen, G., Cugier, P., Schapira, M., Théry, S., Thieu, V., Ménesguen, A., 2019. Managing the agri-food system of watersheds to combat coastal eutrophication: A land-to-sea modelling approach to the french coastal English channel. Geosci. 9, 441. https://doi.org/10.3390/geosciences9100441

Geoghegan, H., Dyke, A., Pateman, R., West, S. & Everett, G., 2016. Understanding Motivations for Citizen Science Motivations: citizen scientists, environmental volunteers and stakeholders, United Kingdom Environmental Observation Framework.

Giandon P., A., 2016. CARTA DELLA CAPACITÀ PROTETTIVA E DEL RISCHIO DI PERCOLAZIONE DELL'AZOTO DEI SUOLI DELLA PIANURA VENETA.

Giani, M., Djakovac, T., Degobbis, D., Cozzi, S., Solidoro, C., Umani, S.F., 2012. Recent changes in the marine ecosystems of the northern Adriatic Sea. Estuar. Coast. Shelf Sci. 115, 1–13. https://doi.org/10.1016/J.ECSS.2012.08.023

Gjyli, L., Bacu, A., Kolitari, J., Gjyli, S., 2016. Estimation of N/P Ratios Levels in a Coastal Bay, Southern Adriatic Sea. J. Agric. Ecol. Res. Int. 8, 1–9. https://doi.org/10.9734/JAERI/2016/25052

Glibert, P.M., Burford, M.A., 2017. Globally Changing Nutrient Loads and Harmful Algal

Blooms: Recent Advances, New Paradigms, and Continuing Challenges. Oceanography 30, 58–69. https://doi.org/10.2307/24897842

Glibert, P.M., Icarus Allen, J., Artioli, Y., Beusen, A., Bouwman, L., Harle, J., Holmes, R., Holt, J., 2014a. Vulnerability of coastal ecosystems to changes in harmful algal bloom distribution in response to climate change: Projections based on model analysis. Glob. Chang. Biol. 20, 3845–3858. https://doi.org/10.1111/gcb.12662

Glibert, P.M., Maranger, R., Sobota, D.J., Bouwman, L., 2014b. The Haber Bosch–harmful algal bloom (HB–HAB) link. Environ. Res. Lett. 9, 105001. https://doi.org/10.1088/1748-9326/9/10/105001

Gommet, C., Lauerwald, R., Ciais, P., Guenet, B., Zhang, H., Regnier, P., 2022. Spatiotemporal patterns and drivers of terrestrial dissolved organic carbon (DOC) leaching into the European river network. Earth Syst. Dyn. 13, 393–418. https://doi.org/10.5194/ESD-13-393-2022

Gong, J., Zhang, J., Zhang, Y., Zhu, Y., Jin, T., Xu, C., 2021. Do Forest Landscape Pattern Planning and Optimization Play a Role in Enhancing Soil Conservation Services in Mountain Areas of Western China? Chinese Geogr. Sci. 31, 848–866. https://doi.org/10.1007/S11769-021-1230-8/METRICS

Goodchild, M.F., 2007. Citizens as sensors: The world of volunteered geography. GeoJournal 69, 211–221. https://doi.org/10.1007/S10708-007-9111-Y/FIGURES/8

Gratziou, Maria, Gratziou, M, Chrisochoidou, P., 2013. Cost analysis of wastewater nitrogen removal in Greece. Fresenius Environ. Bull. 22.

Grizzetti, B., Bouraoui, F., Aloe, A., 2012. Changes of nitrogen and phosphorus loads to European seas. Glob. Chang. Biol. 18, 769–782. https://doi.org/10.1111/j.1365-2486.2011.02576.x

Gumiero, B., Boz, B., 2017. How to stop nitrogen leaking from a Cross compliant buffer strip? Ecol. Eng. 103, 446–454. https://doi.org/10.1016/j.ecoleng.2016.05.031

Gumiero, B., Cornelio, P., Boz, B., 2011. Nitrogen removal by an irrigated wooded buffer area. Water Pract. Technol. 6. https://doi.org/10.2166/wpt.2011.042

Guo, Z., Wang, Y., Wan, Z., Zuo, Y., He, L., Li, D., Yuan, F., Wang, N., Liu, J., Song, Y., Song, C., Xu, X., 2020. Soil dissolved organic carbon in terrestrial ecosystems: Global budget, spatial distribution and controls. Glob. Ecol. Biogeogr. 29, 2159–2175. https://doi.org/10.1111/GEB.13186

Guswa, A.J., Hamel, P., Meyer, K., 2017. Curve Number Approach to Estimate Monthly and Annual Direct Runoff. J. Hydrol. Eng. 23, 04017060.

https://doi.org/10.1061/(ASCE)HE.1943-5584.0001606

Haklay, M., 2013. Citizen science and volunteered geographic information: Overview and typology of participation. Crowdsourcing Geogr. Knowl. Volunt. Geogr. Inf. Theory Pract. 9789400745872, 105–122. https://doi.org/10.1007/978-94-007-4587-2_7/COVER

Hallegatte, S., 2009. Strategies to adapt to an uncertain climate change. Glob. Environ. Chang. 19, 240–247. https://doi.org/10.1016/J.GLOENVCHA.2008.12.003

Hamel, P., Guswa, A.J., 2015. Uncertainty analysis of a spatially explicit annual water-balance model: Case study of the Cape Fear basin, North Carolina. Hydrol. Earth Syst. Sci. 19, 839–853. https://doi.org/10.5194/HESS-19-839-2015

Hamel, P., Valencia, J., Schmitt, R., Shrestha, M., Piman, T., Sharp, R.P., Francesconi, W., Guswa, A.J., 2020. Modeling seasonal water yield for landscape management: Applications in Peru and Myanmar. J. Environ. Manage. 270, 110792. https://doi.org/10.1016/J.JENVMAN.2020.110792

Hansen, A.M., Kraus, T.E.C., Pellerin, B.A., Fleck, J.A., Downing, B.D., Bergamaschi, B.A., 2016. Optical properties of dissolved organic matter (DOM): Effects of biological and photolytic degradation. Limnol. Oceanogr. 61, 1015–1032. https://doi.org/10.1002/LNO.10270

Harrison, J.A., Caraco, N., Seitzinger, S.P., 2005. Global patterns and sources of dissolved organic matter export to the coastal zone: Results from a spatially explicit, global model. Global Biogeochem. Cycles 19. https://doi.org/10.1029/2005GB002480

Hejzlar, J., Anthony, S., Arheimer, B., Behrendt, H., Bouraoui, F., Grizzetti, B., Groenendijk, P., Jeuken, M.H.J.L., Johnsson, H., Lo Porto, A., Kronvang, B., Panagopoulos, Y., Siderius, C., Silgram, M., Venohr, M., Žaloudík, J., 2009. Nitrogen and phosphorus retention in surface waters: An inter-comparison of predictions by catchment models of different complexity. J. Environ. Monit. 11, 584–593. https://doi.org/10.1039/b901207a

Hernes, P.J., Spencer, R.G.M., Dyda, R.Y., Pellerin, B.A., Bachand, P.A.M., Bergamaschi, B.A., 2013. DOM composition in an agricultural watershed: Assessing patterns and variability in the context of spatial scales. Geochim. Cosmochim. Acta 121, 599–610. https://doi.org/10.1016/J.GCA.2013.07.039

Hernes, P.J., Spencer, R.G.M., Dyda, R.Y., Pellerin, B.A., Bachand, P.A.M., Bergamaschi, B.A., 2008. The role of hydrologic regimes on dissolved organic carbon composition in an agricultural watershed. Geochim. Cosmochim. Acta 72, 5266–5277. https://doi.org/10.1016/J.GCA.2008.07.031

Hiederer, R., 2013. Mapping Soil Properties for Europe - Spatial Representation of Soil

Database Attributes. EUR26082EN Scientific and Technical Research series, JRC Technical Reports. Publications Office of the European Union, Luxembourg. https://doi.org/10.2788/94128

Hill, R.D., Rinker, R.G., Dale Wilson, H., 1980. Atmospheric Nitrogen Fixation by Lightning. J. Atmos. Sci. 37, 179–192. https://doi.org/10.1007/978-3-642-27833-4_438-5

Hodgkiss, I.J., Lu, S., 2004. The effects of nutrients and their ratios on phytoplankton abundance in Junk Bay, Hong Kong. Asian Pacific Phycol. 21st Century Prospect. Challenges 215–229. https://doi.org/10.1007/978-94-007-0944-7_29

Holland, A., McInerney, P.J., Shackleton, M.E., Rees, G.N., Bond, N.R., Silvester, E., 2020. Dissolved organic matter and metabolic dynamics in dryland lowland rivers. Spectrochim. Acta Part A Mol. Biomol. Spectrosc. 229, 117871. https://doi.org/10.1016/J.SAA.2019.117871

Houlton, B.Z., Boyer, E., Finzi, A., Galloway, J., Leach, A., Liptzin, D., Melillo, J., Rosenstock, T.S., Sobota, D., Townsend, A.R., 2013. Intentional versus unintentional nitrogen use in the United States: Trends, efficiency and implications. Biogeochemistry 114, 11–23. https://doi.org/10.1007/S10533-012-9801-5/FIGURES/4

Huang, P.M., Wang, M.K., Chiu, C.Y., 2005. Soil mineral–organic matter–microbe interactions: Impacts on biogeochemical processes and biodiversity in soils. Pedobiologia (Jena). 49, 609–635. https://doi.org/10.1016/J.PEDOBI.2005.06.006

Hurrell, J.W., Kushnir, Y., Ottersen, G., Visbeck, M., 2003. An overview of the north atlantic oscillation. Geophys. Monogr. Ser. 134, 1–35. https://doi.org/10.1029/134GM01

Iannuccilli, M., Bartolini, G., Betti, G., Crisci, A., Grifoni, D., Gozzini, B., Messeri, A., Morabito, M., Tei, C., Torrigiani Malaspina, T., Vallorani, R., Messeri, G., 2021. Extreme precipitation events and their relationships with circulation types in Italy. Int. J. Climatol. 41, 4769–4793. https://doi.org/10.1002/JOC.7109

IPCC, 2021. Climate Change 2021: The Physical Science Basis | Climate Change 2021: The Physical Science Basis [WWW Document]. URL https://www.ipcc.ch/report/ar6/wg1/ (accessed 1.30.23).

IPCC, 2019a. IPCC special report on climate change, desertification, land degradation, sustainable land management, food security, and greenhouse gas fluxes in terrestrial ecosystems [WWW Document]. URL https://www.ipcc.ch/srccl/ (accessed 1.29.23).

IPCC, 2019b. IPCC, 2019: Climate Change and Land: an IPCC special report on climate change, desertification, land degradation, sustainable land management, food security,

and greenhouse gas fluxes in terrestrial ecosystems [WWW Document]. URL https://scholar.googleusercontent.com/scholar?q=cache:52WbLPsPDU4J:scholar.google.com/+IPCC+Climate+Change+and+Land+Report+(2019)&hl=it&as_sdt=0,5&as_vis=1 (accessed 8.9.21).

IPCC, 2014. Climate Change 2014: Synthesis Report. Contribution of Working Groups I, II and III to the Fifth Assessment Report of the Intergovernmental Panel on Climate Change, Kristin Seyboth (USA). Gian-Kasper Plattner, Geneva, Switzerland.

IPCC, 2006. "2006 IPCC Guidelines for National Greenhouse Gas Inventories, Prepared by the National Greenhouse Gas Inventories Programme. Eggleston H.S., Buendia L., Miwa K., Ngara T. and Tanabe K. (eds), in: Eggleston, S., Buendia, L., Miwa, K., Ngara, T., Tanabe, K. (Eds.), . IGES, Hayama, Japan, pp. 1–89.

IR, 2006. Decreto Legislativo 3 aprile 2006, n. 152, Gazzetta Ufficiale. GU Serie Generale n.88 del 14-04-2006 - Suppl. Ordinario n. 96).

Iravani, M., White, S.R., Farr, D.R., Habib, T.J., Kariyeva, J., Faramarzi, M., 2019. Assessing the provision of carbon-related ecosystem services across a range of temperate grassland systems in western Canada. Sci. Total Environ. 680, 151–168. https://doi.org/10.1016/J.SCITOTENV.2019.05.083

Irwin, A., 1995. Citizen Science : A Study of People, Expertise and Sustainable Development. Routledge. https://doi.org/10.4324/9780203202395

ISPRA, 2020. Istituto Superiore per la Protezione e la Ricerca Ambientale, SINAnet. DEM 20 m Italy [WWW Document]. URL http://www.sinanet.isprambiente.it/it/sia-ispra/download-mais/dem20/view (accessed 1.8.23).

ISPRA, 2019. Report | Annuario dei Dati Ambientali [WWW Document]. URL https://annuario.isprambiente.it/ada/downreport/html/6976 (accessed 1.30.23).

ISPRA, 2018. Corine Land Cover 2018 IV livello | Uso, copertura e consumo di suolo [WWW Document]. URL https://groupware.sinanet.isprambiente.it/uso-copertura-e-consumo-di-suolo/library/copertura-del-suolo/corine-land-cover/corine-land-cover-2018-iv-livello (accessed 1.8.23).

ISPRA, 2013. Climate change, naturalità diffusa e pianificazione territoriale. Periodici tecnici, Reticula. Rome.

Jabłońska, E., Wiśniewska, M., Marcinkowski, P., Grygoruk, M., Walton, C.R., Zak, D., Hoffmann, C.C., Larsen, S.E., Trepel, M., Kotowski, W., 2020. Catchment-Scale Analysis Reveals High Cost-Effectiveness of Wetland Buffer Zones as a Remedy to Non-Point Nutrient Pollution in North-Eastern Poland. Water 2020, Vol. 12, Page 629

12, 629. https://doi.org/10.3390/W12030629

Jax, K., Barton, D.N., Chan, K.M.A., de Groot, R., Doyle, U., Eser, U., Görg, C., Gómez-Baggethun, E., Griewald, Y., Haber, W., Haines-Young, R., Heink, U., Jahn, T., Joosten, H., Kerschbaumer, L., Korn, H., Luck, G.W., Matzdorf, B., Muraca, B., Neßhöver, C., Norton, B., Ott, K., Potschin, M., Rauschmayer, F., von Haaren, C., Wichmann, S., 2013. Ecosystem services and ethics. Ecol. Econ. 93, 260–268. https://doi.org/10.1016/J.ECOLECON.2013.06.008

Jiang, F., Beck, M.B., Cummings, R.G., Rowles, K., Russell, D., 2004. Estimation Of Costs Of Phosphorus Removal In Wastewater Treatment Facilities: Construction De Novo.

Jin, R., Liu, T., Liu, G., Zhou, J., Huang, J., Wang, A., 2015. Simultaneous Heterotrophic Nitrification and Aerobic Denitrification by the Marine Origin Bacterium Pseudomonas sp. ADN-42. Appl. Biochem. Biotechnol. 175, 2000–2011. https://doi.org/10.1007/S12010-014-1406-0/METRICS

Jutras, M.F., Nasr, M., Castonguay, M., Pit, C., Pomeroy, J.H., Smith, T.P., Zhang, C. fu, Ritchie, C.D., Meng, F.R., Clair, T.A., Arp, P.A., 2011. Dissolved organic carbon concentrations and fluxes in forest catchments and streams: DOC-3 model. Ecol. Modell. 222, 2291–2313. https://doi.org/10.1016/J.ECOLMODEL.2011.03.035

Kabisch, N., Qureshi, S., Haase, D., 2015. Human–environment interactions in urban green spaces — A systematic review of contemporary issues and prospects for future research. Environ. Impact Assess. Rev. 50, 25–34. https://doi.org/10.1016/J.EIAR.2014.08.007

Kalbitz, K., Schmerwitz, J., Schwesig, D., Matzner, E., 2003. Biodegradation of soil-derived dissolved organic matter as related to its properties. Geoderma 113, 273–291. https://doi.org/10.1016/S0016-7061(02)00365-8

Kalev, S., Toor, G.S., 2020. Concentrations and Loads of Dissolved and Particulate Organic Carbon in Urban Stormwater Runoff. Water 2020, Vol. 12, Page 1031 12, 1031. https://doi.org/10.3390/W12041031

Keeler, B.L., Polasky, S., Brauman, K.A., Johnson, K.A., Finlay, J.C., O'Neille, A., Kovacs, K., Dalzell, B., 2012. Linking water quality and well-being for improved assessment and valuation of ecosystem services. Proc. Natl. Acad. Sci. U. S. A. 109, 18619–18624. https://doi.org/10.1073/pnas.1215991109

Kelling, S., Hochachka, W.M., Fink, D., Riedewald, M., Caruana, R., Ballard, G., Hooker, G., 2009. Data-intensive science: A new paradigm for biodiversity studies. Bioscience 59, 613–620. https://doi.org/10.1525/BIO.2009.59.7.12/2/BIO.2009.59.7.12-F03.JPEG

Kim, J.K., Jung, S., Eom, J. sung, Jang, C., Lee, Y., Owen, J.S., Jung, M.S., Kim, B., 2013.

Dissolved and particulate organic carbon concentrations in stream water and relationships with land use in multiple-use watersheds of the Han River (Korea). http://dx.doi.org/10.1080/02508060.2013.769411 38, 326–339. https://doi.org/10.1080/02508060.2013.769411

Koistinen, J., Sjöblom, M., Spilling, K., 2020. Determining Inorganic and Organic Phosphorus. Methods Mol. Biol. 1980, 87–94. https://doi.org/10.1007/7651_2017_104

Kremen, C., Ullman, K.S., Thorp, R.W., 2011. Evaluating the Quality of Citizen-Scientist Data on Pollinator Communities. Conserv. Biol. 25, 607–617. https://doi.org/10.1111/J.1523-1739.2011.01657.X

Krinner, G., Viovy, N., de Noblet-Ducoudré, N., Ogée, J., Polcher, J., Friedlingstein, P., Ciais, P., Sitch, S., Prentice, I.C., 2005. A dynamic global vegetation model for studies of the coupled atmosphere-biosphere system. Global Biogeochem. Cycles 19, 1–33. https://doi.org/10.1029/2003GB002199

Kunkel, K.E., Karl, T.R., Brooks, H., Kossin, J., Lawrimore, J.H., Arndt, D., Bosart, L., Changnon, D., Cutter, S.L., Doesken, N., Emanuel, K., Groisman, P.Y., Katz, R.W., Knutson, T., O'brien, J., Paciorek, C.J., Peterson, T.C., Redmond, K., Robinson, D., Trapp, J., Vose, R., Weaver, S., Wehner, M., Wolter, K., Wuebbles, D., 2013. Monitoring and Understanding Trends in Extreme Storms: State of Knowledge. Bull. Am. Meteorol. Soc. 94, 499–514. https://doi.org/10.1175/BAMS-D-11-00262.1

Lal, R., 2005. Forest soils and carbon sequestration. For. Ecol. Manage. 220, 242–258. https://doi.org/10.1016/J.FORECO.2005.08.015

Lancelot, C., Thieu, V., Polard, A., Garnier, J., Billen, G., Hecq, W., Gypens, N., 2011. Cost assessment and ecological effectiveness of nutrient reduction options for mitigating Phaeocystis colony blooms in the Southern North Sea: An integrated modeling approach. Sci. Total Environ. 409, 2179–2191. https://doi.org/10.1016/j.scitotenv.2011.02.023

Lasanta, T., Arnáez, J., Pascual, N., Ruiz-Flaño, P., Errea, M.P., Lana-Renault, N., 2017. Space–time process and drivers of land abandonment in Europe. CATENA 149, 810–823. https://doi.org/10.1016/J.CATENA.2016.02.024

Law Al, A.T., Adeloju, S.B., 2013. Progress and recent advances in phosphate sensors: A review. Talanta 114, 191–203. https://doi.org/10.1016/J.TALANTA.2013.03.031

Lee, F.Z., Lai, J.S., Sumi, T., 2022. Reservoir Sediment Management and Downstream River Impacts for Sustainable Water Resources; Case Study of Shihmen Reservoir. Water 2022, Vol. 14, Page 479 14, 479. https://doi.org/10.3390/W14030479

Lehr, J.L., Fowler, S., 2006. Social Justice Pedagogies and Scientific Knowledge: Remaking

Citizenship in the Non-Science Classroom.

Lessels, J.S., Tetzlaff, D., Carey, S.K., Smith, P., Soulsby, C., 2015. A coupled hydrology–biogeochemistry model to simulate dissolved organic carbon exports from a permafrost-influenced catchment. Hydrol. Process. 29, 5383–5396. https://doi.org/10.1002/HYP.10566

Li, M., Peng, C., Wang, M., Xue, W., Zhang, K., Wang, K., Shi, G., Zhu, Q., 2017. The carbon flux of global rivers: A re-evaluation of amount and spatial patterns. Ecol. Indic. 80, 40–51. https://doi.org/10.1016/J.ECOLIND.2017.04.049

Li, M., Peng, C., Zhou, X., Yang, Y., Guo, Y., Shi, G., Zhu, Q., 2019. Modeling Global Riverine DOC Flux Dynamics From 1951 to 2015. J. Adv. Model. Earth Syst. 11, 514–530. https://doi.org/10.1029/2018MS001363

Li, X., Chen, H., Jiang, X., Yu, Z., Yao, Q., 2017. Impacts of human activities on nutrient transport in the Yellow River: The role of the Water-Sediment Regulation Scheme. Sci. Total Environ. 592, 161–170. https://doi.org/10.1016/J.SCITOTENV.2017.03.098

Li, Y., Wu, J., Liu, S., Shen, J., Huang, D., Su, Y., Wei, W., Syers, J.K., 2012. Is the C:N:P stoichiometry in soil and soil microbial biomass related to the landscape and land use in southern subtropical China? Global Biogeochem. Cycles 26. https://doi.org/10.1029/2012GB004399

Lidskog, R., 2008. Scientised citizens and democratised science. Re-assessing the expert-lay divide. J. Risk Res. 11, 69–86. https://doi.org/10.1080/13669870701521636

Lindström, G., Johansson, B., Persson, M., Gardelin, M., Bergström, S., 1997. Development and test of the distributed HBV-96 hydrological model. J. Hydrol. 201, 272–288. https://doi.org/10.1016/S0022-1694(97)00041-3

Link, W.A., Sauer, J.R., Niven, D.K., 2006. A Hierarchical Model for Regional Analysis of Population Change Using Christmas Bird Count Data, with Application to the American Black Duck. Condor 108, 13–24. https://doi.org/10.1093/CONDOR/108.1.13

Liu, J., Han, G., 2020. Major ions and δ34SSO4 in Jiulongjiang River water: Investigating the relationships between natural chemical weathering and human perturbations. Sci. Total Environ. 724, 138208. https://doi.org/10.1016/J.SCITOTENV.2020.138208

Liu, X., Beusen, A.H.W., Van Beek, L.P.H., Mogollón, J.M., Ran, X., Bouwman, A.F., 2018. Exploring spatiotemporal changes of the Yangtze River (Changjiang) nitrogen and phosphorus sources, retention and export to the East China Sea and Yellow Sea. Water Res. 142, 246–255. https://doi.org/10.1016/j.watres.2018.06.006

Lobbes, J.M., Fitznar, H.P., Kattner, G., 2000. Biogeochemical characteristics of dissolved

and particulate organic matter in Russian rivers entering the Arctic Ocean. Geochim. Cosmochim. Acta 64, 2973–2983. https://doi.org/10.1016/S0016-7037(00)00409-9

Loiselle, S.A., Bracchini, L., Cózar, A., Dattilo, A.M., Tognazzi, A., Rossi, C., 2009a. Variability in photobleaching yields and their related impacts on optical conditions in subtropical lakes. J. Photochem. Photobiol. B Biol. 95, 129–137. https://doi.org/10.1016/J.JPHOTOBIOL.2009.02.002

Loiselle, S.A., Bracchini, L., Dattilo, A.M., Ricci, M., Tognazzi, A., Cózar, A., Rossi, C., 2009b. The optical characterization of chromophoric dissolved organic matter using wavelength distribution of absorption spectral slopes. Limnol. Oceanogr. 54, 590–597. https://doi.org/10.4319/LO.2009.54.2.0590

Loiselle, S.A., Cunha, D.G.F., Shupe, S., Valiente, E., Rocha, L., Heasley, E., Belmont, P.P., Baruch, A., 2016. Micro and Macroscale Drivers of Nutrient Concentrations in Urban Streams in South, Central and North America. PLoS One 11, e0162684. https://doi.org/10.1371/JOURNAL.PONE.0162684

Loiselle, S.A., Frost, P.C., Turak, E., Thornhill, I., 2017. Citizen scientists supporting environmental research priorities. Sci. Total Environ. https://doi.org/10.1016/j.scitotenv.2017.03.142

Luo, X., Bai, X., Tan, Q., Ran, C., Chen, H., Xi, H., Chen, F., Wu, L., Li, C., Zhang, S., Zhong, X., Tian, S., 2022. Particulate organic carbon exports from the terrestrial biosphere controlled by erosion. CATENA 209, 105815. https://doi.org/10.1016/J.CATENA.2021.105815

Ma, T., Zhao, N., Ni, Y., Yi, J., Wilson, J.P., He, L., Du, Y., Pei, T., Zhou, C., Song, C., Cheng, W., 2020. China's improving inland surface water quality since 2003. Sci. Adv. 6, eaau3798. https://doi.org/10.1126/sciadv.aau3798

Maavara, T., Lauerwald, R., Regnier, P., Van Cappellen, P., 2017. Global perturbation of organic carbon cycling by river damming. Nat. Commun. 2017 81 8, 1–10. https://doi.org/10.1038/ncomms15347

Madsen, E.L., 2011. Microorganisms and their roles in fundamental biogeochemical cycles. Curr. Opin. Biotechnol. 22, 456–464. https://doi.org/10.1016/J.COPBIO.2011.01.008

Mainstone, C.P., Parr, W., 2002. Phosphorus in rivers — ecology and management. Sci. Total Environ. 282–283, 25–47. https://doi.org/10.1016/S0048-9697(01)00937-8

Malavasi, M., Carranza, M.L., Moravec, D., Cutini, M., 2018. Reforestation dynamics after land abandonment: a trajectory analysis in Mediterranean mountain landscapes. Reg. Environ. Chang. 2018 188 18, 2459–2469. https://doi.org/10.1007/S10113-018-1368-9

Malone, T.C., Newton, A., 2020. The Globalization of Cultural Eutrophication in the Coastal Ocean: Causes and Consequences. Front. Mar. Sci. 7, 670. https://doi.org/10.3389/FMARS.2020.00670/BIBTEX

Maniquiz, M.C., Lee, S., Kim, L.H., 2010. Multiple linear regression models of urban runoff pollutant load and event mean concentration considering rainfall variables. J. Environ. Sci. 22, 946–952. https://doi.org/10.1016/S1001-0742(09)60203-5

Massicotte, P., Asmala, E., Stedmon, C., Markager, S., 2017. Global distribution of dissolved organic matter along the aquatic continuum: Across rivers, lakes and oceans. Sci. Total Environ. 609, 180–191. https://doi.org/10.1016/J.SCITOTENV.2017.07.076

Matomela, N., Li, T., Ikhumhen, H.O., Raimundo Lopes, N.D., Meng, L., 2022. Soil erosion spatio-temporal exploration and Geodetection of driving factors using InVEST-sediment delivery ratio and Geodetector models in Dongsheng, China. https://doi.org/10.1080/10106049.2022.2076912. https://doi.org/10.1080/10106049.2022.2076912

Matos Valerio, A. DE, Kampel, M., Vantrepotte, V., Ward, Nicholas D, Oliveira Sawakuchi, H., Fernanda Silva Less, D. DA, Neu, V., Cunha, A., Richey, J., Kaplan, L.A., Findlay, S., Hopkinson, C.S., Marti, E., Packman, A.I., Newbold, J.D., Sabater, F., Ward, N D, Bianchi, T.S., Medeiros, P.M., Seidel, M., Richey, J.E., Keil, R.G., Sawakuchi, H.O., 2018. Using CDOM optical properties for estimating DOC concentrations and pCO_2 in the Lower Amazon River. Opt. Express, Vol. 26, Issue 14, pp. A657-A677 26, A657–A677. https://doi.org/10.1364/OE.26.00A657

Mayer, P.M., Reynolds, S.K., McCutchen, M.D., Canfield, T.J., 2007. Meta-Analysis of Nitrogen Removal in Riparian Buffers. J. Environ. Qual. 36, 1172–1180. https://doi.org/10.2134/jeq2006.0462

McCrackin, M.L., Muller-Karulis, B., Gustafsson, B.G., Howarth, R.W., Humborg, C., Svanbäck, A., Swaney, D.P., 2018. A Century of Legacy Phosphorus Dynamics in a Large Drainage Basin. Global Biogeochem. Cycles 32, 1107–1122. https://doi.org/10.1029/2018GB005914

McKinley, D.C., Miller-Rushing, A.J., Ballard, H.L., Bonney, R., Brown, H., Cook-Patton, S.C., Evans, D.M., French, R.A., Parrish, J.K., Phillips, T.B., Ryan, S.F., Shanley, L.A., Shirk, J.L., Stepenuck, K.F., Weltzin, J.F., Wiggins, A., Boyle, O.D., Briggs, R.D., Chapin, S.F., Hewitt, D.A., Preuss, P.W., Soukup, M.A., 2017. Citizen science can improve conservation science, natural resource management, and environmental protection. Biol. Conserv. 208, 15–28. https://doi.org/10.1016/J.BIOCON.2016.05.015

MEA, 2005. Millennium Ecosystem Assessment (MEA) - Ecosystems and Human Well-being: Wetland nad Water Synthesis. Washington, DC.

Medina-Villar, S., Castro-Díez, P., Alonso, A., Cabra-Rivas, I., Parker, I.M., Pérez-Corona, E., 2015. Do the invasive trees, Ailanthus altissima and Robinia pseudoacacia, alter litterfall dynamics and soil properties of riparian ecosystems in Central Spain? Plant Soil 396, 311–324. https://doi.org/10.1007/S11104-015-2592-4/FIGURES/4

Meehl, G.A., Covey, C., Delworth, T., Latif, M., McAvaney, B., Mitchell, J.F.B., Stouffer, R.J., Taylor, K.E., 2007. THE WCRP CMIP3 Multimodel Dataset: A New Era in Climate Change Research. Bull. Am. Meteorol. Soc. 88, 1383–1394. https://doi.org/10.1175/BAMS-88-9-1383

Melillo, J.M., McGuire, A.D., Kicklighter, D.W., Moore, B., Vorosmarty, C.J., Schloss, A.L., 1993. Global climate change and terrestrial net primary production. Nat. 1993 3636426 363, 234–240. https://doi.org/10.1038/363234a0

Mello, K. de, Randhir, T.O., Valente, R.A., Vettorazzi, C.A., 2017. Riparian restoration for protecting water quality in tropical agricultural watersheds. Ecol. Eng. 108, 514–524. https://doi.org/10.1016/j.ecoleng.2017.06.049

Melton, J.R., Arora, V.K., Wisernig-Cojoc, E., Seiler, C., Fortier, M., Chan, E., Teckentrup, L., 2020. CLASSIC v1.0: The open-source community successor to the Canadian Land Surface Scheme (CLASS) and the Canadian Terrestrial Ecosystem Model (CTEM)-Part 1: Model framework and site-level performance. Geosci. Model Dev. 13, 2825–2850. https://doi.org/10.5194/GMD-13-2825-2020

Michalzik, B., Tipping, E., Mulder, J., Gallardo Lancho, J.F., Matzner, E., Bryant, C.L., Clarke, N., Lofts, S., Vicente Esteban, M.A., 2003. Modelling the production and transport of dissolved organic carbon in forest soils. Biogeochemistry 66, 241–264. https://doi.org/10.1023/B:BIOG.0000005329.68861.27/METRICS

Miller-Rushing, A., Primack, R., Bonney, R., 2012. The history of public participation in ecological research. Front. Ecol. Environ. 10, 285–290. https://doi.org/10.1890/110278

Miller, W.L., Moran, M.A., 1997. Interaction of photochemical and microbial processes in the degradation of refractory dissolved organic matter from a coastal marine environment. Limnol. Oceanogr. 42, 1317–1324. https://doi.org/10.4319/LO.1997.42.6.1317

Mills, M.M., Moore, C.M., Langlois, R., Milne, A., Achterberg, E., Nachtigall, K., Lochte, K., Geider, R.J., La Roche, J., 2008. Nitrogen and phosphorus co-limitation of bacterial productivity and growth in the oligotrophic subtropical North Atlantic. Limnol. Oceanogr. 53, 824–834. https://doi.org/10.4319/LO.2008.53.2.0824

Minaudo, C., Meybeck, M., Moatar, F., Gassama, N., Curie, F., 2015. Eutrophication mitigation in rivers: 30 Years of trends in spatial and seasonal patterns of biogeochemistry of the Loire River (1980-2012). Biogeosciences 12, 2549–2563. https://doi.org/10.5194/bg-12-2549-2015

Moss, R., Babiker, M., Brinkman, S., Calvo, E., Carter, T., Edmonds, J., Elgizouli, I., Emori, S., Erda, L., Hibbard, K., Jones, R., Kainuma M., Kelleher, J., Lamarque, J.F., Manning, M., Matthews, B., Meehl, J., Meyer, L., Mitchell, J., Nakicenovic, N., O'Neill, B., Pichs, R., Riahi, K., Rose, S., Runci, P., Stouffer, R., van Vuuren, D., Weyant, J., Wilbanks, T., van Ypersele, J.P., Zurek, M., 2008. Towards New Scenarios for Analysis of Emissions, Climate Change, Impacts, and Response Strategies. . Geneva.

Naiman, R.J., Décamps, H., 2003. The Ecology of Interfaces: Riparian Zones. https://doi.org/10.1146/annurev.ecolsys.28.1.621 28, 621–658. https://doi.org/10.1146/ANNUREV.ECOLSYS.28.1.621

Nakhavali, M., Lauerwald, R., Regnier, P., Guenet, B., Chadburn, S., Friedlingstein, P., 2021. Leaching of dissolved organic carbon from mineral soils plays a significant role in the terrestrial carbon balance. Glob. Chang. Biol. 27, 1083–1096. https://doi.org/10.1111/GCB.15460

Neff, J.C., Asner, G.P., 2001. Dissolved organic carbon in terrestrial ecosystems: Synthesis and a model. Ecosystems 4, 29–48. https://doi.org/10.1007/S100210000058/METRICS

Némery, J., Mano, V., Coynel, A., Etcheber, H., Moatar, F., Meybeck, M., Belleudy, P., Poirel, A., 2013. Carbon and suspended sediment transport in an impounded alpine river (Isère, France). Hydrol. Process. 27, 2498–2508. https://doi.org/10.1002/HYP.9387

Newman, G., Wiggins, A., Crall, A., Graham, E., Newman, S., Crowston, K., 2012. The future of Citizen science: Emerging technologies and shifting paradigms. Front. Ecol. Environ. https://doi.org/10.1890/110294

Nistor, M.M., Man, T.C., Benzaghta, M.A., Nedumpallile Vasu, N., Dezsi, Ş., Kizza, R., 2018. Land cover and temperature implications for the seasonal evapotranspiration in europe. Geogr. Tech. 13, 85–108. https://doi.org/10.21163/GT_2018.131.09

NNB, 2021. Progetto Vegetazione Riparia. Network Nazionale della Biodiversità (NNB) [WWW Document]. URL https://www.nnb.isprambiente.it/vegetazioneriparia/index.html (accessed 1.29.23).

NOAA, 2018. NCEP/NCAR Reanalysis 1: NOAA Physical Sciences Laboratory [WWW Document]. URL https://psl.noaa.gov/data/gridded/data.ncep.reanalysis.html (accessed 8.10.21).

Nodvin, S.C., Driscoll, C.T., Likens; Gene E., 1986. Simple partitioning of anions and dissolved organic carbon in a forest soil. Soil Sci. 142, 27–35.

Nonini, L., Fiala, M., 2021. Estimation of carbon storage of forest biomass for voluntary carbon markets: preliminary results. J. For. Res. 32, 329–338. https://doi.org/10.1007/S11676-019-01074-W/FIGURES/4

NRCS-USDA, 2007. NRCS Engineering Manuals and Handbooks | Natural Resources Conservation Service [WWW Document]. URL https://www.nrcs.usda.gov/conservation-basics/conservation-by-state/north-dakota/nrcs-engineering-manuals-and-handbooks (accessed 1.8.23).

Orem, W., Newman, S., Osborne, T.Z., Reddy, K.R., 2014. Projecting Changes in Everglades Soil Biogeochemistry for Carbon and Other Key Elements, to Possible 2060 Climate and Hydrologic Scenarios. Environ. Manage. 55, 776–798. https://doi.org/10.1007/S00267-014-0381-0/FIGURES/9

Ortiz-Hernández, J., Lucho-Constantino, C., Lizárraga-Mendiola, L., Beltrán-Hernández, R.I., Coronel-Olivares, C., Vázquez-Rodríguez, G., 2016. Quality of urban runoff in wet and dry seasons: a case study in a semi-arid zone. Environ. Sci. Pollut. Res. 23, 25156–25168. https://doi.org/10.1007/S11356-016-7547-7/FIGURES/3

Ou, Y., Wang, X., Wang, L., Rousseau, A.N., 2016. Landscape influences on water quality in riparian buffer zone of drinking water source area, Northern China. Env. Earth Sci 75, 1–13. https://doi.org/10.1007/s12665-015-4884-7

Ouyang, Y., 2003. Simulating dynamic load of naturally occurring TOC from watershed into a river. Water Res. 37, 823–832. https://doi.org/10.1016/S0043-1354(02)00389-5

Panagos, P., Ballabio, C., Himics, M., Scarpa, S., Matthews, F., Bogonos, M., Poesen, J., Borrelli, P., 2021. Projections of soil loss by water erosion in Europe by 2050. Environ. Sci. Policy 124, 380–392. https://doi.org/10.1016/J.ENVSCI.2021.07.012

Panagos, P., Borrelli, P., Meusburger, K., Alewell, C., Lugato, E., Montanarella, L., 2015a. Estimating the soil erosion cover-management factor at the European scale. Land use policy 48, 38–50. https://doi.org/10.1016/J.LANDUSEPOL.2015.05.021

Panagos, P., Borrelli, P., Meusburger, K., van der Zanden, E.H., Poesen, J., Alewell, C., 2015b. Modelling the effect of support practices (P-factor) on the reduction of soil erosion by water at European scale. Environ. Sci. Policy 51, 23–34. https://doi.org/10.1016/J.ENVSCI.2015.03.012

Panagos, P., Borrelli, P., Meusburger, K., Yu, B., Klik, A., Lim, K.J., Yang, J.E., Ni, J., Miao, C., Chattopadhyay, N., Sadeghi, S.H., Hazbavi, Z., Zabihi, M., Larionov, G.A., Krasnov,

S.F., Gorobets, A. V., Levi, Y., Erpul, G., Birkel, C., Hoyos, N., Naipal, V., Oliveira, P.T.S., Bonilla, C.A., Meddi, M., Nel, W., Al Dashti, H., Boni, M., Diodato, N., Van Oost, K., Nearing, M., Ballabio, C., 2017. Global rainfall erosivity assessment based on high-temporal resolution rainfall records. Sci. Reports 2017 71 7, 1–12. https://doi.org/10.1038/s41598-017-04282-8

Panagos, P., Meusburger, K., Alewell, C., Montanarella, L., 2012. Soil erodibility estimation using LUCAS point survey data of Europe. Environ. Model. Softw. 30, 143–145. https://doi.org/10.1016/J.ENVSOFT.2011.11.002

Panagos, P., Meusburger, K., Ballabio, C., Borrelli, P., Alewell, C., 2014. Soil erodibility in Europe: A high-resolution dataset based on LUCAS. Sci. Total Environ. 479–480, 189–200. https://doi.org/10.1016/j.scitotenv.2014.02.010

Panagos, P., Van Liedekerke, M., Borrelli, P., Köninger, J., Ballabio, C., Orgiazzi, A., Lugato, E., Liakos, L., Hervas, J., Jones, A., Montanarella, L., 2022. European Soil Data Centre 2.0: Soil data and knowledge in support of the EU policies. Eur. J. Soil Sci. 73. https://doi.org/10.1111/EJSS.13315

Pandeya, B., Buytaert, W., Potter, C., 2021. Designing citizen science for water and ecosystem services management in data-poor regions: Challenges and opportunities. Curr. Res. Environ. Sustain. 3, 100059. https://doi.org/10.1016/J.CRSUST.2021.100059

Panthou, G., Mailhot, A., Laurence, E., Talbot, G., 2014. Relationship between Surface Temperature and Extreme Rainfalls: A Multi-Time-Scale and Event-Based Analysis. J. Hydrometeorol. 15, 1999–2011. https://doi.org/10.1175/JHM-D-14-0020.1

Pärn, J., Pinay, G., Mander, Ü., 2012. Indicators of nutrients transport from agricultural catchments under temperate climate: A review. Ecol. Indic. https://doi.org/10.1016/j.ecolind.2011.10.002

Parton, W.J., Scurlock, J.M.O., Ojima, D.S., Gilmanov, T.G., Scholes, R.J., Schimel, D.S., Kirchner, T., Menaut, J. -C, Seastedt, T., Garcia Moya, E., Kamnalrut, A., Kinyamario, J.I., 1993. Observations and modeling of biomass and soil organic matter dynamics for the grassland biome worldwide. Global Biogeochem. Cycles 7, 785–809. https://doi.org/10.1029/93GB02042

Passy, P., Le Gendre, R., Garnier, J., Cugier, P., Callens, J., Paris, F., Billen, G., Riou, P., Romero, E., 2016. Eutrophication modelling chain for improved management strategies to prevent algal blooms in the Bay of Seine. Mar. Ecol. Prog. Ser. 543, 107–125. https://doi.org/10.3354/meps11533

Perdue, E.M., Reuter, J.H., Ghosal, M., 1980. The operational nature of acidic functional

group analyses and its impact on mathematical descriptions of acid-base equilibria in humic substances. Geochim. Cosmochim. Acta 44, 1841–1851. https://doi.org/10.1016/0016-7037(80)90233-1

Pereda, O., von Schiller, D., García-Baquero, G., Mor, J.R., Acuña, V., Sabater, S., Elosegi, A., 2021. Combined effects of urban pollution and hydrological stress on ecosystem functions of Mediterranean streams. Sci. Total Environ. 753, 141971. https://doi.org/10.1016/J.SCITOTENV.2020.141971

Pessacg, N., Flaherty, S., Brandizi, L., Solman, S., Pascual, M., 2015. Getting water right: A case study in water yield modelling based on precipitation data. Sci. Total Environ. 537, 225–234. https://doi.org/10.1016/J.SCITOTENV.2015.07.148

Pettine, M., Capri, S., Manganelli, M., Patrolecco, L., Puddu, A., Zoppini, A., 2001. The Dynamics of DOM in the Northern Adriatic Sea. Estuar. Coast. Shelf Sci. 52, 471–489. https://doi.org/10.1006/ECSS.2000.0752

Pettine, M., Patrolecco, L., Camusso, M., Crescenzio, S., 1998. Transport of Carbon and Nitrogen to the Northern Adriatic Sea by the Po River. Estuar. Coast. Shelf Sci. 46, 127–142. https://doi.org/10.1006/ecss.1997.0303

Picco, L., Comiti, F., Mao, L., Tonon, A., Lenzi, M.A., 2017. Medium and short term riparian vegetation, island and channel evolution in response to human pressure in a regulated gravel bed river (Piave River, Italy). CATENA 149, 760–769. https://doi.org/10.1016/J.CATENA.2016.04.005

Pocock, M.J.O., Tweddle, J.C., Savage, J., Robinson, L.D., Roy, H.E., 2017. The diversity and evolution of ecological and environmental citizen science. PLoS One 12, e0172579. https://doi.org/10.1371/journal.pone.0172579

Porter, E.M., Bowman, W.D., Clark, C.M., Compton, J.E., Pardo, L.H., Soong, J.L., 2012. Interactive effects of anthropogenic nitrogen enrichment and climate change on terrestrial and aquatic biodiversity. Biogeochem. 2012 1141 114, 93–120. https://doi.org/10.1007/S10533-012-9803-3

Prairie, Y.T., 2011. Carbocentric limnology: looking back, looking forward. https://doi.org/10.1139/f08-011 65, 543–548. https://doi.org/10.1139/F08-011

Prentice, I.C., Farquhar, G.D., Fasham, M.J.R., Goulden, M.L., Heimann, M., Jaramillo, V.J., Kheshgi, H.S., Quéré, C. Le, Scholes, R.J., Wallace, D.W.R., Archer, D., Ashmore, M.R., Aumont, O., Baker, D., Battle, M., Bender, M., Bopp, L.P., Bousquet, P., Caldeira, K., Ciais, P., Cox, P.M., Cramer, W., Dentener, F., Enting, I.G., Field, C.B., Friedlingstein, P., Holland, E.A., Houghton, R.A., House, J.I., Ishida, A., Jain, A.K.,

Janssens, I.A., Joos, F., Kaminski, T., Keeling, C.D., Keeling, R.F., Kicklighter, D.W., Kohfeld, K.E., Knorr, W., Law, R., Lenton, T., Lindsay, K., Maier-Reimer, E., Manning, A.C., Matear, R.J., Mcguire, A.D., Melillo, J.M., Meyer, R., Mund, M., Orr, J.C., Piper, S., Plattner, K., Rayner, P.J., Sitch, S., Slater, R., Taguchi, S., Tans, P.P., Tian, H.Q., Weirig, M.F., Whorf, T., Yool, A., 2001. The carbon cycle and atmospheric carbon dioxide, in: Houghton, J.T., Ding, Y., Griggs, D.J., Noguer, M., van der Linden, P.J., Dai, X., Maskell, K., Johnson, C.. (Eds.), Climate Change 2001: The Scientific Basis, Intergovernmental Panel on Climate Change. Cambridge University Press, Cambridge, pp. 185–237.

Price, J.I., Heberling, M.T., 2018. The Effects of Source Water Quality on Drinking Water Treatment Costs: A Review and Synthesis of Empirical Literature. Ecol. Econ. 151, 195–209. https://doi.org/10.1016/J.ECOLECON.2018.04.014

QGIS Development Team, 2022. QGIS Geographic Information System. Open Source Geospatial Foundation Project. QGIS v.3.22. Geographic Information System API Documentation. QGIS Association. [WWW Document]. URL https://qgis.org/en/site/ (accessed 1.8.23).

Qi, J., Du, X., Zhang, X., Lee, S., Wu, Y., Deng, J., Moglen, G.E., Sadeghi, A.M., McCarty, G.W., 2020. Modeling riverine dissolved and particulate organic carbon fluxes from two small watersheds in the northeastern United States. Environ. Model. Softw. 124, 104601. https://doi.org/10.1016/J.ENVSOFT.2019.104601

Qu, H.J., Kroeze, C., 2010. Past and future trends in nutrients export by rivers to the coastal waters of China. Sci. Total Environ. 408, 2075–2086. https://doi.org/10.1016/J.SCITOTENV.2009.12.015

Rabalais, N.N., Turner, R.E., Scavia, D., 2002. Beyond science into policy: Gulf of Mexico hypoxia and the Mississippi River. Bioscience 52, 129–142. https://doi.org/10.1641/0006-3568(2002)052[0129:BSIPGO]2.0.CO;2

Raddick, J., Lintott, C., Bamford, S., Land, K., Locksmith, D., Murray, P., Nichol, B., Schawinski, K., Slosar, A., Szalay, A., Thomas, D., Vandenberg, J., Andreescu, D., 2008. Galaxy Zoo: Motivations of Citizen Scientists. AAS 212, 40.01.

Raimonet, M., Thieu, V., Silvestre, M., Oudin, L., Rabouille, C., Vautard, R., Garnier, J., 2018. Landward perspective of coastal eutrophication potential under future climate change: The Seine River case (France). Front. Mar. Sci. 5, 136. https://doi.org/10.3389/fmars.2018.00136

Raudsepp-Hearne, C., Peterson, G.D., Bennett, E.M., 2010. Ecosystem service bundles for

analyzing tradeoffs in diverse landscapes. Proc. Natl. Acad. Sci. 107, 5242–5247. https://doi.org/10.1073/PNAS.0907284107

Raymond, P.A., Hamilton, S.K., Stanley, E., Del Giorgio, P., 2018. Anthropogenic influences on riverine fluxes of dissolved inorganic carbon to the oceans. Limnol. Oceanogr. Lett. 3, 143–155. https://doi.org/10.1002/LOL2.10069

Raymond, P.A., Saiers, J.E., Sobczak, W. V., 2016. Hydrological and biogeochemical controls on watershed dissolved organic matter transport: pulse-shunt concept. Ecology 97, 5–16. https://doi.org/10.1890/14-1684.1

Redfield, A.C., Ketchum, B.H., Richards, F.A., 1963. The influence of organisms on the composition of sea-water . Sea 2, 26–76.

Redhead, J.W., May, L., Oliver, T.H., Hamel, P., Sharp, R., Bullock, J.M., 2018. National scale evaluation of the InVEST nutrient retention model in the United Kingdom. Sci. Total Environ. 610–611, 666–677. https://doi.org/10.1016/j.scitotenv.2017.08.092

Regelink, I.C., Weng, L., Lair, G.J., Comans, R.N.J., 2015. Adsorption of phosphate and organic matter on metal (hydr)oxides in arable and forest soil: a mechanistic modelling study. Eur. J. Soil Sci. 66, 867–875. https://doi.org/10.1111/EJSS.12285

Reichstein, M., Bahn, M., Ciais, P., Frank, D., Mahecha, M.D., Seneviratne, S.I., Zscheischler, J., Beer, C., Buchmann, N., Frank, D.C., Papale, D., Rammig, A., Smith, P., Thonicke, K., Van Der Velde, M., Vicca, S., Walz, A., Wattenbach, M., 2013. Climate extremes and the carbon cycle. Nat. 2013 5007462 500, 287–295. https://doi.org/10.1038/nature12350

Richardson, D.M., Holmes, P.M., Esler, K.J., Galatowitsch, S.M., Stromberg, J.C., Kirkman, S.P., Pyšek, P., Hobbs, R.J., 2007. Riparian vegetation: degradation, alien plant invasions, and restoration prospects. Divers. Distrib. 13, 126–139. https://doi.org/10.1111/J.1366-9516.2006.00314.X

Rocchini, D., Perry, G.L.W., Salerno, M., Maccherini, S., Chiarucci, A., 2006. Landscape change and the dynamics of open formations in a natural reserve. Landsc. Urban Plan. 77, 167–177. https://doi.org/10.1016/J.LANDURBPLAN.2005.02.008

Romero, E., Garnier, J., Lassaletta, L., Billen, G., Le Gendre, R., Riou, P., Cugier, P., 2013. Large-scale patterns of river inputs in southwestern Europe: Seasonal and interannual variations and potential eutrophication effects at the coastal zone. Biogeochemistry 113, 481–505. https://doi.org/10.1007/s10533-012-9778-0

Roulet, N., Moore, T.R., 2006. Browning the waters. Nat. 2006 4447117 444, 283–284. https://doi.org/10.1038/444283a

Roy, H.E., Pocock, M.J.O., Preston, C.D., Roy, D.B., Savage, J., Tweddle, J.C., Robinson, L.D., 2012. Understanding citizen science and environmental monitoring: final report on behalf of UK Environmental Observation Framework.

Royer, T. V., 2020. Stoichiometry of nitrogen, phosphorus, and silica loads in the Mississippi-Atchafalaya River basin reveals spatial and temporal patterns in risk for cyanobacterial blooms. Limnol. Oceanogr. 65, 325–335. https://doi.org/10.1002/LNO.11300

Ruckelshaus, M., McKenzie, E., Tallis, H., Guerry, A., Daily, G., Kareiva, P., Polasky, S., Ricketts, T., Bhagabati, N., Wood, S.A., Bernhardt, J., 2015. Notes from the field: Lessons learned from using ecosystem service approaches to inform real-world decisions. Ecol. Econ. 115, 11–21. https://doi.org/10.1016/J.ECOLECON.2013.07.009

Saalfeld, D.T., Reutebuch, E.M., Dickey, R.J., Seesock, W.C., Webber, C., Bayne, D.R., 2012. Effects of landscape characteristics on water quality and fish assemblages in the Tallapoosa River Basin, Alabama. Southeast. Nat. 11, 239–252. https://doi.org/10.1656/058.011.0206

Sabater, S., Butturini, A., Clement, J.-C., Burt, T., Dowrick, D., Hefting, M., Matre, V., Pinay, G., Postolache, C., Rzepecki, M., Sabater, F., 2003. Nitrogen Removal by Riparian Buffers along a European Climatic Gradient: Patterns and Factors of Variation. Ecosyst. 2003 61 6, 0020–0030. https://doi.org/10.1007/S10021-002-0183-8

Sagan, V., Peterson, K.T., Maimaitijiang, M., Sidike, P., Sloan, J., Greeling, B.A., Maalouf, S., Adams, C., 2020. Monitoring inland water quality using remote sensing: potential and limitations of spectral indices, bio-optical simulations, machine learning, and cloud computing. Earth-Science Rev. 205, 103187. https://doi.org/10.1016/J.EARSCIREV.2020.103187

Samson, C.C., Rajagopalan, B., Summers, R.S., 2016. Modeling Source Water TOC Using Hydroclimate Variables and Local Polynomial Regression. Environ. Sci. Technol. 50, 4413–4421. https://doi.org/10.1021/ACS.EST.6B00639/SUPPL_FILE/ES6B00639_SI_001.PDF

Sánchez-Canales, M., López-Benito, A., Acuña, V., Ziv, G., Hamel, P., Chaplin-Kramer, R., Elorza, F.J., 2015. Sensitivity analysis of a sediment dynamics model applied in a Mediterranean river basin: Global change and management implications. Sci. Total Environ. 502, 602–610. https://doi.org/10.1016/J.SCITOTENV.2014.09.074

Sass-Klaassen, U., Fonti, P., Cherubini, P., Gričar, J., Robert, E.M.R., Steppe, K., Bräuning, A., 2016. A tree-centered approach to assess impacts of extreme climatic events on forests. Front. Plant Sci. 7, 1069. https://doi.org/10.3389/FPLS.2016.01069/BIBTEX

Scanes, E., Scanes, P.R., Ross, P.M., 2020. Climate change rapidly warms and acidifies Australian estuaries. Nat. Commun. 2020 111 11, 1–11. https://doi.org/10.1038/s41467-020-15550-z

Scholz, R.W., Roy, A.H., Hellums, D.T., 2014. Sustainable phosphorus management: A transdisciplinary challenge. Sustain. Phosphorus Manag. A Glob. Transdiscipl. Roadmap 1–128. https://doi.org/10.1007/978-94-007-7250-2_1/TABLES/8

Schröter, M., Kraemer, R., Mantel, M., Kabisch, N., Hecker, S., Richter, A., Neumeier, V., Bonn, A., 2017. Citizen science for assessing ecosystem services: Status, challenges and opportunities. Ecosyst. Serv. 28, 80–94. https://doi.org/10.1016/J.ECOSER.2017.09.017

Schröter, M., van der Zanden, E.H., van Oudenhoven, A.P.E., Remme, R.P., Serna-Chavez, H.M., de Groot, R.S., Opdam, P., 2014. Ecosystem Services as a Contested Concept: a Synthesis of Critique and Counter-Arguments. Conserv. Lett. 7, 514–523. https://doi.org/10.1111/CONL.12091

Scott, A.B., Frost, P.C., 2017. Monitoring water quality in Toronto's urban stormwater ponds: Assessing participation rates and data quality of water sampling by citizen scientists in the FreshWater Watch. Sci. Total Environ. 592, 738–744. https://doi.org/10.1016/J.SCITOTENV.2017.01.201

Seddon, N., Chausson, A., Berry, P., Girardin, C.A.J., Smith, A., Turner, B., 2020. Understanding the value and limits of nature-based solutions to climate change and other global challenges. Philos. Trans. R. Soc. B 375. https://doi.org/10.1098/RSTB.2019.0120

Seeber, J., Seeber, G.U.H., 2005. Effects of land-use changes on humus forms on alpine pastureland (Central Alps, Tyrol). Geoderma 124, 215–222. https://doi.org/10.1016/J.GEODERMA.2004.05.002

Shang, P., Lu, Y.H., Du, Y.X., Jaffé, R., Findlay, R.H., Wynn, A., 2018. Climatic and watershed controls of dissolved organic matter variation in streams across a gradient of agricultural land use. Sci. Total Environ. 612, 1442–1453. https://doi.org/10.1016/J.SCITOTENV.2017.08.322

Sharp, R., Tallis, H.T., Ricketts, T., Guerry, A.D., Wood, S.A., Chaplin-Kramer, R., Nelson, E., D., E., Wolny, S., Olwero, N., Vigerstol, K., Pennington, D., Mendoza, G., Aukema, J., Foster, J., Forrest, J., Cameron, D., Arkema, K., Lonsdorf, E., Kennedy, C., Verutes, G., Kim, C.K., Guannel, G., Papenfus, M., Toft, J., Marsik, M., Bernhardt, J., Griffin, R., Glowinski, K., Chaumont, N., Perelman, A., Lacayo, M., Mandle, L., Hamel, P., Vogl, A.L., Rogers, L., Bierbower, W., Denu, D., Douglass, J., 2018. InVEST 3.6.0 User's Guide [WWW Document]. Nat. Cap. Proj. URL

http://data.naturalcapitalandresilienceplatform.org/invest-releases/documentation/current_release/index.html

Shirk, J.L., Ballard, H.L., Wilderman, C.C., Phillips, T., Wiggins, A., Jordan, R., Mccallie, E., Minarchek, M., Lewenstein, B. V, Krasny, M.E., Bonney, R., 2012. Public Participation in Scientific Research: a Framework for Deliberate Design. Ecol. Soc. 17. https://doi.org/10.5751/ES-04705-170229

Silvertown, J., 2009. A new dawn for citizen science. Trends Ecol. Evol. 24, 467–71. https://doi.org/10.1016/j.tree.2009.03.017

Siudek, P., Frankowski, M., Siepak, J., 2015. Seasonal variations of dissolved organic carbon in precipitation over urban and forest sites in central Poland. Environ. Sci. Pollut. Res. 22, 11087–11096. https://doi.org/10.1007/S11356-015-4356-3/FIGURES/5

Škerlep, M., Steiner, E., Axelsson, A.L., Kritzberg, E.S., 2020. Afforestation driving long-term surface water browning. Glob. Chang. Biol. 26, 1390–1399. https://doi.org/10.1111/GCB.14891

Smil, V., 2004. Enriching the Earth: Fritz Haber, Carl Bosch, and the Transformation of World Food Production, Enriching the Earth. The MIT Press. https://doi.org/10.7551/MITPRESS/2767.001.0001

Smith, J., Gottschalk, P., Bellarby, J., Chapman, S., Lilly, A., Towers, W., Bell, J., Coleman, K., Nayak, D., Richards, M., Hillier, J., Flynn, H., Wattenbach, M., Aitkenhead, M., Yeluripati, J., Farmer, J., Milne, R., Thomson, A., Evans, C., Whitmore, A., Falloon, P., Smith, P., 2010. Estimating changes in Scottish soil carbon stocks using ECOSSE. I. Model description and uncertainties. Clim. Res. 45, 179–192. https://doi.org/10.3354/CR00899

Smith, M.L., 2014. Citizen Science in Archaeology. Am. Antiq. 79, 749–762. https://doi.org/10.7183/0002-7316.79.4.749

Smith, T.M., Smith, L.R., 2014. Elements of Ecology, 9th ed. Pearson, San Francisco.

Soares, A.R.A., Lapierre, J.F., Selvam, B.P., Lindström, G., Berggren, M., 2019. Controls on Dissolved Organic Carbon Bioreactivity in River Systems. Sci. Reports 2019 91 9, 1–9. https://doi.org/10.1038/s41598-019-50552-y

Spencer, R.G.M., Butler, K.D., Aiken, G.R., 2012. Dissolved organic carbon and chromophoric dissolved organic matter properties of rivers in the USA. J. Geophys. Res. Biogeosciences 117, 3001. https://doi.org/10.1029/2011JG001928

Spencer, R.G.M., Hernes, P.J., Ruf, R., Baker, A., Dyda, R.Y., Stubbins, A., Six, J., 2010. Temporal controls on dissolved organic matter and lignin biogeochemistry in a pristine

tropical river, Democratic Republic of Congo. J. Geophys. Res. Biogeosciences 115, 3013. https://doi.org/10.1029/2009JG001180

Spillman, C.M., Imberger, J., Hamilton, D.P., Hipsey, M.R., Romero, J.R., 2007. Modelling the effects of Po River discharge, internal nutrient cycling and hydrodynamics on biogeochemistry of the Northern Adriatic Sea. J. Mar. Syst. 68, 167–200. https://doi.org/10.1016/j.jmarsys.2006.11.006

Stallard, R.F., 1998. Terrestrial sedimentation and the carbon cycle: Coupling weathering and erosion to carbon burial. Global Biogeochem. Cycles 12, 231–257. https://doi.org/10.1029/98GB00741

Stanley, E.H., Powers, S.M., Lottig, N.R., Buffam, I., Crawford, J.T., 2012. Contemporary changes in dissolved organic carbon (DOC) in human-dominated rivers: is there a role for DOC management? Freshw. Biol. 57, 26–42. https://doi.org/10.1111/J.1365-2427.2011.02613.X

Steinberg, C.E.W., 2003. Ecology of Humic Substances in Freshwaters, 1st ed, Ecology of Humic Substances in Freshwaters. Springer Berlin Heidelberg, Berlin, Heidelberg. https://doi.org/10.1007/978-3-662-06815-1

Steinfeld, H., Wassenaar, T., 2007. The Role of Livestock Production in Carbon and Nitrogen Cycles. https://doi.org/10.1146/annurev.energy.32.041806.143508 32, 271–294. https://doi.org/10.1146/ANNUREV.ENERGY.32.041806.143508

Sterner, R.W., Elser, J.J., 2017. Ecological Stoichiometry, Ecological Stoichiometry. Princeton University Press. https://doi.org/10.1515/9781400885695/HTML

Stocker, T.F., Qin, D., Plattner, G.-K., Tignor, M., Allen, S.K., Boschung, J., Nauels, A., Xia, Y., Bex, V., Midgley, P.M., 2013. IPCC, 2013: Summary for Policymakers 2013 — European Environment Agency [WWW Document]. Cambridge Univ. Press. URL https://www.eea.europa.eu/data-and-maps/indicators/global-and-european-temperature-9/ipcc-2013-summary-for-policymakers-2013 (accessed 8.10.21).

Straile, D., Livingstone, D.M., Weyhenmeyer, G.A., George, D.G., 2003. The response of freshwater ecosystems to climate variability associated with the North Atlantic oscillation 263–279. https://doi.org/10.1029/134GM12

Strickland, J.D.H., Parsons, T.R., 1972. A Practical Handbook of Seawater Analysis. Bull. Fish. Res. Board Canada 167, 405. https://doi.org/10.2307/1979241

Strohmeier, S., Knorr, K.H., Reichert, M., Frei, S., Fleckenstein, J.H., Peiffer, S., Matzner, E., 2013. Concentrations and fluxes of dissolved organic carbon in runoff from a forested catchment: Insights from high frequency measurements. Biogeosciences 10, 905–916.

https://doi.org/10.5194/BG-10-905-2013

Strokal, M., Kroeze, C., Wang, M., Bai, Z., Ma, L., 2016. The MARINA model (Model to Assess River Inputs of Nutrients to seAs): Model description and results for China. Sci. Total Environ. 562, 869–888. https://doi.org/10.1016/j.scitotenv.2016.04.071

Stutter, M.I., Graeber, D., Evans, C.D., Wade, A.J., Withers, P.J.A., 2018. Balancing macronutrient stoichiometry to alleviate eutrophication. Sci. Total Environ. 634, 439–447. https://doi.org/10.1016/J.SCITOTENV.2018.03.298

Surian, N., Rinaldi, M., Pellegrini, L., Audisio, C., Maraga, F., Teruggi, L., Turitto, O., Ziliani, L., 2009. Channel adjustments in northern and central Italy over the last 200 years. Spec. Pap. Geol. Soc. Am. 451, 83–95. https://doi.org/10.1130/2009.2451(05)

Sutton, M.A., Howard, C.M., Erisman, J.W., Billen, G., Bleeker, A., Grennfelt, P., van Grinsven, H., Grizzetti, B., 2011. The European Nitrogen Assessment: Sources, Effects and Policy Perspectives. Cambridge University Press, Cambridge. https://doi.org/10.1017/CBO9780511976988

Tabacchi, E., Lambs, L., Guilloy, H., Planty-Tabacchi, A.-M., Muller, E., Décamps, H., 2000. Impacts of riparian vegetation on hydrological processes - Tabacchi - 2000 - Hydrological Processes - Wiley Online Library. Hydrol. Process. 14, 2959–2976.

Tague, C.L., Band, L.E., 2004. RHESSys: Regional Hydro-Ecologic Simulation System—An Object-Oriented Approach to Spatially Distributed Modeling of Carbon, Water, and Nutrient Cycling. Earth Interact. 8, 1–42. https://doi.org/10.1175/1087-3562(2004)8<1:rrhsso>2.0.co;2

Tanaka, M.O., de Souza, A.L.T., Moschini, L.E., de Oliveira, A.K., 2016. Influence of watershed land use and riparian characteristics on biological indicators of stream water quality in southeastern Brazil. Agric. Ecosyst. Environ. 216, 333–339. https://doi.org/10.1016/j.agee.2015.10.016

Tarr, A.P., Smith, I.J., Rodger -, C.J., Joseph, B., Kaetzl, K., Hensgen, F., -, al, Choueiri, Y., Lund, J., Daccache, A., Ciurana, J.S., Rodriguez Diaz, J.A., Knox, J.W., 2014. Water and energy footprint of irrigated agriculture in the Mediterranean region. Environ. Res. Lett. 9, 124014. https://doi.org/10.1088/1748-9326/9/12/124014

Tasser, E., Mader, M., Tappeiner, U., 2003. Effects of land use in alpine grasslands on the probability of landslides. Basic Appl. Ecol. 4, 271–280. https://doi.org/10.1078/1439-1791-00153

Thomson, A.M., Calvin, K. V., Smith, S.J., Kyle, G.P., Volke, A., Patel, P., Delgado-Arias, S., Bond-Lamberty, B., Wise, M.A., Clarke, L.E., Edmonds, J.A., 2011. RCP4.5: A

pathway for stabilization of radiative forcing by 2100. Clim. Change 109, 77–94. https://doi.org/10.1007/S10584-011-0151-4/FIGURES/12

Thornhill, I., Chautard, A., Loiselle, S., 2018. Monitoring Biological and Chemical Trends in Temperate Still Waters Using Citizen Science. Water 2018, Vol. 10, Page 839 10, 839. https://doi.org/10.3390/W10070839

Thornhill, I., Loiselle, S., Lind, K., Ophof, D., 2016. The citizen science opportunity for researchers and agencies. Bioscience. https://doi.org/10.1093/biosci/biw089

Thurman, E.M., 1985. Organic Geochemistry of Natural Waters, 1st ed, Organic Geochemistry of Natural Waters. Springer Netherlands. https://doi.org/10.1007/978-94-009-5095-5

Tian, H., Xu, R., Canadell, J.G., Thompson, R.L., Winiwarter, W., Suntharalingam, P., Davidson, E.A., Ciais, P., Jackson, R.B., Janssens-Maenhout, G., Prather, M.J., Regnier, P., Pan, N., Pan, S., Peters, G.P., Shi, H., Tubiello, F.N., Zaehle, S., Zhou, F., Arneth, A., Battaglia, G., Berthet, S., Bopp, L., Bouwman, A.F., Buitenhuis, E.T., Chang, J., Chipperfield, M.P., Dangal, S.R.S., Dlugokencky, E., Elkins, J.W., Eyre, B.D., Fu, B., Hall, B., Ito, A., Joos, F., Krummel, P.B., Landolfi, A., Laruelle, G.G., Lauerwald, R., Li, W., Lienert, S., Maavara, T., MacLeod, M., Millet, D.B., Olin, S., Patra, P.K., Prinn, R.G., Raymond, P.A., Ruiz, D.J., van der Werf, G.R., Vuichard, N., Wang, J., Weiss, R.F., Wells, K.C., Wilson, C., Yang, J., Yao, Y., 2020. A comprehensive quantification of global nitrous oxide sources and sinks. Nat. 2020 5867828 586, 248–256. https://doi.org/10.1038/s41586-020-2780-0

Tian, H., Yang, Q., Najjar, R.G., Ren, W., Friedrichs, M.A.M., Hopkinson, C.S., Pan, S., 2015. Anthropogenic and climatic influences on carbon fluxes from eastern North America to the Atlantic Ocean: A process-based modeling study. J. Geophys. Res. Biogeosciences 120, 757–772. https://doi.org/10.1002/2014JG002760

Timofeeva, A., Galyamova, M., Sedykh, S., 2022. Prospects for Using Phosphate-Solubilizing Microorganisms as Natural Fertilizers in Agriculture. Plants 2022, Vol. 11, Page 2119 11, 2119. https://doi.org/10.3390/PLANTS11162119

Torrecilla, N.J., Galve, J.P., Zaera, L.G., Retamar, J.F., Álvarez, A.N.A., 2005. Nutrient sources and dynamics in a mediterranean fluvial regime (Ebro river, NE Spain) and their implications for water management. J. Hydrol. 304, 166–182. https://doi.org/10.1016/j.jhydrol.2004.07.029

Totti, C., Romagnoli, T., Accoroni, S., Coluccelli, A., Pellegrini, M., Campanelli, A., Grilli, F., Marini, M., 2019. Phytoplankton communities in the northwestern Adriatic Sea:

Interdecadal variability over a 30-years period (1988–2016) and relationships with meteoclimatic drivers. J. Mar. Syst. 193, 137–153. https://doi.org/10.1016/J.JMARSYS.2019.01.007

Trabucco, A., Zomer, R.J., 2018. Global Aridity Index and Potential Evapo-Transpiration (ET0) Climate Database v2. CGIAR Consortium for Spatial Information (CGIAR-CSI) [WWW Document]. CGIAR-CSI GeoPortal. URL https://cgiarcsi.community (accessed 1.8.23).

Tranvik, L.J., Downing, J.A., Cotner, J.B., Loiselle, S.A., Striegl, R.G., Ballatore, T.J., Dillon, P., Finlay, K., Fortino, K., Knoll, L.B., Kortelainen, P.L., Kutser, T., Larsen, S., Laurion, I., Leech, D.M., Leigh McCallister, S., McKnight, D.M., Melack, J.M., Overholt, E., Porter, J.A., Prairie, Y., Renwick, W.H., Roland, F., Sherman, B.S., Schindler, D.W., Sobek, S., Tremblay, A., Vanni, M.J., Verschoor, A.M., Von Wachenfeldt, E., Weyhenmeyer, G.A., 2009. Lakes and reservoirs as regulators of carbon cycling and climate. Limnol. Oceanogr. 54, 2298–2314. https://doi.org/10.4319/LO.2009.54.6_PART_2.2298

Turner, B.L., Lambin, E.F., Reenberg, A., 2007. The emergence of land change science for global environmental change and sustainability. Proc. Natl. Acad. Sci. U. S. A. https://doi.org/10.1073/pnas.0704119104

Turner, R.E., Rabalais, N.N., 1994. Coastal eutrophication near the Mississippi river delta. Nature 368, 619–621. https://doi.org/10.1038/368619a0

Turner, R.E., Rabalais, N.N., Justic, D., Dortch, Q., 2003. Global patterns of dissolved N, P and Si in large rivers. Biogeochemistry 64, 297–317. https://doi.org/10.1023/A:1024960007569/METRICS

UN, 2015. Transforming our world: the 2030 Agenda for Sustainable Development | Department of Economic and Social Affairs.

UNFCCC, 2022. COP 27 [WWW Document]. URL https://unfccc.int/event/cop-27 (accessed 1.31.23).

Valipour, M., Johnson, C.E., Battles, J.J., Campbell, J.L., Fahey, T.J., Fakhraei, H., Driscoll, C.T., 2021. Simulation of the effects of forest harvesting under changing climate to inform long-term sustainable forest management using a biogeochemical model. Sci. Total Environ. 767, 144881. https://doi.org/10.1016/J.SCITOTENV.2020.144881

van den Berg, L.J.L., Shotbolt, L., Ashmore, M.R., 2012. Dissolved organic carbon (DOC) concentrations in UK soils and the influence of soil, vegetation type and seasonality. Sci. Total Environ. 427–428, 269–276. https://doi.org/10.1016/J.SCITOTENV.2012.03.069

Vigerstol, K.L., Aukema, J.E., 2011. A comparison of tools for modeling freshwater ecosystem services. J. Environ. Manage. https://doi.org/10.1016/j.jenvman.2011.06.040

Vigiak, O., Borselli, L., Newham, L.T.H., McInnes, J., Roberts, A.M., 2012. Comparison of conceptual landscape metrics to define hillslope-scale sediment delivery ratio. Geomorphology 138, 74–88. https://doi.org/10.1016/J.GEOMORPH.2011.08.026

Vira, B., Adams, W.M., 2009. Ecosystem services and conservation strategy: beware the silver bullet. Conserv. Lett. 2, 158–162. https://doi.org/10.1111/J.1755-263X.2009.00063.X

Von Wachenfeldt, E., Tranvik, L.J., 2008. Sedimentation in boreal lakes - The role of flocculation of allochthonous dissolved organic matter in the water column. Ecosystems 11, 803–814. https://doi.org/10.1007/S10021-008-9162-Z/FIGURES/5

Wade, A.J., Butterfield, D., Whitehead, P.G., 2006. Towards an improved understanding of the nitrate dynamics in lowland, permeable river-systems: Applications of INCA-N. J. Hydrol. 330, 185–203. https://doi.org/10.1016/J.JHYDROL.2006.04.023

Wåhlström, I., Höglund, A., Almroth-Rosell, E., MacKenzie, B.R., Gröger, M., Eilola, K., Plikshs, M., Andersson, H.C., 2020. Combined climate change and nutrient load impacts on future habitats and eutrophication indicators in a eutrophic coastal sea. Limnol. Oceanogr. 65, 2170–2187. https://doi.org/10.1002/lno.11446

Wang, H., Yang, Z., Saito, Y., Liu, J.P., Sun, X., 2006. Interannual and seasonal variation of the Huanghe (Yellow River) water discharge over the past 50 years: Connections to impacts from ENSO events and dams. Glob. Planet. Change 50, 212–225. https://doi.org/10.1016/j.gloplacha.2006.01.005

Waraich, E.A., Ahmad, R., Yaseen Ashraf, M., Saifullah, S., Ahmad, M., 2011. Improving agricultural water use efficiency by nutrient management in crop plants. http://dx.doi.org/10.1080/09064710.2010.491954 61, 291–304. https://doi.org/10.1080/09064710.2010.491954

WCD, 2000. World Commission on Dams. Dams and Development: A New Framework for Decision-Making | International Rivers [WWW Document]. URL https://archive.internationalrivers.org/resources/dams-and-development-a-new-framework-for-decision-making-3939 (accessed 1.29.23).

Wei, P., Chen, S., Wu, M., Deng, Y., Xu, H., Jia, Y., Liu, F., 2021. Using the InVEST Model to Assess the Impacts of Climate and Land Use Changes on Water Yield in the Upstream Regions of the Shule River Basin. Water 2021, Vol. 13, Page 1250 13, 1250. https://doi.org/10.3390/W13091250

Wheatcroft, R.A., Goñi, M.A., Hatten, J.A., Pasternack, G.B., Warrick, J.A., 2010. The role of effective discharge in the ocean delivery of particulate organic carbon by small, mountainous river systems. Limnol. Oceanogr. 55, 161–171. https://doi.org/10.4319/LO.2010.55.1.0161

Whitehead, P.G., Wilby, R.L., Battarbee, R.W., Kernan, M., Wade, A.J., 2009. A review of the potential impacts of climate change on surface water quality. Hydrol. Sci. J. https://doi.org/10.1623/hysj.54.1.101

Wiggins, A., Crowston, K., 2011. From conservation to crowdsourcing: A typology of citizen science, in: Proceedings of the Annual Hawaii International Conference on System Sciences. https://doi.org/10.1109/HICSS.2011.207

WMO, 2022. World Meteorological Organization (WMO) Greenhouse Gas Bulletin (GHG Bulletin) - No.18. WMO, Geneva.

Worrall, F., Burt, T., 2005. Predicting the future DOC flux from upland peat catchments. J. Hydrol. 300, 126–139. https://doi.org/10.1016/J.JHYDROL.2004.06.007

Worrall, F., Harriman, R., Evans, C.D., Watts, C.D., Adamson, J., Neal, C., Tipping, E., Burt, T., Grieve, I., Monteith, D., Naden, P.S., Nisbet, T., Reynolds, B., Stevens, P., 2004. Trends in dissolved organic carbon in UK rivers and lakes. Biogeochemistry 70, 369–402. https://doi.org/10.1007/S10533-004-8131-7/METRICS

Wu, H., Peng, C., Moore, T.R., Hua, D., Li, C., Zhu, Q., Peichl, M., Arain, M.A., Guo, Z., 2014. Modeling dissolved organic carbon in temperate forest soils: TRIPLEX-DOC model development and validation. Geosci. Model Dev. 7, 867–881. https://doi.org/10.5194/gmd-7-867-2014

Xu, H., Gao, Q., Yuan, B., 2022. Analysis and identification of pollution sources of comprehensive river water quality: Evidence from two river basins in China. Ecol. Indic. 135, 108561. https://doi.org/10.1016/J.ECOLIND.2022.108561

Xu, Z., Fan, W., Wei, H., Zhang, P., Ren, J., Gao, Z., Ulgiati, S., Kong, W., Dong, X., 2019. Evaluation and simulation of the impact of land use change on ecosystem services based on a carbon flow model: A case study of the Manas River Basin of Xinjiang, China. Sci. Total Environ. 652, 117–133. https://doi.org/10.1016/J.SCITOTENV.2018.10.206

Yang, H., Wang, G., Wang, L., Zheng, B., 2016. Impact of land use changes on water quality in headwaters of the Three Gorges Reservoir. Environ. Sci. Pollut. Res. 23, 11448–11460. https://doi.org/10.1007/s11356-015-5922-4

Yang, H., Yang, D., Lei, Z., Sun, F., 2008. New analytical derivation of the mean annual water-energy balance equation. Water Resour. Res. 44, 3410.

https://doi.org/10.1029/2007WR006135

Yang, Q., Zhang, X., 2016. Improving SWAT for simulating water and carbon fluxes of forest ecosystems. Sci. Total Environ. 569–570, 1478–1488. https://doi.org/10.1016/J.SCITOTENV.2016.06.238

Yang, W., Liu, Y., Ou, C., Gabor, S., 2016. Examining water quality effects of riparian wetland loss and restoration scenarios in a southern ontario watershed. J. Environ. Manage. 174, 26–34. https://doi.org/10.1016/j.jenvman.2016.03.001

Yates, C.A., Johnes, P.J., Spencer, R.G.M., 2016. Assessing the drivers of dissolved organic matter export from two contrasting lowland catchments, U.K. Sci. Total Environ. 569–570, 1330–1340. https://doi.org/10.1016/J.SCITOTENV.2016.06.211

Yin, G., Wang, X., Zhang, X., Fu, Y., Hao, F., Hu, Q., 2020. InVEST Model-Based Estimation of Water Yield in North China and Its Sensitivities to Climate Variables. Water 2020, Vol. 12, Page 1692 12, 1692. https://doi.org/10.3390/W12061692

Yoshimura, C., Fujii, M., Omura, T., Tockner, K., 2010. Instream release of dissolved organic matter from coarse and fine particulate organic matter of different origins. Biogeochemistry 100, 151–165. https://doi.org/10.1007/S10533-010-9412-Y/FIGURES/8

Zhang, C., Zhang, W., Huang, Y., Gao, X., 2017. Analysing the correlations of long-term seasonal water quality parameters, suspended solids and total dissolved solids in a shallow reservoir with meteorological factors. Environ. Sci. Pollut. Res. 24, 6746–6756. https://doi.org/10.1007/S11356-017-8402-1/FIGURES/8

Zhang, H., Lauerwald, R., Ciais, P., Van Oost, K., Guenet, B., Regnier, P., 2022. Global changes alter the amount and composition of land carbon deliveries to European rivers and seas. Commun. Earth Environ. 2022 31 3, 1–11. https://doi.org/10.1038/s43247-022-00575-7

Zhang, L., Hickel, K., Dawes, W.R., Chiew, F.H.S., Western, A.W., Briggs, P.R., 2004. A rational function approach for estimating mean annual evapotranspiration. Water Resour. Res. 40, 2502. https://doi.org/10.1029/2003WR002710

Zhang, L., Nan, Z., Xu, Y., Li, S., 2016. Hydrological Impacts of Land Use Change and Climate Variability in the Headwater Region of the Heihe River Basin, Northwest China. PLoS One 11, e0158394. https://doi.org/10.1371/JOURNAL.PONE.0158394

Zhang, X., Izaurralde, R.C., Arnold, J.G., Williams, J.R., Srinivasan, R., 2013. Modifying the Soil and Water Assessment Tool to simulate cropland carbon flux: Model development and initial evaluation. Sci. Total Environ. 463–464, 810–822.

https://doi.org/10.1016/J.SCITOTENV.2013.06.056

Zhang, X., Liu, X., Zhang, M., Dahlgren, R.A., Eitzel, M., 2010. A Review of Vegetated Buffers and a Meta-analysis of Their Mitigation Efficacy in Reducing Nonpoint Source Pollution. J. Environ. Qual. 39, 76–84. https://doi.org/10.2134/jeq2008.0496

Zhou, M., Deng, J., Lin, Y., Belete, M., Wang, K., Comber, A., Huang, L., Gan, M., 2019. Identifying the effects of land use change on sediment export: Integrating sediment source and sediment delivery in the Qiantang River Basin, China. Sci. Total Environ. 686, 38–49. https://doi.org/10.1016/J.SCITOTENV.2019.05.336